

Dissertation zur Erlangung des Doktorgrades
der Fakultät für Chemie und Pharmazie
der Ludwig-Maximilians-Universität München

**Development of spider silk protein particles
for pharmaceutical applications**

Markus Michael Hofer

aus

Ingolstadt, Deutschland

2013

Erklärung

Diese Dissertation wurde im Sinne von §7 der Promotionsordnung vom 28. November 2011 von Herrn Prof. Dr. Gerhard Winter betreut.

Eidesstattliche Versicherung

Diese Dissertation wurde eigenständig und ohne unerlaubte Hilfe erarbeitet.

München, 04.10.2013

.....
Markus Hofer

Dissertation eingereicht am: 04.10.2013

- 1. Gutachter: Prof. Dr. Gerhard Winter
- 2. Gutachter: Prof. Dr. Wolfgang Frieß

Mündliche Prüfung am: 04.11.2013

Für meine Familie

In Liebe und Dankbarkeit

ACKNOWLEDGEMENTS

The present thesis was prepared under the supervision of Prof. Dr. Gerhard Winter at the Department of Pharmacy, Pharmaceutical Technology and Biopharmaceutics at the Ludwig-Maximilians-University (LMU) in Munich, Germany.

Foremost, I would like to express my deepest gratitude to my supervisor Prof. Dr. Gerhard Winter for offering the possibility to join his team and for his dedicated scientific guidance throughout all phases of this work. Also I would like to thank him for providing an outstanding working and team atmosphere and the opportunity to attend scientific conferences all over Europe and the USA. Last but not least, I want to highlight his elaborated advice and guidance on my personal development over the last years.

This work was further supervised by Dr. Julia Myschik. I would like to thank Julia for her outstanding scientific and personal support from the first day of our project, for proof reading of all publications and this thesis, and for her never-fading encouragement and enthusiasm in my work.

I would like to thank Prof. Dr. Wolfgang Frieß for his enduring interest in this topic, for his scientific input and advice over the last years, for his support on organizing the practical course 'Biopharmacy', and for kindly being the co-referee of this work.

I deeply appreciate that both Prof. Dr. Gerhard Winter and Prof. Dr. Wolfgang Frieß encourage the whole team to organize and attend numerous social events creating an outstanding working and personal climate that made the preparation of this thesis a precious and exciting time.

During the preparation of this thesis, an application prepared by the LMU, the University of Bayreuth and the AMSilk GmbH (Martinsried, Germany) was approved by the Federal Ministry of Education and Research (BMBF) in the cluster 'BioTransporter – Effizienter Wirkstofftransport in biologischen Systemen'. For this reason, the BMBF as well as AMSilk GmbH are acknowledged for the financial support of this work.

My special thanks go to the entire team at AMSilk GmbH and especially to Dr. Ute Slotta, Dr. Lin Roemer, Dr. Axel Leimer and Dr. Stephan Reschauer for providing the spider silk protein, the inspiring scientific discussions and the structural work on the submitted patent.

With regard to the research on spider silk proteins, I would like to express my thanks to Prof. Dr. Thomas Scheibel from the University of Bayreuth. Without his outstanding scientific achievements and his willingness to cooperate with Prof. Dr. Gerhard Winter, this work would not have been possible.

I would like to especially thank Dr. Andreas Lammel and Dr. Martin Schwab who introduced me to the world of spider silk proteins. Their excellent previous work provided the basis for this thesis.

My tremendous gratitude is expressed to all my colleagues from the research groups of Prof. Dr. Winter and Prof. Dr. Frieß. I very much appreciate the scientific and personal support from each of you: Dr. Ahmed Besheer, Thomas Bosch, Dr. Sarah Claus, Dr. Yibin Deng, Marie-Paule Even, Dr. Angelika Freitag, Dr. Sebastian Fuchs, Raimund Geidobler, Elisabeth Härtl, Sebastian Hertel, Alice Hirschmann, Kerstin Höger, Dr. Julia Kasper, Dr. Sarah Küchler, Imke Leitner, Robert Lieber, Matthias Lucke, Roman Mathäs, Philipp Matthias, Tim Menzen, Christian Neuhofer, Matthäus Noga, Dr. Miriam Printz, Dr. Eva-Maria Ruberg, Dr. Gerhard Sax, Dr. Lars Schiefelbein, Dr. Katja Schmid, Dr. Tim Serno, Ayla Tekbudak, Madeleine Witting, Dr. Sarah Zölls.

Elsa Etzl, thank you so much for being more than just a labmate. Dr. Winfried Schlögl, thanks a lot for our daily 'breakfast time' and your loyal friendship. Elisa Agostini, I like your Italian spirit so much. Christian Hildebrandt, just chillax and thank you for your intimate friendship.

Furthermore, all students which have contributed to the preparation of this work are acknowledged for providing valuable scientific input and results: Janek Kibat, who even had the heart to work twice under my supervision, Friederike Voge and Katrin Ottinger, Sandra Crößmann and Regina Siebachmeyer, and Alexandra Partenhauser. Good job, it was a great time to work with you all.

From the Department of Chemistry of the LMU Munich, I want to thank Christian Minke for his extensive support with SEM analysis.

I would like to thank Prof. Dr. Stefan Zahler at the Department of Pharmaceutical Biology and Dr. Yibin Deng for their help with confocal laser scanning microscopy.

Finally, I would like to thank my parents and my sister Pamela for all your encouragement and support throughout all the years. Thank you for always being there for me.

TABLE OF CONTENTS

CHAPTER 1: GENERAL INTRODUCTION

1.1	INTRODUCTION	1
1.2	DRUG DELIVERY SYSTEMS FOR THERAPEUTIC PROTEINS	3
1.3	PROTEIN-BASED DRUG DELIVERY SYSTEMS	6
1.3.1	PREPARATION TECHNIQUES FOR PROTEIN PARTICLES AS DRUG CARRIERS.....	6
1.3.1.1	Emulsion / Solvent extraction	6
1.3.1.2	Coacervation – Non-solvent	7
1.3.1.3	Coacervation – Salt precipitation	7
1.3.2	ALBUMIN	8
1.3.3	GELATIN.....	8
1.3.4	SILK.....	9
1.3.4.1	Structure and properties of silk proteins	10
1.3.4.2	Natural assembly process	12
1.3.4.3	Immunogenicity and biodegradation of silk proteins	13
1.3.4.4	Silkworm silk for drug delivery	14
1.4	SPIDER SILK PROTEINS	19
1.4.1	DEVELOPMENT OF RECOMBINANT SPIDER SILK PROTEINS	19
1.4.1.1	Types of spider silk proteins	19
1.4.1.2	Engineered spider silk proteins.....	20
1.4.2	SPIDER SILK PROTEIN eADF4(C16).....	21
1.4.2.1	Characteristics of eADF4(C16).....	21
1.4.2.2	Processing of eADF4(C16).....	22
1.4.2.3	eADF4(C16) for drug delivery.....	26
1.5	OBJECTIVES OF THE THESIS	28
1.6	REFERENCES	30

CHAPTER 2: MATERIALS AND METHODS

2.1	MATERIALS	41
2.1.1	PROTEINS	41
2.1.1.1	Spider silk protein eADF4(C16).....	41
2.1.1.2	Lysozyme	42
2.1.1.3	Nerve growth factor	42

2.1.2	REAGENTS, CHEMICALS AND EXCIPIENTS.....	43
2.2	METHODS APPLIED FOR SPIDER SILK PROTEIN OR SPIDER SILK PARTICLES	45
2.2.1	PREPARATION OF LIQUID eADF4(C16) FORMULATIONS.....	45
2.2.2	CHARACTERIZATION OF LIQUID eADF4(C16) FORMULATIONS	45
2.2.2.1	Asymmetrical flow field-flow fractionation	45
2.2.2.2	Incubation at elevated temperature	46
2.2.2.3	Size exclusion chromatography.....	46
2.2.2.4	Sodium dodecyl sulphate polyacrylamide gel electrophoresis	46
2.2.2.5	Nephelometry.....	47
2.2.2.6	Light obscuration.....	47
2.2.3	PREPARATION OF eADF4(C16) PARTICLES	48
2.2.3.1	Micromixing system.....	48
2.2.3.2	Dialysis.....	49
2.2.3.3	Ultrasonic nozzle.....	49
2.2.3.4	Ultrasonic treatment and purification	50
2.2.3.5	Gravimetric determination of particle concentration	50
2.2.3.6	Freeze-drying of nanosuspensions.....	51
2.2.4	CHARACTERIZATION OF eADF4(C16) PARTICLES	51
2.2.4.1	Dynamic light scattering	51
2.2.4.2	Laser diffraction.....	52
2.2.4.3	Fourier transformed infrared spectroscopy	53
2.2.4.4	Scanning electron microscopy.....	53
2.2.4.5	Colloidal stability of eADF4(C16) particles.....	53
2.2.4.6	Determination of residual moisture	53
2.2.4.7	Differential scanning calorimetry.....	54
2.2.5	REMOTE LOADING OF SPIDER SILK PARTICLES.....	55
2.2.5.1	Loading procedure	55
2.2.5.2	Determination of loading and loading efficiency.....	55
2.2.5.3	Confocal laser scanning microscopy	56
2.2.6	ENCAPSULATION OF DRUGS INTO SPIDER SILK PARTICLES	57
2.2.6.1	Co-precipitation of Rhodamine B.....	57
2.2.6.2	Co-precipitation of lysozyme	57
2.2.7	<i>IN VITRO</i> RELEASE FROM SPIDER SILK PARTICLES.....	59
2.2.7.1	Experimental setup.....	59
2.2.7.2	Micro BCA protein assay	61
2.2.7.3	Size exclusion chromatography – Lysozyme.....	61
2.2.7.4	Activity assay – Lysozyme.....	61

2.3	METHODS APPLIED FOR STUDIES WITH NERVE GROWTH FACTOR	63
2.3.1	FORCED DEGRADATION OF NERVE GROWTH FACTOR.....	63
2.3.1.1	Experimental setup.....	63
2.3.1.2	Desorption procedure.....	64
2.3.1.3	Freeze-thaw	65
2.3.1.4	Stirring.....	65
2.3.1.5	Light exposure.....	65
2.3.1.6	Incubation at elevated temperature	66
2.3.2	ANALYTICAL METHODS	66
2.3.2.1	Size exclusion chromatography.....	66
2.3.2.2	Reversed phase chromatography.....	66
2.3.2.3	Nephelometry.....	67
2.3.2.4	Light obscuration.....	67
2.3.2.5	Sodium dodecyl sulphate polyacrylamide gel electrophoresis	67
2.3.2.6	Microcalorimetry.....	68
2.4	REFERENCES	69

CHAPTER 3: PREPARATION TECHNIQUES, CHARACTERIZATION AND FORMULATION DEVELOPMENT OF SPIDER SILK PARTICLES

3.1	INTRODUCTION	71
3.2	PREPARATION OF eADF4(C16) PARTICLES	74
3.2.1	SPIDER SILK NANOPARTICLES	74
3.2.2	SPIDER SILK MICROPARTICLES.....	80
3.2.2.1	Simultaneous atomization of eADF4(C16) solution and potassium phosphate solution	80
3.2.2.2	Atomization of eADF4(C16) into potassium phosphate solutions.....	82
3.2.2.3	Atomization of potassium phosphate into eADF4(C16) solutions.....	84
3.3	CHARACTERIZATION OF LIQUID eADF4(C16) FORMULATIONS	88
3.3.1	CHARACTERIZATION OF eADF4(C16) BY AF4	88
3.3.2	STABILITY OF eADF4(C16) AT ELEVATED TEMPERATURE	93
3.4	COLLOIDAL STABILITY OF SPIDER SILK NANOPARTICLES	96
3.5	FREEZE-DRYING OF eADF4(C16) NANOSUSPENSIONS	99
3.5.1	FEASIBILITY STUDY	99
3.5.2	FORMULATION DEVELOPMENT	101
3.6	SUMMARY AND CONCLUSIONS	104

3.7 REFERENCES.....	106
----------------------------	------------

CHAPTER4: SPIDER SILK PARTICLES FOR DRUG DELIVERY

4.1 INTRODUCTION	109
4.2 PROTEIN LOADED eADF4(C16) PARTICLES VIA REMOTE LOADING.....	112
4.2.1 LYSOZYME	112
4.2.2 NERVE GROWTH FACTOR	116
4.2.3 INVESTIGATION OF LOADING MECHANISM.....	119
4.2.4 <i>IN VITRO</i> RELEASE FROM PROTEIN LOADED SPIDER SILK PARTICLES.....	123
4.2.4.1 Influence of pH, ionic strength and payload.....	123
4.2.4.2 Analysis of drug release from remote loaded eADF4(C16) particles.....	125
4.2.4.3 <i>In vitro</i> release in the presence of albumin	129
4.3 ENCAPSULATION OF DRUGS INTO eADF4(C16) PARTICLES.....	131
4.3.1 RHODAMINE B.....	132
4.3.2 LYSOZYME	133
4.3.2.1 Lysozyme-loaded nanoparticles	134
4.3.2.2 Lysozyme-loaded microparticles	137
4.4 SUMMARY AND CONCLUSIONS	140
4.5 REFERENCES.....	142

CHAPTER 5: SPIDER SILK PARTICLES AS NOVEL EXCIPIENT FOR THE STABILIZATION OF NERVE GROWTH FACTOR

5.1 INTRODUCTION	145
5.2 DEVELOPMENT OF A STANDARD DESORPTION PROCEDURE.....	148
5.3 FORCED DEGRADATION STUDIES.....	151
5.3.1 FREEZE-THAW STUDY	151
5.3.2 STIRRING	155
5.3.3 LIGHT EXPOSURE.....	159
5.3.4 INCUBATION AT ELEVATED TEMPERATURE	164
5.4 SUMMARY AND CONCLUSIONS	170
5.5 REFERENCES.....	172

CHAPTER 6: FINAL SUMMARY AND CONCLUSION

FINAL SUMMARY AND CONCLUSION 175

LIST OF ABBREVIATIONS

ADF	<i>Araneus diadematus</i> fibroin
AF4	Asymmetrical flow field-flow fractionation
API	Active pharmaceutical ingredient
AUC	Area under the curve
BMP	Bone morphogenetic protein
BSA	Bovine serum albumin
CLSM	Confocal laser scanning microscopy
DDS	Drug delivery system
DLS	Dynamic light scattering
dn/dc	Differential index of refraction, specific refractive index increment
DOPC	1,2-Dioleoyl-sn-glycero-3-phosphocholine
DSC	Differential scanning calorimetry
μDSC	Microcalorimetry
eADF4	Engineered <i>Araneus diadematus</i> fibroin 4
FDA	US Food and Drug Administration
FITC	Fluorescein isothiocyanate
FNU	Formazine nephelometric units
FTIR	Fourier transformed infrared spectroscopy
HP-SEC	High performance size exclusion chromatography
HRP	Horseradish peroxidase
HSA	Human serum albumin
HPW	Highly purified water
ID	Inner diameter
IEP	Isoelectric point
IGF	Insulin-like growth factor
MA silk protein	Major ampullate silk protein
mp	Melting point
MV	Methyl violet 2B
NGF	Recombinant human nerve growth factor
PBS	Phosphate buffered saline
PI	Polydispersity index
PLGA	Poly(lactic-co-glycolic acid)
PVDF	Polyvinylidene fluoride
rpm	rounds per minute

RP-HPLC	Reversed phase high performance liquid chromatography
SD	Standard deviation
SDS-PAGE	Sodium dodecyl sulphate polyacrylamide gel electrophoresis
SEM	Scanning electron microscopy
SLS	Static light scattering / Laser diffraction
SOP	Standard operation procedure
TFA	Trifluoric acid
T_g'	Glass transition temperature of the maximally freeze-dried solution
T_g	Glass transition temperature
THF	Tetrahydrofuran
T_m	Melting temperature
TRIS	Tris(hydroxyethyl)-aminomethane

CHAPTER 1

GENERAL INTRODUCTION

1.1 INTRODUCTION

Today, protein drugs including cytokines and monoclonal antibodies still represent a growing and upcoming class of therapeutic molecules as they had been for the last 20 years even if the rate of approvals for new biopharmaceuticals has slowed down [1, 2]. Furthermore, the pipelines of pharmaceutical companies are loaded with new types and variants of therapeutic proteins such as antibody fragments or antibody-drug-conjugates [3]. Protein drugs are well established pharmaceuticals for the treatment of serious life-threatening and chronic diseases such as cancer, rheumatoid arthritis and hepatitis [1].

In contrast to low molecular weight drugs, proteins exhibit a fragile, three-dimensional macromolecular structure and are much more susceptible to different chemical and physical degradation. Short half-lives further complicate the application of therapeutic proteins [4].

Therefore, the development of suitable protein formulations as well as the development of new strategies for protein delivery is a major challenge for R&D in pharmaceutical industry in order to overcome the restriction to frequent parenteral administration of pharmaceutical proteins [5].

Sustained delivery of protein drugs can reduce application frequency and systemic burden for patients. Several delivery systems, e.g. colloidal formulations (liposomes, microparticles etc.) and implants have been investigated in order to achieve a controlled and sustained release of protein drugs [6, 7]. As poly-lactid acid (PLA) and poly-lactic-co-glycolic acid (PLGA) implants and microparticles had already been approved by regulatory authorities, these synthetic polymers were employed first for developing protein depot formulations [8]. Peptides such as Leuprolide and Octreotide were successfully embedded and released from such systems, but protein delivery appeared more difficult and complex. Nutropin Depot[®] (recombinant human growth hormone, PLGA microparticles) has been the only protein depot formulation approved by the US Food and Drug Administration (FDA), but was withdrawn from the market in 2004. It was explained by manufacturing and commercializing issues according to Alkermers Inc. and Genentech Inc (press release). No implant or colloidal formulation for sustained delivery of a therapeutic protein is on the market today.

Another important reason for this situation is the lack of innovation in the area of pharmaceutical excipients. Global excipient research and development has faced challenges

in the regulatory and safety framework [9]. FDA does not allow for approval of a new excipient outside the dossier of a new drug approval (NDA) although the need for new excipients is obvious. For this reason, the International Pharmaceutical Excipient Council (IPEC) published guidelines on the development of novel excipients to support industry [10]. This effort led to the approval and monograph for Solutol[®] HS15 in 2010.

In academia, various innovative synthetic polymers and biomaterials have been employed for *in vitro* and *in vivo* delivery of protein drugs during the last decade [8, 11]. Therein, silk as a well-known material with unique mechanical properties gained increasing attention also for biomedical applications. Silk proteins including silk fibroin from *Bombyx mori* and spider silk proteins showed excellent biocompatibility, customizable properties and easy processing into various morphologies like scaffolds, films and spheres [12-16]. Silk fibroin has already been employed for the delivery of different kind of active ingredients including e.g. growth factors [12, 17]. However, silk fibroin from *Bombyx mori* is an entirely natural product. The quality of the protein can vary between species and individuals of the same species, and an elaborate degumming process has to be applied to remove Sericin from the natural product. Finally, quality control of this material is difficult with regard to regulatory approval [12].

The engineered spider silk protein eADF4(C16) was developed by Scheibel et al. [18, 19]. The protein sequence was adopted from the natural occurring spider silk protein ADF4 which is produced by the European garden spider *Araneus diadematus* for the use as dragline silk fiber. This spider silk protein can be produced in large quantities as a recombinant protein in *E. coli*. The manufacturing process is by now performed by AMSilk GmbH (Martinsried, Germany), which has been founded as a spin-off company from the group of Prof. Scheibel. Previous studies on the assembly process of the recombinant protein showed that smooth protein spheres with high β -sheet content are formed by an easy salting-out process avoiding organic solvents [20, 21]. The particle preparation process was further evaluated and drug loading and release were performed using eADF4(C16) submicron particles and low molecular weight drugs [22-24]. These studies revealed promising results regarding a controlled and sustained drug release.

Nevertheless, spider silk particles are especially of high interest for depot formulations of therapeutic proteins and for an application in the area of vaccination. Therefore, the focus of this thesis was on the evaluation of the recombinant spider silk protein eADF4(C16) as a new colloidal drug carrier for protein therapeutics.

1.2 DRUG DELIVERY SYSTEMS FOR THERAPEUTIC PROTEINS

Protein drugs usually have to be administered by subcutaneous injection or intravenous infusion due to their inherent instability in the gastrointestinal tract [5, 6]. As frequent applications are necessary because of short circulating half-lives of most proteins, Langer and Folkman introduced non-degradable polymers as matrix material for parenteral protein depots [25]. Since that time, numerous polymers have been evaluated for their suitability as matrix for protein depots [26]. Besides this early work on non-degradable polymers, biodegradable polymers are preferred from a patient perspective as no second medical intervention for implant removal is necessary. Thus, synthetic and natural biodegradable polymers have been developed and investigated as matrix-forming polymers for protein delivery. Selected biodegradable polymers are listed in Table 1.1.

Implants and microspheres made of polylactic acid (PLA) and polylactic-co-glycolic acid (PLGA) were approved by regulatory authorities for the delivery of small molecules and peptides. Due to their proven safety and biocompatibility record, polyesters are still the most frequent used class of polymers. Many therapeutic proteins were embedded into PLGA-based drug delivery systems (DDS) such as interferon- α [27] and erythropoietin [28, 29]. However, inherent shortcomings of the PLA/PLGA-systems were also observed. Both chemical (e.g. solvent evaporation/extraction) and physical preparation processes (e.g. spray drying) require the loading of an organic polymer solution with the protein drug due to the low solubility of PLGA in water. This was shown to be detrimental for protein stability as proteins tend to unfold and aggregate in hydrophobic environments and at interfaces [30]. Additionally, destructive conditions for proteins are generated within the polyester matrix during the time period of sustained drug release. The degradation products lactic and glycolic acid are trapped within the polymer matrix and create altered environmental conditions for the incorporated proteins, including a significant drop in pH and an increase of osmotic pressure [7, 31-34]. Despite all partially successful attempts to overcome these shortcomings, no formulation using polyesters for therapeutic protein delivery is on the market today.

Table 1.1. Selected biodegradable polymers used for delivery of protein drugs

Synthetic polymers	Natural polymers	
<i>Biodegradable</i>	<i>Polysaccharides</i>	<i>Proteins</i>
Polyesters: PLA, PLGA	Chitosan	Albumin
Polycarbonates	Alginate	Gelatin
Lipids		Silk

Besides the strategy to invent varieties of synthetic polymeric constructs, natural polymers represent promising materials for the use as DDS as well.

Among this group, polysaccharides like chitosan and alginate have been investigated in great depths. Chitosan, a biomaterial obtained by alkaline deacetylation of chitin, is regarded as non-toxic, biocompatible and biodegradable. It is water-soluble and positively charged at physiological conditions, which allows for interaction with negatively charged molecules and polyanions in an aqueous environment. However, the use of chitosan is so far limited by a rapid water absorption and a high swelling degree, leading to fast drug release from non-modified chitosan delivery systems [35-37].

Alginate is a polysaccharide isolated from brown seaweed and its sodium or calcium salts are also regarded as non-toxic and biocompatible. Divalent or multivalent metal ions (e.g. calcium ions) easily form gels or colloidal precipitates with alginate in aqueous media. A large number of proteins have been encapsulated in mainly alginate hydrogels for applications in tissue engineering [38-40].

However, there remains a need for biomaterials that fulfill the high requirements in terms of composition and sequence, structure, mechanical properties and function [12]. For the development and the optimization of such release systems, it is crucial to understand how drug release is controlled.

Detailed mechanistic studies on the release from non-degradable matrices revealed that protein release occurs via diffusion through a complex porous pathway within the inert matrix [41]. At first, water penetrates into the matrix and dissolves the water-soluble drug. Likewise, hydrophilic excipients are dissolved and a porous microstructure is created. The subsequent leaching out of the drug and excipients further alters the matrix morphology. Randomly distributed pores and channels are formed, enabling the diffusion of the protein into the bulk fluid. However, this tortuosity of the porous structure cannot fully explain why proteins are released in such a sustained manner. Thus, Siegel and Langer suggested that, besides tortuosity, the connection of the pores through narrow channels contributes to the retardation of protein release [42]. The protein performs a random walk and will therefore need a certain time until it reaches the next pore. In addition, release kinetics depends on the drug loading and particle size of the incorporated drug. Higher drug loading enables a complete protein release due to a fully interconnected network, and large particle size results in a faster release of the protein.

The release from degradable polymer matrices is a more complicated process governed by diffusion through a water-filled pore network, degradation of the polymer and possible swelling of the polymer matrix. In the majority of cases, a combination of all three processes was observed [8, 109]. Protein release from PLGA microspheres shows a pulsatile liberation profile. A burst release of surface located and poorly encapsulated protein is followed by a

phase of lower release rates controlled by diffusion. Finally, increased release occurs due to starting polymer degradation [43].

To address all these requirements of a suitable DDS, proteins were also broadly explored as matrix materials for controlled drug delivery. Therein, silk proteins have gained more and more interest over the last few years.

1.3 PROTEIN-BASED DRUG DELIVERY SYSTEMS

Drug delivery systems composed of proteinaceous materials, e.g. albumin, gelatin and silk, benefit from their compatibility with biological systems and have served as alternative biomaterial to synthetic polyesters [44]. Especially solid protein particles have been in focus because particulate DDS offer the possibilities of systematic drug delivery via different administration routes and prevention of non-specific biodistribution. They can be applied for new imaging techniques and targeting of specific tissue dependent on their physico-chemical properties and particle size. However, safety concerns like folding pattern-derived or sequence derived immunogenicity as well as contamination with transmissible diseases are often associated with protein-based materials [45]. For this reason, careful choice of the source of the natural material is necessary and even better, recombinant material should be used wherever possible. Recombinant proteins are in the meantime available for the most important representatives such as albumin, gelatin and silk.

1.3.1 PREPARATION TECHNIQUES FOR PROTEIN PARTICLES AS DRUG CARRIERS

Several distinct methods have been developed for the preparation of solid particles in a particle size range from micrometers down to approx. 100 nm. It should be mentioned that each method needs to be optimized for entrapment of a drug of interest at high efficiency and retention of its pharmacologic activity [44]. With regard to protein therapeutics, the latter necessity is one of the major challenges.

1.3.1.1 EMULSION / SOLVENT EXTRACTION

The emulsion / solvent extraction technique, which is the most employed procedure for particles made of polyesters, requires a primary emulsion of the aqueous protein solution in an organic solution of the polymer and is therefore known to be critical for protein stability [46, 47]. However, further development of the process towards a W/O/W double-emulsion method enabled the encapsulation of hydrophilic drugs and proteins [28, 29, 48].

Solvent extraction processes for the preparation of proteinaceous drug carriers are adapted from the emulsion technique applied for synthetic polymers. In brief, the protein is dissolved in an aqueous buffer and a W/O emulsion is created by the addition of a non-solvent. After removal of both solvents, solid protein particles are obtained. However, this methods lacks from comparatively large particle sizes as reported for BSA (100 to 800 nm) in dependence of protein concentration and relative W/O volume ratio [49].

With regard to protein-based materials, other preparation methods are more common which will be described in section 1.3.1.2 and 1.3.1.3.

1.3.1.2 COACERVATION – NON-SOLVENT

The coacervation/desolvation process was the most frequently applied method in the last decade for the preparation of protein-based nanoparticles due to comparatively mild process conditions. In brief, the protein matrix is dissolved in a solvent (e.g. aqueous buffer) and subsequently extracted into a non-solvent phase (e.g. ethanol). By phase separation, a phase with a colloidal component / coacervate and a second phase with a solvent / non-solvent mixture are formed [44, 50]. Consequently, solvent and non-solvent have to be miscible in order to be able to form the second phase (e.g. ethanol/water or acetone/water). A stable particle size is reached after an initial process period so that further desolvation (addition of non-solvent) solely leads to an increased particle yield. As the coacervation process is faster and more efficient at conditions of zero net charge (isoelectric point of the protein), the pH of the protein solution is of major importance and can be adjusted towards the desired conditions regarding particle size and process yield.

The described process was performed with several proteins such as human serum albumin (HAS) [50-52], bovine serum albumin (BSA) [44], gelatin [53] and β -lactoglobulin [54]. However, all protein nanoparticles had to be stabilized by cross-linking of the prime NH_2 -groups using chemical cross-linkers. Glutaraldehyde was widely employed without negative side effects [50], but as carcinogenic properties of free glutaraldehyde cause regulatory issues, new approaches have to be developed to overcome this critical process limitation.

1.3.1.3 COACERVATION – SALT PRECIPITATION

A simple approach for preparation of protein-based nanoparticles is the salting out of a protein solution to form protein coacervates. Since only aqueous solutions are necessary, this approach seems to be very interesting for DDS employing sensitive therapeutic proteins. Furthermore, certain therapeutic proteins may be directly transformed into particles without a loss of biological activity. This was described e.g. for insulin by exposing the protein solution to high sodium chloride concentrations ($> 0.5 \text{ M}$) at low pH (< 2.0) in order to obtain insulin nanoparticles [55]. The simple technique is also of interest for protein particles acting as drug carriers only (e.g. HSA or silk), because large amount of particles can be easily and continuously produced. However, higher heterogeneity in particle sizes was reported as process parameters may be more difficult to control [44].

1.3.2 ALBUMIN

The most prominent protein used as particulate drug carrier is the blood transporter protein albumin, namely human serum albumin (HSA) or in certain cases for research purposes bovine serum albumin (BSA). HSA had been intensively investigated as drug carrier for several active drug molecules and even successfully entered the market. Two albumin-based formulations were approved for use in humans: Alburnex™ as ultrasound contrast agent and Abraxane™ as a carrier of anticancer drug paclitaxel for treating metastatic breast cancer [56, 57]. However, both formulations do not represent a particulate formulation where the colloidal system comprises solid discrete and uniformly shaped spheres.

Alburnex™ is an ultrasound contrast agent consisting of a slowly diffusing gas C3F6 which is encapsulated by an elastic HSA shell [58]. Thereby, this formulation can be classified as a microbubble formulation with a mean diameter of approx. 4 µm (95% < 10 µm) and an average shell thickness of 30 to 50 nm [59].

Abraxane™ is a self-assembling nanoagglomerate of HSA and paclitaxel which is produced by high pressure homogenization [60]. The particle size of the formulation was determined to be about 130 nm. This drug product was designed for therapy against metastatic breast cancer [61], but was meanwhile evaluated for other anti-cancer treatments such as non-small cell cancer, ovarian cancer and pancreas cancer [62, 63].

In research, albumin nanoparticles were applied for lots of *in vitro* and *in vivo* studies [64]. As albumin exhibits a high binding capacity due to multiple drug binding sites present in the albumin molecule, electrostatic adsorption of positively (e.g. Ganciclovir) and negatively charged (e.g. oligonucleotides) molecules is possible [63]. Furthermore, targeted delivery of anticancer drugs can be achieved because of the presence of albumin-binding proteins such as membrane associated gp60 (albonin) [57]. Albumin-ligand combinations on the nanoparticle's surface can be used for modifying pharmacokinetic parameters (e.g. polysorbate 80 [65]), enhancing the colloidal stability by cationic polymers [66], prolonging the circulation half-life (e.g. coating with PEG [64]), slowing down drug release and specific targeting (e.g. monoclonal antibodies [67]).

1.3.3 GELATIN

Gelatin is a natural polymer derived from animal collagen by acidic (type A) or alkaline (type B) degradation. Collagen itself exhibits high stability due to the unique triple-helix structure consisting of three polypeptide α -chains. Only collagen types I-III are used for the production of gelatin [68]. Gelatin type A is obtained from porcine skin with acidic pretreatment before the extraction process, whereas gelatin type B is derived from ossein and cut hide split from bovine origin. Due to the different preparation processes, both gelatin

types exhibit different isoelectric points (9.0 for type A vs. 5.0 for type B) [69]. Gelatin is classified as 'generally regarded as safe' (GRAS) by the FDA and is known to be biocompatible and biodegradable without toxic degradation products [69, 70]. Moreover, intravenous application of gelatin derivatives as plasma expanders is approved for human use.

The preparation of gelatin nanoparticles using a two-step desolvation method and subsequent chemical cross-linking by glutaraldehyde was introduced by Coester et al. [53]. These nanoparticles exhibited higher storage stability than liposomal liquid formulations and maintained their non-toxic properties throughout the preparation process. Furthermore, good *in vivo* stability upon administration was shown [71]. Even though no undesired effects were associated with chemically cross-linked gelatin particles, an alternative to glutaraldehyde was evaluated [72]. Efficient cross-linking by microbial transglutaminase was demonstrated and particle sizes, size distributions and storage stability were comparable to chemically cross-linked particles so that glutaraldehyde could be substituted in order to ease future clinical trials in humans. Nevertheless, immunogenicity of animal-derived gelatin is still an issue. Therefore, animal-derived gelatin can be replaced by recombinant human gelatin [73].

Similar to albumin, drug delivery applications of gelatin particles covered a wide range throughout the last decade and are reviewed elsewhere [69, 74]. Typical applications like the delivery of anticancer drugs like paclitaxel [75] and further small molecular weight drugs such as chloroquine [76] were investigated. Matrix loading of gelatin particles was shown to improve drug load and delivery [77]. However, gelatin nanoparticles were in particular successfully evaluated as drug carrier for oligonucleotides [78-80]. *In vivo*, immunization with RNA-loaded gelatin nanoparticles led to an increased and efficient antitumoral immune response. Moreover, formulation development regarding freeze-drying of oligonucleotide-loaded gelatin nanoparticles was performed to provide stable and high concentrated formulations [81]. Klier and Fuchs et al. optimized, transferred and successfully implemented this drug delivery platform as the first colloidal nanocarrier-mediated immunotherapy in food-producing animals [82, 83]. Treatment with nebulized CpG-loaded gelatin nanoparticles resulted in partial remission of the allergic condition.

1.3.4 SILK

A rather new material of natural origin used for drug delivery applications are silk proteins. Silk is an ancient material since silk fibers from the mulberry silkworm *Bombyx mori* have been used to produce textiles for thousands of years. The material is known for its attractive luster along with light weight and tear resistance. These extraordinary material characteristics were also responsible for attracting the attention of biomedical research. Silks and especially spider silks combine impressive mechanical stability (see Table 1.2) with

biocompatibility and biodegradability and allow various side chain modifications for functionalization [84]. Silks are produced by about 34,000 known spider species (class *Arachnida*), most of the 113,000 species of the insect order Lepidoptera (including moths and butterflies) and other members of several orders in phylum of arthropods [85]. Among all these different silks, the most intensively investigated and characterized ones are the cocoon silk from the domesticated silkworm *Bombyx mori* and spider silk proteins from two spider species, namely *Nephila clavipes* (golden orb-web spider) and *Araneus diadematus* (European garden cross spider) [86-88]. Silk is a very evolutionary specialized material with outstanding mechanical properties which can be indispensable to the life of animals due to the necessity of silk for prey capture and reproductive success [89].

Table 1.2. Mechanical properties of spider silk fibers and other materials [84]

Material	Stiffness E_{init} (GPa)	Strength G_{max} (GPa)	Extensibility ϵ_{max}	Toughness (MJ*m ⁻³)
<i>Araneus</i> MA silk	10	1.1	0.27	160
<i>Araneus</i> viscid silk	0.003	0.5	2.7	150
<i>Bombyx mori</i> silk	/	0.6	0.18	70
Tendon collagen	1.5	0.15	0.12	7.5
Bone	20	0.16	0.03	4
Wool	0.5	0.2	0.5	60
Elastin	0.001	0.002	1.5	2
Synthetic rubber	0.001	0.05	8.5	100
Nylon fiber	5	0.95	0.18	80
Kevlar 49 fiber	130	3.6	0.027	50
Carbon fiber	300	4	0.013	25
High-tensile steel	200	1.5	0.008	6

1.3.4.1 STRUCTURE AND PROPERTIES OF SILK PROTEINS

Generally, silk fibers have a core shell type structure and are typically composite materials formed of silk protein(s) and other associated molecules such as glycoproteins and lipids [90]. Silk proteins from arthropods are extremely large proteins with molecular weights ranging from 70 to 700 kDa [91]. The proteins are usually produced in epithelial cells, followed by the secretion into the lumen of specialized glands where the silk proteins are stored prior to the spinning process [85].

Despite the variability in primary sequences, all silk proteins show a well-defined organization (see Figure 1.1). The central and by far the largest part of silk fibroin (*Bombyx mori*) is

composed of a repetitive hydrophobic motif (green) and more complex hydrophilic spacers (dark blue) of variable but smaller size. In contrast, the N- and C-terminal sequences (purple and red) are non-repetitive, more hydrophilic and have a more heterogeneous amino acid sequence [92]. Deduced from the characteristic primary structure, silk proteins exhibit a predominantly hydrophobic nature. On this account, silk fibers can resist swelling and dissolution and are insoluble in most solvents, including water, dilute acid and alkali.

Investigations on the composition of silk fibroin from *Bombyx mori* revealed a complex of three proteinaceous components. The heavy-chain fibroin (392 kDa) and light-chain fibroin (26 kDa) are linked by a disulfide bond. The third component is a glycoprotein called P25 which has a molecular weight of about 30 kDa [93, 94]. The core sequence of the heavy chain comprises hydrophobic core repeats with alanine, glycine and serine residues. These core repeats dominate the hydrophobic silk properties.

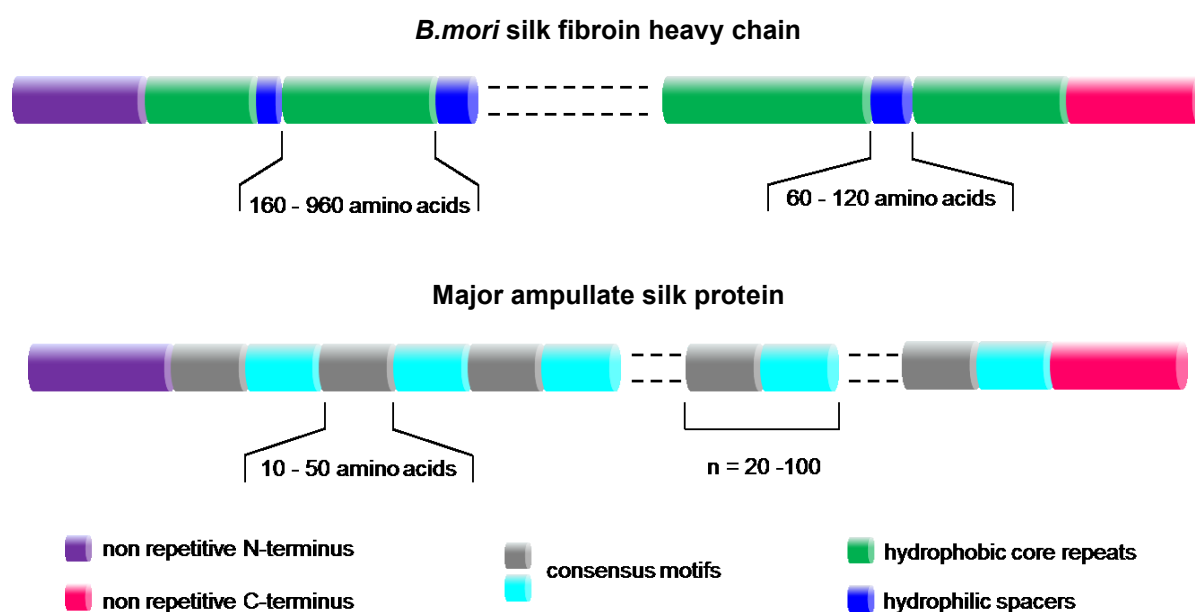


Figure 1.1. Model of primary structures of silk proteins

Major ampullate (MA) silk fibers are composed of two silk proteins which differ in their hydrophobicity [95], e.g. ADF-3 (hydrophilic) and ADF-4 (hydrophobic) in the case of dragline silk produced by the spider *Araneus diadematus* [96]. A major ampullate silk protein is characterized by the repetition of a low complexity consensus motif (grey and blue) wherein the hydrophilic component is already included [18]. The presence of higher contents of charged amino acid residues such as glutamic acid and arginine is another significant difference to *Bombyx mori* silk.

Regarding the different mechanical properties of different silks, structure-function relationships were determined as listed in Table 1.3.

In *Bombyx mori* cocoon silk, the repetitive core motif is GAGAX (where X = A, S, V or T) and is known to be the building block for β -sheet crystals. The non-repetitive, more hydrophilic regions act as spacers between the hydrophobic blocks and may adopt a loop structure, facilitating an anti-parallel β -sheet formation [92, 97-99].

In major ampullate spider silk proteins, polyalanine motifs $(GA)_n / (A)_n$ adopt the crystalline β -sheet structures in assembled fibers. β -sheet stacks and their crystalline characteristics result in a high-tensile strength [100, 101]. Glycine-rich motifs GPGQQ or GGX form β -turn and 3_{10} -helices which connect the crystalline β -sheets. These structures introduce elasticity and flexibility in spider silk fibers [18, 102]. The remarkable combination of strength and extensibility results in toughness greater than that of any other known high performance fibrous material (see Table 1.2) [103]. The central repetitive region is terminated at both ends by non-repetitive (NR) domains, which were found to adopt a mainly helical conformation. Both NR-domains are not influencing mechanical properties, but the C-terminal domain is strongly involved in the protein assembly process [104] and the N-terminal domain is an important signal sequence [105].

Table 1.3. Typical amino acid motifs of *Bombyx mori* cocoon silk and major ampullate silk proteins correlated with their putative structure

Origin	Motif	Putative structure	Property
<i>Bombyx mori</i> cocoon silk	GAGAGS	β -sheet	crystalline
	GAGAGY		
	spacer	random coil	amorphous
	GAAS	β -turn	elastic
Major ampullate spider silk	$(GA)_n / A_n$	β -sheet	crystalline
	GPGQQ	β -turn	elastic
	GGX	3_{10} -helix	amorphous
	NR _N -domain		
	NR _C -domain	α -helical	assembly process

1.3.4.2 NATURAL ASSEMBLY PROCESS

In nature, spiders possess the ability to control, adjust, and rapidly fine-tune silk protein composition, fiber diameter and drawing rate, all leading to silks with highly 'tuned' mechanical properties. Up to date, the highly complex natural spinning process cannot be entirely mimicked *in vitro* [106]. For this reason, several studies were performed in order to clarify the detailed mechanism of the silk fiber formation process [21, 98, 107]. A detailed review on the natural self-assembly process is given by Heim et al. [108].

In brief, silk fibers are formed on demand in the spinning duct by a complex liquid-solid phase transition process which is accompanied by structural changes to form a stable fiber. The phase transition is triggered by several biochemical and physical factors involving slight acidification from pH 7.2 to 6.3, ion exchange of more chaotropic (e.g. Na⁺) to more kosmotropic (e.g. K⁺) ions and water removal. In combination with an elongational flow and shear forces, the unique structure of a spider silk fiber is formed. Once silk proteins have been spun into fibers, extreme conditions such as high salt concentrations or strong acids are required to facilitate resolving of the assembled silk proteins [109]. Interestingly, protein solutions having concentrations of up to 50% are stored in the glands without premature protein aggregation prior to the spinning process. The prevention of aggregation is most likely based on their almost completely random coiled structure [110, 111]. Furthermore, a high concentration of sodium chloride is assumed to stabilize the one-phase solution and to inhibit a premature phase-separation and oligomerisation of silk proteins [96, 112].

Two theories on the molecular mechanism of the silk fiber assembly have been proposed [98, 113]. The first one assumes a liquid crystalline state to be the basis for the formation of intermolecular interactions. This liquid crystalline behavior is a result of the alignment of protein molecules and the increased protein concentration [113]. The second theory describes an assembly into small micelles due to the amphiphilic character of silk proteins. A multitude of these micelles form larger globules and shear stress finally forces these globules into an elongated shape, leading to fiber formation [98].

1.3.4.3 IMMUNOGENICITY AND BIODEGRADATION OF SILK PROTEINS

Silk fibers from *Bombyx mori* have been used as surgical sutures for decades. Besides this proven efficacy, some biological responses to silk proteins have raised questions about its biocompatibility. In contrast to spider silks, core fibers from *Bombyx mori* are encased in a sericin coat. Sericin proteins are a family of glue-like proteins which hold two fibroins together to form the composite fiber of the cocoon case [13]. On this account, silkworm silk is subjected to a degumming procedure and purification steps to almost entirely remove sericin [93]. The core fibroin without sericin appeared to be comparable to other biomaterials when used as suture material [13].

Santin et al. investigated the inflammatory potential of silk membranes [114]. In comparison to polystyrene and poly(2-hydroxyethyl)methacrylat, silk membranes elicited a lower macrophage activation. Panilaitis et al. analyzed native silk fibers and sericin-free silk in an *in vitro* macrophage assay [115]. Only the sericin comprising silk fibroin represented a potential stimulus, whereas sericin-free silk induced neither macrophage activation nor pro-inflammatory cytokines transcription. Likewise, inflammatory responses *in vitro* and *in vivo* were determined to be more conspicuous around collagen and PLA films when compared to

silk fibroin films casted from hexafluoroisopropanol solutions seeded with bone-marrow derived mesenchymal stem cells [116].

It is self-evident that silk proteins are susceptible to proteolytic degradation. However, silk fibers as mechanically robust material showed only long-term degradation characteristics [13, 117]. The *in vivo* degradation of three-dimensional scaffolds made of *Bombyx mori* silk in rats strongly depended on the preparation method (aqueous or hexafluoroisopropanol) and structural characteristics. Therefore, biodegradation could be predicted and controlled to match different needs. All scaffolds investigated were well tolerated and immune responses to silk implants were mild [118]. Native spider silk was shown to combine biodegradability and immunotolerance that equals other commonly used implantable polymers [14]. Further *in vivo* studies also found no evidence for any immunological response to native spider silks [119]. *In vivo* biocompatibility and biodegradation behavior of non-wovens made of the recombinant spider silk protein eADF4(C16) were performed by AMSilk and did not reveal any immunologic responses to the biomaterial (oral communication).

1.3.4.4 SILKWORM SILK FOR DRUG DELIVERY

Due to the described mechanical and non-immunogenic properties, silk fibroin provides an interesting material for an application as surgical threads, biomaterial for tissue engineering and drug delivery system [120]. This section focuses on the latter and describes the published studies on silkworm silk in the field of drug delivery. Tissue engineering and other applications are reviewed elsewhere [121-126]. Silk protein scaffolds are able to support *in vitro* cell adhesion, proliferation and differentiation, and are mainly used in stem-cell based tissue engineering for bone and nerve regeneration.

Drugs that have been employed in delivery systems made of silk fibroin are summarized in Table 1.4. Drug release was controlled by both the characteristics of the incorporated drug and the used polymer matrix. The silk protein matrix is *in vitro* considered as a non-degradable material with regard to release mechanisms, whereby attention should be paid to the swelling of the system. *In vivo*, the matrix is degraded by proteases over a long time period (> 60 days). However, it is assumed that due to the very slow degradation process this will not have a pronounced influence on the release profile of incorporated drugs.

Silk fibroin provides an interesting new coating material. It has been investigated as a potential aqueous film coating agent for solid pharmaceuticals. Theophylline tablets were coated with a silk fibroin solution mixed with polyethylene glycol as plasticizer [127]. A sustained drug release following zero-order kinetics was achieved. Silk coating was further applied to emodin-loaded liposomes [128]. The overall efficacy to breast cancer cells was enhanced due to increased retention of emodin in the cell and protection against fast release

and metabolism. This was achieved by a reduced swelling behavior of silk coated liposomes. Wang et al. coated PLGA and alginate microspheres with silk protein by layer-by-layer assembly technology and investigated the release of encapsulated protein model drugs horseradish peroxidase (HRP) and BSA [129]. A significantly retarded protein release was obtained which could be further enforced by methanol treatment of the silk coating.

Table 1.4. Applications of *Bombyx mori* silk in the field of drug delivery

Silk fibroin coatings and silk films		
Topic	Drug	Reference
Dip coating of theophylline tablets	Theophylline	Bayraktar et al. [127]
Silk coated emodin-loaded liposomes	Emodin	Gobin et al. [128]
PLGA and alginate microspheres coated with silk fibroin	HRP TMR-BSA	Wang et al. [129]
Nanoscale layered coatings on quartz slides	Rhodamine B Evans Blue Azoalbumin	Wang et al. [130]
Silk coatings on tissue culture plates and metallic stents to modulate vascular cell responses	Paclitaxel Clopidogrel Heparin	Wang et al. [131]
Sustained adenosine release in rats	Adenosine	Szybala et al. [132]
Silk coating of solid powder reservoirs for sustained release of adenosine	Adenosine	Pritchard et al. [133]
Release of macromolecules in dependence of crystallinity of the silk films	Dextrans HRP Lysozyme	Hofmann et al. [134]
Silk fibroin/gelatin multilayered films for controlled drug release	Trypan blue FITC-inulin FITC-BSA	Mandal et al. [135]
Release of HRP from silk fibroin films	HRP	Lu et al. [136]
NGF-loaded silk fibroin nerve conduits for peripheral nerve repair	NGF	Uebersax et al. [137]
Silk films for enhanced thermostability of both antibiotics and vaccines	Tetracycline MMR vaccine	Zhang et al. [138]
Silk fibroin particles		
Topic	Drug	Reference
Microspheres using lipid vesicles as templates	HRP	Wang et al. [139]
Growth factor delivery by silk microspheres incorporated into alginate scaffolds	rhBMP-2 rhIGF-I	Wang et al. [140]
Preparation method using silk/PVA blend films and <i>in vitro</i> release evaluation for silk nano- and microspheres	TMR-BSA TMR-Dextran Rhodamine B	Wang et al. [141]
Preparation by vibrational splitting of laminar jet and <i>in vitro</i> drug release studies	Salicylic acid Propranolol IGF-I	Wenk et al. [17]
Silk fibroin microparticles prepared by ethanol addition and drug release of rhBMPs	rhBMPs	Bessa et al. [142]
Preparation by salting out and <i>in vitro</i> release of compounds dependent on the secondary structure	Alcian blue Rhodamine B Crystal violet	Lammel et al. [143]
Silk fibroin-albumin blended nanoparticles	Methotrexate	Subia et al. [144]

The mechanically stable shells stabilized the microspheres and provided an effective diffusion barrier. A multi-layered structure was created by a stepwise deposition of silk fibroin and model drugs by dip-coating on quartz slides as substrate [130]. Higher crystallinity and a thicker silk capping layer suppressed the initial burst and prolonged the duration of release. This multi-layered matrix was shown to be an effective system for drug-eluting coatings, such as for metallic stents when heparin or clopidogrel were incorporated [131]. Several studies were performed in order to evaluate the use of silk fibroin for controlled release of adenosine [132, 133]. Szybala et al. used implants comprising silk microspheres and silk films to release 1000 ng adenosine per day in kindled rats. At least partial anti-epileptogenic effects were observed [132]. Solid adenosine powder reservoirs were coated with silk fibroin to achieve local, sustained and controlled adenosine release from degradable implants. Eight layers of 8% [w/V] silk resulted in a linear and sustained release over 14 days [133].

With regard to silk films and particles, the structure and crystallinity of the silk matrix was shown to be crucial for drug release. The polymer matrix was modified by increasing the employed silk protein concentration, resulting in lower burst and total release rates [17]. Another strong influence on the release profile was observed when the crystallinity of the silk matrix was altered [134, 139]. An increased β -sheet structure led to a strong and molecular weight dependent retardation of the release of FITC-dextran [134]. Silk microparticles were either treated with methanol or sodium chloride in order to induce β -sheet formation by Wang et al. [139]. Methanol was more efficient and caused lower release of HRP compared to sodium chloride treated microparticles. HRP was released in its native and bioactive form, whereas the same post-treatment had a detrimental effect on lysozyme and led to a total loss of activity [134]. Using also HRP as model protein, Lu et al. stated that the loaded protein drugs are present in silk films in at least two states, untrapped and trapped [136]. The ratio and stability of both states depended on the interactions between the enzyme and silk fibroin. Untrapped enzyme was responsible for the burst release, whereas trapped HRP could only be released following very slow dissolution or proteolytic degradation. The entrapment occurred due to physical entrapment as well as hydrophilic and/or hydrophobic interactions. Due to different film treatments, the content of untrapped HRP was decreased to almost 0% [136]. A multilayer system made of silk fibroin/gelatin blend was successfully employed for controlled drug release of different model compounds [135]. The release was shown to be dependent on multilayer film degradation rate rather than on the molar mass of the drug molecules. For this reason, modification of the release rate could be achieved by selective change of the formulation. Controlled release of nerve growth factor (NGF) over 3 weeks was obtained from silk fibroin nerve conduits [137]. The matrices were easily prepared by drying (air-dried or freeze-drying) in suitable molds. The potency of released NGF was retained within all formulations. A different approach was evaluated by Zhang et

al. [138]. Silk film systems were used as an effective carrier material to enhance thermostability of both antibiotics and vaccines, aiming for eliminating the cold chain. Increased stability of the susceptible formulations during storage at higher temperature was achieved by reducing residual moisture.

With regard to the active ingredient, the molecular weight was shown to significantly influence the release kinetics as presented for dextrans with different molar masses [134]. Furthermore, the interaction of the drug with the silk matrix is critical. Wenk et al. demonstrated that propranolol ($pK_a = 9.5$) has a slower release rate compared to salicylic acid ($pK_a = 3.0$), which can be attributed to the opposite interaction forces with the negatively charged silk matrix ($pK_a = 4.2$) [17]. Additionally, dissimilar hydrophobic interactions contributed to the observed release kinetics in this study.

Silk fibroin can also be processed into spheres as a platform for controlled drug delivery. Water-insoluble microspheres were prepared by using the synthetic phospholipid derivate 1,2-Dioleoyl-sn-glycero-3-phosphocholine (DOPC). Silk protein and a model protein drug (HRP) were encapsulated in multilamellar phospholipid vesicles [139]. Smaller unilamellar vesicles were generated by freezing and thawing steps. After lyophilization, the addition of methanol or sodium chloride solutions removed the DOPC, induced β -sheet formation and simultaneously entrapped the protein drug in the silk protein matrix. Silk fibroin was further used as matrix for microsphere-mediated growth factor delivery in polymeric scaffolds for osteochondral tissue engineering [140]. Silk microspheres were more efficient in the delivery of recombinant human bone morphogenetic protein 2 (rhBMP-2) than recombinant human insulin-like growth factor I (rhIGF-I), which was attributed to the different properties of both growth factors. After a release period of 14 days, 70% of rhIGF-I was released whereas only 15% released rhBMP-2 was determined. Wang et al. developed a three-step preparation method for silk nano- and microspheres from silk/PVA blend films [141]. Spherical as well as spindle-shaped particles were obtained. As a proof of concept, tetramethylrhodamine-BSA (TMR-BSA), TMR-Dextran and Rhodamine B were encapsulated. The loading efficiency was 94.5% for RhB, 51.2% for TMR-BSA and 1.2% for TMR-Dextran. The determined high release rate for TMR-Dextran and lower release rates for TMR-BSA and Rhodamine B indicated that the interaction between silk and the encapsulated drug controlled the release rather than diffusion processes. Silk fibroin microparticles were further employed as carrier for the delivery of BMP-2, BMP-9 and BMP-14 [142]. Particles were prepared by addition of an anti-solvent (ethanol). A two-phasic release profile was observed which consisted of a burst release in the first two days followed by a slower release for a period of 14 days. Higher loading resulted in lower release rates. Silk fibroin particles prepared by a simple salting out process using potassium phosphate were presented by Lammel et al. [143]. Loading of small model drugs was achieved by simple absorption and diffusion into the particle matrix in an

incubation step after particle preparation based on electrostatic interactions. *In vitro* release of these compounds revealed a dependency on the drug-specific interaction with the silk matrix (positively charged molecules – more prolonged release) as well as on the crystallinity (secondary structure) of the particles. Silk fibroin-albumin nanoparticles were prepared by a desolvation method without surfactant [144]. Loaded with methotrexate, those particles showed promising results regarding drug release (85% of methotrexate was released within the first 12 days), internalization by cells, viability and biocompatibility.

1.4 SPIDER SILK PROTEINS

Spider silks gained an increasing interest in the group of silk proteins because of their extraordinary mechanical properties by which they are able to outperform every other natural or synthetic material (see Table 1.2). Therefore, applications of spider silks are conceivable in a multitude of different ways ranging from body armor or cosmetics to pharmaceutical and biomedical applications.

However, spider silk materials were not commercialized due to a number of challenges. The major issue was to overcome the limitations of a biomaterial being only available from natural origin at very low amounts compared to e.g. silkworm silk [13]. The group of Prof. Scheibel solved this problem by developing a recombinant production process that is able to produce spider silk-like proteins at high yields and sufficiently high amounts (at least at kilogram scale). This process enabled the broad use of spider silk proteins for the variety of the abovementioned applications.

1.4.1 DEVELOPMENT OF RECOMBINANT SPIDER SILK PROTEINS

1.4.1.1 TYPES OF SPIDER SILK PROTEINS

Spiders evolved the ability to produce a variety of task-specific silks which exhibit surprisingly different mechanical properties. Spiders use their silks for many different purposes compared to insects. Figure 1.2 shows the seven different silks *Araneus diadematus* is able to produce.

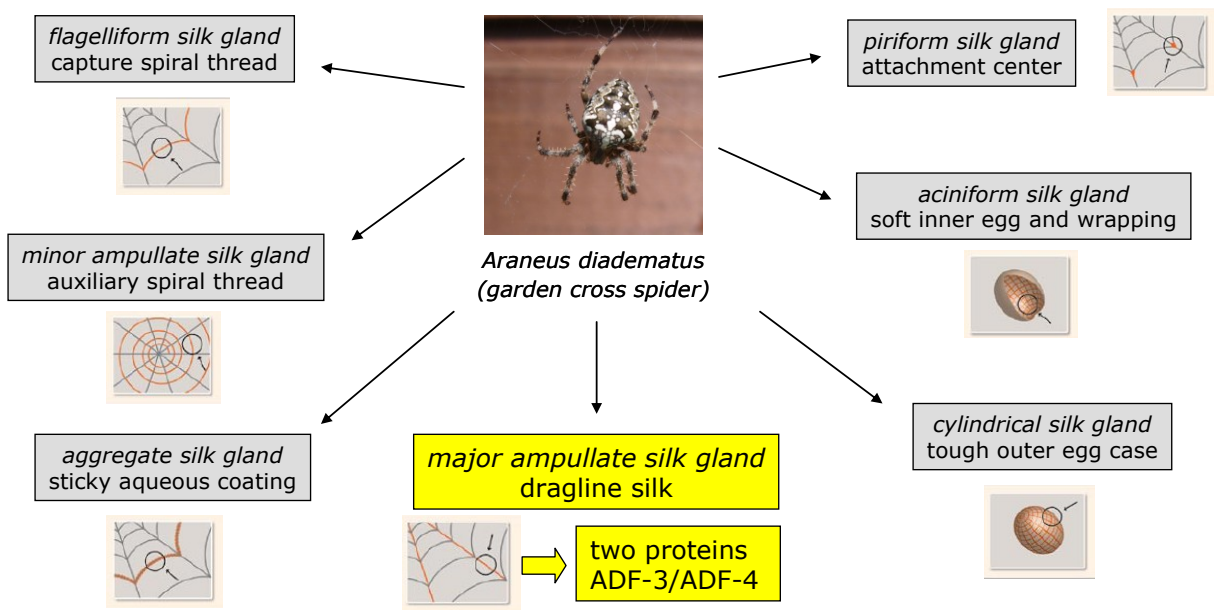


Figure 1.2. Different types of silk produced by the European garden cross spider *Araneus diadematus*. The yellow box highlights the dragline silk consisting of two proteins, namely ADF3 and ADF4.

The dragline and flagelliform silk are the two most interesting silks. The major ampullate glands produce the dragline silk that is utilized for radial threads and spider safety lines. These silk fibers are between 1 and 20 μm in diameter and exhibit very high tensile strength combined with moderate elasticity [100]. Major ampullate silks are composed of two types of silk protein. In the case of *Araneus diadematus*, these proteins are abbreviated as ADF3 and ADF4. All pairs of dragline silk proteins even from different spider species share a common repetitive architecture [95, 97] and additionally display a distinct distribution in hydrophobicity and charge (see section 1.3.4.1) [145].

In contrast to structural silks, flagelliform silks are used for capturing prey where the silk fiber has to withstand the impact energy of flying insects. Consequently, mechanical properties have to be different from dragline silks. As depicted in Table 1.2, elasticity is nearly 9-fold higher. Flagelliform silks consist only of a single protein whose primary sequence is composed of large amounts of proline and valine and reduced alanine content [93].

1.4.1.2 ENGINEERED SPIDER SILK PROTEINS

As mentioned previously, harvesting of spider silk from spiders would not allow for the intended applications of this biomaterial. Therefore, large amounts of spider silk proteins can only be obtained by recombinant production processes as established for other therapeutic proteins. However, spider silk gene sequences comprise some difficulties and limitations concerning recombinant protein production. The highly repetitive nature and length of the gene sequences (over 9,000 base pairs), the large molecular weight and specific codon usage of spiders inhibited a successful expression of full length spider silk clones up to now [18, 146, 147]. The well-known and comparatively cheap host system *E. coli* was not suitable to maintain such highly repetitive protein sequences due to genetic deletions and termination errors during protein synthesis. Thus, other host systems like insect cell lines were studied, but even though these approaches were not successful [120, 146].

Alongside the purpose to create native spider silk proteins, the group of Prof. Scheibel focused on the development of engineered synthetic spider DNA. Finally, they succeeded in producing high yields of spider silk-like proteins in a cheap host system (*E. coli*) [18]. In brief, Huemmerich et al. chose the dragline silk from *Araneus diadematus* as natural model [19]. Single conserved oligonucleotides were engineered and synthesized which encode for the consensus motifs of the original protein (see Figure 1.3). Furthermore, codons of the host system were adapted. Using a seamless cloning strategy, these oligonucleotides were replicated to generate longer silk-encoding gene sequences and finally, authentic non-repetitive regions were linked to the synthetic gene sequence.

ADF3 and ADF4 were used as templates [19]. Only one conserved module C was necessary for the construction of the engineered *Araneus diadematus* fibroin 4 (eADF4). This

engineered eADF4 protein consists of 16 identical modules C as shown in Figure 1.3 and is therefore also called C16.

The recombinant spider silk proteins contain one third fewer polyalanine motifs compared to their natural models. But altogether, these proteins closely resemble the authentic silk proteins and can be produced at high yields and purities in an established bacterial expression system, thereby enabling cost-efficient large scale production [18]. Furthermore, spider silks produced by recombinant techniques offer the possibility to modify gene sequences and to create proteins with specialized characteristics. This was already shown for genetically engineered silkworm silk [148]. Genetic engineering can also lead to a novel family of fusion (= chimeric) proteins which then exhibit tailored properties. The new options for processing and control of material properties may result in important benefits for biomedical applications [149].

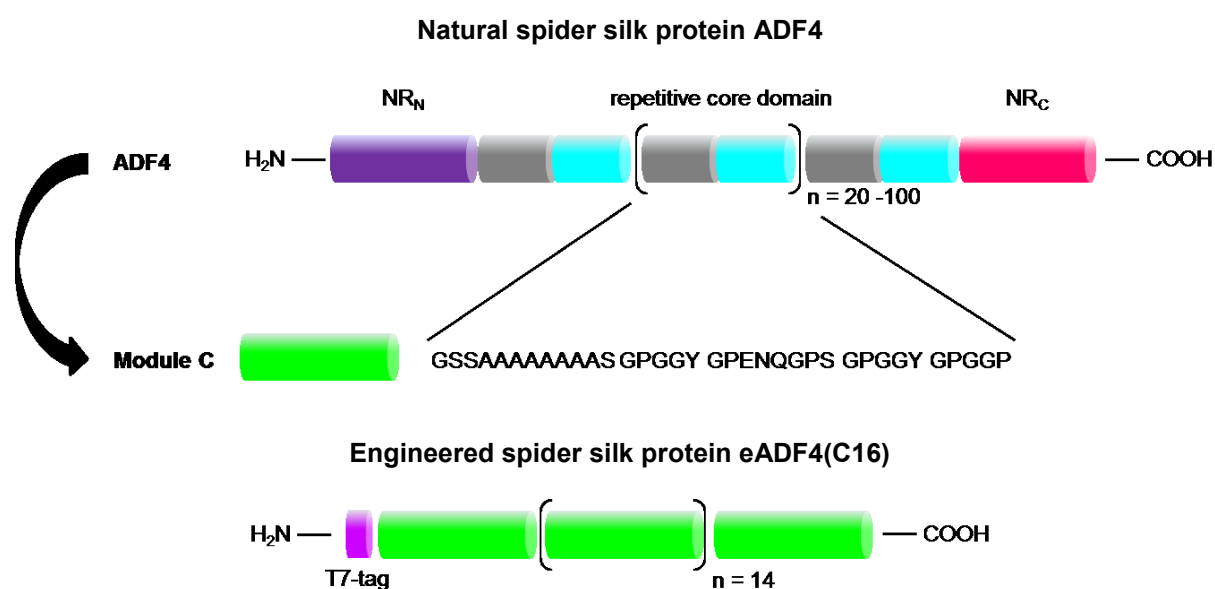


Figure 1.3. Development and structure of the engineered spider silk protein eADF4(C16)

1.4.2 SPIDER SILK PROTEIN eADF4(C16)

1.4.2.1 CHARACTERISTICS OF eADF4(C16)

A detailed characterization is essential to describe and compare the characteristics of eADF4(C16) to other silk proteins or polymers in general. Table 1.5 provides an overview of selected biochemical properties both of the natural protein ADF4 and the engineered protein eADF4(C16). Higher hydrophobicity, expressed by higher mean hydrophobicity, and a lower net charge for ADF-4 compared to eADF4(C16) resulted in a high intrinsic insolubility of the native protein. eADF4(C16) was up to 8% [w/V] soluble in water and gel-like states occurred upon higher concentration [19].

Table 1.5. Selected properties of native spider silk protein and engineered eADF4(C16) [19]

	eADF4(C16)	ADF-4
molecular weight [kDa]	47.7	34.9
no. of charged amino acid residues [pos/neg]	0 / 16	2 / 6
mean hydropathicity	- 0.464	- 0.075
solubility [%, w/V]	8	< 1

Subsequently, the influence of ions on the assembly behavior was studied according to the natural assembly process [19]. Concentrations of 300 mM sodium and potassium chloride did not result in any protein aggregation. However, potassium and sodium phosphate at the same concentration induced precipitation (12%) of eADF4(C16), but in a lower extent compared to the natural protein ADF-4. It was assumed that weaker precipitation tendency can be assigned to the relatively strong net charge of the recombinant protein and missing phosphorylated amino acid residues. Therefore, protonation of glutamate residues of eADF4(C16) is not as efficient as protonating the native ADF-4 protein regarding protein aggregation. Even acidification (pH 1) was not able to promote aggregation by establishing a strong hydrophobic core [150]. Liquid-liquid phase separation occurred at potassium phosphate concentrations higher than 400 mM. Spherical eADF4(C16) particles were spontaneously formed in contrast to nanofibrillar structures at lower concentrations [151].

1.4.2.2 PROCESSING OF eADF4(C16)

The correlation of molecular sequence to mechanical properties and consequently the feasibility to control the properties of the biomaterial have attracted several research groups to produce multi-purpose materials of controlled strength, extensibility and stiffness [152]. The spider silk protein eADF4(C16) can be processed into a diverse set of morphologies including solid spheres, hydrogels, films and microcapsules.

eADF4(C16) particles

Slotta et al. investigated the concentration dependent formation process of solid protein spheres and its underlying mechanism [20]. It is shown in Figure 1.4 that low concentrations of potassium phosphate (< 300 mM) led to protein self-assembly into nanofibrils. These nanofibrils with a diameter between 2 and 10 nm were formed due to a neutralization of the coulombic repulsion between the glutamate residues of eADF4(C16). Therefore, formation of nanofibrils was further influenced by pH and ionic strength of the aqueous buffer solution. Higher concentrations of potassium phosphate (> 400 mM) resulted in the formation of stable and solid protein spheres with a particle size of approx. 1 μm . The underlying mechanism

was described as a phase separation process induced by potassium and phosphate ions which are known to strengthen hydrophobic interactions and to decrease the solubility of nonpolar molecules according to the Hofmeister series [153-155]. A dense protein-rich phase was created which caused the formation of protein nuclei accompanied with structural transition of the protein's secondary structure and further sphere growth [20]. Sphere formation happened fast and was completed after 120 s. The surface analysis revealed smooth protein particles and the secondary structure of the particles' protein matrix showed a significant amount of β -sheet structure (64%).

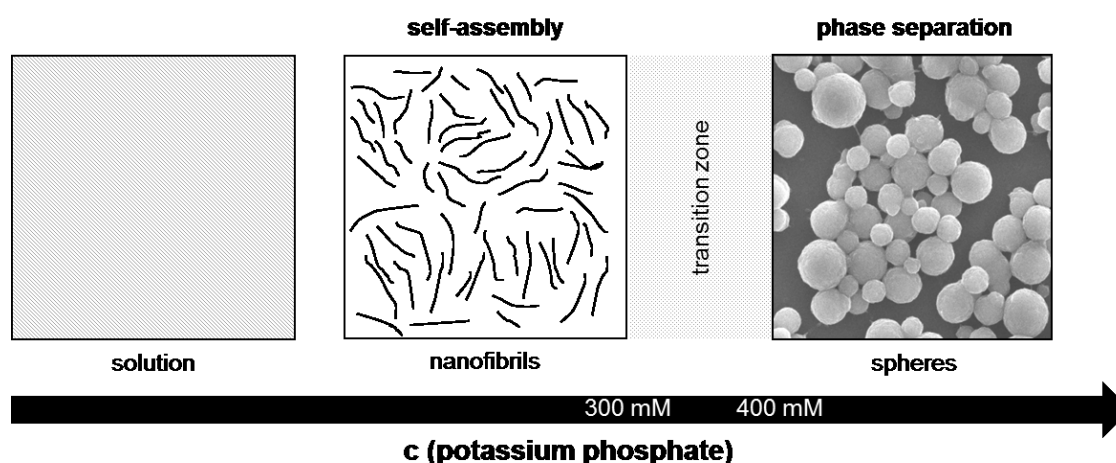


Figure 1.4. Self-assembly and phase separation process of eADF4(C16) in dependence of potassium phosphate concentration.

Detailed insight in the importance of processing conditions for eADF4(C16) particle formation was given by Lammel et al. [22]. The size of eADF4(C16) particles was easily controlled by protein concentration (direct proportionality) and mixing intensity (indirect proportionality). Furthermore, the concentration of potassium phosphate was confirmed to be crucial for the particle formation process. A concentration of 500 mM resulted in large clusters of eADF4(C16) particles which disintegrated upon shear stress. At a concentration of 1 M, fully developed eADF4(C16) particles were formed at an eADF4(16) concentration of 0.5 mg/mL. These protein particles maintained their particle size of about 300 nm during shear stress. The time period for the salting out process at 1 M potassium phosphate was determined to be 30 s.

eADF4(C16) films

Spider silk protein films were easily prepared by casting eADF4(C16) solutions onto substrates and subsequent evaporation of the solvent (see Figure 1.5) [156]. The dried films needed to be peeled off from the support for further usage and could be structurally or chemically modified afterwards [157, 158]. Non-aqueous solvents such as

hexafluoroisopropanol (HFIP) [157, 159] and formic acid [160] were used first due to the high solubility of eADF4(C16) in these organic solvents. However, aqueous protein solutions were employed recently and the different impact of the used solvent on the thermal stability and mechanical properties of the resulting spider silk films was demonstrated [161, 162]. Junghans et al. compared the mechanical properties of films made of recombinant eADF4(C16) protein to other silk proteins such as sericin-free silkworm silk and another recombinant spider silk protein from plants [163]. Thin layers were prepared by spin-coating and casting from HFIP silk protein solutions. The outcome of this study was that only films made of eADF4(C16) combined superior hardness with a predominantly elastic behavior. As a separate research project on the development of eADF4(C16) films for drug delivery was started in our research group in 2010, further details about spider silk films will not be presented in this work.

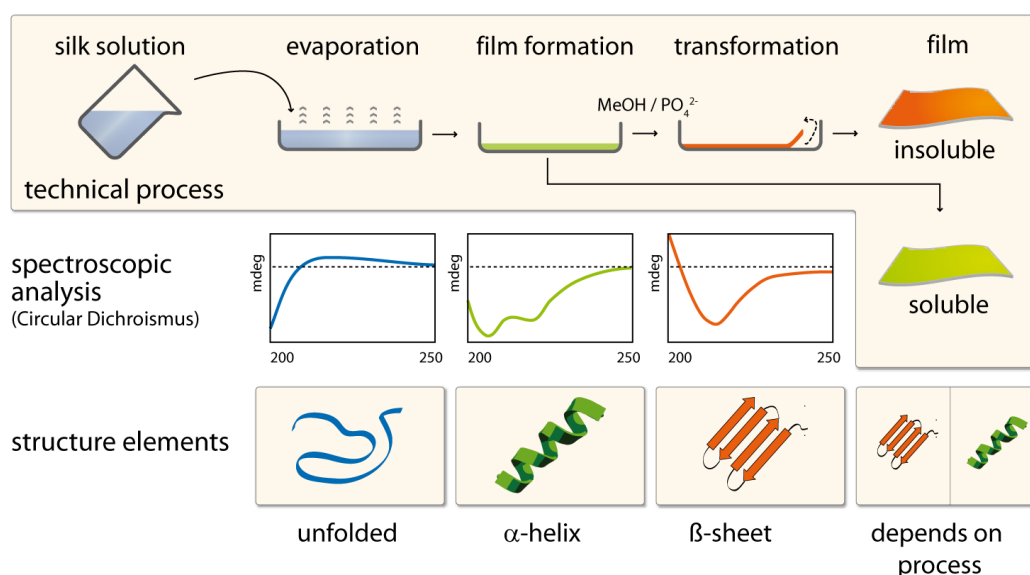


Figure 1.5. Preparation of eADF4(C16) films by casting/evaporation and subsequent post-treatment [156]

eADF4(C16) microcapsules

A second particulate morphology was derived from eADF4(C16) due to its amphiphilicity and controllable structure. Microcapsules were generated by an emulsion process as it is shown in Figure 1.6. The aqueous spider silk protein solution was emulsified in an oily component (e.g. toluene), so that the amphiphilic protein quickly adsorbed at the water-oil interface. A thin protein film was formed at the surface of the aqueous droplets encapsulating its content. During the film formation process, protein conformation changed to a β -sheet rich conformation. Therefore, the obtained microcapsules were stable and could be transferred into an aqueous phase by sedimentation or by the addition of ethanol. The capsule formation process was, similar to sphere formation, a very fast process due to the intrinsically unfolded

structure of eADF4(C16). Microcapsules with diameters from 1 to 30 μm were obtained. The protein shell was determined to be not more than 6 nm in thickness [164].

The microcapsules were further characterized by encapsulating fluorescein isothiocyanate (FITC) labeled dextran with a median molecular weight of 40 kDa. Partial permeation was observed and attributed to a fraction of FITC-dextran with lower molecular weight than the molecular weight cut off of the spider silk capsule [164]. Hence, this cut off was calculated to be 27 kDa by determination of the permeability of FITC-dextran [165]. Permeability varied inside the capsule dispersion, but was always between 16 and 47 kDa. Further investigation of this morphology revealed resistance to osmotic stress, high elasticity and excellent chemical stability against denaturants. The protein capsules were digested by Proteinase K to release encapsulated molecules [164]. Chemical crosslinking of eADF4(C16) with ammonium persulfate (APS) prevented enzymatic digestion.

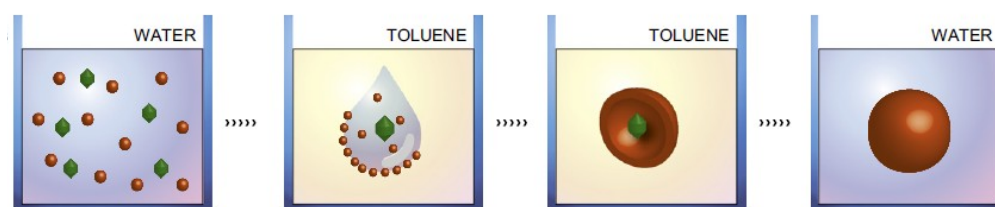


Figure 1.6. Preparation of microcapsules made of eADF4(C16) protein [164]

eADF4(C16) hydrogels

The major disadvantage of hydrogels made of biopolymers for biomedical applications is the limited range of mechanical properties [166]. Therefore, hydrogels made of silk proteins may overcome this drawback.

Rammensee et al. performed a rheological characterization of hydrogels made of eADF4(C16) [167]. The addition of 10% [w/V] methanol to eADF4(C16) solutions with concentrations between 5 and 30 mg/mL led to self-assembly of the spider silk protein into semi-flexible nanofibers which formed branch-like structures in a concentration dependent manner. The obtained hydrogels were transparent and sufficiently viscous. Although being easily disrupted by agitation or shearing, the hydrogels were stable over weeks and had a high elastic modulus due to the persistence length of the semi-flexible spider silk protein network.

1.4.2.3 eADF4(C16) FOR DRUG DELIVERY

All presented morphologies of eADF4(C16) can in principle be applied for drug delivery of active pharmaceutical ingredients. However, the deep understanding of the phase transition behavior of the recombinant protein eADF4(C16) from initially unstructured protein molecules into solid protein spheres [22] and the ease of handling led to the prioritization of studies on eADF4(C16) particles.

Liebmann et al. conducted a proof-of-concept study for the encapsulation of poorly water-soluble substances into spider silk microbeads [168, 169]. eADF4(C16) microbeads were formed by mixing or dialyzing a solution containing eADF4(C16) at 10 mg/mL and β -carotene (30 to 300-fold excess of soluble eADF4) with or against 600 mM potassium phosphate (pH 8.0). β -carotene was chosen due to its strong affinity to hydrophobic surfaces. The study revealed that eADF4(C16) is able to colloiddally stabilize β -carotene in an aqueous solution by encapsulation/co-precipitation of β -carotene (nano)particles into eADF4(C16) protein microbeads. Thereby, further agglomeration of β -carotene particles was prevented. The protein microbeads were qualitatively analyzed by electron microscopy. The microbeads exhibited diameters in the range from 1 to 5 μ m. The surface of microbeads comprising β -carotene particles appeared to be considerably rougher than the surface of empty eADF4(C16) particles. The encapsulated β -carotene was released by proteolytic degradation of the protein microbeads using proteinase K and intestinal fluid (pankreatin), whereas gastric fluid containing pepsin was not able to digest eADF4(C16) particles. Therefore, it was assumed that poorly water-soluble substances can be transported through the stomach and delivered in the intestine by encapsulation into eADF4(C16) microbeads.

A different formulation strategy for drug delivery was carried out by Lammel et al. [23, 24]. eADF4(C16) particles were prepared first and loading with an active pharmaceutical ingredient was performed afterwards. It was shown that small molecules with a positive net charge can diffuse into the negatively charged protein matrix driven by electrostatic interactions. The efficiency of this loading strategy depended on the properties of the small molecules of weak alkaline nature: the distribution coefficient (logD) and the weight (size) of the molecule (M_w) (see Figure 1.7). During this study, constant release rates were obtained for ethacridine lactate and methyl violet at physiological conditions over a period of one month. For this reason, this formulation strategy was chosen for further proceeding employing protein molecules, aiming for efficient loading at gentle conditions and constant release over a sufficiently long time period.

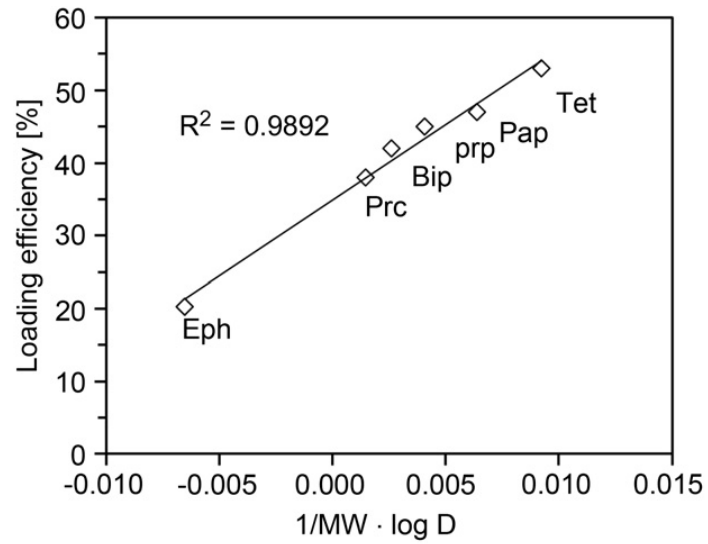


Figure 1.7. Loading efficiencies for model drugs of weak alkaline nature [23]: Ephedrine (Eph), Procain (Prc), Biperiden (Bip), Propranolol (Prp), Papaverine (Pap) and Tetracaine (Tet)

1.5 OBJECTIVES OF THE THESIS

The overall aim of this thesis was a broad investigation of the spider silk protein eADF4(C16) with regard to an application as new biomaterial for colloidal drug delivery systems. The obtained results using eADF4(C16) particles may further be transferred to other morphologies like spider silk protein films or hydrogels.

This project was justified because there is to date still a clear need for biodegradable materials which have to be available in adequate amounts meeting the required quality and safety profile for pharmaceutical excipients. The derived delivery systems have to be easily prepared using an adaptable and upscalable technique. Stability of the encapsulated drugs with special attention to protein therapeutics is a further necessity. A broad field of application makes such a delivery system an exciting technology for investors and pharmaceutical companies.

Thus, the first major objective of this thesis was the clarification of the phase separation process in order to set up a standardized particle preparation technique and manufacturing process (chapter 3). Two different techniques for the preparation of eADF4(C16) nano- and microparticles were evaluated and process limitations as well as critical process parameters were elaborated. The aqueous eADF4(C16) solution as intermediate of the manufacturing procedure was deeply characterized to elucidate its potential influence on the following phase separation process. A second goal of this particular project was the development of a stable colloidal formulation. For this reason, lyophilization of particulate formulations comprising different excipients was developed for empty and lysozyme-loaded eADF4(C16) nanoparticles.

The use of eADF4(C16) particles for drug delivery was recently investigated for small molecular weight drugs [23]. Different types of drugs were loaded on submicron particles by so-called remote loading which means loading during an incubation step after particle preparation. This study was the basis for the second major aim of this thesis: the applicability of eADF4(C16) particles as drug carrier for high molecular weight drugs like protein pharmaceuticals (chapter 4). First, loading was performed according to the explained remote loading procedure and the *in vitro* release was examined. Lysozyme and nerve growth factor (NGF) were employed as protein drugs for this study. The loading mechanism was investigated using different fluorescein isothiocyanate (FITC) labeled macromolecules. Secondly, drug encapsulation was performed as comparison to the remote loading procedure.

Besides an application as potential drug delivery system, another objective of this thesis was the evaluation whether the colloidal formulation consisting of NGF-loaded spider silk particles can be superior to a particle-free NGF formulation regarding the prevention of protein aggregation in forced degradation studies (chapter 5). Especially the determined matrix

loading of particles was supposed to be beneficial as the protein itself is less exposed to stress factors compared to the particle-free formulation. Binding of the protein to the particles driven by electrostatic interactions may also stabilize the native, folded state of the protein. In order to prove these assumptions, forced degradation studies comparing the suspension and the particle-free protein formulation were performed. Freeze-thawing, stirring, light exposure and incubation at elevated temperatures were conducted to obtain an insight into the different processes and mechanisms occurring without or in presence of spider silk particles.

1.6 REFERENCES

- [1] **Walsh G.**, Biopharmaceutical benchmarks 2010. *Nat Biotech* 2010, 28(9), 917-924
- [2] **Pavlou A. K. and Reichert J. M.**, Recombinant protein therapeutics - success rates, market trends and values to 2010. *Nat Biotech* 2004, 22(12), 1513-1519
- [3] **Nelson A. L. and Reichert J. M.**, Development trends for therapeutic antibody fragments. *Nat Biotech* 2009, 27(4), 331-337
- [4] **Wang W.**, Instability, stabilization, and formulation of liquid protein pharmaceuticals. *Int. J. Pharm.* 1999, 185(2), 129-188
- [5] **Moeller E. H. and Jorgensen L.**, Alternative routes of administration for systemic delivery of protein pharmaceuticals. *Drug Discovery Today: Technologies* 2008, 5(2-3), e89-e94
- [6] **Cleland J. L., Daugherty A. and Mrsny R.**, Emerging protein delivery methods. *Curr. Opin. Biotechnol.* 2001, 12(2), 212-219
- [7] **Sinha V. R. and Trehan A.**, Biodegradable microspheres for protein delivery. *J. Control. Release* 2003, 90(3), 261-280
- [8] **Pisal D. S., Kosloski M. P. and Balu-lyer S. V.**, Delivery of therapeutic proteins. *J. Pharm. Sci.* 2010, 99(6), 2557-2575
- [9] **DeMerlis C. C., Goldring J. M., Velagaleti R., Brock W. and Osterberg R.**, Regulatory update: the IPEC novel excipient safety evaluation procedure. *Pharmaceutical Technology* 2009, 33(11), 72-82
- [10] *IPEC Guidelines*. Available from: <http://www.ipeceurope.org/page.asp?pid=59>.
- [11] **Lee K. Y. and Yuk S. H.**, Polymeric protein delivery systems. *Progress in Polymer Science* 2007, 32(7), 669-697
- [12] **Wenk E., Merkle H. P. and Meinel L.**, Silk fibroin as a vehicle for drug delivery applications. *J. Control. Release* 2011, 150(2), 128-141
- [13] **Altman G. H., Diaz F., Jakuba C., Calabro T., Horan R. L., Chen J., Lu H., Richmond J. and Kaplan D. L.**, Silk-based biomaterials. *Biomaterials* 2003, 24(3), 401-416
- [14] **Vollrath F., Barth P., Basedow A., Engstrom W. and List H.**, Local tolerance to spider silks and protein polymers in vivo. *In Vivo* 2002, 16(4), 229-234
- [15] **Spieß K., Lammel A. and Scheibel T.**, Recombinant spider silk proteins for applications in biomaterials. *Macromol. Biosci.* 2010, 10(9), 998-1007
- [16] **Humenik M., Smith A. M. and Scheibel T.**, Recombinant spider silks - biopolymers with potential for future applications. *Polymers* 2011, 3(1), 640-661
- [17] **Wenk E., Wandrey A. J., Merkle H. P. and Meinel L.**, Silk fibroin spheres as a platform for controlled drug delivery. *J. Control. Release* 2008, 132(1), 26-34
- [18] **Scheibel T.**, Spider silks: recombinant synthesis, assembly, spinning, and engineering of synthetic proteins. *microbial cell factories* 2004, 3(1), 14
- [19] **Huemmerich D., Helsen C. W., Quedzuweit S., Oschmann J., Rudolph R. and Scheibel T.**, Primary structure elements of spider dragline silks and their contribution to protein solubility. *Biochemistry* 2004, 43(42), 13604-13612

- [20] **Slotta U., Rammensee S., Gorb S. and Scheibel T.**, An engineered spider silk protein forms microspheres. *Angew. Chem. Int. Ed. Engl.* 2008, 47(24), 4592-4594
- [21] **Rammensee S., Slotta U., Scheibel T. and Bausch A. R.**, Assembly mechanism of recombinant spider silk proteins. *P Natl Acad Sci USA* 2008, 105(18), 6590-6595
- [22] **Lammel A., Schwab M., Slotta U., Winter G. and Scheibel T.**, Processing conditions for the formation of spider silk microspheres. *ChemSusChem* 2008, 1(5), 413-416
- [23] **Lammel A., Schwab M., Hofer M., Winter G. and Scheibel T.**, Recombinant spider silk particles as drug delivery vehicles. *Biomaterials* 2011, 32(8), 2233-2240
- [24] **Lammel A., Scheibel T., Schwab M., Winter G., Hofer M. and Myschik J.**, Spider silk particles for controlled and sustained delivery of compounds, 2011, 2011063990, WO
- [25] **Langer R. and Folkman J.**, Polymers for the sustained release of proteins and other macromolecules. *Nature* 1976, 263(5580), 797-800
- [26] **Dai C., Wang B. and Zhao H.**, Microencapsulation peptide and protein drugs delivery system. *Colloids and Surfaces B: Biointerfaces* 2005, 41(2-3), 117-120
- [27] **Pistel K. F., Bittner B., Koll H., Winter G. and Kissel T.**, Biodegradable recombinant human erythropoietin loaded microspheres prepared from linear and star-branched block copolymers: Influence of encapsulation technique and polymer composition on particle characteristics. *J. Control. Release* 1999, 59(3), 309-325
- [28] **Morlock M., Koll H., Winter G. and Kissel T.**, Microencapsulation of rh-erythropoietin, using biodegradable poly(-lactide-co-glycolide): protein stability and the effects of stabilizing excipients. *Eur. J. Pharm. Biopharm.* 1997, 43(1), 29-36
- [29] **Morlock M., Kissel T., Li Y. X., Koll H. and Winter G.**, Erythropoietin loaded microspheres prepared from biodegradable LPLG-PEO-LPLG triblock copolymers: protein stabilization and in-vitro release properties. *J. Control. Release* 1998, 56(1-3), 105-115
- [30] **Philo J. S. and Arakawa T.**, Mechanisms of Protein Aggregation. *Curr. Pharm. Biotechnol.* 2009, 10(4), 348-351
- [31] **van de Weert M., Hennink W. E. and Jiskoot W.**, Protein instability in poly(lactic-co-glycolic acid) microparticles. *Pharm. Res.* 2000, 17(10), 1159-1167
- [32] **Li L. and Schwendeman S. P.**, Mapping neutral microclimate pH in PLGA microspheres. *J. Control. Release* 2005, 101(1-3), 163-173
- [33] **Brunner A., Mäder K. and Göpferich A.**, pH and osmotic pressure inside biodegradable microspheres during erosion. *Pharm. Res.* 1999, 16(6), 847-853
- [34] **Lucke A., Kiermaier J. and Göpferich A.**, Peptide Acylation by Poly(α -Hydroxy Esters). *Pharm. Res.* 2002, 19(2), 175-181
- [35] **Prabaharan M.**, Review Paper: Chitosan Derivatives as Promising Materials for Controlled Drug Delivery. *J. Biomater. Appl.* 2008, 23(1), 5-36
- [36] **Xu Y. and Du Y.**, Effect of molecular structure of chitosan on protein delivery properties of chitosan nanoparticles. *Int. J. Pharm.* 2003, 250(1), 215-226
- [37] **Amidi M., Romeijn S. G., Borchard G., Junginger H. E., Hennink W. E. and Jiskoot W.**, Preparation and characterization of protein-loaded N-trimethyl chitosan nanoparticles as nasal delivery system. *J. Control. Release* 2006, 111(1-2), 107-116
- [38] **Tonnesen H. H. and Karlsen J.**, Alginate in Drug Delivery Systems. *Drug Dev. Ind. Pharm.* 2002, 28(6), 621 - 630

- [39] **Gombotz W. R. and Wee S.**, Protein release from alginate matrices. *Adv Drug Deliv Rev* 1998, 31(3), 267-285
- [40] **Malafaya P. B., Silva G. A. and Reis R. L.**, Natural-origin polymers as carriers and scaffolds for biomolecules and cell delivery in tissue engineering applications. *Adv Drug Deliv Rev* 2007, 59(4-5), 207-233
- [41] **Langer R. and Moses M.**, Biocompatible controlled release polymers for delivery of polypeptides and growth factors. *J. Cell. Biochem.* 1991, 45(4), 340-345
- [42] **Siegel R. A. and Langer R.**, Controlled Release of Polypeptides and Other Macromolecules. *Pharm. Res.* 1984, 1(1), 2-10
- [43] **Gombotz W. R. and Pettit D. K.**, Biodegradable polymers for protein and peptide drug delivery. *Bioconjug. Chem.* 1995, 6(4), 332-351
- [44] **Wang G. and Uludag H.**, Recent developments in nanoparticle-based drug delivery and targeting systems with emphasis on protein-based nanoparticles. *Expert Opin. Drug Deliv.* 2008, 5(5), 499-515
- [45] **Jiskoot W., Schie R. F., Carstens M. and Schellekens H.**, Immunological Risk of Injectable Drug Delivery Systems. *Pharm. Res.* 2009, 26(6), 1303-1314
- [46] **Raghuvanshi R. S., Goyal S., Singh O. and Panda A. K.**, Stabilization of Dichloromethane-Induced Protein Denaturation During Microencapsulation. *Pharm. Dev. Technol.* 1998, 3(2), 269-276
- [47] **Stureson C. and Carlfors J.**, Incorporation of protein in PLG-microspheres with retention of bioactivity. *J. Control. Release* 2000, 67(2-3), 171-178
- [48] **Zambaux M. F., Bonneaux F., Gref R., Maincent P., Dellacherie E., Alonso M. J., Labrude P. and Vigneron C.**, Influence of experimental parameters on the characteristics of poly(lactic acid) nanoparticles prepared by a double emulsion method. *J. Control. Release* 1998, 50(1-3), 31-40
- [49] **Mishra V., Mahor S., Rawat A., Gupta P. N., Dubey P., Khatri K. and Vyas S. P.**, Targeted brain delivery of AZT via transferrin anchored pegylated albumin nanoparticles. *J. Drug Target.* 2006, 14(1), 45-53
- [50] **Weber C., Coester C., Kreuter J. and Langer K.**, Desolvation process and surface characterisation of protein nanoparticles. *Int. J. Pharm.* 2000, 194(1), 91-102
- [51] **Lin W., Coombes A., Davies M., Davis S. and Illum L.**, Preparation of Sub-100 nm Human Serum Albumin Nanospheres Using a pH-Coacervation Method. *J. Drug Target.* 1993, 1(3), 237-243
- [52] **Langer K., Balthasar S., Vogel V., Dinauer N., von Briesen H. and Schubert D.**, Optimization of the preparation process for human serum albumin (HSA) nanoparticles. *Int. J. Pharm.* 2003, 257(1-2), 169-180
- [53] **Coester C. J., Langer K., Von Briesen H. and Kreuter J.**, Gelatin nanoparticles by two step desolvation - a new preparation method, surface modifications and cell uptake. *J. Microencapsul.* 2000, 17(2), 187-193
- [54] **Ko S. and Gunasekaran S.**, Preparation of sub-100-nm β -lactoglobulin (BLG) nanoparticles. *J. Microencapsul.* 2006, 23(8), 887-898
- [55] **Fan Y. F., Wang Y. N., Fan Y. G. and Ma J. B.**, Preparation of insulin nanoparticles and their encapsulation with biodegradable polyelectrolytes via the layer-by-layer adsorption. *Int. J. Pharm.* 2006, 324(2), 158-167

- [56] **Chirgwin J. and Chua S. L.**, Management of breast cancer with nanoparticle albumin-bound (nab)-paclitaxel combination regimens: A clinical review. *Breast* 2011, 20(5), 394-406
- [57] **Elsadek B. and Kratz F.**, Impact of albumin on drug delivery — New applications on the horizon. *J. Control. Release* 2012, 157(1), 4-28
- [58] **Postema M. and Schmitz G.**, Ultrasonic bubbles in medicine: influence of the shell. *Ultrason. Sonochem.* 2007, 14(4), 438-444
- [59] **Barnhart J., Levene H., Villapando E., Maniquis J., Fernandez J., Rice S., Jablonski E., Gjoen T. and Tolleshaug H.**, Characteristics of Albumex: air-filled albumin microspheres for echocardiography contrast enhancement. *Invest. Radiol.* 1990, 25 Suppl 1(162-164)
- [60] **Moreno-Aspitia A. and Perez E.**, North Central Cancer Treatment Group N0531: Phase II Trial of Weekly Albumin-Bound Paclitaxel (ABI-007; Abraxane®) in Combination with Gemcitabine in Patients with Metastatic Breast Cancer. *Clin. Breast Cancer* 2005, 6(4), 361-364
- [61] **Miele E., Spinelli G. P., Tomao F. and Tomao S.**, Albumin-bound formulation of paclitaxel (Abraxane ABI-007) in the treatment of breast cancer. *Int. J. Nanomedicine* 2009, 4(99-105)
- [62] **Yuan D.-m., Lv Y.-l., Yao Y.-w., Miao X.-h., Wang Q., Xiao X.-w., Yin J., Shi Y., Shi M.-q., Zhang X.-w. and Song Y.**, Efficacy and safety of Abraxane in treatment of progressive and recurrent non-small cell lung cancer patients: A retrospective clinical study. *Thoracic Cancer* 2012, 3(4), 341-347
- [63] **Kratz F.**, Albumin as a drug carrier: Design of prodrugs, drug conjugates and nanoparticles. *J. Control. Release* 2008, 132(3), 171-183
- [64] **Elzoghby A. O., Samy W. M. and Elgindy N. A.**, Albumin-based nanoparticles as potential controlled release drug delivery systems. *J. Control. Release* 2012, 157(2), 168-182
- [65] **Pereverzeva E., Treschalin I., Bodyagin D., Maksimenko O., Langer K., Dreis S., Asmussen B., Kreuter J. and Gelperina S.**, Influence of the formulation on the tolerance profile of nanoparticle-bound doxorubicin in healthy rats: Focus on cardio- and testicular toxicity. *Int. J. Pharm.* 2007, 337(1–2), 346-356
- [66] **Singh H. D., Wang G., Uludağ H. and Unsworth L. D.**, Poly-l-lysine-coated albumin nanoparticles: Stability, mechanism for increasing in vitro enzymatic resilience, and siRNA release characteristics. *Acta Biomater.* 2010, 6(11), 4277-4284
- [67] **Wagner S., Rothweiler F., Anhorn M. G., Sauer D., Riemann I., Weiss E. C., Katsen-Globa A., Michaelis M., Cinatl Jr J., Schwartz D., Kreuter J., von Briesen H. and Langer K.**, Enhanced drug targeting by attachment of an anti α v integrin antibody to doxorubicin loaded human serum albumin nanoparticles. *Biomaterials* 2010, 31(8), 2388-2398
- [68] **Babel W.**, Gelatine – ein vielseitiges Biopolymer. *Chemie in unserer Zeit* 1996, 30(2), 86-95
- [69] **Young S., Wong M., Tabata Y. and Mikos A. G.**, Gelatin as a delivery vehicle for the controlled release of bioactive molecules. *J. Control. Release* 2005, 109(1–3), 256-274
- [70] **Yamamoto M., Ikada Y. and Tabata Y.**, Controlled release of growth factors based on biodegradation of gelatin hydrogel. *J. Biomater. Sci. Polym. Ed.* 2001, 12(1), 77-88
- [71] **Coester C., Nayyar P. and Samuel J.**, In vitro uptake of gelatin nanoparticles by murine dendritic cells and their intracellular localisation. *Eur. J. Pharm. Biopharm.* 2006, 62(3), 306-314
- [72] **Fuchs S., Kutscher M., Hertel T., Winter G., Pietzsch M. and Coester C.**, Transglutaminase: New insights into gelatin nanoparticle cross-linking. *J. Microencapsul.* 2010, 27(8), 747-754

- [73] **Won Y.-W. and Kim Y.-H.**, Preparation and cytotoxicity comparison of type a gelatin nanoparticles with recombinant human gelatin nanoparticles. *Macromolecular Research* 2009, 17(7), 464-468
- [74] **Kumari A., Yadav S. K. and Yadav S. C.**, Biodegradable polymeric nanoparticles based drug delivery systems. *Colloids and Surfaces B: Biointerfaces* 2010, 75(1), 1-18
- [75] **Lu Z., Yeh T.-K., Tsai M., Au J. L.-S. and Wientjes M. G.**, Paclitaxel-Loaded Gelatin Nanoparticles for Intravesical Bladder Cancer Therapy. *Clin. Cancer Res.* 2004, 10(22), 7677-7684
- [76] **Bajpai A. K. and Choubey J.**, Design of gelatin nanoparticles as swelling controlled delivery system for chloroquine phosphate. *Journal of Materials Science: Materials in Medicine* 2006, 17(4), 345-358
- [77] **Ofokansi K., Winter G., Fricker G. and Coester C.**, Matrix-loaded biodegradable gelatin nanoparticles as new approach to improve drug loading and delivery. *Eur. J. Pharm. Biopharm.* 2010, 76(1), 1-9
- [78] **Zwiorek K., Kloeckner J., Wagner E. and Coester C.**, Gelatin nanoparticles as a new and simple gene delivery system. *J. Pharm. Pharm. Sci.* 2005, 7(4), 22-28
- [79] **Zwiorek K., Bourquin C., Battiany J., Winter G., Endres S., Hartmann G. and Coester C.**, Delivery by Cationic Gelatin Nanoparticles Strongly Increases the Immunostimulatory Effects of CpG Oligonucleotides. *Pharm. Res.* 2008, 25(3), 551-562
- [80] **Zillies J. and Coester C.**, Evaluating gelatin based nanoparticles as a carrier system for double stranded oligonucleotides. *J. Pharm. Pharm. Sci.* 2005, 7(4), 17-21
- [81] **Zillies J. C., Zwiorek K., Hoffmann F., Vollmar A., Anchordoquy T. J., Winter G. and Coester C.**, Formulation development of freeze-dried oligonucleotide-loaded gelatin nanoparticles. *Eur. J. Pharm. Biopharm.* 2008, 70(2), 514-521
- [82] **Klier J., Fuchs S., May A., Schillinger U., Plank C., Winter G., Gehlen H. and Coester C.**, A Nebulized Gelatin Nanoparticle-Based CpG Formulation is Effective in Immunotherapy of Allergic Horses. *Pharm. Res.* 2012, 29(6), 1650-1657
- [83] **Fuchs S., Klier J., May A., Winter G., Coester C. and Gehlen H.**, Towards an inhalative in vivo application of immunomodulating gelatin nanoparticles in horse-related preformulation studies. *J. Microencapsul.* 2012, 29(7), 615-625
- [84] **Omenetto F. G. and Kaplan D. L.**, New Opportunities for an Ancient Material. *Science* 2010, 329(5991), 528-531
- [85] **Kaplan D., Adams W. W., Farmer B. and Viney C.**, Silk: biology, structure, properties, and genetics. *ACS Symposium Series* 1994, 544(Silk Polymers), 2-16
- [86] **Scheibel T.**, Protein fibers as performance proteins: new technologies and applications. *Curr. Opin. Biotechnol.* 2005, 16(4), 427-433
- [87] **Kaplan D. L.**, Fibrous proteins - silk as a model system. *Polymer Degradation and Stability* 1998, 59(1-3), 25-32
- [88] **Vendrey C. and Scheibel T.**, Biotechnological Production of Spider-Silk Proteins Enables New Applications. *Macromol. Biosci.* 2007, 7(4), 401-409
- [89] **Craig C. L.**, Importance of unique silk proteins to the ecological and evolutionary diversity of araneid spiders. *ACS Symposium Series* 1994, 544(Silk Polymers), 59-66
- [90] **Sponner A., Vater W., Monajembashi S., Unger E., Grosse F. and Weisshart K.**, Composition and Hierarchical Organisation of a Spider Silk. *PLoS ONE* 2007, 2(10), e998

- [91] **Ayoub N. A., Garb J. E., Tinghitella R. M., Collin M. A. and Hayashi C. Y.**, Blueprint for a High-Performance Biomaterial: Full-Length Spider Dragline Silk Genes. *PLoS ONE* 2007, 2(6), e514
- [92] **Bini E., Knight D. P. and Kaplan D. L.**, Mapping Domain Structures in Silks from Insects and Spiders Related to Protein Assembly. *J. Mol. Biol.* 2004, 335(1), 27-40
- [93] **Hardy J., Roemer L. and Scheibel T.**, Polymeric materials based on silk proteins. *Polymer* 2008, 49(20), 4309-4327
- [94] **Zhou C.-Z., Confalonieri F., Medina N., Zivanovic Y., Esnault C., Yang T., Jacquet M., Janin J., Duguet M., Perasso R. and Li Z.-G.**, Fine organization of *Bombyx mori* fibroin heavy chain gene. *Nucleic Acids Res.* 2000, 28(12), 2413-2419
- [95] **Gatesy J., Hayashi C., Motriuk D., Woods J. and Lewis R.**, Extreme Diversity, Conservation, and Convergence of Spider Silk Fibroin Sequences. *Science* 2001, 291(5513), 2603-2605
- [96] **Exler J. H., Hümmerich D. and Scheibel T.**, The Amphiphilic Properties of Spider Silks Are Important for Spinning. *Angewandte Chemie International Edition* 2007, 46(19), 3559-3562
- [97] **Guerette P. A., Ginzinger D. G., Weber B. H. F. and Gosline J. M.**, Silk Properties Determined by Gland-Specific Expression of a Spider Fibroin Gene Family. *Science* 1996, 272(5258), 112-115
- [98] **Jin H.-J. and Kaplan D. L.**, Mechanism of silk processing in insects and spiders. *Nature* 2003, 424(6952), 1057-1061
- [99] **McGrath K. and Kaplan D.**, *Protein-Based Materials*, ed. Kaplan, D. 1997: Birkhäuser. 429 pp.
- [100] **Winkler S. and Kaplan D. L.**, Molecular biology of spider silk. *Reviews in Molecular Biotechnology* 2000, 74(2), 85-93
- [101] **Parkhe A. D., Seeley S. K., Gardner K., Thompson L. and Lewis R. V.**, Structural studies of spider silk proteins in the fiber. *J. Mol. Recognit.* 1997, 10(1), 1-6
- [102] **van Beek J. D., Hess S., Vollrath F. and Meier B. H.**, The molecular structure of spider dragline silk: Folding and orientation of the protein backbone. *P Natl Acad Sci USA* 2002, 99(16), 10266-10271
- [103] **Gosline J. M., Guerette P. A., Ortlepp C. S. and Savage K. N.**, The mechanical design of spider silks: from fibroin sequence to mechanical function. *J. Exp. Biol.* 1999, 202(23), 3295-3303
- [104] **Ittah S., Michaeli A., Goldblum A. and Gat U.**, A Model for the Structure of the C-Terminal Domain of Dragline Spider Silk and the Role of Its Conserved Cysteine. *Biomacromolecules* 2007, 8(9), 2768-2773
- [105] **Hayashi C. Y. and Lewis R. V.**, Spider flagelliform silk: lessons in protein design, gene structure, and molecular evolution. *Bioessays* 2001, 23(8), 750-756
- [106] **Lammel A., Keerl D., Roemer L. and Scheibel T.**, Proteins: Polymers of natural origin, in *Recent Advances in Biomaterials Research*, Hu, J., Editor. 2008, Transworld Research Network. p. 1-22
- [107] **Lefevre T., Leclerc J., Rioux-Dube J. F., Buffeteau T., Paquin M. C., Rousseau M. E., Cloutier I., Auger M., Gagne S. M., Boudreault S., Cloutier C. and Pezolet M.**, Conformation of Spider Silk Proteins In Situ in the Intact Major Ampullate Gland and in Solution. *Biomacromolecules* 2007, 8(8), 2342-2344

- [108] **Heim M., Keerl D. and Scheibel T.**, Spider Silk: From Soluble Protein to Extraordinary Fiber. *Angewandte Chemie International Edition* 2009, 48(20), 3584-3596
- [109] **Mello C. M., Senecal K., Yeung B., Vouros P. and Kaplan D.**, Initial characterization of *Nephila clavipes* dragline protein. *ACS Symposium Series* 1994, 544(Silk Polymers), 67-79
- [110] **Dicko C., Knight D., Kenney J. M. and Vollrath F.**, Secondary Structures and Conformational Changes in Flagelliform, Cylindrical, Major, and Minor Ampullate Silk Proteins. Temperature and Concentration Effects. *Biomacromolecules* 2004, 5(6), 2105-2115
- [111] **Kenney J. M., Knight D., Wise M. J. and Vollrath F.**, Amyloidogenic nature of spider silk. *Eur. J. Biochem.* 2002, 269(16), 4159-4163
- [112] **Rising A., Nimmervoll H., Grip S., Fernandez-Arias A., Storckenfeldt E., Knight D. P., Vollrath F. and Engstroem W.**, Spider Silk Proteins - Mechanical Property and Gene Sequence. *Zoological Science* 2005, 22(3), 273-281
- [113] **Vollrath F. and Knight D. P.**, Liquid crystalline spinning of spider silk. *Nature* 2001, 410(6828), 541-548
- [114] **Santin M., Motta A., Freddi G. and Cannas M.**, In vitro evaluation of the inflammatory potential of the silk fibroin. *J. Biomed. Mater. Res.* 1999, 46(3), 382-389
- [115] **Panilaitis B., Altman G. H., Chen J., Jin H.-J., Karageorgiou V. and Kaplan D. L.**, Macrophage responses to silk. *Biomaterials* 2003, 24(18), 3079-3085
- [116] **Meinel L., Hofmann S., Karageorgiou V., Kirker-Head C., McCool J., Gronowicz G., Zichner L., Langer R., Vunjak-Novakovic G. and Kaplan D. L.**, The inflammatory responses to silk films in vitro and in vivo. *Biomaterials* 2005, 26(2), 147-155
- [117] **Horan R. L., Antle K., Collette A. L., Wang Y., Huang J., Moreau J. E., Volloch V., Kaplan D. L. and Altman G. H.**, In vitro degradation of silk fibroin. *Biomaterials* 2005, 26(17), 3385-3393
- [118] **Wang Y., Rudym D. D., Walsh A., Abrahamsen L., Kim H.-J., Kim H. S., Kirker-Head C. and Kaplan D. L.**, In vivo degradation of three-dimensional silk fibroin scaffolds. *Biomaterials* 2008, 29(24-25), 3415-3428
- [119] **Allmeling C., Jokuszies A., Reimers K., Kall S., Choi C. Y., Brandes G., Kasper C., Scheper T., Guggenheim M. and Vogt P. M.**, Spider silk fibres in artificial nerve constructs promote peripheral nerve regeneration. *Cell Prolif.* 2008, 41(3), 408-420
- [120] **Wong Po Foo C. and Kaplan D. L.**, Genetic engineering of fibrous proteins: spider dragline silk and collagen. *Adv Drug Deliv Rev* 2002, 54(8), 1131-1143
- [121] **Wang Y., Kim H.-J., Vunjak-Novakovic G. and Kaplan D. L.**, Stem cell-based tissue engineering with silk biomaterials. *Biomaterials* 2006, 27(36), 6064-6082
- [122] **Wang Y., Kim U.-J., Blasioli D. J., Kim H.-J. and Kaplan D. L.**, In vitro cartilage tissue engineering with 3D porous aqueous-derived silk scaffolds and mesenchymal stem cells. *Biomaterials* 2005, 26(34), 7082-7094
- [123] **Meinel L., Betz O., Fajardo R., Hofmann S., Nazarian A., Cory E., Hilbe M., McCool J., Langer R., Vunjak-Novakovic G., Merkle H. P., Rechenberg B., Kaplan D. L. and Kirker-Head C.**, Silk based biomaterials to heal critical sized femur defects. *Bone* 2006, 39(4), 922-931
- [124] **Preda R., Leisk G., Omenetto F. and Kaplan D.**, Bioengineered Silk Proteins to Control Cell and Tissue Functions, in *Protein Nanotechnology*, Gerrard, J.A., Editor. 2013, Humana Press. p. 19-41

- [125] **Allmeling C., Radtke C. and Vogt P.**, Technical and Biomedical Uses of Nature's Strongest Fiber: Spider Silk, in *Spider Ecophysiology*, Nentwig, W., Editor. 2013, Springer Berlin Heidelberg. p. 475-490
- [126] **Uebersax L., Merkle H. P. and Meinel L.**, Insulin-like growth factor I releasing silk fibroin scaffolds induce chondrogenic differentiation of human mesenchymal stem cells. *J. Control. Release* 2008, 127(1), 12-21
- [127] **Bayraktar O., Malay Ö., Özgarip Y. and Batlgün A.**, Silk fibroin as a novel coating material for controlled release of theophylline. *Eur. J. Pharm. Biopharm.* 2005, 60(3), 373-381
- [128] **Gobin A. S., Rhea R., Newman R. A. and Mathur A. B.**, Silk-fibroin-coated liposomes for long-term and targeted drug delivery. *Int. J. Nanomedicine* 2006, 1(1), 81-87
- [129] **Wang X., Wenk E., Hu X., Castro G. R., Meinel L., Wang X., Li C., Merkle H. and Kaplan D. L.**, Silk coatings on PLGA and alginate microspheres for protein delivery. *Biomaterials* 2007, 28(28), 4161-4169
- [130] **Wang X., Hu X., Daley A., Rabotyagova O., Cebe P. and Kaplan D. L.**, Nanolayer biomaterial coatings of silk fibroin for controlled release. *J. Control. Release* 2007, 121(3), 190-199
- [131] **Wang X., Zhang X., Castellot J., Herman I., Iafrazi M. and Kaplan D. L.**, Controlled release from multilayer silk biomaterial coatings to modulate vascular cell responses. *Biomaterials* 2008, 29(7), 894-903
- [132] **Szybala C., Pritchard E. M., Lusardi T. A., Li T., Wilz A., Kaplan D. L. and Boison D.**, Antiepileptic effects of silk-polymer based adenosine release in kindled rats. *Exp. Neurol.* 2009, 219(1), 126-135
- [133] **Pritchard E. M., Szybala C., Boison D. and Kaplan D. L.**, Silk fibroin encapsulated powder reservoirs for sustained release of adenosine. *J. Control. Release* 2010, 144(2), 159-167
- [134] **Hofmann S., Wong Po Foo C. T., Rossetti F., Textor M., Vunjak-Novakovic G., Kaplan D. L., Merkle H. P. and Meinel L.**, Silk fibroin as an organic polymer for controlled drug delivery. *J. Control. Release* 2006, 111(1-2), 219-227
- [135] **Mandal B. B., Mann J. K. and Kundu S. C.**, Silk fibroin/gelatin multilayered films as a model system for controlled drug release. *Eur. J. Pharm. Sci.* 2009, 37(2), 160-171
- [136] **Lu Q., Wang X., Hu X., Cebe P., Omenetto F. and Kaplan D. L.**, Stabilization and Release of Enzymes from Silk Films. *Macromol. Biosci.* 2010, 10(4), 359-368
- [137] **Uebersax L., Mattotti M., Papaloizos M., Merkle H. P., Gander B. and Meinel L.**, Silk fibroin matrices for the controlled release of nerve growth factor (NGF). *Biomaterials* 2007, 28(30), 4449-4460
- [138] **Zhang J., Pritchard E., Hu X., Valentin T., Panilaitis B., Omenetto F. G. and Kaplan D. L.**, Stabilization of vaccines and antibiotics in silk and eliminating the cold chain. *P Natl Acad Sci USA* 2012, 109(30), 11981-11986
- [139] **Wang X., Wenk E., Matsumoto A., Meinel L., Li C. and Kaplan D. L.**, Silk microspheres for encapsulation and controlled release. *J. Control. Release* 2007, 117(3), 360-370
- [140] **Wang X., Wenk E., Zhang X., Meinel L., Vunjak-Novakovic G. and Kaplan D. L.**, Growth factor gradients via microsphere delivery in biopolymer scaffolds for osteochondral tissue engineering. *J. Control. Release* 2009, 134(2), 81-90
- [141] **Wang X., Yucel T., Lu Q., Hu X. and Kaplan D. L.**, Silk nanospheres and microspheres from silk/pva blend films for drug delivery. *Biomaterials* 2010, 31(6), 1025-1035

- [142] **Bessa P. C., Balmayor E. R., Azevedo H. S., Nürnberger S., Casal M., van Griensven M., Reis R. L. and Redl H.**, Silk fibroin microparticles as carriers for delivery of human recombinant BMPs. Physical characterization and drug release. *J. Tissue Eng. Regen. Med.* 2010, 4(5), 349-355
- [143] **Lammel A. S., Hu X., Park S.-H., Kaplan D. L. and Scheibel T. R.**, Controlling silk fibroin particle features for drug delivery. *Biomaterials* 2010, 31(16), 4583-4591
- [144] **Subia B. and Kundu S. C.**, Drug loading and release on tumor cells using silk fibroin–albumin nanoparticles as carriers. *Nanotechnology* 2013, 24(3), 035103
- [145] **Huemmerich D., Scheibel T., Vollrath F., Cohen S., Gat U. and Ittah S.**, Novel Assembly Properties of Recombinant Spider Dragline Silk Proteins. *Curr. Biol.* 2004, 14(22), 2070-2074
- [146] **Kluge J. A., Rabotyagova O., Leisk G. G. and Kaplan D. L.**, Spider silks and their applications. *Trends Biotechnol.* 2008, 26(5), 244-251
- [147] **Arcidiacono S., Mello C., Kaplan D., Cheley S. and Bayley H.**, Purification and characterization of recombinant spider silk expressed in *Escherichia coli*. *Appl. Microbiol. Biotechnol.* 1998, 49(1), 31-38
- [148] **Szela S., Avtges P., Valluzzi R., Winkler S., Wilson D., Kirschner D. and Kaplan D. L.**, Reduction-Oxidation Control of beta-sheet Assembly in Genetically Engineered Silk. *Biomacromolecules* 2000, 1(4), 534-542
- [149] **Wong Po Foo C., Patwardhan S. V., Belton D. J., Kitchel B., Anastasiades D., Huang J., Naik R. R., Perry C. C. and Kaplan D. L.**, Novel nanocomposites from spider silk-silica fusion (chimeric) proteins. *P Natl Acad Sci USA* 2006, 103(25), 9428-9433
- [150] **Zbilut J. P., Scheibel T., Huemmerich D., Webber Jr C. L., Colafranceschi M. and Giuliani A.**, Statistical approaches for investigating silk properties. *Applied Physics A: Materials Science & Processing* 2006, 82(2), 243-251
- [151] **Slotta U., Hess S., Spieß K., Stromer T., Serpell L. and Scheibel T.**, Spider Silk and Amyloid Fibrils: A Structural Comparison. *Macromol. Biosci.* 2007, 7(2), 183-188
- [152] **Metwalli E., Slotta U., Darko C., Roth S. V., Scheibel T. and Papadakis C. M.**, Structural changes of thin films from recombinant spider silk proteins upon post-treatment. *Applied Physics A: Materials Science & Processing* 2007, 89(3), 655-661
- [153] **Baldwin R. L.**, How Hofmeister ion interactions affect protein stability. *Biophys. J.* 1996, 71(4), 2056-2063
- [154] **Hofmeister F.**, Zur Lehre von der Wirkung der Salze. *Archiv für experimentelle Pathologie und Pharmakologie* 1888, 25(1), 1-30
- [155] **Zhang Y. and Cremer P. S.**, Interactions between macromolecules and ions: the Hofmeister series. *Curr. Opin. Chem. Biol.* 2006, 10(6), 658-663
- [156] **Spieß K., Roemer L. and Scheibel T.**, Transparente Folien aus Spinnenseide. *GIT Labor-Fachzeitschrift* 2007, 11), 928-931
- [157] **Huemmerich D., Slotta U. and Scheibel T.**, Processing and modification of films made from recombinant spider silk proteins. *Applied Physics A: Materials Science & Processing* 2006, 82(2), 219-222
- [158] **Chen X., Knight D. P., Shao Z. and Vollrath F.**, Conformation Transition in Silk Protein Films Monitored by Time-Resolved Fourier Transform Infrared Spectroscopy: Effect of Potassium Ions on *Nephila* Spidroin Films. *Biochemistry* 2002, 41(50), 14944-14950

- [159] **Zhao C., Yao J., Masuda H., Kishore R. and Asakura T.**, Structural characterization and artificial fiber formation of Bombyx mori silk fibroin in hexafluoro-iso-propanol solvent system. *Biopolymers* 2003, 69(2), 253-259
- [160] **Um I. C., Kweon H., Park Y. H. and Hudson S.**, Structural characteristics and properties of the regenerated silk fibroin prepared from formic acid. *Int. J. Biol. Macromol.* 2001, 29(2), 91-97
- [161] **Spiess K., Ene R., Keenan C. D., Senker J., Kremer F. and Scheibel T.**, Impact of initial solvent on thermal stability and mechanical properties of recombinant spider silk films. *Journal of Materials Chemistry* 2011, 21(35), 13594-13604
- [162] **Slotta U., Tammer M., Kremer F., Koelsch P. and Scheibel T.**, Structural Analysis of Spider Silk Films. *Supramolecular Chemistry* 2006, 18(5), 465-471
- [163] **Junghans F., Morawietz M., Conrad U., Scheibel T., Heilmann A. and Spohn U.**, Preparation and mechanical properties of layers made of recombinant spider silk proteins and silk from silk worm. *Applied Physics A: Materials Science & Processing* 2006, 82(2), 253-260
- [164] **Hermanson K. D., Huemmerich D., Scheibel T. and Bausch A. R.**, Engineered Microcapsules Fabricated from Reconstituted Spider Silk. *Adv. Mater.* 2007, 19(14), 1810-1815
- [165] **Hermanson K. D., Harasim M. B., Scheibel T. and Bausch A. R.**, Permeability of silk microcapsules made by the interfacial adsorption of protein. *Phys. Chem. Chem. Phys.* 2007, 9(48), 6442-6446
- [166] **Lee K. Y. and Mooney D. J.**, Hydrogels for Tissue Engineering. *Chem. Rev.* 2001, 101(7), 1869-1880
- [167] **Rammensee S., Huemmerich D., Hermanson K. D., Scheibel T. and Bausch A. R.**, Rheological characterization of hydrogels formed by recombinantly produced spider silk. *Applied Physics A: Materials Science & Processing* 2006, 82(2), 261-264
- [168] **Liebmann B.**, Use of amphiphilic self-assembling proteins for formulating poorly water-soluble active agents, 2007, 2007-EP50541, 2007082936, WO
- [169] **Liebmann B., Hümmereich D., Scheibel T. and Fehr M.**, Formulation of poorly water-soluble substances using self-assembling spider silk protein. *Colloids and Surfaces A: Physicochemical and Engineering Aspects* 2008, 331(1-2), 126-132

CHAPTER 2

MATERIALS AND METHODS

2.1 MATERIALS

2.1.1 PROTEINS

2.1.1.1 SPIDER SILK PROTEIN eADF4(C16)

An introduction to the unique properties of spider silk proteins has already been given in section 1.4 of the first chapter. For this reason only the biochemical properties of eADF4(C16) will be explained in the following section.

The amino acid sequence and recombinant production of eADF4(C16) was developed by Prof. Dr. Thomas Scheibel [1]. The protein consists of 16 repetitions of a protein sequence named module C.

GSSAAAAAAAAASGPGGYGPENQGPSGPGGYGPGGP

Figure 2.1. Amino acid sequence of the engineered module C of the spider silk protein eADF4(C16)

Important features can be derived from the primary structure displayed in Figure 2.1. Firstly, the protein is dominated by hydrophobic amino acid residues such as alanine or tyrosine, but hydrophobic blocks are interrupted in each case by hydrophilic side chains such as serine residues resulting in a mean hydropathicity of -0.464 [2]. Secondly, this spider silk protein does not contain any tryptophan residues. This is a very important fact for the separation from other foreign protein species during downstream processing. Thirdly, on account of its amino acid sequence, which includes glutamic acid as the only one charged amino acid residue per module C, eADF4(C16) has a theoretical isoelectric point of 3.48.

The entire protein eADF4(C16) has a molecular weight of 47.7 kDa and was provided by AMSilk GmbH (Martinsried, Germany) after downstream processing and subsequent drying of the final protein solution. Furthermore, at this point of development AMSilk provided the eADF4(C16) protein incorporating a T7-Tag (MASMTGGQMG). This tag was initially coupled to the protein in order to detect the protein in first vivo experiments. eADF4(C16) exhibits a molar extinction coefficient of $46,400 \text{ M}^{-1}\cdot\text{cm}^{-1}$ at 276 nm [2]. The extinction coefficient was used for the concentration determination by UV-spectroscopy which was carried out on an Agilent 8453 UV-VIS diode array spectrophotometer.

2.1.1.2 LYSOZYME

Lysozyme from chicken egg white was purchased as lyophilized powder from Sigma Aldrich (St. Louis, MO, USA). It is a single chain polypeptide of 129 amino acids and exhibits a molecular mass of 14,307 Da. The isoelectric point of lysozyme is 11.35 according to literature [3]. An extinction coefficient of E^{mM} (280 nm) = 36 was used for the calculation of lysozyme concentration by UV-spectroscopy (Agilent 8453 diode array spectrophotometer). The activity was declared to be $\geq 40,000$ units/mg protein, and aqueous solutions should retain their activity for at least one month when stored at 2-8°C [4].

2.1.1.3 NERVE GROWTH FACTOR

Recombinant human nerve growth factor (NGF) was a gift from Roche Diagnostics GmbH, Penzberg, Germany. Nerve growth factor plays an important physiological role in the development and maintenance of both sympathetic and sensory neurons and their neuronal extensions [5] as well as in the regeneration of lesioned peripheral nerves [6]. Therefore, it has been successfully applied in clinical trials (phase II) for the treatment of symptomatic diabetic polyneuropathy [7], but failed in clinical studies (phase III) to show significant beneficial effects [8]. For this reason Genentech stopped further development of NGF [9]. Interestingly, in recent years drug substances against NGF were developed. Tanezumab and other anti-NGF monoclonal antibodies show an analgesic effect and are under clinical investigation for the treatment of pain associated with osteoarthritis or other chronic pain conditions [10].

Nerve growth factor is the best characterized member of the neurotrophin family. Its crystal structure was described over 30 years ago and revealed that one end of the monomer carries a cysteine-knot motif consisting of three disulfide bonds [11]. This cysteine-knot stabilizes the fold and locks the molecules in their conformation. The biologically active form of NGF consists of two monomers which are arranged in a parallel manner to form a close-packed homodimer as illustrated in Figure 2.2, B. The residuals from the β -sheets (AB and CD in Figure 2.2, A) are responsible for the majority of interactions that stabilize the non-covalent dimer structure.



Figure 2.2. Monomer (A) and non-covalent homodimer (B) of human β -nerve growth factor [12]

The bulk drug substance contained NGF at a concentration of 0.5 mg/mL. The protein was formulated in 100 mM acetate buffer at pH 6.0 and stored at -80°C prior to use. Thawing was performed by submersing formulation aliquots of 50 mL, 15 mL or 2 mL into a water bath at ambient temperature and the formulations were used as described in the appropriate sections in this chapter. The molecular weight of the rhNGF monomer and dimer is approximately 13.5 kDa and 27 kDa, respectively. For UV-spectroscopy using an Agilent 8453 diode array photometer an extinction coefficient of $E^{1\text{mg/mL}}(280\text{ nm})=1.5$ was employed [13].

2.1.2 REAGENTS, CHEMICALS AND EXCIPIENTS

The following table gives an overview of all reagents, chemicals and excipients used throughout this work.

Table 2.1. Overview of used reagents, chemicals and excipients

Excipient	Description / Purity	Source
Di-potassium hydrogen phosphate	p.a.	AppliChem (Darmstadt, Germany)
D-Mannitol	p.a.	Boehringer Ingelheim (Ingelheim, Germany)
Ethacridine lactate monohydrate	Ph. Eur.	FAGRON GmbH & Co. KG (Barsbüttel, Germany)
FITC-albumin	From bovine albumin	Sigma Aldrich GmbH (Steinheim, Germany)
FITC-Dextran	Average molecular weight: 21.2 kDa	Sigma Aldrich GmbH (Steinheim, Germany)
Fluorescein isothiocyanate	Isomer I ≥ 90%	Sigma Aldrich GmbH (Steinheim, Germany)
Guanidine thiocyanate	For molecular biology	Sigma Aldrich GmbH (Steinheim, Germany)
HYDRANAL-Coulomat AG	-	Honeywell Riedel de Haen (Seelze, Germany)
Hydrochloric acid	1 mol/L	VWR International GmbH (Darmstadt, Germany)
Hydrochloric acid	32%	Honeywell Riedel de Haen (Seelze, Germany)
Methanol	HPLC grade	VWR International GmbH (Darmstadt, Germany)
Methyl violet	for microscopy, indicator (pH 0.1 – 2.0)	Sigma Aldrich GmbH (Steinheim, Germany)
Micrococcus lysodeikticus ATCC No. 4698	suitable for substrate for the assay of lysozyme	Sigma Aldrich GmbH (Steinheim, Germany)

Materials and methods

Potassium dihydrogen phosphate	p.a.	Merck KGaA (Darmstadt, Germany)
Potassium hydroxide solution	50%	Sigma Aldrich GmbH (Steinheim, Germany)
Propranolol hydrochloride	Ph. Eur.	FAGRON GmbH & Co. KG (Barsbüttel, Germany)
Rhodamine B	p.a., $\geq 90\%$	Merck KGaA (Darmstadt, Germany)
Sodium dodecyl sulphate	$\geq 99.0\%$	Sigma Aldrich GmbH (Steinheim, Germany)
Sodium hydroxide	1 mol/L	VWR International GmbH (Darmstadt, Germany)
Sucrose	p.a.	Boehringer Ingelheim (Ingelheim, Germany)
Trehalose dihydrate	High purity, low endotoxin	Ferro Pfanstiehl Lab., Inc (Waukegan, IL, USA)
Trifluoroacetic acid	p.a.	Merck KGaA (Darmstadt, Germany)
Trizma [®] base	$\geq 99.9\%$	Sigma Aldrich GmbH (Steinheim, Germany)

2.2 METHODS APPLIED FOR SPIDER SILK PROTEIN AND SPIDER SILK PARTICLES

2.2.1 PREPARATION OF LIQUID eADF4(C16) FORMULATIONS

The spider silk protein eADF4(C16) was provided by AMSilk GmbH as a fairly free-flowing powder with a white to slightly brownish color. Drying of the purified protein solution was the final process at the laboratories of AMSilk and was changed from freeze-drying in the beginning to spray-drying due to improved dissolution of the obtained protein powder. Nevertheless, dissolving dried eADF4(C16) protein in aqueous buffer solutions at sufficiently high concentrations was almost impossible or at least too time-consuming for routinely performed processes. Therefore, 6 M Guanidine thiocyanate solutions were used to dissolve dried protein by employing gentle agitation or heating to 40°C. For further processing the denaturing agent had to be removed. Dialysis was performed at 4°C against 10 mM Tris(hydroxymethyl)aminomethane(=Tris)/HCl at pH 8.0 using Spectra/Por® 1 dialysis membranes with a molecular weight cut-off of 6,000-8,000 Da (Spectrum Laboratories Inc., Rancho Dominguez, USA). The buffer was exchanged three times and the overall dialysis time was 24 hours. The resulting protein solution usually contained small amounts of visible particles which were removed by centrifugation at 10,000-15,000 g for a minimum of 15 minutes. The final step of the preparation process was filtration of the supernatant through a 0.45 µm or 0.22 µm cellulose acetate filter membrane (VWR International GmbH, Darmstadt, Germany). The concentration was determined according to section 2.1.1.1 by UV-spectroscopy.

2.2.2 CHARACTERIZATION OF LIQUID eADF4(C16) FORMULATIONS

2.2.2.1 ASYMMETRICAL FLOW FIELD-FLOW FRACTIONATION

A suitable separation method for spider silk proteins such as AF4 was developed to investigate the state of dissolved eADF4(C16) prior to particle preparation. The separation principles of AF4 are reviewed elsewhere [14, 15]. The AF4 system consisted of the main device AF2000 Focus from Postnova Analytics GmbH (Landsberg am Lech, Germany) including focus and tip pump PN 1122, slot pump PN 1610, vacuum degasser PN 7505 and refractive index detector PN 3150. Further components were a SPD-10A UV-detector from Shimadzu (Duisburg, Germany) and a miniDAWN light scattering detector from Wyatt Technology (Dernbach, Germany). The AF4 channel was also produced by Postnova Analytics and had dimensions of 32.0 x 6.0 x 3.7 cm.

For the separation of eADF4(C16) samples this AF4 channel was equipped with a 350 µm spacer and a fixed detection flow rate of 1.0 mL/min was used. The mobile phase was equal

to the formulation buffer using a 10 mM Tris-buffer at pH 8.0 in order to avoid any influence of the mobile phase during separation. During method development different membrane types and cut-offs were evaluated and the amount of injected spider silk protein was varied from 4 to 60 µg. New membranes were always saturated with BSA before sample analysis was performed. An important difference to HP-SEC analysis was that samples were not centrifuged prior to injection. For data analysis the ASTRA software (Wyatt Technology, Dernbach, Germany), an extinction coefficient of $972 \text{ mL} \cdot \text{g}^{-1} \cdot \text{cm}^{-1}$ at 280 nm, and a differential index of refraction (dn/dc) of 0.185 for eADF4(C16) were used.

2.2.2.2 INCUBATION AT ELEVATED TEMPERATURE

Based on the implementation of higher process temperatures during particle preparation (see section 2.2.3.1), the physical stability of eADF4(C16) at higher temperatures was investigated. For this reason, the most commonly used eADF4(C16) formulation consisting of 1.0 mg/mL eADF4(C16) in 10 mM Tris / pH 8.0 was analyzed. 500 µL of the formulation were filled into 2.0 mL polypropylene tubes and incubated at 80°C for 4 hours. Afterwards, 200 µL of the samples were drawn and diluted with formulation buffer to a volume of 2.0 mL to perform turbidity and light obscuration measurements. The residual formulation was centrifuged and used for size exclusion chromatography.

2.2.2.3 SIZE EXCLUSION CHROMATOGRAPHY

After removing potential insoluble aggregates by centrifugation, the supernatants of the corresponding formulations were analyzed by size exclusion chromatography. The separation was carried out on a Shodex OHpak SB-803 column which was made of a polyhydroxymethacrylate matrix and can be used for alkaline running buffers up to pH 10 in contrast to silica-based columns. As mobile phase 100 mM Tris at pH 8.0 was used at a flow rate of 0.38 mL/min. The column was installed in the aforementioned AF4-system replacing the AF4 channel (see section 2.2.2.1). For elution mode during HP-SEC only the tip pump of the system was necessary. All three detectors were available for the calculation of protein content and molar mass of the eluted protein species.

2.2.2.4 SODIUM DODECYL SULPHATE POLYACRYLAMIDE GEL ELECTROPHORESIS

In order to obtain further information about potential spider silk protein aggregates SDS-PAGE was performed under non-reducing conditions. Samples were loaded on NuPAGE® 10% Bis-Tris precast gels (Life technologies GmbH, Darmstadt, Germany), which had been mounted in the XCell II Mini cell system (Novex, San Diego, CA, USA). The sample preparation included the dilution of the samples to an approximate protein

concentration of 0.025 mg/mL in a Tris-buffer at pH 6.8 and the denaturation of the samples at 95°C for 20 minutes. Finally, 10 µL of each sample were loaded into the different wells of the gel. Separation was carried out at a current of 40 mA per gel and the runtime was about 90 minutes. Silver staining was carried out by using the SilverXPRESS® Staining Kit (Invitrogen, Carlsbad, CA, USA). A protein standard (Mark 12® Unstained Standard, Invitrogen, Carlsbad, CA, USA) was loaded onto the gel for the assessment of the molecular weight of protein species.

2.2.2.5 NEPHELOMETRY

The turbidity of spider silk protein formulations after incubation at 80°C was determined using a NEPHLA nephelometer (Dr. Lange, Düsseldorf, Germany). Turbidity was measured in formazine nephelometric units (FNU) by 90° light scattering at a wavelength of 860 nm. Each value represents the average of two measurements to exclude unspecific scattering effects by rotating the cuvette. As the required measurement volume is almost 2.0 mL, formulations were diluted 1:10 with formulation buffer before measurement.

2.2.2.6 LIGHT OBSCURATION

The size and amount of particles between 1 and 200 µm was measured by light obscuration on a SVSS C-40 apparatus equipped with a HCB-LD-25/25 sensor (PAMAS GmbH, Rutesheim, Germany). The light obscuration system was cleaned with highly purified water which had been filtered through a 0.22 µm filter membrane and was essentially free from particles. Cleaning was performed until the total particle count per mL was below 100 and less than 5 particles larger than 10 µm were detected. This cleaning step was performed and recorded before and in between the individual measurements after flushing the system with 5 mL highly purified water.

The light obscuration measurements were performed subsequent to the turbidity measurements. 0.5 mL of the sample was used for flushing the system. Afterwards, three aliquots of 0.3 mL sample volume were analyzed for subvisible particles. The average value of the three aliquots was calculated and related to the total particle number in 1.0 mL. Typically, the range of subvisible particles is divided into three classes of particle sizes: $\geq 1 \mu\text{m}$, $\geq 10 \mu\text{m}$ and $\geq 25 \mu\text{m}$.

2.2.3 PREPARATION OF eADF4(C16) PARTICLES

This section provides an overview of different techniques and devices applied for the preparation of spider silk particles resulting in liquid and dried formulations. As the optimization and results of the individual techniques will be explained in detail in chapter 3, the following descriptions are limited to brief explanations of the employed procedures and devices.

2.2.3.1 MICROMIXING SYSTEM

A syringe pump system consisting of two identical syringe pumps (model 100 DX, Teledyne Isco Inc., USA) and a digital control element (Series D, Teledyne Isco Inc., USA) were implemented for the preparation of particle dispersions with batch sizes of up to a total volume of 200 mL. The dead volume of each pump is approx. 2 mL and the required filling volume for an acceptable particle preparation especially at high flow rates is about 15 - 20 mL. The digital regulation controlling the flow rate of each pump can be set separately. For our purpose an equal flow rate was used for both pumps in between a range of 1.0 to 50 mL/min. The syringe pump system included a heating jacket for both pumps which was tempered between 20 and 80°C using a bath circulator SC100-A10 (Thermo Scientific, Karlsruhe, Germany) as required. One syringe pump was filled with the eADF4(C16) solution (preheated if necessary) (10 mM Tris, pH 8.0). The concentration of the spider silk protein ranged from 0.5 to 2.0 mg/mL. The second pump was filled with a sterile-filtered salt solution. Once the salt solution comes into contact with the spider silk solution, particles are formed due to a phase separation process (see chapter 3, section 3.1) [16]. In the case of the standard operation procedure (SOP), this salt solution was a 2 M potassium phosphate solution at pH 8.0. During process development also 2 M ammonium sulfate (pH 8) was used. Micromixing and precipitation of the particles was performed by connecting the syringe pumps via a T-shaped mixing element with a circular mixing zone. To investigate the impact of the mixing zone on the particle characteristics, an inner diameter of 0.50 mm (P-727 PEEK tee, Upchurch Scientific, Oak Harbor, USA) was compared to a diameter of 1.25 mm (P-728 PEEK tee, Upchurch Scientific, Oak Harbor, USA). The P-727 PEEK tee with the smaller inner diameter (0.50 mm) was used in the SOP.

The resulting spider silk particle suspensions were collected via the third outlet port of the mixing element, subsequently centrifuged (different speeds used for different particle sizes), and excessively washed with purified water.

2.2.3.2 DIALYSIS

The eADF4(C16) solution at a concentration of 1.0 mg/mL was dialyzed against 2 M potassium phosphate (pH 8.0) in a volumetric ratio of 1:50 at room temperature using Spectra/Por® 1 dialysis membrane with a molecular weight cut-off of 6,000-8,000 Da (Spectrum Laboratories Inc., Rancho Dominguez, USA). Afterwards, the spider silk particle suspension was excessively washed with purified water to remove the residual potassium phosphate.

2.2.3.3 ULTRASONIC NOZZLE

An ultrasonic nozzle was employed in order to establish an additional process for the preparation of spider silk particles. The ultrasonic nozzle operates at a specific resonance frequency of 120 kHz generated by a broadband ultrasonic generator (Sono-Tek Corporation, Milton, NY, USA). The nozzle is equipped with a dual liquid feed option bearing a maximum of 10.28 mL/min for the inner and 9.44 mL/min for the outer outlet. The characteristic fine mist spray is created at the atomizing surface of the nozzle tip as it is illustrated in Figure 2.3. In order to atomize the liquid, the vibrational amplitude of the atomizing surface must be carefully controlled. Below the so-called critical amplitude, the energy is insufficient to produce atomized drops. If the amplitude is excessively high, the liquid is ripped apart and large chunks of fluid are ejected. Only within a narrow band of input power is the amplitude ideal for producing the characteristic fine, low velocity mist. According to the manual and with respect to the maximum capacity of 5 W, the optimal input power for atomizing water was validated as 0.8 W. The input power was adjusted in the course of the preliminary tests to 1.6 W which ensured an appropriate spraying pattern for the potassium phosphate solution and low-concentrated protein solutions. High-concentrated protein solutions (> 5 mg/mL) required different settings of the input power up to 4.5 W. For liquid delivery both inlets of the nozzle were connected to an Ismatec® IPC peristaltic pump (IDEX Health & Science GmbH, Wertheim-Mondfeld, Germany).

Different setups were tested regarding the feasibility to produce spider silk particles. In the first experiment the dual liquid feed option was applied and the eADF4(C16) solution was atomized via the inner and a potassium phosphate solution (pH 8.0) via the outer outlet. In a second experiment, phase separation was induced by spraying the aqueous eADF4(C16) solution into 2 M potassium phosphate (pH 8.0) or vice versa. Throughout the experiments different parameters and their impact on the resulting particle characteristics were investigated: eADF4(C16) concentration, potassium phosphate concentration, temperature of both solutions and amount of liquid atomized per unit time (= flow rate of the peristaltic pump) (listed in chapter 3, Table 3.2).



Figure 2.3. Atomization of water at the tip (flat shaped) of the employed ultrasonic nozzle operating at 120 kHz and a spraying rate of 3 mL/min

2.2.3.4 ULTRASONIC TREATMENT AND PURIFICATION

Spider silk particles always showed severe agglomeration after the preparation and washing process as a result of the high salt concentration being present immediately after particle formation. Therefore, aqueous eADF4(C16) particle dispersions were subjected to an ultrasonic treatment. Throughout the work Sonopuls HD 2200 (Bandelin electronic, Berlin, Germany) in the laboratory of Prof. Vollmar, Pharmaceutical Biology, LMU Munich, and a Sonopuls HD 3200 (Bandelin electronic, Berlin, Germany) were used. The duration of the ultrasound treatment did not exceed 15 minutes.

If the eADF4(C16) particles exhibited a particle size below 1 μm , the resulting particle suspension was filtered through 5 μm syringe filters with a surfactant-free cellulose acetate membrane (Minisart[®] NML, Sartorius Stedim Biotech GmbH, Goettingen, Germany) in order to remove any residual agglomerates.

Particles obtained by dialysis and via spraying techniques were also subjected to the ultrasonic treatment, but were not filtered afterwards.

2.2.3.5 GRAVIMETRICAL DETERMINATION OF PARTICLE CONCENTRATION

The eADF4(C16) particle concentration of all suspensions in pure water was determined gravimetrically. For that purpose, aliquots in the range of 50-100 μL were transferred into small aluminum cups and dried at 80°C for a minimum of 3 hours. The concentration was calculated using a minimum of three cups per formulation and the following equation:

$$\text{conc. eADF4(C16) particles} = \frac{m(\text{particles})}{\text{mL}(\text{water})} = \frac{m(\text{cup, dried}) - m(\text{cup, blank})}{(m(\text{cup, susp}) - m(\text{cup, blank}) - m(\text{particles})) / 1 \frac{\text{g}}{\text{mL}}}$$

2.2.3.6 FREEZE-DRYING OF NANOSUSPENSIONS

As suspensions of nanoparticles without further formulation additives usually lack long-term colloidal stability, freeze-drying of suspensions containing eADF4(C16) particles within the nanometer range was performed.

Sucrose, trehalose and mannitol were investigated as excipients for freeze-drying of eADF4(C16) particles. The employed formulations (listed in chapter 3, Table 3.3) were prepared by mixing empty or lysozyme-loaded eADF4(C16) particles with aqueous solutions of the corresponding freeze-drying excipient. Loading of spider silk particles with 15% [w/w] lysozyme was carried out as described in section 2.2.5. The particle concentration of all formulations was set to 1.0 mg/mL. The excipient-to-eADF4(C16) particles mass ratio was varied from 2.5:1 to 50:1. Consequently, the total solid content of the formulations ranged from 0.35 to 5.1% [w/V]. For experiments including lysozyme-loaded eADF4(C16) particles, the same excipient-to-eADF4(C16) particle mass ratio without accounting for the loaded lysozyme amount was used. Particle dispersions were immediately transferred to cleaned 2R glass vials (Schott AG, Mainz, Germany) using a multipette. All samples were freeze-dried in an EPSILON 2 6D pilot scale freeze-dryer (Martin Christ Freeze Dryers GmbH, Osterode, Germany). The formulations were dried as follows: After freezing samples at -50°C for 3 hours (-40°C for sucrose samples with 1.0 mL filling volume), the chamber pressure was reduced to 0.05 mbar. Primary drying included a temperature ramp increasing from -50°C to -20°C during 5 hours and drying at -20°C for another 10 hours. After the shelf temperature was constantly increased from -20°C to 20°C over three hours, secondary drying was conducted at 20°C for 10 hours. Upon completion of the freeze-drying cycle, the drying chamber was vented with nitrogen and vials were plugged under slight vacuum at 800 mbar. Unless stated otherwise, the samples were stored at 2-8°C after drying before analysis. For reconstitution of lyophilized samples, purified water was used to end up with the the original filling volume. In addition, for formulations containing sucrose reconstitution at lower volumes was tested in order to concentrate the resulting particle suspension (see chapter 3, Table 3.3).

2.2.4 CHARACTERIZATION OF eADF4(C16) PARTICLES

2.2.4.1 DYNAMIC LIGHT SCATTERING

The eADF4(C16) particle size represented by the Z-average value and the width of the particle size distribution expressed by the polydispersity index (PI) were determined by dynamic light scattering (DLS) using a Zetasizer Nano ZS (Malvern Instruments, Worcestershire, UK). All samples were diluted directly before the measurement to a concentration of 0.01 mg/mL in the corresponding buffer and filled into disposable PMMA

cuvettes. Each measurement consisted of three runs of at least 10 subruns and was started after an equilibration time of 90 seconds at 25°C. The measurement principles as well as limitations of this technique are summarized elsewhere [17].

The zeta-potential of eADF4(C16) particles was equally determined with the Zetasizer Nano ZS at the same particle concentration and temperature as used for particle size measurements, but measurements required the use of the disposable capillary cell (DTS1061, Malvern Instruments, Worcestershire, UK).

The Zetasizer Nano ZS was equipped with the MPT-2 Autotitrator (Malvern Instruments, Worcestershire, UK) which allows the automatic determination of particle size and zeta-potential as a function of pH, conductivity and other parameters. One important application of this setup is the determination of the isoelectric point of particles or protein molecules by DLS which was employed in this work for eADF4(C16) particles, lysozyme and nerve growth factor. As the zeta-potential is strongly dependent on the dispersion medium, a constant background of 10 mM sodium chloride was chosen for these measurements. The pH was adjusted by automatic titration of 0.25 M hydrochloric acid or sodium hydroxide to the sample solution. In order to avoid aggregation the starting point of each titration was set at the opposite pH range of the IEP, that means that e.g. the titration of eADF4(C16) particles with an estimated IEP around 4 started above the IEP (pH 9) and finished at pH 2. A concentration of 0.25 mg/mL was used for eADF4(C16) particles, whereas lysozyme was directly dissolved at 10 mg/mL in the dispersion medium. NGF was concentrated to 4.4 mg/mL after dialysis using VIVASPIN 20 centrifugal concentrators with a PES membrane and a MWCO of 5,000 Da (Sartorius Stedim Biotech GmbH, Goettingen, Germany). Particle size and zeta-potential were determined in intervals of 0.5 pH-values at 25°C. The isoelectric point was calculated after the titration by the Zetasizer APS software (Malvern Instruments, Worcestershire, UK).

2.2.4.2 LASER DIFFRACTION

The size and size distribution of eADF4(C16) particles were determined by static light scattering or also called laser diffraction spectrometry (Horiba Practica LA-950, Horiba Scientific, Japan). Refractive indices of 1.33 for water and 1.60 for eADF4(C16) were used for the calculation of particle sizes and their distribution. The device is equipped with two different lasers (405 and 650 nm), one detector in forward direction, and 23 separate wide angle detectors (side and reverse direction) so that particle sizes from 0.01 – 3000 µm can be measured [18]. This technique was primarily used for spider silk particles in the range from 0.5 to 10 µm throughout this work. All results from laser diffraction were obtained from volume based distributions if not otherwise stated.

2.2.4.3 FOURIER TRANSFORMED INFRARED SPECTROSCOPY

A small droplet of particle dispersion was vacuum-dried on a CaF₂-crystal. Measurements were conducted in transmission mode using a Tensor 27 spectrometer with the Hyperion microscope (Bruker Optik GmbH, Ettlingen, Germany). Background measurements of the CaF₂-crystal were carried out before measurement of each sample. Opus software Version 6.5 was used for data analysis.

2.2.4.4 SCANNING ELECTRON MICROSCOPY

eADF4(C16) particles were immobilized by vacuum drying on Thermanox™ coverslips (Thermo Scientific/Nunc, Langensfeld, Germany), which were stucked on Leit-Tabs (Plano GmbH, Wetzlar, Germany) and connected with a conductive copper tape (Plano GmbH, Wetzlar, Germany) to the sample holder. Samples were carbon sputtered under vacuum and analyzed by a Joel JSM-6500F field emission scanning electron microscope (Joel Inc., Peabody, USA).

2.2.4.5 COLLOIDAL STABILITY OF eADF4(C16) PARTICLES

The colloidal stability of eADF4(C16) particles was studied at three different pH (3, 5 and 7) at constant ionic strength of 30 mM and at different ionic strength (30 mM, 60 mM, 100 mM and 154 mM) at constant pH of 5 and 7, respectively. All buffers were prepared at concentrations of 10 mM and the ionic strength was adjusted with sodium chloride. The particle concentration was set to 0.25 mg/mL after centrifugation of the stock dispersion and samples with a total volume of 1.0 mL were allowed to stand at room temperature without agitation. Samples were analyzed directly after redispersion as well as after one hour and 24 hours for particle size, size distribution and zeta-potential using the Zetasizer Nano ZS as described in sections 2.2.4.1. Storage stability of the eADF4(C16) stock dispersion in purified water was investigated at 2-8°C over a period of 6 months.

2.2.4.6 DETERMINATION OF RESIDUAL MOISTURE

Residual moisture of lyophilized samples was measured by using an Aqua 40.00 titrator comprising a headspace module (Analytik Jena AG, Halle, Germany). Samples were analyzed either directly using the original vial from freeze-drying or after sample preparation in a dry-nitrogen-purged glove box to avoid hydration resulting from atmosphere. The net weight of the analyzed samples ranged from 1 to 51 mg. In order to obtain reliable results blank values were obtained from empty vials which were identically treated to the verum samples. For the measurement the sample vials was placed in the headspace module and

heated up to 80°C. The evaporated water was evacuated by a needle system and transferred into the titration solution where the amount of water was automatically determined by Karl Fischer titration.

The obtained results from the headspace module were cross-checked with results derived from methanol extraction and subsequent Karl Fischer titration. No significant difference was detected.

2.2.4.7 DIFFERENTIAL SCANNING CALORIMETRY

A Netzsch 204 Phoenix[®] DSC (Netzsch-Gerätebau GmbH, Selb, Germany) was used for determination of the glass transition temperature of the maximally freeze-concentrated solution (T_g'), the glass transition temperature of the amorphous matrix (T_g) and melting point (mp) of mannitol.

Table 2.2. DSC temperature programs for sucrose, trehalose and mannitol

sucrose + trehalose				mannitol	
T_g'		T_g		$T_g + mp$	
T [°C]	time heating rate	T [°C]	time heating rate	T [°C]	time heating rate
20	1 min	0	1 min	0	1 min
20 → -70	5 K/min	0 → 80	10 K/min	0 → 80	10 K/min
-70	1 min	80	1 min	80	1 min
-70 → 20	10 K/min	80 → 20	10 K/min	80 → -10	10 K/min
		-20	1 min	-10	1 min
		-20 → 180	10 K/min	-10 → 180	10 K/min
		180	1 min	180	1 min
		180 → 20	10 K/min	180 → 20	10 K/min

For the measurement of T_g' 20 μ L of the formulation were analyzed in crimped aluminum crucibles. After lyophilization, hydration of the dried samples had to be avoided. Therefore, sample preparation was carried out in a dry-nitrogen-purged glove box. The relative humidity during sample preparation was kept below 10%. Sample amounts of 2 to 6 mg were used for the measurements and two samples of each formulation were analyzed regarding T_g or mp. Both values were calculated with the Netzsch Proteus[®] Software whereupon the point of inflection and the onset temperature were determined as T_g and mp, respectively. The different temperature programs are listed in Table 2.2.

2.5 REMOTE LOADING OF SPIDER SILK PARTICLES

This section refers to the loading of eADF4(C16) particles after particle preparation which is further called remote loading of spider silk particles.

2.2.5.1 LOADING PROCEDURE

Loading of eADF4(C16) particles was performed with different kind of drugs such as low molecular weight drugs on the basis of previous studies [19] and proteins like lysozyme and nerve growth factor. If not otherwise stated, the so-called standard loading procedure was carried out in a loading buffer comprising 10 mM phosphate buffer at pH 7.0 and a total ionic strength of 30 mM adjusted with sodium chloride. In additional studies loading buffers exhibiting different total ionic strengths of 60 mM and 100 mM (adjusted with sodium chloride) were prepared in order to investigate the influence of ionic strength on the loading efficiency.

The loading procedure was implemented as follows: A stock dispersion of spider silk particles in purified water was centrifuged (15,000 g, 30 min) and redispersed in the desired buffer media before loading. A second stock solution comprising the appropriate drug was prepared by dissolving the drug in the identical buffer solution or by dialysis (NGF). Appropriate volumes of spider silk particle suspension and drug stock solution were mixed to obtain a final spider silk particle concentration of 0.5 mg/mL and the desired w/w-ratio [%] of drug to spider silk particles. After 30 minutes of incubation at room temperature under gentle agitation (horizontal shaker with 40 rpm (GFL 3015, Burgwedel, Germany)), 20 μ L of the particle suspension were used for dynamic light scattering measurements. Simultaneously, samples were centrifuged (15,000 g, 30 min) and the supernatant was analyzed for residual drug content (see section 2.2.5.2).

2.2.5.2 DETERMINATION OF LOADING AND LOADING EFFICIENCY

In order to determine the amount of drug loaded onto eADF4(C16) particles the supernatant obtained after centrifugation was analyzed for residual drug content.

Low molecular weight drugs

The sensitivity of UV-spectroscopy was sufficiently high to allow for the quantification of low molecular weight drugs via common UV-spectroscopy. The characteristics of the employed substances are listed in Table 2.3.

Table 2.3. Characteristics of employed low molecular weight drugs

Drug molecule	M _w [Da]	A _{max} [nm]	pK _a
Methyl violet 2B	408.0	590	N.A.
Ethacridine lactate * 1H ₂ O	361.4	365	11.04
Propranolol hydrochloride	295.8	290	9.46

Lysozyme and nerve growth factor

In case of lysozyme and nerve growth factor more sensitive methods had to be employed for protein quantification at low concentrations of several $\mu\text{g/mL}$. Therefore, the Micro BCA Protein Assay Kit (Thermo Scientific, Rockford, USA) was used. A standard calibration curve for both proteins in the corresponding buffer allowed the quantification of the protein concentration in the range from 0.5 - 40 $\mu\text{g/mL}$. Nevertheless, it had to be proven that no dissolved spider silk protein interferes the quantification for which reason control groups of empty eADF4(C16) particles were included. Furthermore, size exclusion chromatography of lysozyme and NGF containing supernatants was performed to quantify the residual protein and to prove in particular the absence of soluble spider silk protein. Both HP-SEC methods will be explained in section 2.2.7.3 and 2.3.2.1 of this chapter.

Loading efficiencies [%, w/w] and loading [%, w/w] were determined using equation (1) and (2), respectively.

$$\text{Loading efficiency [\%]} = \frac{\text{lysozyme loaded on eADF4(C16) particles } [\mu\text{g}]}{\text{lysozyme initially added } [\mu\text{g}]} \times 100 \quad (1)$$

$$\text{Loading [\%]} = \frac{\text{lysozyme loaded on eADF4(C16) particles } [\mu\text{g}]}{\text{eADF4(C16) particles } [\mu\text{g}]} \times 100 \quad (2)$$

2.2.5.3 CONFOCAL LASER SCANNING MICROSCOPY

For the detailed analysis of the loading mechanism, eADF4(C16) particles were prepared by dialysis and loaded with FITC-labeled albumin, FITC-dextran and FITC-labeled lysozyme. The latter was prepared as described previously [20]. Briefly, 225 mg lysozyme and 9 mg fluorescein isothiocyanate (Isomer I) were dissolved in 45 mL of 100 mM borate buffer (pH 8.5). The fluorescein isothiocyanate solution was added dropwise to the stirred lysozyme solution and the complete mixture was stirred for another 16 hours at room temperature. The solution was afterwards extensively dialyzed against purified water to remove unbound fluorescein isothiocyanate. The resulting FITC-lysozyme solution was freeze-dried using a conservative freeze-drying protocol.

eADF4(C16) particles obtained by dialysis were remote loaded (see section 2.2.5) with three different types of FITC-labeled macromolecules both at pH 2.0 (10 mM phosphate, 30 mM

ionic strength) and pH 7.0 (10 mM phosphate, 30 mM ionic strength). The FITC-labeled macromolecules were dissolved in the same buffer as employed for the loading procedure. In all cases the w/w-ratio of the FITC-labeled macromolecule to the spider silk particles was set to 15% [w/V] at a fixed eADF4(C16) particle concentration of 2.0 mg/mL. All samples were investigated in the liquid state with a confocal scanning laser microscope (Zeiss LSM 510 Meta, Carl Zeiss Microscope Systems, Jena, Germany).

2.2.6 ENCAPSULATION OF DRUGS INTO SPIDER SILK PARTICLES

In contrast to remote loading of spider silk particles drugs can be also co-precipitated during particle preparation in order to encapsulate the drug in the spider silk matrix. Two different drugs were employed in this study, namely Rhodamine B as low molecular weight substance, and lysozyme as model protein.

Spider silk particles were prepared by phase separation using an eADF4(C16) solution in 10 mM Tris pH 8 and 2 M potassium phosphate pH 8 as described in section 2.2.3. By doing this it is in principle possible to add the drug both to the spider silk protein solution or the 2 M potassium phosphate solution in order to co-precipitate the drug. However, the drugs were mixed solely with the spider silk protein prior to co-precipitation.

2.2.6.1. CO-PRECIPIATION OF RHODAMINE B

The main objective of this experiment was the clarification if uncharged molecules at the employed pH can be incorporated at significant amounts by co-precipitation. Thus, Rhodamine B was added to the aqueous eADF4(C16) solution with a protein concentration of 1.0 mg/mL at mass ratios of 0 / 1 / 2.5 / 5 / 7.5 / 10 / 15 and 30% [w/w] with regard to the mass of spider silk protein. 0.5 mL of this solution comprising eADF4(C16) and Rhodamine B was prepared immediately before phase separation was carried out by mixing it with 0.5 mL of a 2 M potassium phosphate at pH 8.0. The resulting particle suspension was centrifuged (15,000 g, 30 min), washed three times with purified water and subjected to ultrasonic treatment before DLS measurements were performed. The supernatants were collected and analyzed by UV-spectroscopy for Rhodamine B content. This easy determination by UV-spectroscopy was possible due to sufficiently different absorption maxima of Rhodamine B and eADF4(C16). Loading and loading efficiencies were calculated according to equation (1) and (2) explained in section 2.2.5.2.

2.2.6.2 CO-PRECIPIATION OF LYSOZYME

It was not possible to dissolve lysozyme at the required concentrations in a 2 M potassium phosphate solution so that co-precipitation was only performed by adding lysozyme to the

aqueous eADF4(C16) solution. In order to evaluate the impact of particle size on the resulting drug release lysozyme was co-precipitated at conditions where nanoparticles and microparticles were formed.

Preparation of lysozyme-loaded nanoparticles

Lysozyme was added to an eADF4(C16) solution at a concentration of 1.0 mg/mL at mass ratios of 0 / 5 / 10 / 30 / 50 / 100 and 200% [w/w] with regard to the mass of spider silk protein. 2.0 mL of the spider silk solution containing lysozyme were prepared by dissolving lysozyme directly in 10 mM Tris-buffer at pH 8.0 and mixing the required amounts of lysozyme with the spider silk solution directly before precipitation was performed. Due to the small volumes and large sample number precipitation was conducted not via the syringe pumps but using a 10 mL pipette. 2.0 mL of 2 M potassium phosphate solution were provided in 8 mL polypropylene tubes (VWR International GmbH, Darmstadt, Germany) and the same volume of eADF4(C16)/lysozyme solution was added by intense mixing. Spider silk particles were formed immediately and subsequently centrifuged (15,000 g, 30 min). The obtained supernatant was analyzed for lysozyme and eADF4(C16) content, whereas the pellet was washed 3 times with purified water to remove salt and protein residuals. Each particle suspension was subjected to an ultrasonic treatment (2 minutes, 20% amplitude, pulsation 5 sec / 1 sec) prior to DLS measurements.

Preparation of lysozyme-loaded microparticles

Lysozyme was added to an eADF4(C16) solution at a concentration of 10 mg/mL at mass ratios of 0 / 5 / 10 / 30 and 50% [w/w] with regard to the mass of spider silk protein. 3.0 mL of the spider silk solution containing lysozyme were prepared by dissolving lysozyme directly in 10 mM Tris-buffer at pH 8.0 and mixing the required amounts of lysozyme with the spider silk solution directly before particle preparation was performed. In order to obtain microparticles, the setup using an ultrasonic nozzle as described in section 2.2.3.3 was employed. The eADF4(C16)/lysozyme solution was provided in one well of a 6 well-plate. 3.0 mL of 2 M potassium phosphate solution were atomized into this solution via the ultrasonic nozzle at an atomization rate of 3 mL/min. The formed particles were subsequently centrifuged (10,000 g, 30 min). The obtained supernatant was analyzed for lysozyme and eADF4(C16) content, whereas the pellet was washed 3 times with purified water to remove salt and protein residuals. Each particle suspension was subjected to an ultrasonic treatment (2 minutes, 20% amplitude, pulsation 5 sec / 1 sec) prior to SLS measurements.

Quantification of lysozyme and eADF4(C16) content in the supernatants

So far the particle preparation yield had always been at least 99%. Thus, the amount of eADF4(C16) in the supernatant would be negligible, but the impact of other proteins on the

phase separation process was unknown. The quantification of lysozyme in a potential presence of eADF4(C16) was performed by UV-spectroscopy at 280 nm, but as a prerequisite the absence of eADF4(C16) in the supernatant had to be demonstrated. For this reason, SDS-PAGE was carried out. Lysozyme and eADF4(C16) standards were included and the supernatants obtained after the first centrifugation step were diluted to a lysozyme concentration of 50 µg/mL. All supernatants including those from washing steps were analyzed and loading and loading efficiencies were calculated according to equation (1) and (2) explained in section 2.2.5.2.

2.2.7 *IN VITRO* RELEASE FROM SPIDER SILK PARTICLES

2.2.7.1 EXPERIMENTAL SETUP

All *in vitro* release experiments were conducted at 37°C and at an eADF4(C16) particle concentration of 1.0 mg/mL. The pellet with loaded particles was resuspended in polypropylene tubes (1.5 or 2.0 mL total volume, VWR International GmbH, Darmstadt, Germany) with 37°C preheated release medium. At predetermined time points the medium was almost completely removed after centrifugation (15,000 g, 30 min) and replaced with 980 µL of fresh release medium. The supernatant was analyzed for drug content using different methods as described in the following sections. The percentage of cumulative drug release was examined as a function of incubation time. Each release experiment was performed at least in triplicate.

Low molecular weight drugs

Spider silk particles were loaded with three different low molecular weight drugs, namely methyl violet, ethacridine lactate and propranolol-hydrochloride, at a payload of 10% [w/w]. The *in vitro* release for all three substances was investigated in the release medium consisting of 10 mM phosphate and 160 mM ionic strength at pH 7.4 (see Table 2.4). In the case of methyl violet the release medium at pH 7.4 was varied regarding its ionic strength to almost 0 (purified water), 50 mM and 100 mM. The samples were drawn every hour over a total period of 4 hours.

Lysozyme

The release of lysozyme was investigated as a function of pH and ionic strength of the release medium. All release experiments were conducted with a total theoretical payload of 15% [w/w] lysozyme. In order to examine the release mechanism non-physiological conditions such as pH 2 and pH 4 were included in the *in vitro* release studies. Lysozyme loaded eADF4(C16) particles were centrifuged after the loading procedure and redispersed in the corresponding type and volume of the release medium as listed in Table 2.4.

In order to evaluate the influence of total payload on the resulting release profile eADF4(C16) particles loaded with 5, 10 and 15% [w/w] lysozyme were prepared as described in section 2.2.5.1. After loading, the physiological release medium consisting of 10 mM phosphate and 160 mM ionic strength at pH 7.4 was used for investigation of lysozyme release.

In addition to the release setup using polypropylene tubes and centrifugation, the release of lysozyme was investigated using well-inserts. Wells of a 12 well-plate were filled with 1 mL of preheated release medium before placing a 12 well millicell hanging cell culture insert (0.4 μm , PET, Millipore, Germany). A pellet of loaded particles was resuspended with 500 μL of preheated release medium in a polypropylene tube. This volume was transferred and filled into the insert. The well plate was incubated at 37°C. After each hour inserts were taken out and release medium in the well was completely refreshed.

The *in vitro* release of co-precipitated lysozyme was investigated for nano- and microparticles prepared at a lysozyme to eADF4(C16) mass ratio of 10, 30 and 50%. A release medium comprising 10 mM phosphate and 160 mM ionic strength at pH 7.4 was used. The calculated payloads were set as 100% and the percentage of released lysozyme was determined using the activity assay for lysozyme as described in section 2.2.7.4.

Table 2.4. Experimental setup for the *in vitro* release studies of lysozyme from eADF4(C16) particles

eADF4(C16) particles [μg]	Lysozyme payload [μg]	Release medium
1000	150	pH 2.0 / 10 mM phosphate / ionic strength 50 mM
1000	150	pH 4.0 / 10 mM formate / ionic strength 50 mM
1000	150	pH 6.0 / 10 mM MES / ionic strength 50 mM
1000	150	pH 7.4 / 10 mM phosphate / ionic strength 50 mM
1000	150	pH ~ 7.4 / highly purified water (HPW)
1000	150	pH 7.4 / 10 mM phosphate / ionic strength 100 mM
1000	150	pH 7.4 / 10 mM phosphate / ionic strength 160 mM

Nerve growth factor

Based on the knowledge from results obtained for lysozyme, the *in vitro* release of NGF was investigated at pH 7.4 and the same variations in ionic strength namely 50 mM, 100 mM and 160 mM. NGF was loaded onto eADF4(C16) particles with a total payload of 2.5, 5 and 10% [w/w]. All other parameters were equal to those described for lysozyme. The amount of released NGF was determined by the Micro BCA Protein Assay Kit as described in section 2.2.7.2 and size exclusion chromatography (see section 2.3.2.1).

Release at physiological conditions including serum albumin

In order to further mimic physiological conditions albumin was integrated in the release medium at a concentration of 40 mg/mL. Human serum albumin as well as bovine serum albumin was employed and the release of methyl violet and lysozyme was investigated as described in this section. The concentration of methyl violet was determined by UV-spectroscopy, whereas the amount of released lysozyme was calculated using the activity assay (section 2.2.7.4) as the large excess of albumin interfered with the determination of lysozyme by size exclusion chromatography significantly.

2.2.7.2 MICRO BCA PROTEIN ASSAY

To determine the amount of lysozyme and nerve growth factor a Micro BCA protein assay (Thermo Scientific, Rockford, USA) was performed. 150 μ L of protein standard or sample material and 150 μ L of BCA reagent were filled into wells of a 96 well-plate. After 2 hours of incubation at 37°C the absorption of each well was measured photometrically by a microplate reader (BMG Labtech Fluostar Omega, Ortenberg, Germany). The amount of protein in the range of 0.5 – 40 μ g/mL was calculated using standard curves of both proteins in the corresponding release media.

2.2.7.3 SIZE EXCLUSION CHROMATOGRAPHY – LYSOZYME

The stability of released lysozyme was analyzed by size exclusion chromatography on a Dionex HPLC system (P680, ASI-100, UVD170, RF2000, Dionex Softron GmbH, Germering, Germany). Separation was performed using a Superose 12 10/300 GL column (GE Healthcare Europe GmbH, Freiburg, Germany) at a flow rate of 0.6 mL/min using 200 mM sodium phosphate at pH 6.8 as mobile phase. UV-detection was carried out at 215 nm and 280 nm. 100 μ L of the supernatant were injected and the protein was quantified by calibration curves of lysozyme standards dissolved in the corresponding release medium.

2.2.7.4 ACTIVITY ASSAY – LYSOZYME

The activity of lysozyme was determined by measuring the change of absorption of a *Micrococcus lysodeikticus* ATCC No. 4698 suspension at 450 nm. Due to the large number of samples the assay procedure was transferred from cuvettes with 1 cm path length to 96 well-plates using a microplate reader. For that purpose lyophilized cells were suspended in 66 mM phosphate buffer, pH 6.2, at a concentration of 0.5 mg/mL. The cell suspension was prepared freshly each day. 200 μ L of this suspension were provided in one well and 100 μ L sample volume was added. The measurement was started directly after sample addition and the absorption at 450 nm was determined over a period of 3 minutes in intervals

of 5 seconds. Nevertheless, for calculation of lysozyme activity only the slope of the first 60 seconds was determined by linear regression as this part of the assay shows an almost linear decrease in the range of 1 – 20 $\mu\text{g/mL}$. Based on this procedure, it was possible to measure eight samples simultaneously.

2.3 METHODS APPLIED FOR STUDIES WITH NERVE GROWTH FACTOR

2.3.1 FORCED DEGRADATION OF NERVE GROWTH FACTOR

In this study, spider silk particles were tested as a stabilizing excipient during forced degradation studies of nerve growth factor which has been shown to be an excellent protein molecule for loading onto eADF4(C16) particles. In order to evaluate the potential of spider silk particles to stabilize bound NGF molecules, different stress studies using a particle-free NGF formulation and eADF4(C16) suspensions loaded with different payloads of NGF were performed. A standard procedure had to be developed that allows for reproducible and gentle desorption of NGF from eADF4(C16) particles after the stress testing was performed.

2.3.1.1 EXPERIMENTAL SETUP

Four different NGF containing formulations with or without eADF4(C16) particles were prepared as shown in Table 2.5.

Table 2.5. Formulations used for the forced degradation of nerve growth factor

Sample	conc. NGF [mg/mL]	conc. eADF4(C16) particles [mg/mL]	NGF payload [%, m/m]
Particle-free NGF	0.5	0	0
0.5% eADF4(C16)	0.5	5	10
1% eADF4(C16)	0.5	10	5
2% eADF4(C16)	0.5	20	2.5

Preparation of particle-free NGF formulations

Appropriate aliquots of the NGF bulk solution were dialyzed against a buffer comprising 10 mM phosphate and adjusted with sodium chloride to a total ionic strength of 30 mM at pH 7.0. This buffer had been routinely used for the remote loading procedure (see section 2.2.5.1) and was used as formulation buffer in this study. The dialysis was performed over 24 hours at 4°C using a Cellu Sep T1 dialysis membrane with a nominal molecular weight cut off of 3,500 Da (Membrane Filtration Products Inc, Seguin, TX, USA). The buffer was exchanged three times. Afterwards, the solution was filtered through a 0.22 µm Acrodisc® syringe filter with PVDF membrane (Pall GmbH, Dreieich, Germany) and the protein concentration was determined by UV-spectroscopy. This formulation was used without further dilution or concentration steps. The concentrations of the resulting NGF solutions were in the range of 0.48 - 0.50 mg/mL. In order to obtain equal concentrations as in the spider silk particle containing formulations, 15 µL of water were placed in

polypropylene centrifugal tubes (2.0 mL, VWR International GmbH, Darmstadt, Germany) and 300 μ L of the NGF formulation were added.

Preparation of remote loaded NGF formulations

The appropriate volumes of the spider silk particle stock suspension (suspension medium: purified water) were transferred into polypropylene centrifugal tubes (2.0 mL, VWR International GmbH, Germany) and centrifuged at 15,000 g for at least 30 minutes. The clear supernatant was discarded with only a small residue of water remaining in the tubes (15 μ L). The particle pellet was resuspended using 300 μ L of the prepared NGF formulation and incubated for at least 30 minutes. This straightforward procedure was possible because it had been shown throughout the remote loading studies with NGF that at these given protein to eADF4(C16) ratios no residual protein could be detected in the supernatant. Therefore, all NGF molecules were loaded onto the spider silk particles before applying different stress methods.

2.3.1.2 DESORPTION PROCEDURE

Different procedures were evaluated in order to achieve a sufficient high desorption of NGF from the spider silk particles after the stress testing, whereas 80% desorption of the originally loaded NGF content was defined as target value. Due to the NGF concentration of 0.5 mg/mL, a dilution factor of 1:2 should not be exceeded. During this initial evaluation, the eADF4(C16) particle concentration was set to 5 mg/mL with a payload of 10% [w/w] NGF and the suspensions were mixed with equal volumes of the desorption solutions.

Finally, the desorption procedure was determined as follows: 300 μ L of a buffer solution (pH 8.0, 200 mM sodium phosphate, 800 mM sodium chloride) were added to all formulations (300 μ L) and the resulting mixtures were incubated for 30 minutes at 50°C and 600 rpm using a Thermomixer compact (Eppendorf, Hamburg, Germany). Subsequently, formulations containing spider silk particles were centrifuged at 15,000 g for 30 minutes. Thus, the final concentration was approx. 0.25 mg/mL. Samples which were treated according to this procedure are further referred as 'Liquid NGF WP'.

Particle-free formulations were mixed with 300 μ L loading buffer as a control. These samples are further referred as 'Liquid NGF FB'. The control samples were equally incubated at 50°C for 30 minutes in order to clarify the impact of the high salt concentration and higher pH of the solution required for desorption.

All samples were analyzed by size exclusion chromatography (see section 2.3.2.1), reversed phase chromatography (see section 2.3.2.2) and SDS-PAGE (see section 2.3.2.5). As the formulations comprising spider silk particles had to be centrifuged in order to obtain clear

supernatants, nephelometry (see section 2.3.2.3) and light obscuration (see section 2.3.2.4) measurements could be performed only for particle-free NGF samples.

2.3.1.3 FREEZE-THAW STRESS

Samples were prepared by filling the total volume (approx. 315 μ L) of the respective formulation into 2.0 mL polypropylenes tubes. The tubes were immersed into liquid nitrogen for 5 min to ensure complete freezing of the samples. To thaw the samples tubes were kept in a Thermomixer compact (Eppendorf, Hamburg, Germany) for 15 min at 25°C without agitation. The freeze-thaw cycles were repeated 5, 10 and 15 times. Afterwards, samples were drawn from the tubes and the desorption procedure as described in section 2.3.1.2 was carried out.

2.3.1.4 STIRRING

Stirring stress onto the NGF formulations was performed at a constant stirring speed of 400 rpm by placing glass vials with screw caps (max. filling volume: 1.5 mL; VWR International GmbH, Darmstadt, Germany) vertically onto a multi-position magnetic stirring device (VariomagTM Magnetic stirrer, Thermo Electron GmbH, Langensfeld, Germany). Washed 3 mm \times 3 mm Teflon coated stirring bars (VWR International GmbH, Darmstadt, Germany) were placed into the vials and the corresponding formulations were added. Stirring was stopped after 24, 48 and 92 hours, whereby at each time point the complete sample volume was drawn before the desorption step as described in section 2.3.1.2 was applied. Samples were tested in triplicates and control samples without stirring bars were analyzed to proof that protein degradation was only induced by mechanical stress.

2.3.1.5 LIGHT EXPOSURE

For the evaluation of NGF stability during light exposure, formulations were filled into glass vials with screw caps (max. filling volume: 1.5 mL; VWR International GmbH, Darmstadt, Germany) and placed into the Suntest[®] CPS device (Hereaus, Hanau, Germany). The radiation energy of the xenon arc lamp instrument was set to 60 watt hours per square meter what represented medium illumination intensity. Samples were removed completely after 8, 16 and 24 hours and subsequently analyzed after desorption of NGF had been conducted (see section 2.3.1.2). In order to exclude contribution from thermally induced change to the total observed change, dark control samples wrapped in aluminum foil were additionally analyzed.

2.3.1.6 INCUBATION AT ELEVATED TEMPERATURE

In order to investigate NGF stability at elevated temperature formulations were filled into glass vials with screw caps (max. filling volume: 1.5 mL; VWR International GmbH, Darmstadt, Germany) and incubated at 60°C for a maximum of 7 days. Samples were drawn after 1 and 3 days of incubation. For each sampling point separate vials were prepared. In accordance to the other stress tests, the standard desorption procedure was applied after the removal of the samples from the hot-air cabinet (see section 2.3.1.2).

In a second study, the same formulations were incubated at 40°C and 60°C, respectively. Samples were only analyzed after 1 and 3 days.

2.3.2 ANALYTICAL METHODS

2.3.2.1 SIZE EXCLUSION CHROMATOGRAPHY

After removal of insoluble aggregates by centrifugation the supernatants were analyzed by size exclusion high performance liquid chromatography (HP-SEC) on a Dionex HPLC system (P680, ASI-100, UVD170, RF2000, Dionex Softron GmbH, Germering, Germany) or an Ultimate[®] 3000-system (Dionex Softron GmbH, Germering, Germany). 50 µL sample volume were injected onto an YMC-Pack Diol-120 – column (YMC Europe GmbH, Dinslaken, Germany) and a flow rate of 0.5 mL/min was used. The mobile phase consisted of 200 mM potassium phosphate and 450 mM potassium chloride at pH 7.0. The detection was carried out using a UV-VIS variable detector at 215 nm and 280 nm as well as a fluorescence detector using an excitation wavelength of 288 nm and an emission wavelength of 344 nm. The area of dimer, tetramer und high molecular weight aggregates was integrated and monitored throughout the different forced degradation experiments. The percentage of total protein recovery as well as of the respective soluble protein species was calculated by dividing the area obtained from incubated samples by the area of untreated control samples. Control samples at t₀ were treated as described in section 2.3.1.2.

Due to the centrifugation step before injection, the amount of insoluble aggregates was indirectly calculated by the difference between the total protein recovery at t₀ and the different sampling points. Data analysis was performed with Chromeleon[®] software (Dionex GmbH, Germering, Germany).

2.3.2.2 REVERSED PHASE CHROMATOGRAPHY

In accordance to sample preparation for size exclusion chromatography insoluble aggregates were removed by centrifugation prior to injection. Likewise, 50 µL of the corresponding sample were injected onto a reversed phase C4 Eurosil[®] Bioselect column (Knauer, Berlin, Germany) and the separation was carried out on an Ultimate[®] 3000-system (Dionex Softron

GmbH, Germering, Germany) or on a Dionex HPLC system (P680, ASI-100, UVD170, RF2000, Dionex Softron GmbH, Germering, Germany). The applied gradient consisted of two mobile phases, namely solvent (A) water + 0.1% [m/m] TFA and solvent (B) 100% acetonitrile + 0.1% [m/m] TFA. Each run started with 5 minutes of 100% solvent (A) and was followed by an increase of solvent (B) from 25% to 28% over 35 minutes. Residual protein was washed from the column by 100% solvent (B) and the run stopped with equilibration of the column at 100% solvent (A). The detection was carried out on a UV-VIS variable detector at 215 nm and 280 nm as well as on a fluorescence detector using an excitation wavelength of 288 nm and an emission wavelength of 344 nm. The calculations regarding protein recovery were performed according to the procedure described in section 2.3.2.1.

2.3.2.3 NEPHELOMETRY

The turbidity of particle-free NGF formulations was determined using a NEPHLA nephelometer (Dr. Lange, Düsseldorf, Germany). Nephelometry was measured in formazine nephelometric units (FNU) by 90° light scattering at a wavelength of 860 nm. This procedure is described in the European Pharmacopoeia (method 2.2.1). Each value represents the average of two measurements to exclude unspecific scattering effects.

As the required measurement volume is 1.8 mL, all NGF formulations were diluted 1:10 with loading buffer before measurement. Therefore, the total dilution for turbidity and light obscuration measurements was 1:20 including the dilution step during the desorption procedure.

2.3.2.4 LIGHT OBSCURATION

The size and amount of particles between 1 and 200 µm was measured for particle-free NGF formulations by light obscuration using a SVSS C-40 apparatus equipped with a HCB-LD-25/25 sensor (PAMAS GmbH, Rutesheim, Germany).

The detailed measurement procedure was already described for the measurement of spider silk protein formulations and it is therefore referred to section 2.2.2.6.

2.3.2.5 SODIUM DODECYL SULPHATE POLYACRYLAMIDE GEL ELECTROPHORESIS

In order to obtain further information about NGF aggregates SDS-PAGE was performed under non-reducing conditions. Samples were loaded on NuPAGE® 10% Bis-Tris precast gels (Life technologies GmbH, Darmstadt, Germany), which had been mounted in the XCell II Mini cell system (Novex, San Diego, CA, USA). The sample preparation included the dilution of the samples to an approximate protein concentration of 0.10 mg/mL in a tris-buffer

at pH 6.8 and the denaturation of the samples at 95°C for 20 minutes. Finally, 10 µL or 5 µL of each sample were loaded into the different wells of the gel for coomassie staining or for silver staining, respectively. Separation was carried out at a current of 40 mA per gel and the runtime was about 90 minutes.

Coomassie staining of the gels was performed using the Imperial[®] protein stain solution (Thermo Fisher, Rockford, IL, USA). The gels were incubated in the staining solution for about 3 hours and washed excessively with purified water over night.

Silver staining was carried out by using the SilverXPRESS[®] Staining Kit (Invitrogen, Carlsbad, CA, USA).

Regardless of the staining procedure, the same protein standard (Mark 12[®] Unstained Standard, Invitrogen, Carlsbad, CA, USA) was loaded onto each gel for the assessment of the molecular weight of protein species.

2.3.2.6 MICROCALORIMETRY

Thermal stability of NGF in the formulation buffer was investigated using high sensitivity differential scanning calorimetry (µDSC) on a MicroCal differential scanning calorimeter (MicroCal Inc., MA, USA). After degassing, the NGF formulations were filled into the measurement cells of the calorimeter using a hamilton syringe. The samples were heated up from 20 to 90°C with a heating rate of 1°C/min. The reversibility of the unfolding process was controlled by a second consecutive heating scan.

The thermogram of water samples was subtracted from the thermogram of the NGF formulations and the melting temperature (midpoint of unfolding, T_m) of the transition was determined using Origin 7.0 software.

2.4 REFERENCES

- [1] **Scheibel T.**, Spider silks: recombinant synthesis, assembly, spinning, and engineering of synthetic proteins. *microbial cell factories* 2004, 3(1), 14
- [2] **Huemmerich D., Helsen C. W., Quedzuweit S., Oschmann J., Rudolph R. and Scheibel T.**, Primary structure elements of spider dragline silks and their contribution to protein solubility. *Biochemistry* 2004, 43(42), 13604-13612
- [3] **Aune K. C. and Tanford C.**, Thermodynamics of the denaturation of lysozyme by guanidine hydrochloride. I. Dependence on pH at 25°. *Biochemistry* 1969, 8(11), 4579-4585
- [4] *Lysozyme product information.* Available from: <http://www.sigmaaldrich.com/etc/medialib/docs/Sigma/Datasheet/7/16876dat.Par.0001.File.tmp/16876.pdf>.
- [5] **Levi-Montalcini R.**, The nerve growth factor 35 years later. *Science* 1987, 237(4819), 1154-1162
- [6] **Raivich G. and Kreutzberg G. W.**, Peripheral nerve regeneration: Role of growth factors and their receptors. *Int. J. Dev. Neurosci.* 1993, 11(3), 311-324
- [7] **Apfel S. C., Kessler J. A., Adornato B. T., Litchy W. J., Sanders C., Rask C. A. and Group* T. N. S.**, Recombinant human nerve growth factor in the treatment of diabetic polyneuropathy. *Neurology* 1998, 51(3), 695-702
- [8] **Apfel S. C., Schwartz S., Adornato B. T., Freeman R., Biton V., Rendell M., Vinik A., Giuliani M., Clarke Stevens J., Barbano R. and Dyck P. J.**, Efficacy and safety of recombinant human nerve growth factor in patients with diabetic polyneuropathy: A randomized controlled trial. *JAMA: The Journal of the American Medical Association* 2000, 284(17), 2215-2221
- [9] **Apfel S. C.**, Nerve growth factor for the treatment of diabetic neuropathy: What went wrong, what went right, and what does the future hold?, in *Int. Rev. Neurobiol.*, David, T., Editor. 2002, Academic Press. p. 393-413
- [10] *Clinical trials for Tanezumab.* Available from: <http://www.clinicaltrials.gov/ct2/results?term=Tanezumab&phase=1>.
- [11] **McDonald N. Q., Lapatto R., Rust J. M., Gunning J., Wlodawer A. and Blundell T. L.**, New protein fold revealed by a 2.3-Å resolution crystal structure of nerve growth factor. *Nature* 1991, 354(6352), 411-414
- [12] **Wiesmann C. and de Vos A. M.**, Nerve growth factor: structure and function. *Cell. Mol. Life Sci.* 2001, 58(5), 748-759
- [13] **Rattenholl A., Lilie H., Grossmann A., Stern A., Schwarz E. and Rudolph R.**, The pro-sequence facilitates folding of human nerve growth factor from *Escherichia coli* inclusion bodies. *Eur. J. Biochem.* 2001, 268(11), 3296-3303
- [14] **Fraunhofer W. and Winter G.**, The use of asymmetrical flow field-flow fractionation in pharmaceuticals and biopharmaceuticals. *Eur. J. Pharm. Biopharm.* 2004, 58(2), 369-383
- [15] **Cao S., Pollastrini J. and Jiang Y.**, Separation and Characterization of Protein Aggregates and Particles by Field Flow Fractionation. *Curr. Pharm. Biotechnol.* 2009, 10(4), 382-390
- [16] **Slotta U., Rammensee S., Gorb S. and Scheibel T.**, An engineered spider silk protein forms microspheres. *Angew. Chem. Int. Ed. Engl.* 2008, 47(24), 4592-4594

- [17] **Zöls S., Tantipolphan R., Wiggerhorn M., Winter G., Jiskoot W., Friess W. and Hawe A.**, Particles in therapeutic protein formulations, Part 1: Overview of analytical methods. *J. Pharm. Sci.* 2012, 101(3), 914-935
- [18] *Function & Features: LA-950.* Available from: <http://www.retsch-technology.com/rt/products/laser-light-scattering/la-950/function-features/>.
- [19] **Lammel A., Schwab M., Hofer M., Winter G. and Scheibel T.**, Recombinant spider silk particles as drug delivery vehicles. *Biomaterials* 2011, 32(8), 2233-2240
- [20] **Van Tomme S. R., De Geest B. G., Braeckmans K., De Smedt S. C., Siepmann F., Siepmann J., van Nostrum C. F. and Hennink W. E.**, Mobility of model proteins in hydrogels composed of oppositely charged dextran microspheres studied by protein release and fluorescence recovery after photobleaching. *J. Control. Release* 2005, 110(1), 67-78

CHAPTER 3

PREPARATION TECHNIQUES, CHARACTERIZATION AND FORMULATION DEVELOPMENT OF SPIDER SILK PARTICLES

3.1 INTRODUCTION

As described in the introduction of this thesis particles made from biodegradable polymers represent a promising platform for drug delivery with a broad variety of potential applications [1-3]. For particle preparation several different strategies and techniques have been developed which are summarized elsewhere [4, 5]. Therein, the most employed techniques are emulsion-based preparation methods which are primarily used for particles made of polyesters such as poly(lactic-co-glycolic acid). The emulsion-based techniques can be used for microparticle as well as for nanoparticle preparation, but protein denaturation or aggregation is a severe issue during encapsulation due to the presence of water/organic solvent interfaces [6]. In the field of protein-based carriers most notably albumin, gelatin and silk particles have been developed throughout the last decade [7-10]. However, none of the investigated carriers is able to meet all requirements which are necessary for successful delivery of protein drugs. Gelatin nanoparticles have been successfully applied *in vivo* as nebulized drug carriers for immunostimulating agents like cytosine-phosphate-guanine-oligodeoxynucleotides (CpG-ODN) in immunotherapy of allergic horses [11]. Nevertheless, particle preparation of gelatin nanoparticles by one or two-step desolvation exhibits important drawbacks such as the necessary use of glutaraldehyde and acetone as well as limited ability to upscale the process. This is quite critical regarding a potential commercialization of this drug delivery platform. Using silk fibroin from *Bombyx mori*, microspheres and nanoparticles were prepared by different and predominantly quite sophisticated preparation techniques: using lipid-based templates [12-14], film casting and subsequent sonication [15], vibrational splitting of laminar jet [16], usage of water-miscible organic solvents [17] and salting-out with lyotropic salts [18].

In summary, these examples show that there is still a need for new biodegradable materials which have to be available in adequate amounts meeting the required quality and safety for pharmaceutical excipients. These materials should be easily prepared using an adaptable and upscalable technique.

After development of the recombinant production of eADF4(C16), first studies on the specific assembly process of this protein were carried out [19, 20]. The group of Prof. Scheibel showed that smooth protein spheres with high β -sheet content were formed by a salting-out process with potassium phosphate as lyotropic salt. The underlying mechanism was described as liquid-liquid phase separation into a protein-poor and a protein-rich phase in which particulate protein aggregates were formed. Spherical growth of the protein aggregates stopped when the protein concentration was below the equilibrium of solubility [19]. The spider silk particles were shown to be chemically stable even at harsh conditions such as 6 M urea and could only be dissolved in the very strong denaturant 6 M guanidine thiocyanate [21]. Based on these results, the preparation conditions and the resulting eADF4(C16) particle sizes and size distributions were evaluated [22]. Lammel et al. observed that the size of eADF4(C16) particles can be easily controlled by the mixing intensity and the concentrations of potassium phosphate and eADF4(C16). Figure 3.1 summarizes all impact factors on the phase separation process which lead to the formation of β -sheet dominated particles made of the originally unfolded eADF4(C16) protein. As a major advantage over the aforementioned preparation processes of other biodegradable particles it has to be highlighted that the entire particle preparation process using spider silk protein is performed in an aqueous environment avoiding any organic solvent and harsh preparation conditions.

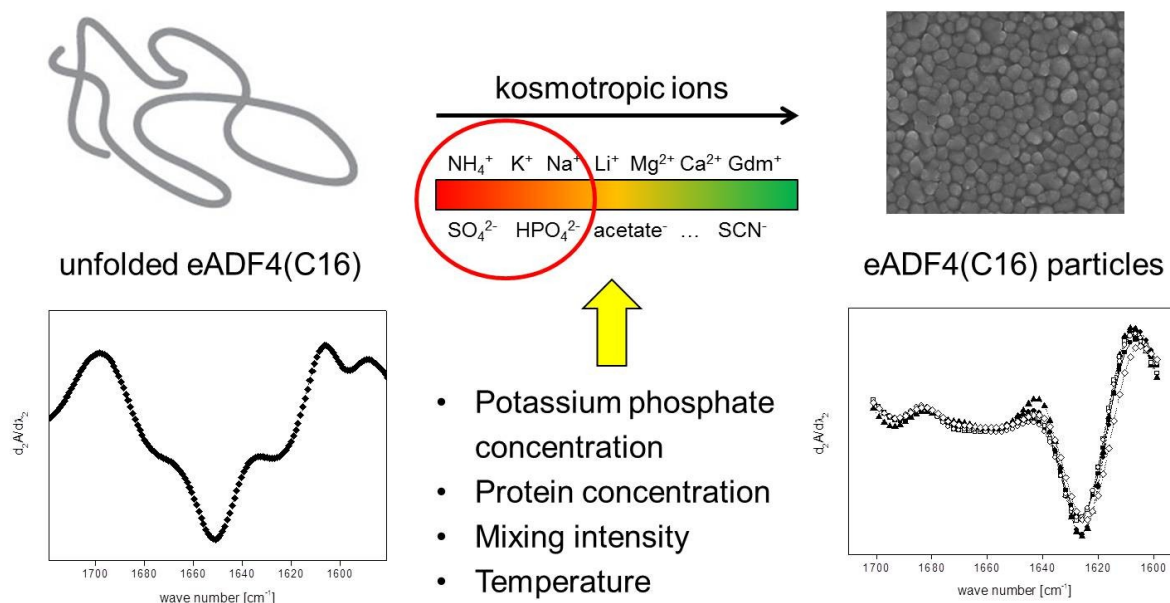


Figure 3.1. Liquid-liquid phase separation and structure formation of eADF4(C16) particles

However, results so far only covered the evaluation of the particle preparation process to some extent which was owed in particular to the limited availability of recombinant eADF4(C16) protein at the time. As protein production at AMSilk improved and protein amounts of up to 1 g were available, each single part of the phase separation process was investigated in more detail in this chapter.

At first, different techniques for particle preparation were compared. In the course of this work, the need emerged for both small nanoparticles for approaches in the field of vaccination and for larger microparticles for application in other areas of drug delivery. Our work on optimizing the preparation techniques, identifying process limitations and defining critical process parameters will be described in section 3.2 of this chapter.

Secondly, the improvement of the recombinant production process at AMSilk and results from particle preparation employing different protein qualities raised the demand for a detailed investigation of the liquid eADF4(C16) intermediate. So far it is known that the spider silk protein is intrinsically unfolded [19], but no data is available about its physical stability or its potential influence on the phase separation process. Therefore, section 3.3 deals with the characterization of liquid eADF4(C16) formulations using different analytical techniques and the investigation of eADF4(C16) stability during incubation at elevated temperatures.

Thirdly, the obtained eADF4(C16) particles suspensions were analyzed regarding their colloidal stability at different conditions in section 3.4. So far no information was available from literature about the performance of spider silk particles after preparation which is obviously of great importance regarding their future application. Lyophilization of nanosuspensions is often applied in order to optimize the long-term stability of suspensions [23-25]. A feasibility study employing sucrose as lyoprotectant as well as the comparison of different formulations were carried out and are described in section 3.5.

3.2 PREPARATION OF eADF4(C16) PARTICLES

Slotta et al. [19] and Lammel et al. [22] performed first studies in order to evaluate the mechanism of phase separation, different particle preparation techniques and the resulting particle size distributions. They found that above a potassium phosphate concentration of 500 mM (pH 8) spider silk spheres were formed in aqueous solution [19]. The effect of different mixing conditions was investigated by simple mixing with a pipette, dialysis and micromixing within a t-shaped mixing element. At 500 mM potassium phosphate clusters of spider silk spheres were formed with all examined preparation methods, whereas the observed particles at 1 M potassium phosphate were separated and well-shaped. eADF4(C16) concentrations of 0.5 and 1.0 mg/mL were employed throughout the study and particles in the range of 250 - 510 nm were obtained by micromixing and mixing with a pipette. A particle size around 1.6 μm was measured for spider silk particles prepared by dialysis. After all, it was concluded that sphere size increases with increasing protein concentration and decreases with the mixing intensity [22].

Based on these findings, two different strategies were developed to fulfill the emerging need for significantly different particle sizes.

3.2.1 SPIDER SILK NANOPARTICLES

The required particle size of drug delivery systems depends on the desired application. In the case of spider silk particles an application in the field of vaccination is very promising as polymeric particles were already successfully evaluated as vaccine delivery systems [26]. For that purpose a perfect particle size cannot be defined, but in our case a particle size of 500 nm is the invariable maximum. Much better would be a particle size below 300 nm so that the optimization of the particle preparation aimed to decrease the particle size as much as possible.

Figure 3.2 gives an overview of the established preparation process of eADF4(C16) particles based on the micromixing method via a syringe pump system. The individual process steps are described in detail in chapter 2, section 2.2. The implementation of the syringe pump system has several advantages compared to the preparation by other mixing techniques such as using a pipette or dialysis: high reproducibility of the employed flow-rates due to digital controlling, temperature control due to the connection of the heating jackets to a batch circulator and broad tunable spectrum of both process parameters. Besides, upscaling of this technique is possible and the syringe pumps can be cleaned with almost each kind of solvent, acid or base so that an endotoxin-free preparation is feasible as well.

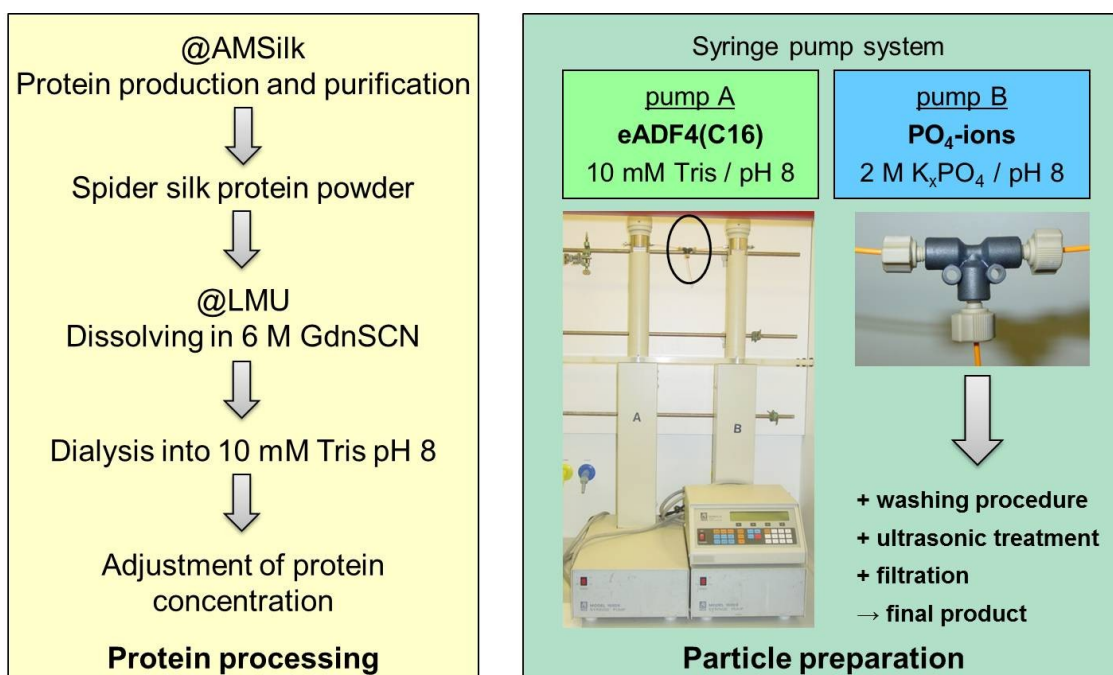


Figure 3.2. Overview of the preparation process of eADF4(C16) particles using the micromixing device

As it is shown in Figure 3.2 an ultrasonic treatment and filtration step were implemented in addition to the washing procedure. The reason therefore is illustrated in Figure 3.3, where the obtained particle size distributions are compared. Due to the high ionic strength necessary for phase separation, the already formed particles immediately agglomerated into large clusters which were responsible for a distorted size distribution of the bulk suspension after the washing procedure. Neither the first peak around 300 nm nor the second one in the micrometer range indicated the actual particle size. Simple filtration through a 1.2 μm membrane removed the agglomeration peak, but the size distribution still demonstrated too large particle sizes compared to microscopic images from SEM (data not shown). Therefore, an ultrasonic treatment was established which enabled the disintegration of agglomerated eADF4(C16) particles without altering the particles' secondary structure (data not shown). The significant decrease in particle size was also detected by dynamic light scattering (see Figure 3.3). It has to be mentioned that this method is much more sensitive towards small amounts of larger particles/agglomerates, because the resulting particle size/size distribution is based on the scattering intensity which depends on the particle diameter to the power of six in the Rayleigh approximation $I \approx d^6$ [27]. For this reason, the mean hydrodynamic diameter – usually reported as Z-average diameter – was significantly higher in the bulk suspension and in the 1.2 μm filtrate. Both SLS- and DLS-measurements reflected only minor differences between an ultrasonic treatment of 5 and 15 minutes for which reason shorter time periods were preferred. Additional filtration of the suspensions showed a positive effect on the Z-average diameter and is therefore recommended for the standard particle preparation procedure. Both sizing techniques revealed furthermore almost the identical particle size which argues for a correct analytical determination of the observed particle size.

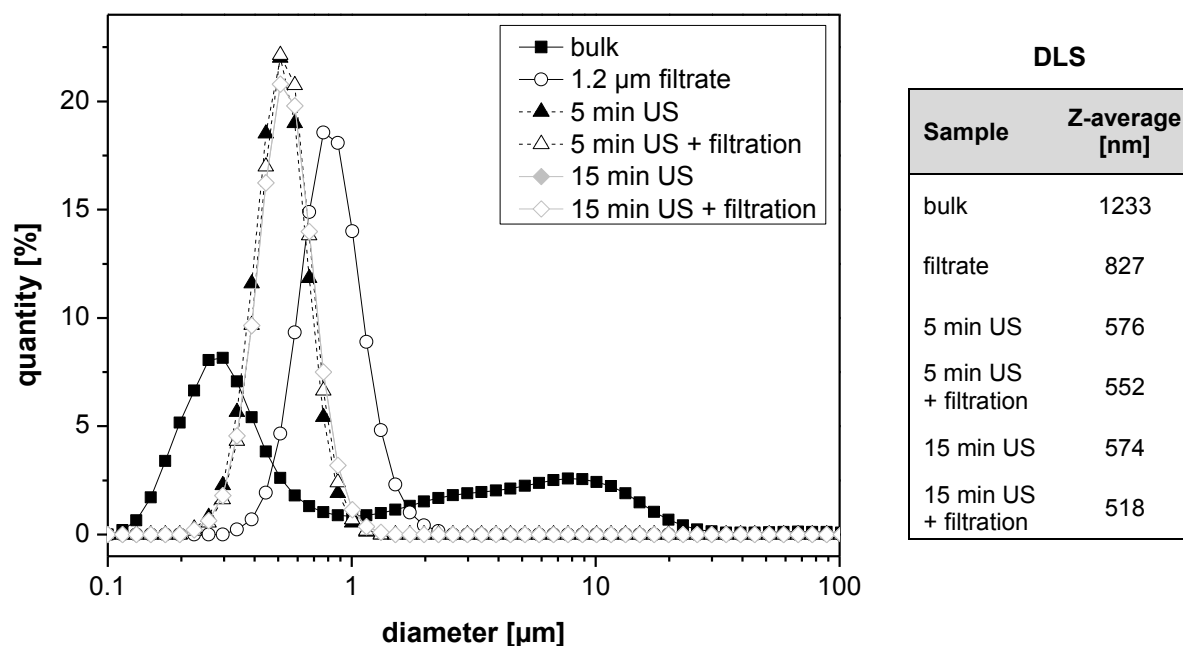


Figure 3.3. Particle size distributions determined by static light scattering during the preparation process. The results from DLS-measurements of the corresponding samples are tabulated alongside the diagram

However, ultrasonic treatment may not be a suitable process when drugs and especially proteins are encapsulated during the particle preparation process. Several studies have shown that ultrasound can be detrimental for protein stability, e.g. for lysozyme [28]. Nevertheless, the effect on the drug will be case-specific and strongly dependent on the applied process [29, 30]. Maybe the incorporation and interaction with the silk matrix can also stabilize the employed drug molecules.

After the establishment of the preparation procedure, different settings and parameters were varied and the micromixing system was again compared to other preparation techniques. eADF4(C16) concentration was set to 1.0 mg/mL and a 2 M potassium phosphate solution at pH 8.0 was used for the salting out of the spider silk protein. The resulting Z-average diameters and polydispersity indices are listed in table 3.1. Raising the flow rate from 1 mL/min to 50 mL/min slightly reduced the resulting particle size and PI, but a clear trend towards larger particles and especially broader size distributions were observed when an inner diameter of the circular mixing zone of 1.25 mm was employed. Mixing both solutions with a pipette resulted in a mean diameter of 531 nm. This particle size was quite comparable to the micromixing technique, but the PI value revealed a broader size distribution than micromixing in the small circular mixing zone. As already reported by Lammel et al. [22], eADF4(C16) particles formed by dialysis exhibited the largest diameter of all preparation techniques with an Z-average of 1.4 µm. However, due to the slow and more or less uncontrolled mixing process the particle suspension was very polydisperse.

To sum it up, phase separation can be very well controlled by the use of the micromixing system leading to monodisperse particle distributions, whereas dialysis and mixing with a

pipette result in more polydisperse suspensions. With regard to the aim of preparing eADF4(C16) nanoparticles as small as possible, the highest available flow rate of 50 mL/min and the T-shaped mixing element with an inner diameter of 0.50 mm were used for further particle preparation processes if not otherwise stated.

Table 3.1. Particle size and polydispersity indices (PI) of differently prepared eADF4(C16) particles as determined by dynamic light scattering. Each preparation technique was performed once. The standard deviation was calculated from three subruns performed for each particle batch

Preparation technique	Settings		Z-average [nm]	PI
	Flow rate	ID		
Micromixing system	1 mL/min	0.50 mm	518.1 ± 8.0	0.188 ± 0.033
Micromixing system	50 mL/min	0.50 mm	490.6 ± 7.8	0.187 ± 0.018
Micromixing system	1 mL/min	1.25 mm	560.4 ± 15.1	0.280 ± 0.018
Micromixing system	50 mL/min	1.25 mm	510.1 ± 8.2	0.245 ± 0.029
Pipette	N.A.	N.A.	531.0 ± 8.7	0.232 ± 0.022
Dialysis	N.A.	N.A.	1369.4 ± 56.2	0.757 ± 0.156

Nevertheless, the obtained particle sizes of around 500 nm were still quite large related to their potential application in vaccination studies. Therefore, further optimization of the process had to be established which means that the phase separation process had to be further accelerated. For this purpose, three different strategies were followed: variation of the lyotropic salt, decrease of the protein concentration and implementation of higher process temperatures. The results from these process modifications are depicted in Figure 3.4. The use of a 2 M ammonium sulphate solution in exchange for the 2 M potassium phosphate solution did not significantly alter the resulting particle distributions even though ammonium and sulphate ions are described to be more lyotropic [31]. But, process temperature and protein concentration had a strong impact on the kinetics of the phase separation process. On this account it was possible to reduce the particle size to diameters slightly below 300 nm if a protein concentration of 0.5 mg/mL and a process temperature of 80°C were used. The corresponding polydispersity index below 0.15 completed the convincing outcome obtained by this modification of the preparation procedure.

The suspensions were vacuum-dried on Thermanox™ cover slips (Thermo Scientific / Nunc, Langenselbold, Germany) and analyzed by scanning electron microscopy in order to confirm the determined particle sizes. It is clearly visible that smooth and round particles with a quite dense surface were formed (see Figure 3.5). The size of the particles appears to be slightly smaller compared to DLS/SLS measurements, but the shrinkage can be likely attributed to

the drying step necessary prior to SEM investigation. The obtained micrographs (magnification: 9,500x) shown in Figure 3.5 are indicative of all particle batches produced throughout the work regarding shape and surface characteristics.

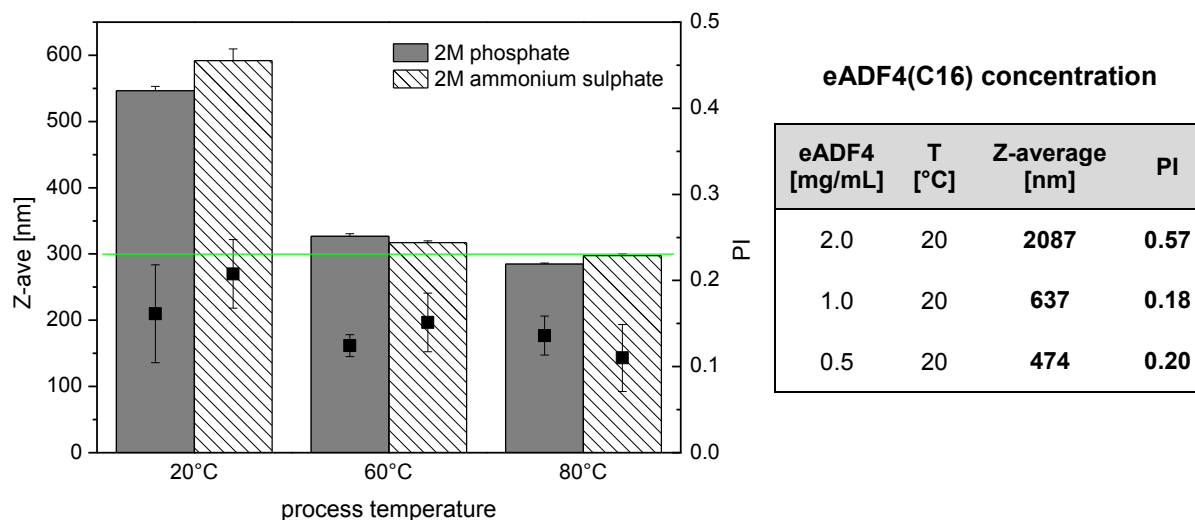


Figure 3.4. Particle size and polydispersity indices after preparation of eADF4(C16) particles at different temperatures (diagram) as well as after employing different eADF4(C16) concentrations (inserted table)

Altogether, the development of a standardized preparation procedure was achieved and written down in a standard operation procedure. The particle size of eADF4(C16) nanoparticles can be tailored by variation of process parameters such as protein concentration or process temperature. The micromixing technique is moreover upscalable and should allow for adequate cleaning in place in order to produce endotoxin-free particles for vaccination studies.

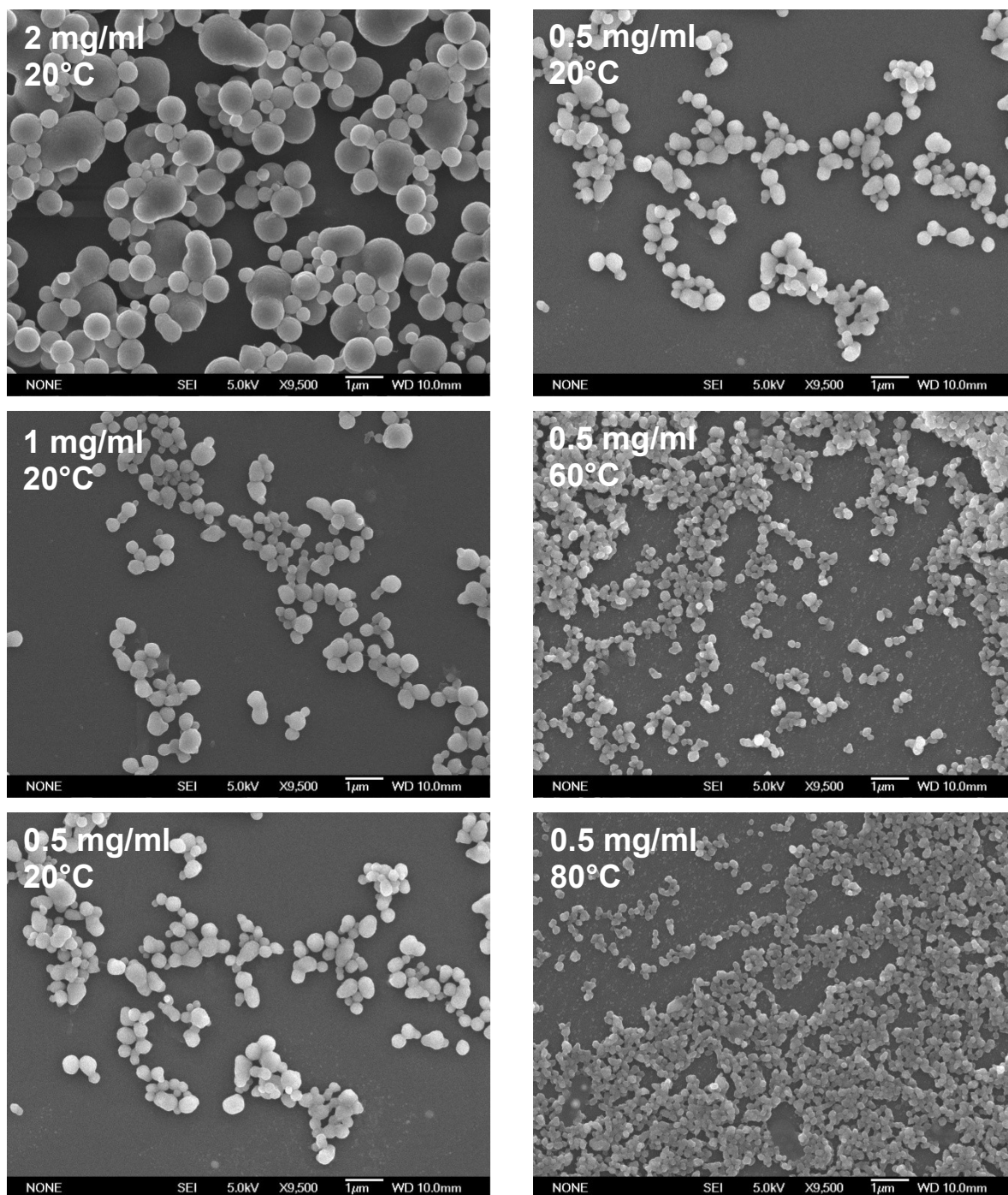


Figure 3.5. Scanning electron micrographs (magnification: 9,500x) of eADF4(C16) particles prepared at conditions specified in the upper left corner of each micrograph

3.2.2 SPIDER SILK MICROPARTICLES

Microparticles made of biodegradable polymers are commonly used drug delivery systems for different kind of applications. For example, PLA and PLGA-based microspheres were approved for parenteral depot formulations of leuprolide acetate for endometriosis or prostate cancer (Lupron[®] depot) and octreotide for acromegaly (Somatostatin[®] LAR), respectively. In order to develop depot formulations made of spider silk protein, larger eADF4(C16) spheres are needed compared to the prepared nanoparticles in section 3.2.1. The use of the straightforward preparation process based on phase separation should be continued, but in contrast to the nanoparticles' preparation the thermodynamic kinetics of the process has to be slowed down. For this reason, an ultrasonic nozzle was employed for particle preparation using different setups to form eADF4(C16) particles (further details see chapter 2, section 2.2.3.3). The different settings are listed in table 3.2.

Table 3.2. Ultrasonic nozzle – Different settings for the preparation of eADF4(C16) particles

	conc. (eADF4) [mg/mL]	c (PO ₄ ³⁻) / Volume	Temperature [°C]	Atomization rate [mL/min]
<i>Simultaneous atomization</i>				
A	0.5 / 1.0 / 2.0	2 M / 100 mL	RT	3
	2.0 / 5.0	4 M / 100 mL	55	3
<i>Atomization of eADF4(C16) into potassium phosphate solutions</i>				
B	0.5 / 1.0 / 2.0 / 5 / 10 / 15	2 M / 3 mL	RT	3
	0.5 / 1.0 / 2.0	2 M / 30 mL / 60 mL	RT	3
	0.5 / 1.0 / 2.0	2 M / 3 mL	60 / 80	3
<i>Atomization of potassium phosphate into eADF4(C16) solutions</i>				
C	0.5 / 1.0 / 2.0 / 5 / 10 / 15	2 M / 3 mL	RT	3
	0.5 / 2.0 / 10	2 M / 3 mL	4	3
	0.5 / 2.0 / 10	1 M / 3 mL	RT	3
	5	2 M / 3 mL	RT	1.5 / 0.5

3.2.2.1 SIMULTANEOUS ATOMIZATION OF eADF4(C16) SOLUTION AND POTASSIUM PHOSPHATE SOLUTION

As the ultrasonic nozzle is equipped with a dual liquid feed option, both the protein and the potassium phosphate solution can be atomized at the tip of the nozzle simultaneously. At best, solid particles are created during the spraying period and prior to the collection of the spraying mist. In this study, 2 M potassium phosphate solutions and eADF4(C16) solutions with concentrations of 0.5 to 2.0 mg/mL were atomized into 100 mL purified water (see

Table 3.2, A). All prepared samples contained unfortunately significant amount of threads and fibrils and remained comparatively transparent (see Figure 3.6, A). For this reason it was concluded that almost no particle formation took place during the spraying period. This fact was controlled by spraying simultaneously into a 2 M potassium phosphate solution instead of purified water (see Figure 3.6, B). The resulting solutions exhibited higher turbidity as a result of phase separation / particle formation occurring after the spraying phase.

Taken together, it can be stated that simultaneous atomization creates a situation where the phosphate to eADF4(C16) ratio is too low to form solid spider silk spheres, leading to fibrils and threads. Residual eADF4(C16) protein self-assembles into particulate aggregates primarily after spraying and not during the spraying period. In order to reduce aggregation into filaments and to promote particle formation during spraying, the process was thermodynamically accelerated by raising the potassium phosphate concentration to 4 M and the process temperature to 55°C, respectively. Nevertheless, fibril formation could not be prevented even if more smooth and round particles in the size between 300 – 500 nm were formed at a protein concentration of 2 mg/mL (SEM data not shown). The orifice congested due to severe creation of threads at the atomizing surface at higher protein concentration of 5 mg/mL and prohibited further evaluation of the simultaneous atomization setup.

Finally, simultaneous atomization of both solutions did not result in satisfying particle dispersions so far. The major issue was the formation of fibrils or other macroscopic agglomerates which occurred at every investigated experimental condition. This uncontrolled aggregation appeared due to the slow phase separation process and a too low potassium phosphate to eADF4(C16) ratio present in the created mist after atomization. Moreover, even if macroscopic agglomerates did not appear, the obtained eADF4(C16) particles exhibited particle sizes below 1 μm . For this reason, the approach described here seems not to be suitable for eADF4(C16) microparticle preparation.

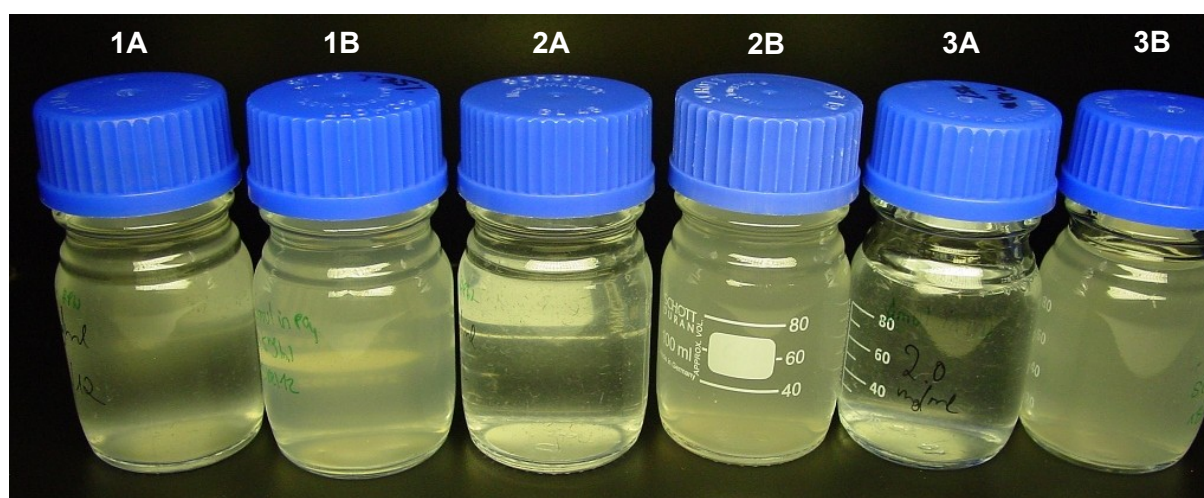


Figure 3.6. Suspensions obtained by simultaneous atomization of eADF4(C16) and 2 M potassium phosphate. eADF4(C16) concentrations of 0.5 mg/mL (1A, 1B), 1.0 mg/mL (2A, 2B) and 2.0 mg/mL (3A, 3B) were sprayed into 100 mL of purified water (A) or 2 M potassium phosphate solutions (B).

3.2.2.2. ATOMIZATION OF eADF4(C16) INTO POTASSIUM PHOSPHATE SOLUTIONS

This approach (see Table 3.2, B) was assumed to lead doubtlessly to the formation of spider silk particles. Six different protein concentrations from 0.5 to 15 mg/mL were evaluated by spraying 3 mL protein solution into an equal volume of a stirred 2 M potassium phosphate solution. The obtained particle suspensions were subjected to the standard purification procedure including washing and ultrasonic treatment of the suspensions. SEM micrographs (magnification: 9,500x) of the resulting particle batches are displayed in Figure 3.7. In contrast to nanoparticles prepared by the micromixing system (see section 3.2.1), striking difficulties to separate the occurring aggregates appeared and resulted in high PI and span values (data not shown). SEM micrographs further indicate that particle formation was rather incomplete as particles were not really defined in shape and still stuck together closely in large particle clusters. Interestingly, the obtained spider silk particles exhibited smaller diameters compared to approaches A and C so that spraying this way was further optimized towards smaller nanoparticles by accelerating the phase separation process.

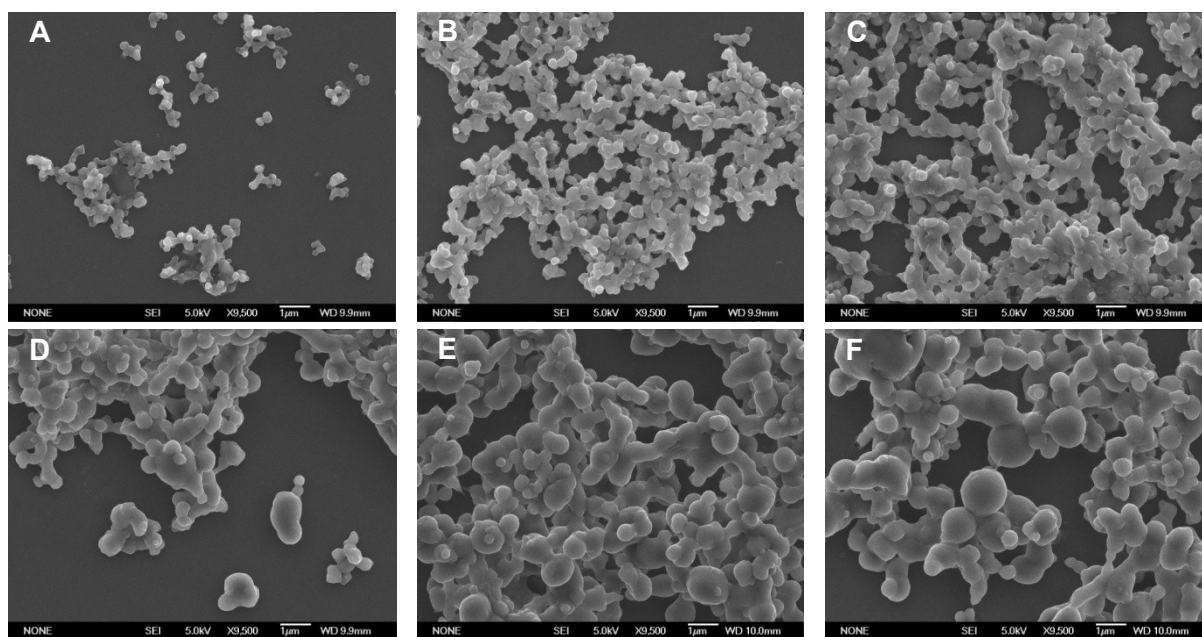


Figure 3.7. SEM micrographs (magnification: 9,500x) of eADF4(C16) particles prepared by the atomization of an eADF4(C16) solution with (A) 0.5 mg/mL, (B) 1.0 mg/mL, (C) 2.0 mg/mL, (D) 5.0 mg/mL, (E) 10 mg/mL and (F) 15 mg/mL into a potassium phosphate solution (2 M, pH 8)

This acceleration was achieved by increasing the process temperature or the volume of the phosphate solution and the corresponding results are illustrated in Figure 3.8, A and B. Only low concentrated spider silk solutions (0.5 – 2.0 mg/mL) were used in this study. An increase of the volume of the potassium phosphate solution means an increase in the phosphate to eADF4(C16)-ratio. It was thereby possible to accelerate the particle preparation process significantly as well-defined particles with sizes between 300 and 500 nm were formed

(see SEM micrograph in Figure 3.8, A). Nevertheless, particle dispersions were still quite polydisperse with polydispersity indices above 0.2. Smaller particles and more narrow size distributions were obtained when both solutions were preheated to 60°C and 80°C, respectively. Well-shaped particles between 250 and 350 nm could be prepared with sufficiently low polydispersity indices below 0.15. This implied that an elevated temperature had stronger accelerating effects on the phase separation process than a higher phosphate to eADF4(C16) ratio. Furthermore, increasing the phosphate to protein ratio goes along with 10- or 20-fold higher suspension volumes which have to be purified afterwards. Compared to other preparation techniques these eADF4(C16) particles were the smallest ever obtained, especially at protein concentrations of 1.0 or 2.0 mg/mL which allow for acceptable process yields. Therefore, this approach seems to be very suitable for the preparation of quite small nanoparticles with reasonable yields.

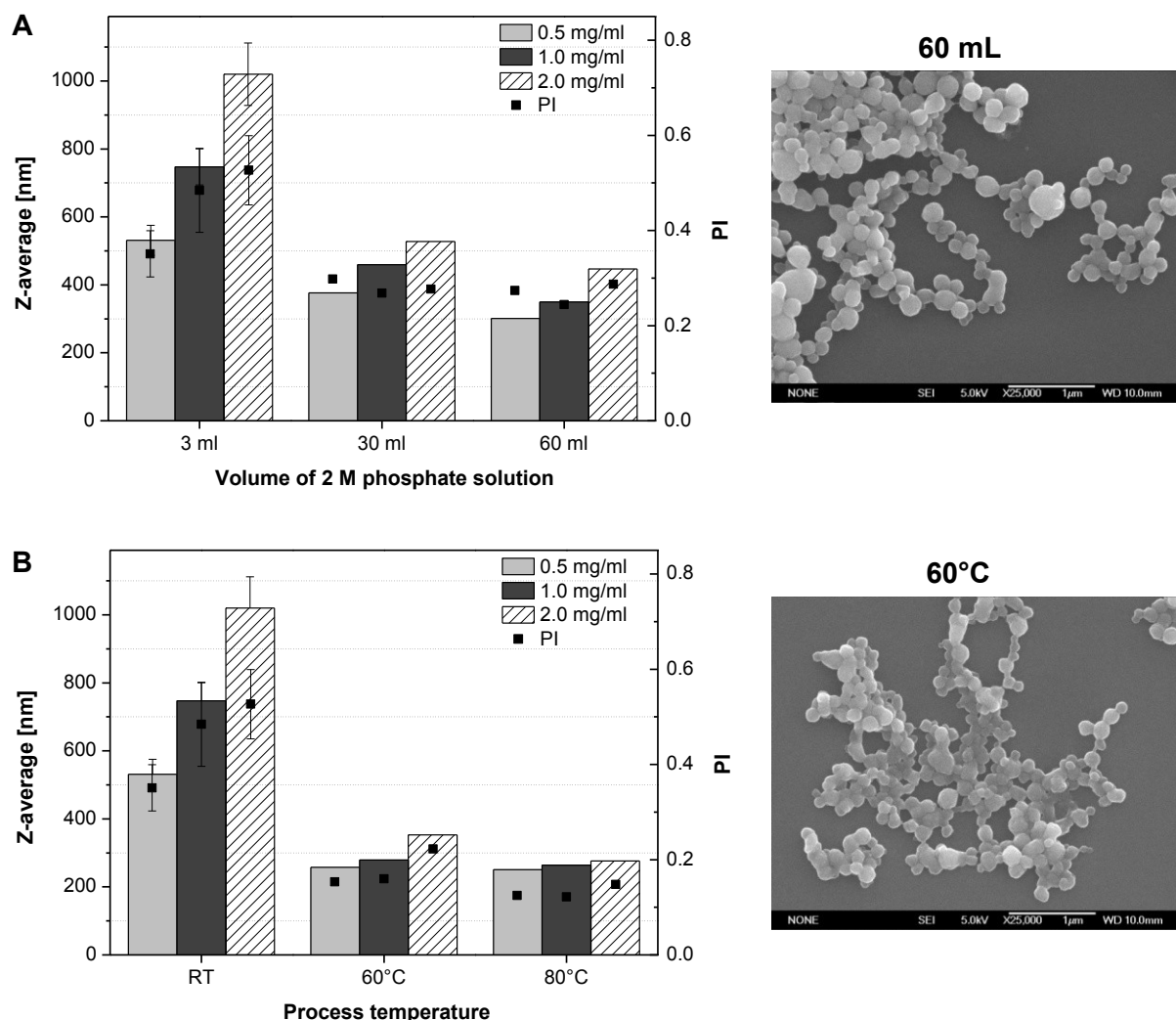


Figure 3.8. Particle size and polydispersity indices of eADF4(C16) particles prepared by using different volumes of potassium phosphate solutions (A) or different process temperatures (B). The corresponding SEM pictures (magnification: 25,000x) are shown on the right hand side.

3.2.2.3 ATOMIZATION OF POTASSIUM PHOSPHATE INTO eADF4(C16) SOLUTIONS

In a third approach (see Table 3.2, C), the potassium phosphate solution was atomized by the ultrasonic nozzle and the spraying mist was collected in an equal volume of stirred eADF4(C16) solutions. The same protein concentrations as employed for atomizing eADF4(C16) solutions were used throughout this study. Turbidity emerged suddenly after several seconds of the spraying process, but definitely not right at the beginning. Furthermore, the time point when visible turbidity occurred was solely dependent on the phosphate concentration gradient being created in the stirred solution and independent of the employed protein concentration. These facts indicate that the initiation of the phase separation for both approaches is different, leading to different particle size distributions. Interestingly, using this approach a sonication time of 2 minutes was sufficient to disintegrate agglomerates, even for suspensions prepared at higher protein concentrations. The resulting particle sizes and span values ($D_{90}-D_{10}/D_{50}$) as determined by static light scattering are shown in Figure 3.9.

For the first time, eADF4(C16) particles with diameters above 2 μm were obtained, whereupon the maximum particle size of approx. 5 μm was reached at an eADF4(C16) concentration of 10 and 15 mg/mL, respectively. As it can be deduced from SEM micrographs (see Figure 3.9, A-F), the produced particles possessed a smooth surface and round shaped morphology. Regarding the polydispersity it could be shown that especially at high protein concentration tight and monodisperse size distributions were achieved. However, SEM micrographs also illustrate a remarkable amount of smaller spider silk particles being present next to large microspheres and may suggest that further purification of the obtained particle dispersions would be necessary.

Next, a deceleration of the self-assembly process was intended to further increase the particle size. Therefore, three process parameters were altered towards a slower kinetic process: temperature, phosphate concentration and atomization rate. The effect of a decreased process temperature and potassium phosphate concentration was studied at eADF4(C16) concentrations of 0.5, 2.0 and 10 mg/mL. A protein concentration of 5.0 mg/mL was used for the evaluation of slower atomization rates.

At first, both employed solutions were precooled to 4°C prior to atomization. However, after purification and sonication the obtained eADF4(C16) particles exhibited nearly the same particle size as after preparation at room temperature (see Figure 3.10, A). Furthermore, with respect to their shape and surface characteristics it seems that particle formation was at least partially incomplete and rather rough particle surfaces were developed. Figure 3.10 B indicates that larger microspheres were formed if a 1 M potassium phosphate solutions were used. Microspheres with a mean diameter of 6.6 μm and a particle size distribution with a span value of 0.97 were obtained at a concentration of 10 mg/mL. Their macroscopic

appearance was satisfying as no clusters or shape-altered particles were observed. In a final step, the flow rate of the peristaltic pump was reduced from 3 mL/min to 1.5 mL/min and 0.5 mL/min, respectively. As the drop size in an ultrasonically produced spray is governed by the vibration frequency, surface tension and density of the liquid being atomized, the created droplet size should not be affected significantly by a change of the atomization rate. Nevertheless, the decelerated addition of the salt resulted in larger microspheres compared to the standard flow rate of 3 mL/min as shown in Figure 3.10, C. The particle size could be increased by 60%, which is the highest percentage increase of all modified preparation procedures without affecting the particles' morphology.

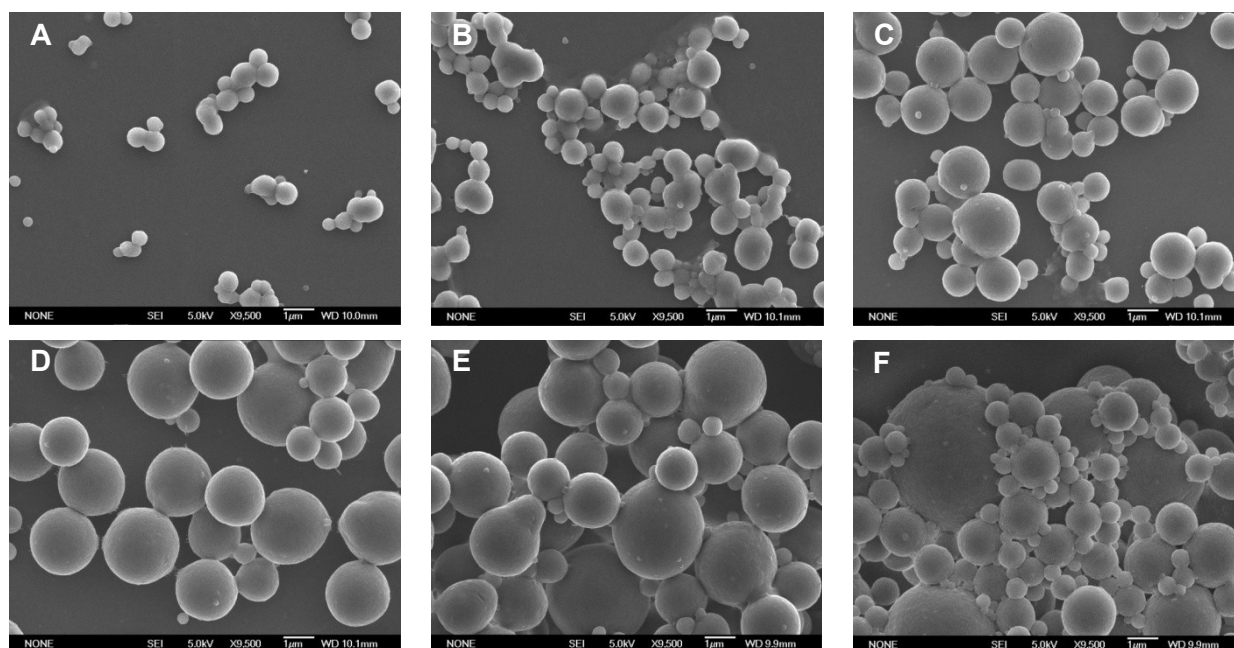
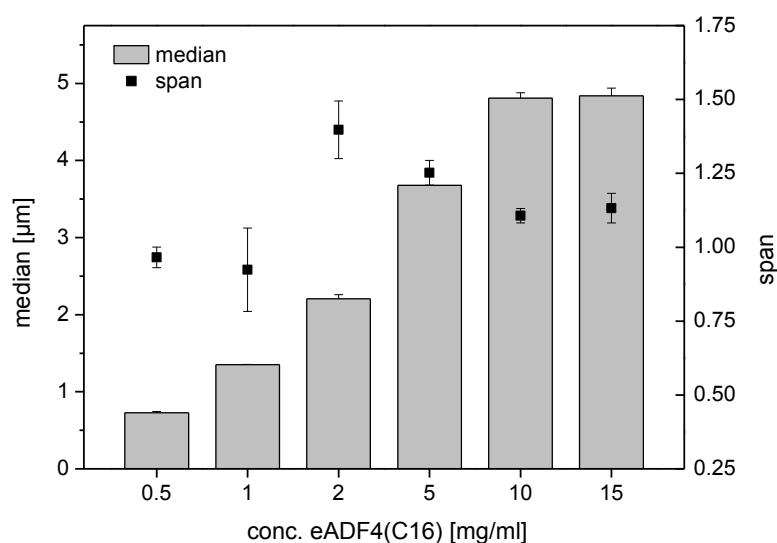


Figure 3.9. Median and span of eADF4(C16) particles prepared by atomization of potassium phosphate into eADF4(C16) solutions. Images A to F show the corresponding SEM micrographs (magnification: 9,500x) starting from (A) 0.5 mg/mL to (F) 15 mg/mL. Each setup was performed in triplicate.

The corresponding span values around 1 indicated that the obtained particle size distributions exhibit a homogenous, almost Gaussian-like distribution curve.

In summary, preparation of microspheres using an ultrasonic nozzle was successful. However, the initial idea to form spider silk particles within the spraying mist by simultaneous atomization of 2 M potassium phosphate and eADF4(C16) solutions was not possible so far. This is likely due to an inadequate phosphate to eADF4(C16)-ratio present at the atomizing surface and in the atomized droplet mixture as the situation could be improved by kinetically accelerating the phase separation process. Nevertheless, fibril formation was observed in all experiments using the simultaneous atomization so that this approach was put aside.

Interestingly, rather small nanoparticles were obtained by the atomization of a spider silk solution into 2 M potassium phosphate. Indeed, this was not initially intended, but it could be shown that particle sizes around 300 nm were achieved at the time when both solutions were preheated to 60 or 80°C.

Spraying vice versa enabled the formation of microspheres in the single-digit micrometer range. Especially atomization at lower flow rates and employing 1 M potassium phosphate solutions significantly increased the obtained particle sizes. The remarkable amount of smaller spider silk particles as shown by SEM can be reduced in the future by centrifugation at very low centrifugal forces or by separation using centrifugal filters with pore sizes around 1 µm (e.g. Vivaclear Mini, 0.8 µm PES membrane, Sartorius Sedim Biotech GmbH, Goettingen) to retain large particles upon the filter membrane.

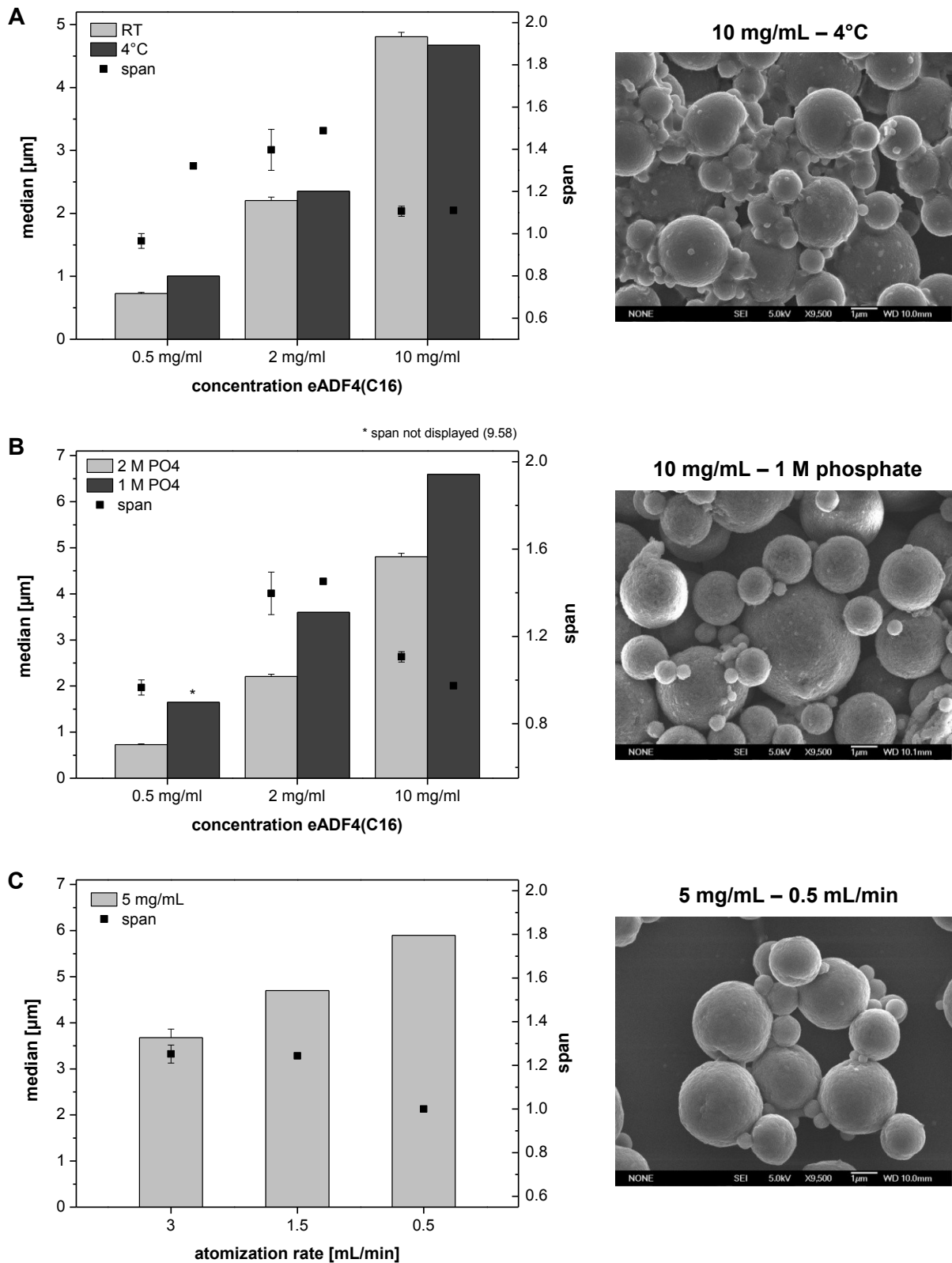


Figure 3.10. Particle size and span values of eADF4(C16) particles prepared at 4°C (A), by using 1 M potassium phosphate (B) or at different flow rates (C). The corresponding SEM micrographs (magnification: 9,500x) are displayed on the right hand side.

3.3 CHARACTERIZATION OF LIQUID eADF4(C16) FORMULATIONS

As described in the previous section, spider silk particle preparation is based on mixing an aqueous eADF4(C16) formulation with a high concentrated salt solution to induce phase separation. However, only little information is available in the literature on the characteristics of the aqueous spider silk protein solution. It is well established that recombinant eADF4(C16) protein behaves different to globular proteins as it is initially unfolded in an aqueous environment as determined by far-UV circular dichroism [32]. This statement was confirmed by FTIR-spectroscopy of an eADF4(C16) solution formulated at 10 mM Tris-buffer at pH 8.0 (see Figure 3.1). The minimum of the second derivation at approx. 1650 cm^{-1} is assigned to a primarily random coiled structure of the protein molecule according to Hu et al. [33]. Nevertheless, besides the determination of the protein's conformation no data was published so far concerning the investigation of the physical or chemical stability of eADF4(C16) or other spider silk proteins. This characterization is obviously necessary for the establishment of reproducible and robust preparation processes of all kind of morphologies made of eADF4(C16). For this reason, analytical methods, which are commonly used for the characterization of protein formulations, have to be established. But, it has to be considered that eADF4(C16) is by nature a hydrophobic and very aggregation-prone protein molecule and therefore significantly different to therapeutic proteins like monoclonal antibodies. This aspect was taken into account by developing a suitable method for asymmetrical flow field-flow fractionation (AF4) as described in section 3.3.1. Furthermore, the eADF4(C16) formulation was analyzed after incubation at 80°C due to the need of high process temperatures for the previously explained preparation process of spider silk nanoparticles. Altogether, the information obtained on the stability of eADF4(C16) will be very useful for further optimization of the protein formulation and subsequent preparation processes.

3.3.1 CHARACTERIZATION OF eADF4(C16) BY AF4

In order to gain insight into the physical state of solubilized eADF4(C16), the analytical technique called asymmetrical flow field-flow fractionation was employed. This method is a suitable tool for separating both soluble and insoluble protein aggregates even though size exclusion chromatography (HP-SEC) is still the default method for characterizing soluble protein aggregates in pharmaceutical industry. In the case of analyzing eADF4(C16) the following drawbacks of HP-SEC are of particular interest: (1) adsorption of protein and/or protein aggregates to the column matrix, (2) dissociation and/or formation of protein aggregates during the course of a sample run, (3) incapability of HP-SEC to resolve larger soluble protein aggregates (void volume) and (4) inability to separate soluble and insoluble protein aggregates simultaneously [34]. Adsorption to the column matrix can be avoided by increasing the ionic strength of the mobile phase, but regarding eADF4(C16) high ionic

strength causes severe protein aggregation. Furthermore, the pH of mobile phases is recommended to be slightly acidic (pH 4-7) for commonly used silica- or agarose-based matrices, but acidic conditions were shown to be detrimental for eADF4(C16) solubility [35]. It was also reported for eADF4(C16) that formation of nanofibrils having a length of several hundred nanometer can occur [36] so that standard HP-SEC conditions would not be able to resolve those morphologies or rather the column frit would be rapidly clogged. Altogether, it seemed to be worth to develop an alternative method to HP-SEC so that AF4 was employed to characterize amount, size and molecular weight of protein species in eADF4(C16) formulations.

The detailed principles and mechanisms of separation in AF4 are described elsewhere [37, 38]. Briefly, differences in hydrodynamic diameter and corresponding diffusion coefficients lead to a different diffusion into the center of the parabolic flow so that species exhibiting a smaller hydrodynamic diameter are eluted first. After separation, protein species are detected by UV-Vis, refractive index and multiple angle light scattering detectors. A suitable AF4 method should exhibit an adequate separation of protein species with a consistent recovery and a solid reproducibility.

During preliminary method development different membrane materials and molecular weight cut-offs were tested. The most accurate and reproducible results were obtained using a 10 kDa cut-off and a membrane made of regenerated cellulose. The formulation buffer was chosen (10 mM Tris-buffer, pH 8.0) as mobile phase in order to avoid any artificial effect or result created by the running buffer during separation. As described in chapter 2, section 2.2.2.1, the detector flow was kept constant at 1.0 mL/min and a channel height of 350 μm was used. Method development included primarily the optimization of the cross flow profile which can be divided in general into four sections: (I) injection and focusing cross flow, (II) elution cross flow, (III) rinsing step and (IV) washing step (see Figure 3.11). The cross flow of each section was varied and optimized to obtain the most suitable elution profile.

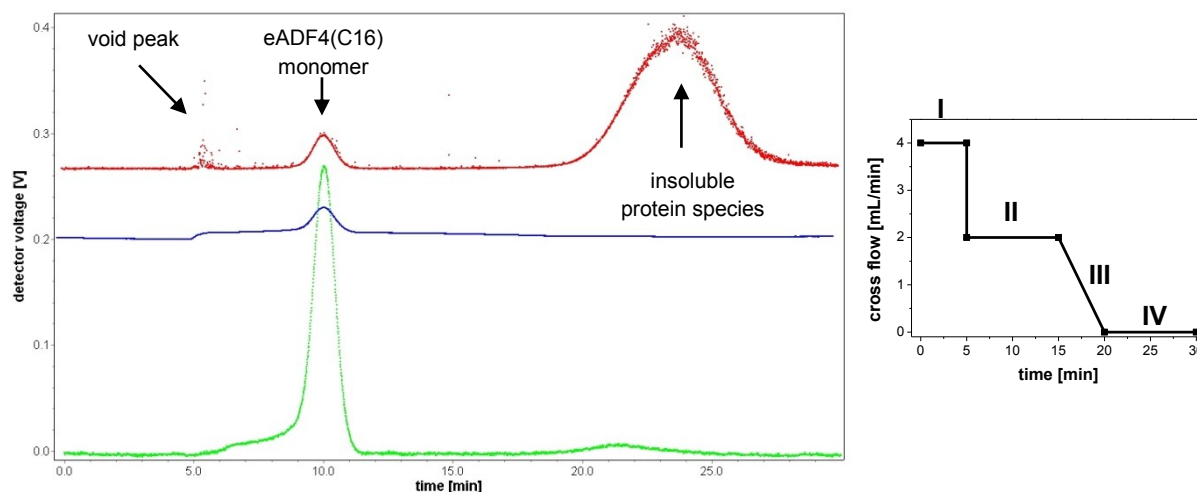


Figure 3.11. Separation of eADF4(C16) by AF4 using the developed cross flow profile. Red: Light scattering at 90°C; blue: Refractive index; green: UV-detection at 280 nm

Finally, an optimal resolution and determination of eADF4(C16) was achieved using the cross flow profile displayed in Figure 3.11. The corresponding chromatogram of the three employed detectors is also shown in this figure. First, a cross flow of 4.0 mL/min was applied for 5 minutes in order to focus the sample on the membrane which is necessary for high separation capacity. The monomeric form of eADF4(C16) eluted after approx. 10 minutes during a constant cross flow of 2.0 mL/min. Cross flow was stopped after 20 min. The shape of the detected protein peak shows a slight but unavoidable fronting. The corresponding UV-signal at 280 nm was used for the calculation of recovery and molar mass of eADF4(C16) as shown in Figure 3.12.

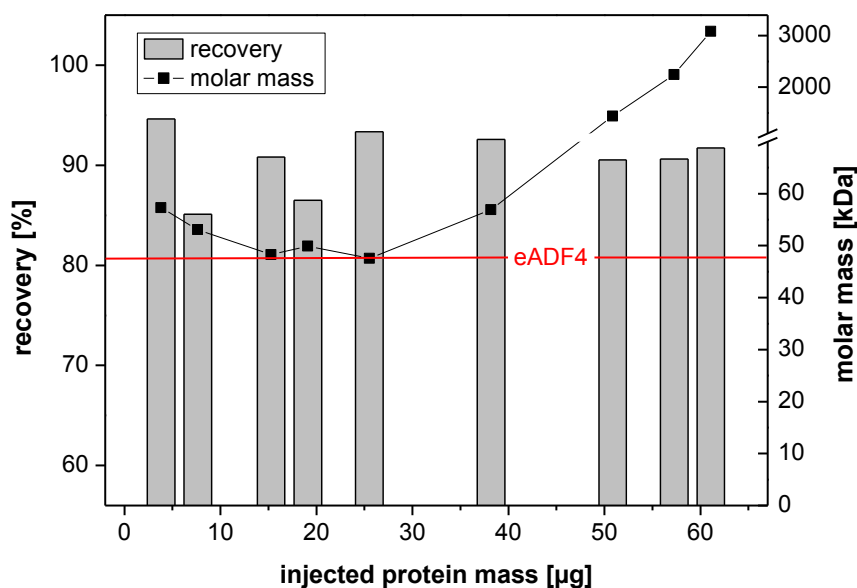


Figure 3.12. Recovery and molar mass of eADF4(C16) determined by AF4 using UV-detection at 280 nm and the developed cross flow profile

Different protein masses were injected in order to evaluate the range for precise determination of molar mass and acceptable protein recovery. It was found that above an injection mass of 40 µg protein recovery is still acceptable (above 80%), but the calculated molar mass is completely out of any tolerable limit. The reason for this result is already observable in the chromatograms of the respective samples (see Figure 3.13, A). Whereas the UV-signals of the monomer peak were proportionally increasing with increasing injection mass (see small graph in Figure 3.13, A), the corresponding light scattering signals at approx. 10 minutes run time were multiple-fold stronger than expected just from higher protein masses. On the contrary, in the range from 15 to 25 µg injected protein mass the calculated molar mass perfectly matched the theoretical value of 47.7 kDa. Therefore, the eluted conformation of eADF4(C16) had to undergo a certain conformational change during the elution in the AF4 channel if higher protein masses are injected. It is known that during the so-called 'focusing phase' after injection, protein specimens are focused in a thin band

and concentrated towards the membrane. Interestingly, the protein specimens can be concentrated up to 100-fold or more potentially leading to *in situ* protein association/aggregation (oral contribution from Wyatt technologies). As the aggregation mechanism of eADF4(C16) protein is very sensitive towards higher protein concentration, it is likely that protein association or conformational change takes place resulting in unmodified retention times and UV-signals, but extremely high light scattering. Therefore, the mass of injected eADF4(C16) has to be considered prior to analysis and should be in the range of 10 to 30 μg .

As it can be seen in Figure 3.11, a second weak UV-signal with a strong light scattering signal is detected after stopping the cross flow at 20 minutes run time. From that moment on every species or particle that has not been eluted so far is washed from the membrane. Based on the light scattering signal, the root mean square (rms) radius, meaning the radius of gyration, was calculated. Figure 3.13 displays the light scattering signals and rms radii vs. time obtained with different injection masses and after different sample preparation.

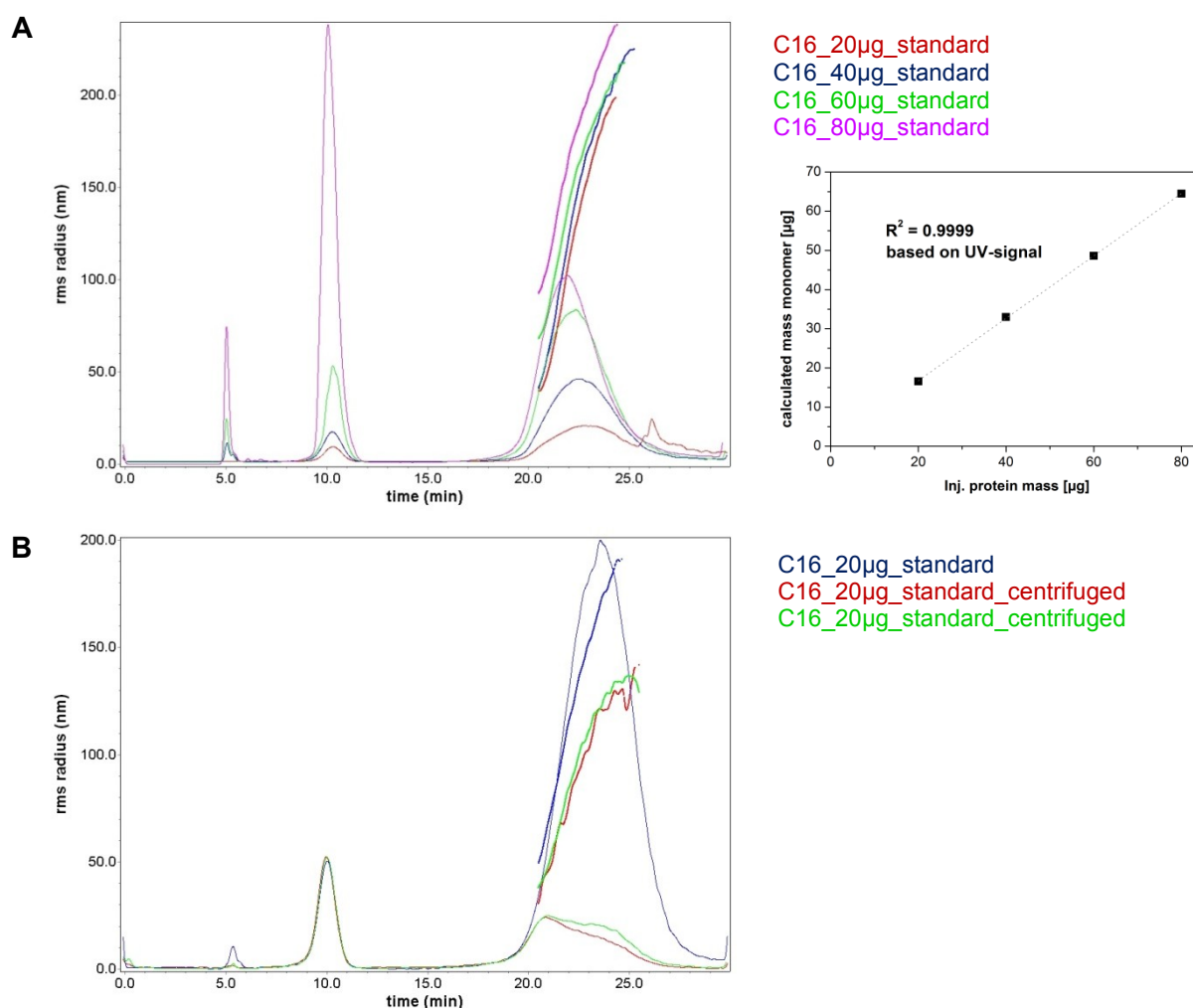


Figure 3.13. Light scattering signals and calculated rms radii of eADF4(C16) samples vs. time as analyzed by AF4. (A) Injection of different masses of eADF4(C16), (B) AF4 analysis without or after centrifugation of the formulation.

The calculated rms radii revealed that besides monomeric eADF4(C16) small amounts of insoluble protein species with sizes between 50 and 200 nm were present in the protein formulations. The determined rms radii were independent of the injected eADF4(C16) mass, but the light scattering signal was significantly reduced by centrifugation of the formulation (15,000 g, 30 min). This indicates that an *in situ* formation as described for the monomer peak at high injection masses can be excluded. However, the corresponding UV-signal did not change upon centrifugation and remained at approx. 7% of the total eluted protein mass. For this reason, it is assumed that this UV-signal at the start of the rinsing step is mainly generated by soluble eADF4(C16) molecules which have not been eluted during the elution cross flow due to strong interaction with the AF4 membrane. The described insoluble species then overlay with these protein molecules.

Therefore, appropriate sample preparation is recommended for future reproducible production of eADF4(C16) nano- and microparticles as these detected impurities may slightly alter phase separation processes.

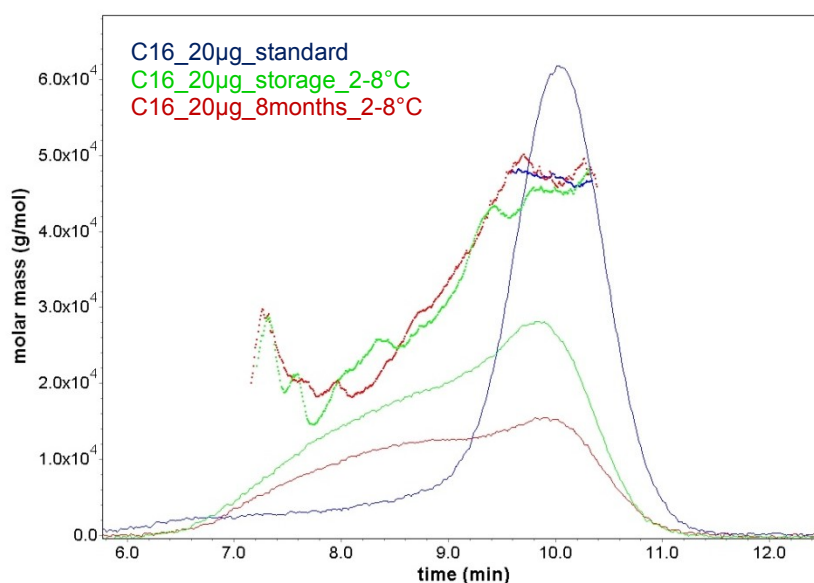


Figure 3.14. UV-absorbance at 280 nm and calculated molar mass of eADF4(C16) formulations during long-term storage at 2-8°C

Throughout the work eADF4(C16) formulations were prepared and processed within a few days so that longer storage periods prior to particle preparation did not occur. Furthermore, differences between formulations from multiple preparation processes, that means different dissolving and dialysis processes (protein concentration, duration of dialysis), could not be detected by AF4 analysis (data not shown). All formulations showed only the same peak representing the eADF4(C16) monomer and small amounts of the described aggregates in the nanometer range. Soluble aggregates of eADF4(C16) were not observed at all. This was true except two formulations which residuals after particle preparation were stored in the

fridge at 2-8°C for a maximum storage time of 8 months. The corresponding chromatograms are displayed in Figure 3.14 and show that fronting of the monomer peak was clearly increased after storage. Lower retention time results in lower molar mass of the eluting species according to the separation principle of AF4. However, the obtained information is so far too insufficient to reasonably claim protein degradation of eADF4(C16) over time.

3.3.2 STABILITY OF eADF4(C16) AT ELEVATED TEMPERATURE

As described earlier, preparation of eADF4(C16) nanoparticles requires preheating of the protein solution to 60°C and 80°C, respectively. Therefore, stability of the spider silk protein formulation was investigated at 80°C over a period of 4 hours. The concentration was set to 1.0 mg/mL and the commonly used formulation comprising a 10 mM Tris-buffer at pH 8.0 was employed.

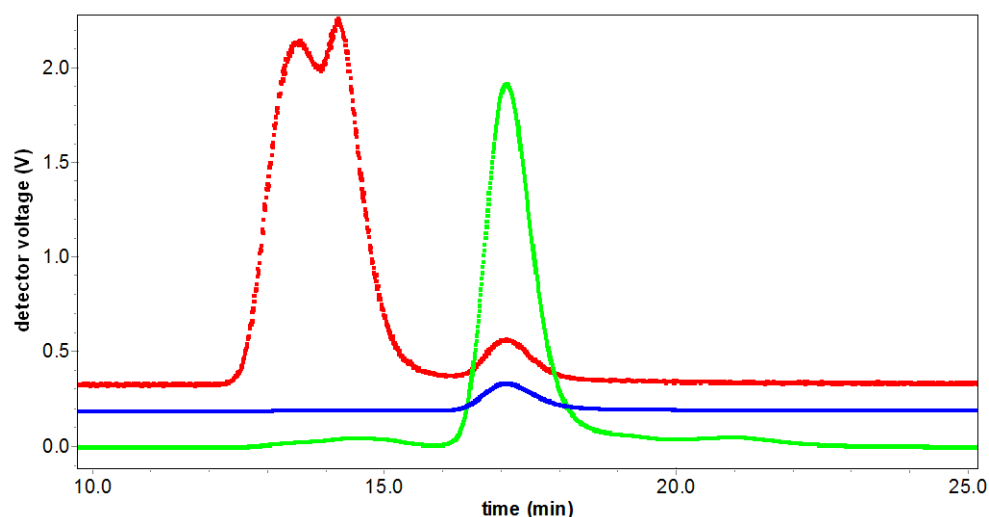


Figure 3.15. Separation of eADF4(C16) on a Shodex OHPak SB-803 SEC-column. Red: Light scattering at 90°C; blue: refractive index; green: UV-detection at 280 nm

The samples were analyzed using a HP-SEC method developed by AMSilk. The resulting chromatogram of an unstressed eADF4(C16) formulation is shown in Figure 3.15. The order of the eluting peaks was vice versa as obtained by AF4 so that first high molecular weight (HMW) species with a huge light scattering signal were detected. This peak was followed by the monomer peak of eADF4(C16) and a slight tailing of the peak as it was also detected by AF4 (fronting). Throughout the incubation at 80°C the height and AUC of the monomer peak decreased continuously, whereas the amount of HMW-species and the tailing were not altered (data not shown). The total protein recovery decreased to 88% after 1 hour and 63% after 4 hours of incubation, respectively (see Figure 3.16, A). The result from HP-SEC was confirmed by SDS-PAGE under non-reducing conditions (see Figure 3.16, B). A decrease of the coloration of the monomer band was clearly detectable (line 4 vs. 7). More importantly

and in agreement with HP-SEC results, no further protein species occurred during incubation indicating that no soluble protein aggregates were formed. For this reason, the loss in protein content has to be accompanied by the formation of insoluble aggregates, but light obscuration measurements did not reveal a significant increase of subvisible particles (see Figure 3.16, C) as total particle counts around 2000 particles per mL (1:10 dilution) could not explain a protein loss of approx. 400 µg eADF4(C16). However, in all formulations large visible aggregates were formed, but these aggregates were not of particulate nature as it is usually found for aggregated protein drugs. Figure 3.16, D shows that spider silk fiber formation took place during incubation at 80°C in the 10 mM Tris-buffer at pH 8.0.

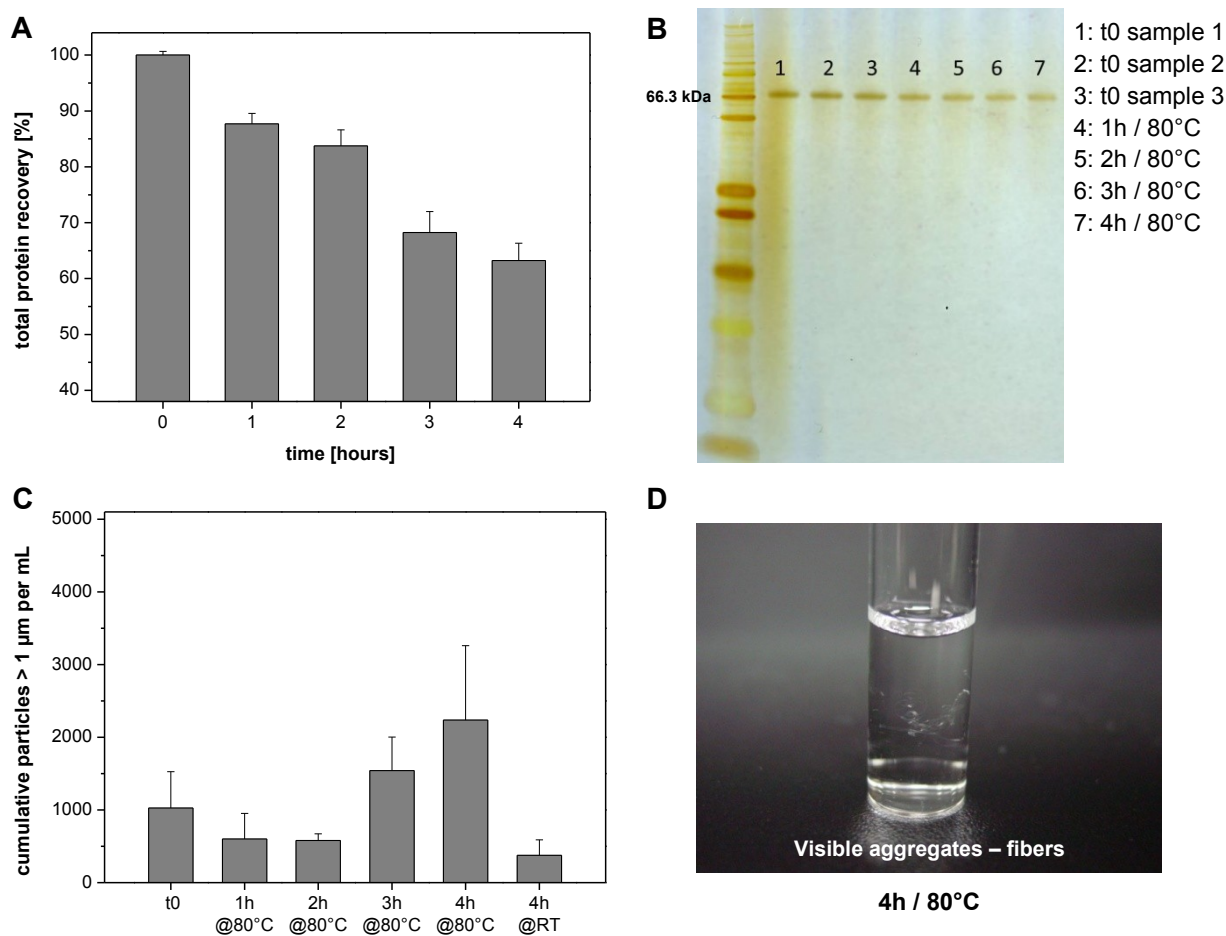


Figure 3.16. Stability of an aqueous eADF4(C16) solution at 80°C. (A) Total protein recovery determined by size exclusion chromatography. (B) SDS-PAGE (non-reducing conditions) and (C) light obscuration (1:10 dilution) results of the corresponding formulations. (D) Photographic image of the formulation after 4 hours at 80°C (1:10 dilution)

Summing up, section 3.3 of this chapter describes the implementation of analytical techniques for characterizing the physical stability of eADF4(C16) formulations. An AF4 method was developed and established as an orthogonal method to size exclusion chromatography. The results from both analytics agreed concerning detected protein species and revealed that eADF4(C16) formulations contained low amounts of high molecular weight

aggregates, but no soluble protein oligomers. SDS-PAGE showed only the protein band representing the monomeric eADF4(C16), but due to the large size of the HMW-aggregates it is likely that they were not able to enter the gel and therefore not detected by silver staining. The amount of these HMW-aggregates could only be reduced by long centrifugation times which are not commonly used for HP-SEC sample preparation.

The degradation process of eADF4(C16) induced by incubation at 80°C solely led to the formation of large visible protein fibers. The aggregation pathway is therefore different to globular therapeutic proteins like monoclonal antibodies or cytokines where soluble aggregates and subvisible particles play a major role in protein degradation [39]. The assembly of the spider silk protein eADF4(C16) starts with intrinsically random coiled protein molecules in the aqueous environment. Therefore, it is very likely that aggregates are formed directly by self-association of unfolded protein molecules which act as aggregation nucleus on their own. As a result and dependent on the environmental conditions like ionic strength, eADF4(C16) aggregates are easily formed and were determined in literature as fibrils at low and solid spheres at high potassium phosphate concentrations [19, 36, 40, 41]. In the case of heat-induced aggregation at low ionic strength (10 mM Tris buffer), it is assumed that those fibrils only occur as intermediates which are instantly transformed to larger protein fibers due to the increased kinetics of the aggregation process.

As a consequence for the particle preparation procedure, two different preventive actions can be derived. At first, if a preheating of the formulation is intended, the salting-out process should be performed as quickly as possible. The technical requirements allow a filling of the pump with 100 mL in 5 minutes and the mixing takes 2 minutes at a flow rate of 50 mL/min. Therefore, the time period at which the formulation is processed at elevated temperature can be kept below a total of 10 minutes. Compared to the loss in protein recovery this short time period does not raise a problem for the preparation process. Secondly, in order to achieve a spider silk formulation without or at least with very low amounts of aggregates it is not only sufficient to filtrate the solution, but also long centrifugation times or ultracentrifugation should be applied shortly before particle preparation is carried out.

3.4 COLLOIDAL STABILITY OF SPIDER SILK NANOPARTICLES

Stability issues regarding nanosuspensions have been widely investigated and can be categorized into physical and chemical stability. The latter is certainly specific for each drug delivery system and depends on the corresponding polymer and delivered drug. Physical stability is a common issue for nanosuspensions and includes primarily sedimentation and agglomeration effects. Sedimentation can be minimized by decreasing particle size and increasing medium viscosity to overcome the occurrence of deflocculated suspensions [42]. In the case of eADF4(C16) particles slow sedimentation effects were visually observed during storage, but redispersion was achieved quite easily. In general, the large surface area of nanoparticles creates high total surface energy which is thermodynamically unfavorable and leads to problems in terms of agglomeration [43]. As far as no steric stabilizers are added, the potential energy of interactions between particles can be explained by the Derjaguin-Landau-Verwey-Overbeek (D.L.V.O.) theory. Therein, the potential energy is the sum of repulsive forces due to the overlay of electrical double layers and attractive forces due to van der Waal's forces [44]. The repulsive forces depend on several factors including the zeta-potential of the system, the particle radius, the interparticular distance and the dielectric constant of the medium, whereas van der Waal's forces are affected by interparticular distance and particle radius. For this reason, one of the key parameters to predict the physical stability of a suspension is the zeta-potential, which is defined as the electrical potential at the shear plane around particles in the dispersion medium [43]. The higher the absolute value of the zeta-potential, the more stable is the suspension. On this account, the colloidal stability of spider silk particles was investigated at different pH and ionic strength in terms of particle size, polydispersity and zeta-potential.

In order to evaluate the maximal range of the zeta-potential and to determine the isoelectric point of eADF4(C16) particles, a pH-titration was performed using a 10 mM sodium chloride solution as dispersion medium. The corresponding zeta-potentials and particle sizes are plotted vs. pH in Figure 3.17, A. An isoelectric point of 3.97 was determined and the zeta-potential of eADF4(C16) particles at neutral pH (pH 6-8) is around -28 mV in 10 mM sodium chloride. The derived value for the isoelectric point of eADF4(C16) particles corresponds well to the calculated isoelectric point of 3.5 for the eADF4(C16) molecule including the T7-tag.

Furthermore, the zeta-potential of eADF4(C16) particles was determined at different pH and ionic strengths as shown in Figure 3.17, B. The absolute value of the zeta-potential decreased from (-)27 mV at pH 7.0 and 30 mM ionic strength to (-)10 mV at pH 5 and 100 mM ionic strength. The zeta-potential adopted positive values when the pH of the formulation was below the isoelectric point (pH 3, 30 mM ionic strength).

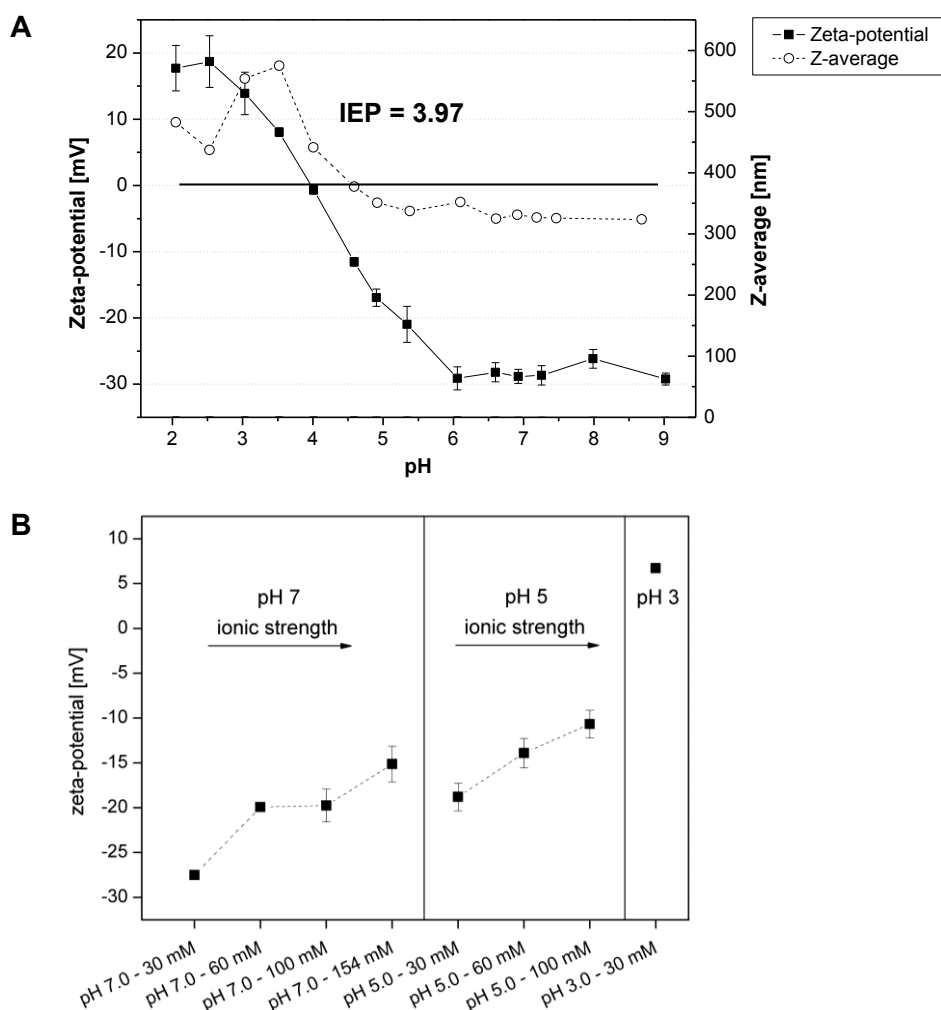


Figure 3.17. (A) Determination of the isoelectric point of eADF4(C16) particles by dynamic light scattering (dispersion medium: 10 mM sodium chloride). (B) Zeta-potential of eADF4(C16) particles at pH 3 / 5 / 7 and an ionic strength of 30 / 60 / 100 / 154 mM

Next, the impact of the decreased zeta-potential concerning the colloidal stability was investigated. Spider silk nanosuspensions were analyzed at pH 3, pH 5 and pH 7 and an overall ionic strength of 30 mM. It was found that eADF4(C16) particles were colloidal stable at pH 7 over a period of 24 hours, whereas a decrease in pH towards (pH 5) or below (pH 3) the isoelectric point of eADF4(C16) resulted in significant particle agglomeration (see Figure 3.18, A). As ionic strength strongly influences the zeta-potential, its impact on the physical stability at pH 5 and pH 7 was investigated as shown in Figure 3.18, B. Spider silk particles were not colloidal stable at any ionic strength at pH 5. This was expected because eADF4(C16) particles showed already agglomeration at an ionic strength of 30 mM. In contrast, particle size and PI remained almost constant over 24 hours at pH 7 and an ionic strength of 30 mM. A further increase of the ionic strength to 100 mM or even 154 mM resulted in only minor changes in particle size and PI after 24 hours of incubation compared to the stock dispersion in purified water. To evaluate the long-term stability of eADF4(C16) particles in highly purified water, the particle size and size distribution was monitored over a

storage period of 6 months at 2-8°C (see Figure 3.18, C). Interestingly, colloidal stability was maintained during storage as the increase in particle size was only 5.7% and the PI remained below 0.20.

In conclusion, these results indicate that eADF4(C16) nanosuspensions are colloidally stable only in liquid formulations with low ionic strength and a formulation pH higher than pH 5.

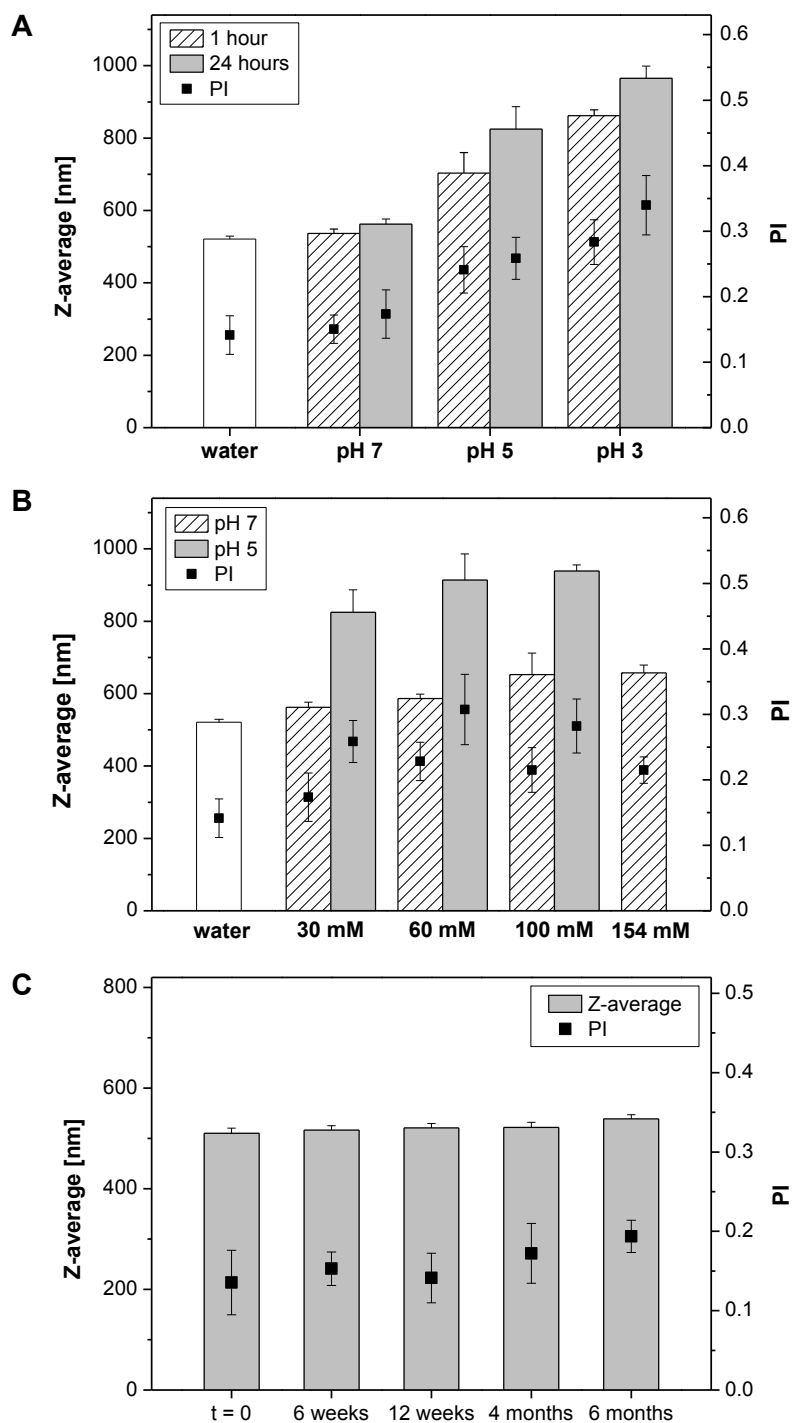


Figure 3.18. (A) Particle size and PI of eADF4(C16) particles after 1 and 24 hours storage at pH 7.0 (10 mM phosphate), pH 5.0 (10 mM acetate) and pH 3.0 (10 mM phosphate). The overall ionic strength of all buffers was adjusted to 30 mM with sodium chloride. (B) Particle size and PI of eADF4(C16) particles incubated for 24 hours at pH 5.0 and pH 7.0 at different ionic strengths. (C) Storage stability of eADF4(C16) particles in stock dispersions (purified water). The standard deviation was calculated from three analytical subruns performed for each corresponding particle batch.

3.5 FREEZE-DRYING OF eADF4(C16) NANOSUSPENSIONS

Two different strategies can be applied in order to overcome the limited physical and chemical stability of suspensions during storage. On the one hand, stabilizers are used to avoid a loss in physical stability due to steric stabilization and increased electrostatic repulsion [42]. On the other hand, pharmaceutical drying techniques are employed to withdraw the water from aqueous suspensions. For that purpose, freeze-drying is the most commonly used drying technique [23]. As one advantage of freeze-drying is the excellent stabilization of sensitive drugs like therapeutic proteins [45], freeze-drying was applied to the development of stable protein loaded eADF4(C16) particle formulations. Previous knowledge of other groups, which already reported on freeze-drying of nanosuspensions, gives indications concerning the choice of possible excipients (lyo- and cryoprotectants) and formulation parameters [23, 24, 46, 47]. An overview of all investigated formulations and parameters in this work is given in Table 3.3.

Table 3.3. Freeze-drying of empty and lysozyme-loaded eADF4(C16) particles using different types of excipients, excipient-to-eADF4(C16) particles ratios [w/w] and reconstitution volumes after lyophilization

Excipient	Filling volume [mL]	Excipient-to-eADF4(C16) particles weight ratio	Reconstitution volume [mL]
<i>empty eADF4(C16) particles</i>			
sucrose	1.0	0 / 5 / 10 / 30 / 50	0.1 / 0.2 / 1.0
sucrose	0.5	2.5 / 5 / 20 / 50	0.5
trehalose	0.5	2.5 / 5 / 20 / 50	0.5
mannitol	0.5	2.5 / 5 / 20 / 50	0.5
<i>lysozyme-loaded eADF4(C16) particles</i>			
sucrose	0.5	30	0.5
trehalose	0.5	30	0.5
mannitol	0.5	30	0.5

3.5.1 FEASIBILITY STUDY

The focus was to test the feasibility of freeze-drying eADF4(C16) nanosuspensions. Therefore, a conventional lyophilization cycle could be employed because spider silk particles had shown no influence on Tg' compared to placebo formulations (data not shown). Results from this freeze-drying cycle with empty eADF4(C16) particles and different concentrations of sucrose as freeze-drying excipient are displayed in Figure 3.19. Compared to particle sizes and polydispersity indices of the suspensions before lyophilization, none of the freeze-dried formulations containing 10:1 [w/w] or more sucrose showed increased values after reconstitution with the original filling volume of 1.0 mL (dashed bars). In contrast, freeze-drying of formulations lacking sucrose or comprising sucrose at a w/w-ratio of 5:1

resulted in agglomerated particles represented by the increase in particle size and PI. Therefore, a minimum excipient-to-eADF4(C16) particle ratio of 10:1 [w/w] is considered to be required for a sufficient stabilization of spiders silk particles during freeze-drying.

Moreover, the effect of reduced reconstitution volumes was investigated according to Zillies et al. [25] as an opportunity to concentrate the formulations after freeze-drying. For instance, this technique may be necessary to obtain a required nanoparticle concentration and the corresponding drug load for a potential *in vitro* or *in vivo* study. An impact of reduced reconstitution volumes was only observed at an excipient-to-eADF4(C16) particles ratio of 5:1 [w/w]. Herein, reduced volumes led to an increase in particle size and polydispersity index, indicating that reconstitution with low volumes creates agglomerated spider silk particles. At excipient-to-eADF4(C16) particles ratios of 10:1 [w/w] or above, the lower reconstitution volumes of 1/5th and 1/10th of the original volume led to only minor changes in particle size and PI. Therefore, the impact of the reconstitution volume can be neglected above the determined threshold and an increase of the nanoparticle concentration after lyophilization is possible without modification of the spider silk particles' colloidal properties.

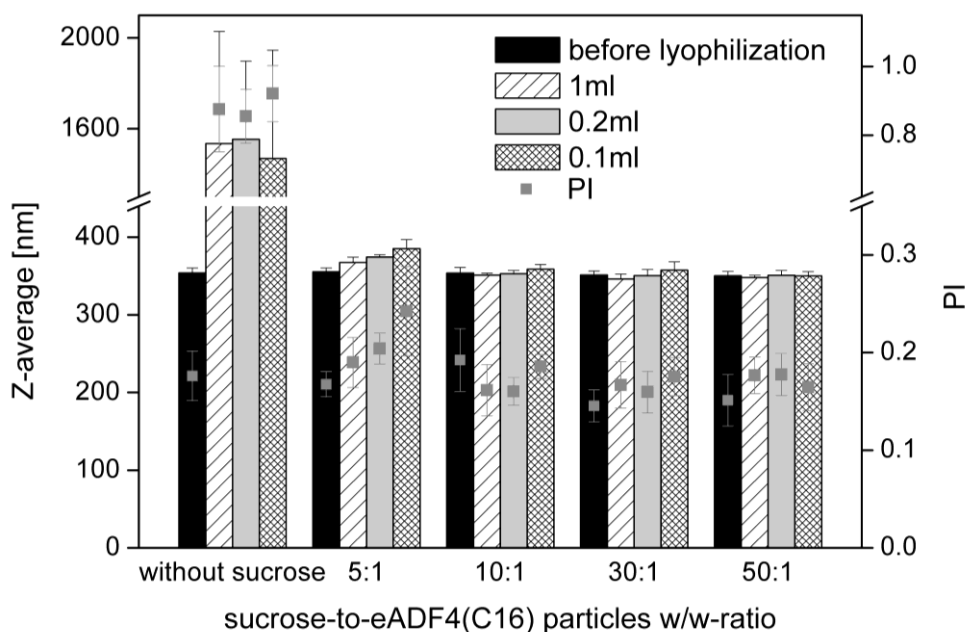


Figure 3.19. Particle size of reconstituted empty eADF4(C16) particles right after freeze-drying using sucrose as freeze-drying excipient at different sucrose-to-eADF4(C16) particles ratios [w/w] and using different reconstitution volumes from 1.0 to 0.1 mL

3.5.2 FORMULATION DEVELOPMENT

In a second set of freeze-drying experiments, two commonly used disaccharides, namely sucrose and trehalose as amorphous lyo- and cryoprotectants, and mannitol as bulking agent were compared regarding their ability to stabilize the physical properties of eADF4(C16) suspensions during freeze-drying (see Figure 3.20). As it can be concluded from the increased particle size after reconstitution, none of the three excipients was able to sufficiently prevent eADF4(C16) particles from agglomeration at an excipient-to-eADF4(C16) particles ratio of 5:1 [w/w] or less. The results above the determined threshold of a w/w-ratio of 10:1 were different. All formulations comprising either sucrose or trehalose showed no significant changes in eADF4(C16) particle size and no difference between the employed excipients. It is commonly known that freeze-dried formulations containing mannitol exhibit a different nature compared to sucrose or trehalose as mannitol readily crystallizes during freeze-drying. Hence, decreased protein drug recovery was detected after freeze-drying of different proteins with mannitol due to the prevention of requisite hydrogen bonding [48]. Nevertheless, it was described that in the case of freeze-drying particulate formulations mannitol was able to maintain nanoparticles' integrity [25]. The authors explained their results by the so-called particle isolation theory which describes that almost any excipient disregarded of its behavior during freeze-drying is able to separate particles in the unfrozen fraction if sufficient amounts of the excipients are used. Our results confirm this hypothesis as an excipient-to-eADF4(C16) particle ratio of 10:1 is the threshold for sufficient stabilization of eADF4(C16) particles independent from the excipient used in the different formulations.

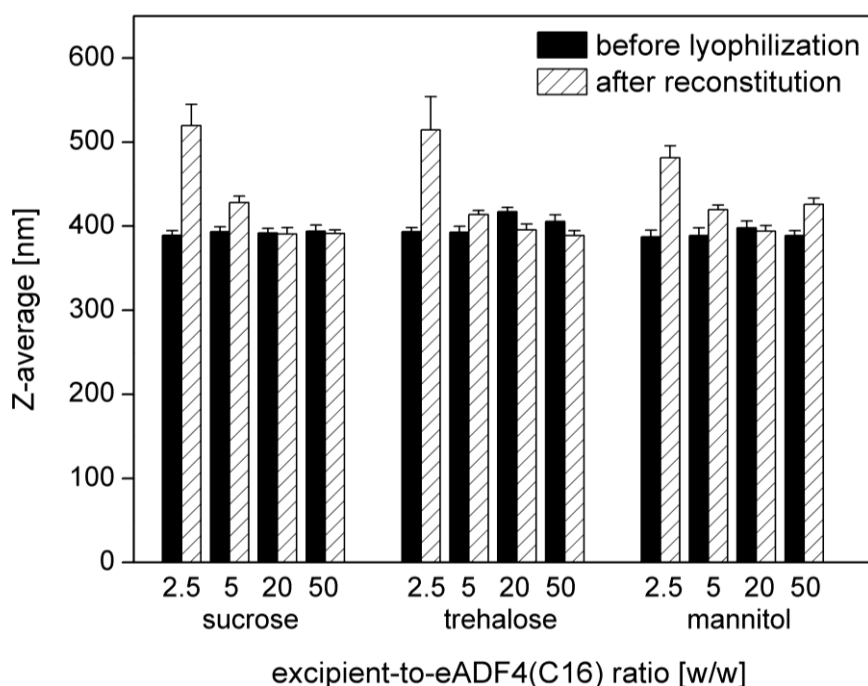


Figure 3.20. Particle size of empty eADF4(C16) particles after freeze-drying with sucrose, trehalose or mannitol at different excipient-to-eADF4(C16) particles ratios

Nevertheless, the three employed excipients exhibit different properties regarding their stabilizing mechanism during freeze-drying and further storage of dried formulations. Sucrose and trehalose act as amorphous and glassy matrix formers which can be distinguished by their glass transition temperature. As shown in Figure 3.21, freeze-dried trehalose formulations possess a significantly higher T_g than sucrose formulations at almost equal residual moisture contents of around 1%. A higher T_g is known to be superior during storage stability of dried protein formulations so that trehalose containing formulations are recommended in the case of freeze-drying eADF4(C16) nanosuspensions. Mannitol containing formulations exhibited a typical crystalline structure represented by the melting point detected at 170°C. Therefore, mannitol does not possess any lyoprotectant activity regarding the stabilization of protein molecules [49]. The macroscopic appearance of sucrose containing formulations of the second freeze-drying experiment is exemplarily shown in Figure 3.21. The porosity of the resulting cake increased with decreasing solid content, but all investigated formulations exhibited an acceptable appearance after freeze-drying.

50:1 [w/w] formulation			
excipient	residual moisture [%]	T_g [°C]	mp [°C]
sucrose	1.11	46.1	-
trehalose	0.86	120.6	-
mannitol	0.32	-	170.1

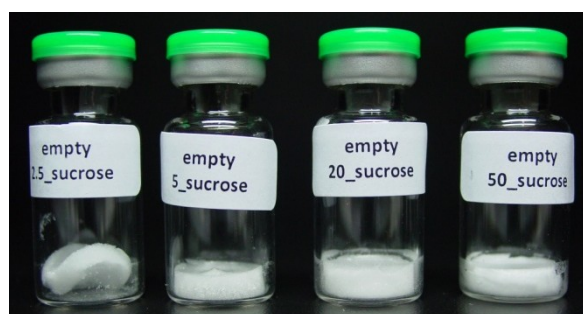


Figure 3.21. Residual moisture and glass transition or melting temperature of freeze-dried formulations comprising a 50:1 [w/w]-ratio of excipient to eADF4(C16) particles. On the right hand side the macroscopic appearance of sucrose containing formulations is illustrated.

In addition to empty eADF4(C16) particles, 15% [w/w] lysozyme-loaded eADF4(C16) particles (via remote loading) were freeze-dried either with sucrose, trehalose or mannitol at an excipient-to-particles weight ratio of 30:1 using the same freeze-drying cycle as before. All investigated formulations exhibited the same particle size and PI after lyophilization and reconstitution (see Figure 3.22).

Therefore, two conclusions can be drawn from the set of freeze-drying studies. At first, freeze-drying of empty as well as lysozyme-loaded eADF4(C16) particles with an excipient-to-eADF4(C16) particles weight ratio of at least 10:1 is possible without losing the physical properties of the original eADF4(C16) particle nanosuspensions. Secondly, trehalose at a mass ratio of 30:1 or 50:1 is the recommended excipient concerning the storage stability of lyophilized eADF4(C16) formulations as the highest T_g was obtained and the colloidal properties of the initial suspensions were maintained throughout lyophilization.

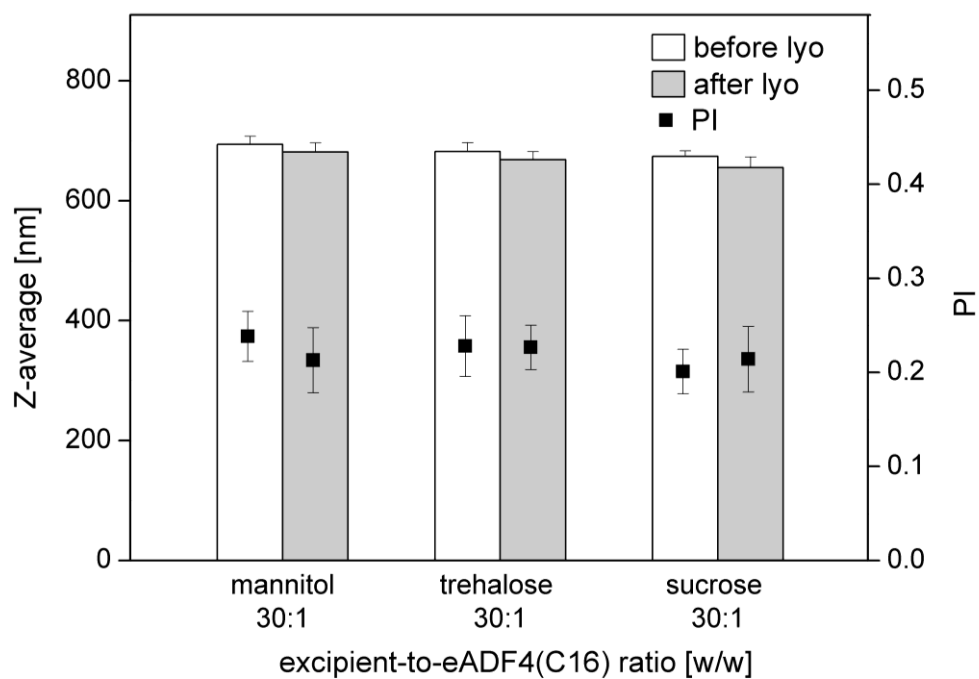


Figure 3.22. Particle size and polydispersity indices of reconstituted lysozyme-loaded eADF4(C16) particles using sucrose, mannitol or trehalose as freeze-drying excipients at a w/w-ratio of 30:1

3.6 SUMMARY AND CONCLUSIONS

The preparation, characterization and formulation development of eADF4(C16) particles was described in this chapter. Furthermore, liquid eADF4(C16) formulations were characterized by multiple analytical techniques and subjected to incubation at elevated temperature.

First of all, the phase separation process leading to solid eADF4(C16) spheres was analyzed in detail in order to obtain nanoparticles not significantly larger than 300 nm and microparticles with diameters of at least 5 μm . Both targeted particle sizes were achieved using the same phase separation mechanism, but different preparation techniques. In terms of nanosized spider silk particles a micromixing system consisting of two digitally controlled syringe pumps and a T-shaped mixing element with an inner diameter of 500 μm was established as standard preparation procedure due to its upscalability and excellent reproducibility. It was shown previously that the phase separation process of eADF4(C16) into solid spheres can be influenced by the mixing intensity and protein concentration [22], but further parameters altering the kinetics of the process were not evaluated so far. Especially an elevated process temperature of 60°C or 80°C dramatically reduced the resulting particle size and polydispersity of eADF4(C16) particles so that finally batches with homogenous particle size distributions and particle sizes slightly below 300 nm were obtained. eADF4(C16) microparticles were prepared by using an ultrasonic spray nozzle equipped with a dual liquid feed system. However, the simultaneous atomization of potassium phosphate and aqueous spider silk formulations resulted only in non-spherical protein aggregates like threads and fibrils at all investigated conditions. In contrast, microparticles were easily obtained by the atomization of potassium phosphate into eADF4(C16) solutions. This approach was further optimized by applying slower atomization rates and/or lower potassium phosphate concentrations so that it was able to prepare microparticles between 5 and 7 μm .

As the aqueous eADF4(C16) protein solution is one important component of the phase separation process, different analytical techniques were developed and employed for the characterization of eADF4(C16) formulations after incubation at 80°C. The analysis by AF4 and other techniques such as size exclusion chromatography and subvisible particle counting revealed that the spider silk protein formulation exhibits only limited protein stability over a period of 4 hours at 80°C. The protein loss accounted for around 40% at a protein concentration of 1.0 mg/mL and was mainly attributed to the formation of large and visible protein aggregates which formed thin spider silk fibers at the investigated conditions. Significant amounts of soluble eADF4(C16) aggregates could not be detected throughout heat-induced degradation. Consequently, the particle preparation procedure as described beforehand is not significantly affected as long as the liquid protein formulation is heated up and directly processed in the micromixing device.

eADF4(C16) particles in the submicron range were analyzed regarding their colloidal stability at different pH and ionic strength. The nanoparticles exhibit a zeta-potential around -30 mV at neutral pH and low ionic strength (10 mM sodium chloride) and a determined isoelectric point of 3.97. It was shown that nanosuspensions without further stabilizers are physically stable at low ionic strength (30 mM) and a pH above 5. The stock suspension in purified water can be stored for 6 months at 2-8°C without an altering the particle size distribution. Another step in formulation development was done by the implementation of freeze-drying to spider silk nanosuspensions. Sucrose, trehalose and mannitol were employed and analyzed regarding their ability to maintain the particle characteristics throughout the drying process. A threshold of an excipient-to-particles ratio [w/w] of 10:1 was determined as all excipients were able to stabilize eADF4(C16) particles at or above this ratio. The results therefore confirm the particle isolation theory described in literature for drying of nanosuspensions. Furthermore, lysozyme-loaded eADF4(C16) particles (remote loading) were successfully freeze-dried. For this reason, freeze-drying enables the preparation of stable drug-loaded nanosuspensions.

3.7 REFERENCES

- [1] **Kumari A., Yadav S. K. and Yadav S. C.,** Biodegradable polymeric nanoparticles based drug delivery systems. *Colloids and Surfaces B: Biointerfaces* 2010, 75(1), 1-18
- [2] **Singh R. and Lillard Jr J. W.,** Nanoparticle-based targeted drug delivery. *Exp. Mol. Pathol.* 2009, 86(3), 215-223
- [3] **Tan M. L., Choong P. F. M. and Dass C. R.,** Recent developments in liposomes, microparticles and nanoparticles for protein and peptide drug delivery. *Peptides* 2010, 31(1), 184-193
- [4] **Park J., Ye M. and Park K.,** Biodegradable Polymers for Microencapsulation of Drugs. *Molecules* 2005, 10(1), 146-161
- [5] **Vrignaud S., Benoit J.-P. and Saulnier P.,** Strategies for the nanoencapsulation of hydrophilic molecules in polymer-based nanoparticles. *Biomaterials* 2011, 32(33), 8593-8604
- [6] **van de Weert M., Hennink W. E. and Jiskoot W.,** Protein instability in poly(lactic-co-glycolic acid) microparticles. *Pharm. Res.* 2000, 17(10), 1159-1167
- [7] **Langer K., Anhorn M. G., Steinhäuser I., Dreis S., Celebi D., Schrickel N., Faust S. and Vogel V.,** Human serum albumin (HSA) nanoparticles: Reproducibility of preparation process and kinetics of enzymatic degradation. *Int. J. Pharm.* 2008, 347(1-2), 109-117
- [8] **Coester C. J., Langer K., Von Briesen H. and Kreuter J.,** Gelatin nanoparticles by two step desolvation - a new preparation method, surface modifications and cell uptake. *J. Microencapsul.* 2000, 17(2), 187-193
- [9] **Pritchard E. M. and Kaplan D. L.,** Silk fibroin biomaterials for controlled release drug delivery. *Expert Opin. Drug Deliv.* 2011, 8(6), 797-811
- [10] **Wenk E., Merkle H. P. and Meinel L.,** Silk fibroin as a vehicle for drug delivery applications. *J. Control. Release* 2011, 150(2), 128-141
- [11] **Klier J., Fuchs S., May A., Schillinger U., Plank C., Winter G., Gehlen H. and Coester C.,** A Nebulized Gelatin Nanoparticle-Based CpG Formulation is Effective in Immunotherapy of Allergic Horses. *Pharm. Res.* 2012, 29(6), 1650-1657
- [12] **Wilz A., Pritchard E. M., Li T., Lan J.-Q., Kaplan D. L. and Boison D.,** Silk polymer-based adenosine release: therapeutic potential for epilepsy. *Biomaterials* 2008, 29(26), 3609-3616
- [13] **Wang X., Wenk E., Matsumoto A., Meinel L., Li C. and Kaplan D. L.,** Silk microspheres for encapsulation and controlled release. *J. Control. Release* 2007, 117(3), 360-370
- [14] **Wang X., Wenk E., Zhang X., Meinel L., Vunjak-Novakovic G. and Kaplan D. L.,** Growth factor gradients via microsphere delivery in biopolymer scaffolds for osteochondral tissue engineering. *J. Control. Release* 2009, 134(2), 81-90
- [15] **Wang X., Yucel T., Lu Q., Hu X. and Kaplan D. L.,** Silk nanospheres and microspheres from silk/pva blend films for drug delivery. *Biomaterials* 2010, 31(6), 1025-1035
- [16] **Wenk E., Wandrey A. J., Merkle H. P. and Meinel L.,** Silk fibroin spheres as a platform for controlled drug delivery. *J. Control. Release* 2008, 132(1), 26-34
- [17] **Zhang Y.-Q., Shen W.-D., Xiang R.-L., Zhuge L.-J., Gao W.-J. and Wang W.-B.,** Formation of silk fibroin nanoparticles in water-miscible organic solvent and their characterization. *Journal of Nanoparticle Research* 2007, 9(5), 885-900

- [18] **Lammel A. S., Hu X., Park S.-H., Kaplan D. L. and Scheibel T. R.**, Controlling silk fibroin particle features for drug delivery. *Biomaterials* 2010, 31(16), 4583-4591
- [19] **Slotta U., Rammensee S., Gorb S. and Scheibel T.**, An engineered spider silk protein forms microspheres. *Angew. Chem. Int. Ed. Engl.* 2008, 47(24), 4592-4594
- [20] **Rammensee S., Slotta U., Scheibel T. and Bausch A. R.**, Assembly mechanism of recombinant spider silk proteins. *P Natl Acad Sci USA* 2008, 105(18), 6590-6595
- [21] **Huemmerich D., Scheibel T., Vollrath F., Cohen S., Gat U. and Ittah S.**, Novel Assembly Properties of Recombinant Spider Dragline Silk Proteins. *Curr. Biol.* 2004, 14(22), 2070-2074
- [22] **Lammel A., Schwab M., Slotta U., Winter G. and Scheibel T.**, Processing conditions for the formation of spider silk microspheres. *ChemSusChem* 2008, 1(5), 413-416
- [23] **Abdelwahed W., Degobert G., Stainmesse S. and Fessi H.**, Freeze-drying of nanoparticles: formulation, process and storage considerations. *Adv Drug Deliv Rev* 2006, 58(15), 1688-1713
- [24] **Anhorn M. G., Mahler H.-C. and Langer K.**, Freeze drying of human serum albumin (HSA) nanoparticles with different excipients. *Int. J. Pharm.* 2008, 363(1-2), 162-169
- [25] **Zillies J. C., Zwirok K., Hoffmann F., Vollmar A., Anchordoquy T. J., Winter G. and Coester C.**, Formulation development of freeze-dried oligonucleotide-loaded gelatin nanoparticles. *Eur. J. Pharm. Biopharm.* 2008, 70(2), 514-521
- [26] **Rice-Ficht A. C., Arenas-Gamboa A. M., Kahl-McDonagh M. M. and Ficht T. A.**, Polymeric particles in vaccine delivery. *Curr. Opin. Microbiol.* 2010, 13(1), 106-112
- [27] **Zölls S., Tantipolphan R., Wiggernhorn M., Winter G., Jiskoot W., Friess W. and Hawe A.**, Particles in therapeutic protein formulations, Part 1: Overview of analytical methods. *J. Pharm. Sci.* 2012, 101(3), 914-935
- [28] **Krishnamurthy R., Lumpkin J. A. and Sridhar R.**, Inactivation of lysozyme by sonication under conditions relevant to microencapsulation. *Int. J. Pharm.* 2000, 205(1-2), 23-34
- [29] **Rokhina E. V., Lens P. and Virkutyte J.**, Low-frequency ultrasound in biotechnology: state of the art. *Trends Biotechnol.* 2009, 27(5), 298-306
- [30] **Morlock M., Koll H., Winter G. and Kissel T.**, Microencapsulation of rh-erythropoietin, using biodegradable poly(-lactide-co-glycolide): protein stability and the effects of stabilizing excipients. *Eur. J. Pharm. Biopharm.* 1997, 43(1), 29-36
- [31] **Zhang Y. and Cremer P. S.**, Interactions between macromolecules and ions: the Hofmeister series. *Curr. Opin. Chem. Biol.* 2006, 10(6), 658-663
- [32] **Huemmerich D., Slotta U. and Scheibel T.**, Processing and modification of films made from recombinant spider silk proteins. *Applied Physics A: Materials Science & Processing* 2006, 82(2), 219-222
- [33] **Hu X., Kaplan D. and Cebe P.**, Determining Beta-Sheet Crystallinity in Fibrous Proteins by Thermal Analysis and Infrared Spectroscopy. *Macromolecules* 2006, 39(18), 6161-6170
- [34] **Carpenter J. F., Randolph T. W., Jiskoot W., Crommelin D. J. A., Middaugh C. R. and Winter G.**, Potential inaccurate quantitation and sizing of protein aggregates by size exclusion chromatography: Essential need to use orthogonal methods to assure the quality of therapeutic protein products. *J. Pharm. Sci.* 2010, 99(5), 2200-2208
- [35] **Slotta U.**, Charakterisierung von Assemblierungsformen rekombinanter Spinnenseidenproteine (2009), *Dissertation*, Fakultät für Chemie, Technische Universität München

- [36] **Slotta U., Hess S., Spieß K., Stromer T., Serpell L. and Scheibel T.**, Spider Silk and Amyloid Fibrils: A Structural Comparison. *Macromol. Biosci.* 2007, 7(2), 183-188
- [37] **Fraunhofer W. and Winter G.**, The use of asymmetrical flow field-flow fractionation in pharmaceuticals and biopharmaceuticals. *Eur. J. Pharm. Biopharm.* 2004, 58(2), 369-383
- [38] **Cao S., Pollastrini J. and Jiang Y.**, Separation and Characterization of Protein Aggregates and Particles by Field Flow Fractionation. *Curr. Pharm. Biotechnol.* 2009, 10(4), 382-390
- [39] **Wang W., Nema S. and Teagarden D.**, Protein aggregation—Pathways and influencing factors. *Int. J. Pharm.* 2010, 390(2), 89-99
- [40] **Huemmerich D., Helsen C. W., Quedzuweit S., Oschmann J., Rudolph R. and Scheibel T.**, Primary structure elements of spider dragline silks and their contribution to protein solubility. *Biochemistry* 2004, 43(42), 13604-13612
- [41] **Rammensee S., Huemmerich D., Hermanson K. D., Scheibel T. and Bausch A. R.**, Rheological characterization of hydrogels formed by recombinantly produced spider silk. *Applied Physics A: Materials Science & Processing* 2006, 82(2), 261-264
- [42] **Nutan M. T. H. and Reddy I. K.**, General Principles of Suspensions, in *Pharmaceutical Suspensions*, Kulshreshtha, A.K., Singh, O.N. and Wall, G.M., Editors. 2010, Springer New York. p. 39-65
- [43] **Wu L., Zhang J. and Watanabe W.**, Physical and chemical stability of drug nanoparticles. *Adv Drug Deliv Rev* 2011, 63(6), 456-469
- [44] **Matthews B. A. and Rhodes C. T.**, Use of the derjaguin, landau, verwey, and overbeek theory to interpret pharmaceutical suspension stability. *J. Pharm. Sci.* 1970, 59(4), 521-525
- [45] **Tang X. and Pikal M.**, Design of freeze-drying processes for pharmaceuticals: practical advice. *Pharm. Res.* 2004, 21(2), 191-200
- [46] **Schwarz C. and Mehnert W.**, Freeze-drying of drug-free and drug-loaded solid lipid nanoparticles (SLN). *Int. J. Pharm.* 1997, 157(2), 171-179
- [47] **Carpenter J. F., Pikal M. J., Chang B. S. and Randolph T. W.**, Rational Design of Stable Lyophilized Protein Formulations: Some Practical Advice. *Pharm. Res.* 1997, 14(8), 969-975
- [48] **Wang W.**, Lyophilization and development of solid protein pharmaceuticals. *Int. J. Pharm.* 2000, 203(1-2), 1-60
- [49] **Izutsu K., Yoshioka S. and Terao T.**, Effect of mannitol crystallinity on the stabilization of enzymes during freeze-drying. *Chem. Pharm. Bull. (Tokyo)* 1994, 42(1), 5-8

CHAPTER 4

SPIDER SILK PARTICLES FOR DRUG DELIVERY

4.1 INTRODUCTION

Particulate drug delivery systems made of different types of biodegradable polymers have been in the focus of research for decades due to their excellent controllability [1]. Nanoparticles as well as microspheres have been employed for controlled delivery of various therapeutic agents including anticancer and antifungal drugs as well as peptides and proteins [2]. The latter class of pharmaceutical compounds requires special formulation due to their susceptibility to proteolysis, chemical modification and denaturation/aggregation during storage [3]. The polymer used as drug carrier system has to fulfill a number of requirements: protection of the protein drug from denaturation or degradation, control of drug release, biodegradability, no toxicity, low cost and easy processability [4]. Commonly used polymeric carriers for this purpose are of synthetic origin. Polyesters like polylactic-co-glycolic acid (PLGA) are the most extensively studied among them [5, 6]. However, polyester-based matrices were often not suitable for protein drugs due to the required usage of organic solvents during preparation. In addition, an acidic microenvironment can occur by polymer degradation [6-9]. Therefore, research on hydrophilic polymers of natural origin, which can be easily processed in an aqueous environment, has received growing attention. Herein, especially chitosan was applied as a particulate drug carrier for protein delivery [10-13]. Nevertheless, non-modified chitosan particles and also gelatin nanoparticles often require the utilization of toxic cross-linking agents so that their application for parenteral protein delivery is limited [14, 15].

In order to overcome the aforementioned limitations, new biomaterials are required as polymers for drug delivery applications. Silk proteins including silk fibroin from *Bombyx mori* and recombinant spider silk proteins represent very promising candidates regarding their non-cytotoxic and customizable properties as well as their easy processability into various morphologies like scaffolds, films and spheres [16-21]. Different kind of therapeutic agents have been incorporated into those systems and acceptable *in vitro* release profiles have been reported. However, the preparation techniques applied were quite sophisticated. Moreover, the used silk fibroin from *Bombyx mori* is a natural product and the quality of the protein may vary between individuals of the same species and depends on the required

degumming process [4]. For these reasons, quality control of such a biomaterial will be an issue as it may become difficult to obtain regulatory approval for such a material.

The engineered spider silk protein eADF4(C16) represents a more favorable biomaterial due to its recombinant production process in *E. coli* [22]. As described in chapter 3, smooth protein spheres with high β -sheet content can be formed by a salting-out process with potassium phosphate as lyotropic salt, thereby avoiding the usage of any organic solvent. In order to evaluate these particles as a drug carrier system, small molecular weight drugs were recently loaded on eADF4(C16) particles using an incubation step after particle preparation [23]. Briefly, high loading efficiencies of almost 100% was achieved with positively charged and sufficiently hydrophobic drug molecules and constant *in vitro* release rates were obtained. The supposed mechanism for drug loading and release is displayed in Figure 4.1. Drug molecules are attracted through electrostatic forces in media with low ionic strength (1) and adsorb first to the particle's surface. After saturation of the surface, drug molecules diffuse into the particle matrix (2) and are bound by a combination of hydrophobic and electrostatic forces (3). Redispersion of drug-loaded spider silk particles in release medium leads to a migration of drug molecules to the surface due to the present concentration gradient (4) and results in constant release rates over time (5).

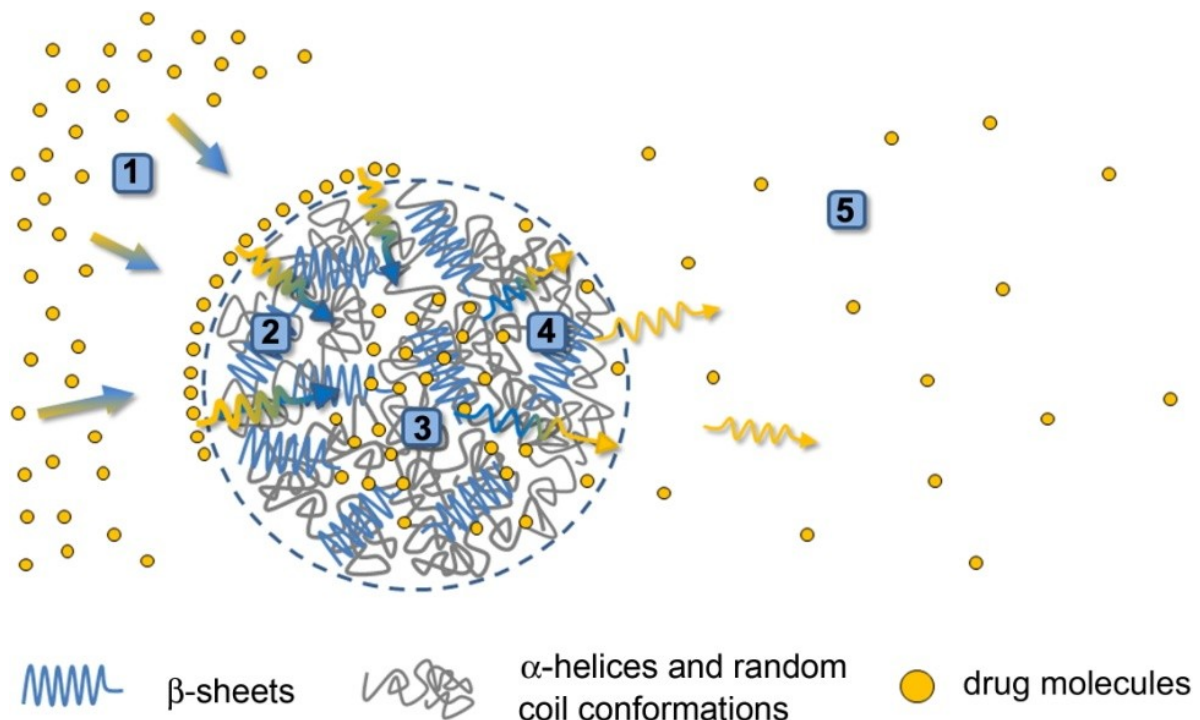


Figure 4.1. Loading and release mechanism for small drug molecules and spider silk particles taken from Lammel et al. [23]

The aim of the work described in this chapter was to investigate the applicability of eADF4(C16) particles as drug carrier for high molecular weight drugs like protein pharmaceuticals. In accordance to the study using small drug molecules, loading was carried out after particle preparation, the so-called 'remote loading' procedure. Two different proteins, namely lysozyme and nerve growth factor, were employed as they represent a model protein and a potential therapeutic drug candidate. Furthermore, the loading mechanism was investigated using fluorescein isothiocyanate (FITC) labeled macromolecules for loading on eADF4(C16) particles and subsequent analysis of the corresponding particle dispersions by confocal laser scanning microscopy (CLSM). The *in vitro* release of the proteins was investigated in dependence of ionic strength and pH of the release medium.

Secondly, the different but common approach of drug encapsulation was performed. Rhodamine B and lysozyme were added to the aqueous protein solution and co-precipitated during phase separation. The resulting loading and release behavior was examined and is reported in section 4.3. Altogether, this chapter gives a detailed overview of the applicability of spider silk particles as a drug carrier system for protein delivery.

4.2 PROTEIN LOADED eADF4(C16) PARTICLES VIA REMOTE LOADING

As it has already been shown in chapter 3, eADF4(C16) particles exhibit an isoelectric point of approx. 4.0. Attractive electrostatic interactions at neutral pH can therefore only occur between spider silk particles and positively charged drug molecules. It has been reported previously that the interactions between spider silk particles and low molecular weight substances, which belong to the class of weak organic bases, depend further on the partition coefficient $\log P$ and the molecular weight of the drug [23]. Strong bases like ethacridine lactate or molecules with a permanently positive charge like methyl violet showed the highest loading efficiency at comparable loading conditions. In order to transfer these findings to protein molecules, one has to consider the complex and completely different structure of proteins compared to small molecules. The charge of a protein molecule at a given pH is primarily determined by the amino acid residues being present in the primary sequence so that an overall net charge of the protein can be defined [24]. Nevertheless, the folding of the molecule plays a very important role in the interaction with other protein molecules as well as with solvent molecules or spider silk particles. The native conformation of a protein in an aqueous solution is usually characterized by presenting hydrophilic amino acid residues towards the solvent molecules, whereas hydrophobic residues are buried inside the globular protein molecule. As a consequence, the known contribution and relation of electrostatic and hydrophobic forces to the interaction of small molecules with spider silk particles has to be reassessed for the interaction of protein molecules with eADF4(C16) particles.

4.2.1 LYSOZYME

The overall net charge of a protein can be determined by dynamic light scattering as it is known for particles or polymers [24]. The resulting pH titration profile of zeta-potential and hydrodynamic diameter for lysozyme is shown in Figure 4.2.

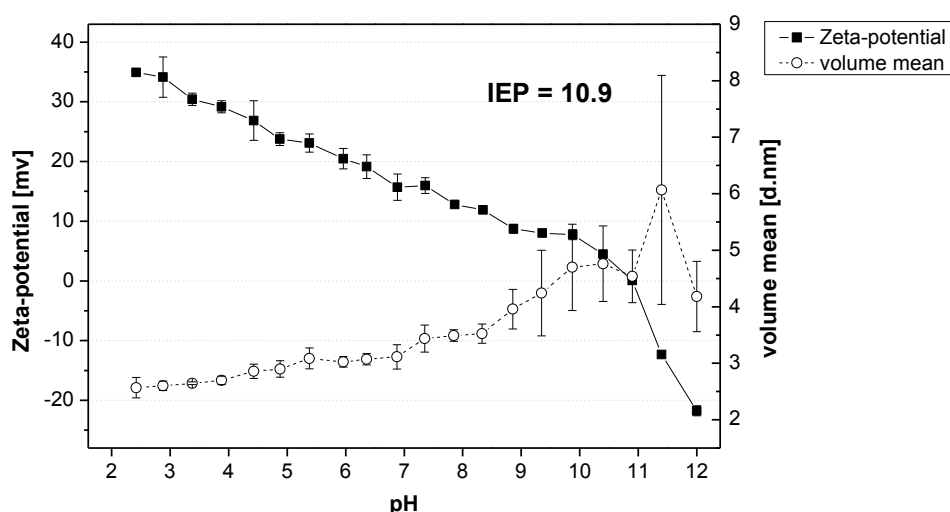


Figure 4.2. Zeta-potential, hydrodynamic diameter and calculated isoelectric point of lysozyme as determined by dynamic light scattering (conc. = 10 mg/mL, background: 10 mM sodium chloride)

The isoelectric point of lysozyme was determined at 10.9 so that a distinct positive overall net charge of the lysozyme molecule is present at neutral pH. Lysozyme with a molecular weight of 14.3 kDa was therefore chosen for the evaluation of protein loading on eADF4(C16) particles.

In order to facilitate electrostatic interactions, ensure protein stability and avoid particle agglomeration, the standard buffer for remote loading was defined as follows: 10 mM phosphate buffer, pH 7.0, addition of sodium chloride (0.573 g/L) to achieve a total ionic strength of 30 mM. Using this standard loading buffer enabled a loading of lysozyme on eADF4(C16) particles in large quantities, which is illustrated in Figure 4.3, A. At this ionic strength of 30 mM, it was possible to load more than 30% [w/w] lysozyme by incubation of eADF4(C16) particles in the lysozyme containing phosphate buffer. The associated loading efficiencies remained upon 95% for w/w-ratios during incubation ranging from 6 to 20%, representing a very effective loading of lysozyme and a strong interaction between eADF4(C16) particles and lysozyme. Figures 4.3, B and C, show the corresponding zeta-potentials and particle sizes of lysozyme-loaded eADF4(C16) particles.

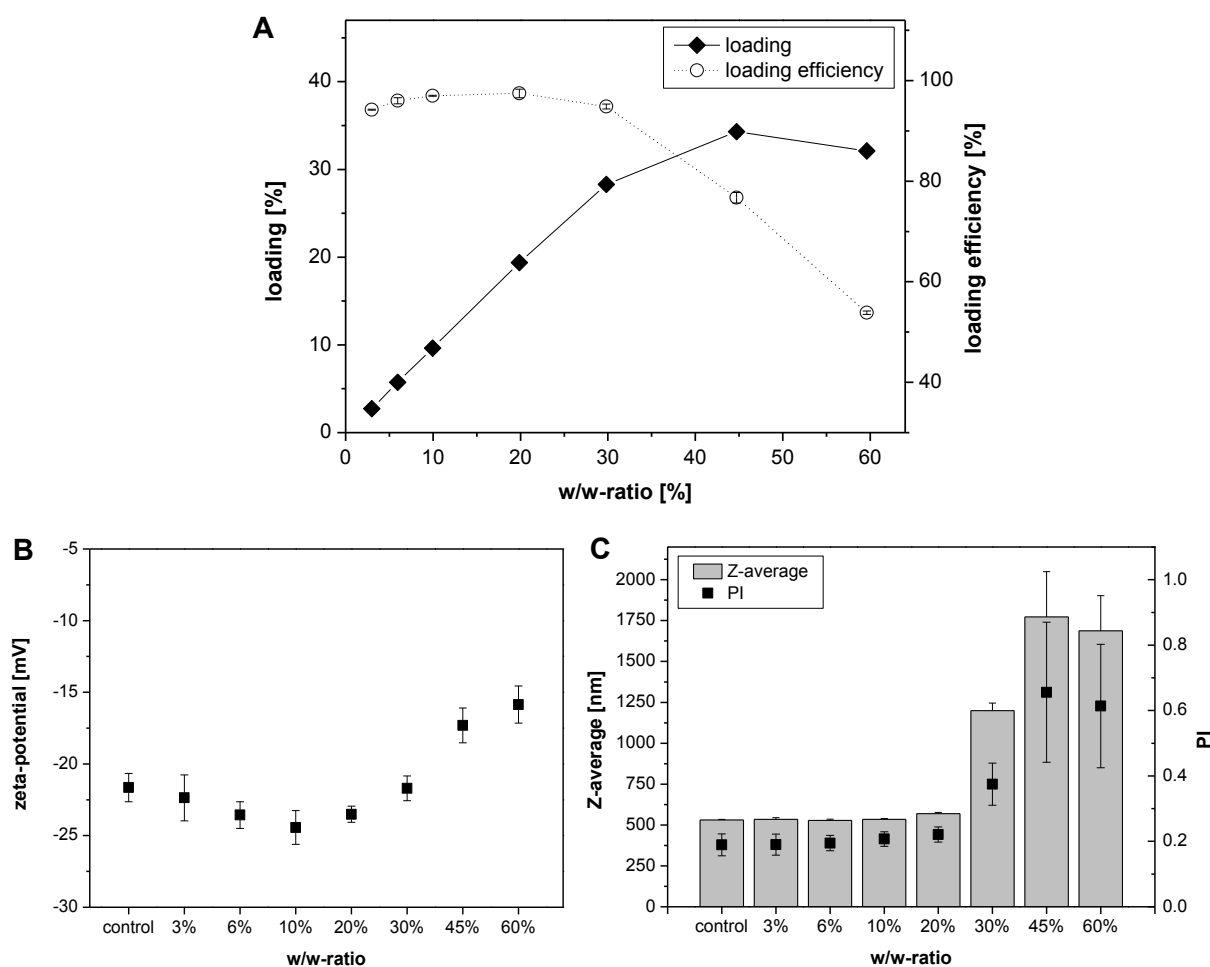


Figure 4.3. Remote loading of eADF4(C16) particles with lysozyme. (A) Loading and loading efficiencies as a function of w/w-ratio of lysozyme-to-eADF4(C16) particles during incubation at pH 7.0/30 mM ionic strength. Zeta-potential (B) and particle size (C) of different lysozyme-loaded eADF4(C16) particles at pH 7.0 / 30 mM ionic strength.

If we assume that only surface loading takes place on eADF4(C16) particles, an increase in particle size combined with a decrease of the absolute value of the zeta-potential should be detectable due to the adsorption of lysozyme molecules to the particles' surface. However, we observed that loading of eADF4(C16) particles with lysozyme does not lead to a significant change in the zeta-potential up to a loading of 30% (see Figure 4.3, B). Simultaneously, the particle size of the corresponding lysozyme-loaded eADF4(C16) particles did not significantly increase during loading up to a w/w-ratio of 20% during incubation (see Figure 4.3, C).

The strong increase in the mean hydrodynamic diameter at higher w/w-ratios detected by dynamic light scattering was further analyzed by scanning electron microscopy. One example of the obtained particle dispersions is demonstrated in Figure 4.7, D, using nerve growth factor. The SEM micrographs of protein-loaded eADF4(C16) particles demonstrated that the high Z-average values were only the result of particle agglomeration but not of larger individual particles due to the protein payload.

Altogether, it is assumed that a substantial fraction of the overall loaded lysozyme diffuses into the protein matrix of eADF4(C16) particles and is not only loaded on the particles' surface. This aspect will further be discussed in detail in section 4.2.3.

The influence of ionic strength on loading and loading efficiencies is shown in Figure 4.4, A and B. An increase in ionic strength from 30 to 100 mM led to a significant decrease in loading and loading efficiencies. For example, loading at 30% w/w-ratio was reduced from 28% at 30 mM to 24% at 60 mM and 20% at 100 mM. The decreased loading caused by higher ionic strength clearly indicates that loading of negatively charged eADF4(C16) particles with positively charged lysozyme is driven by electrostatic interactions.

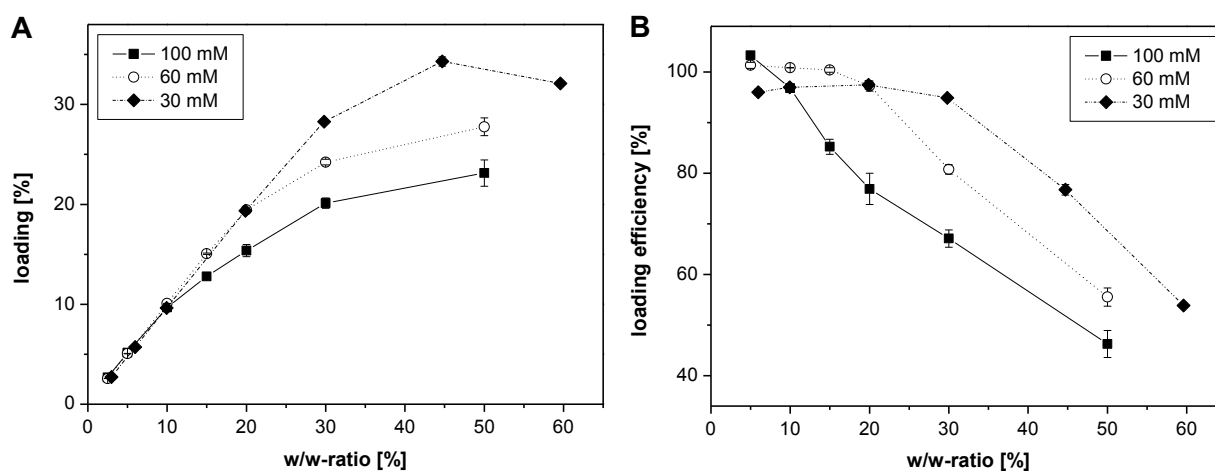


Figure 4.4. (A) Loading of eADF4(C16) particles with lysozyme at different ionic strengths at pH 7.0. (B) Loading efficiencies of lysozyme at different ionic strengths at pH 7.0

In order to describe the hydrophilic/hydrophobic character of a protein, the grand average of hydropathicity (GRAVY) value for a peptide or protein can be calculated as the sum of the individual hydropathy values of the protein's amino acids divided by the number of residues in the sequence [25]. A negative value represents hydrophilic and a positive value more hydrophobic proteins. The GRAVY of the employed lysozyme is -0.472 calculated on its amino acid sequence (ExPASy, ProtParam tool, [26]). The corresponding hydropathicity plot is displayed in Figure 4.5, A. The GRAVY values and hydropathicity plot clearly indicate that lysozyme has more negative hydropathy values and therefore a more hydrophilic character compared to nerve growth factor (see Figure 4.5, B) or eADF4(C16) (see Figure 4.5, C). Consequently, loading of lysozyme is most likely driven by predominantly electrostatic interactions rather than hydrophobic van der Waal's forces.

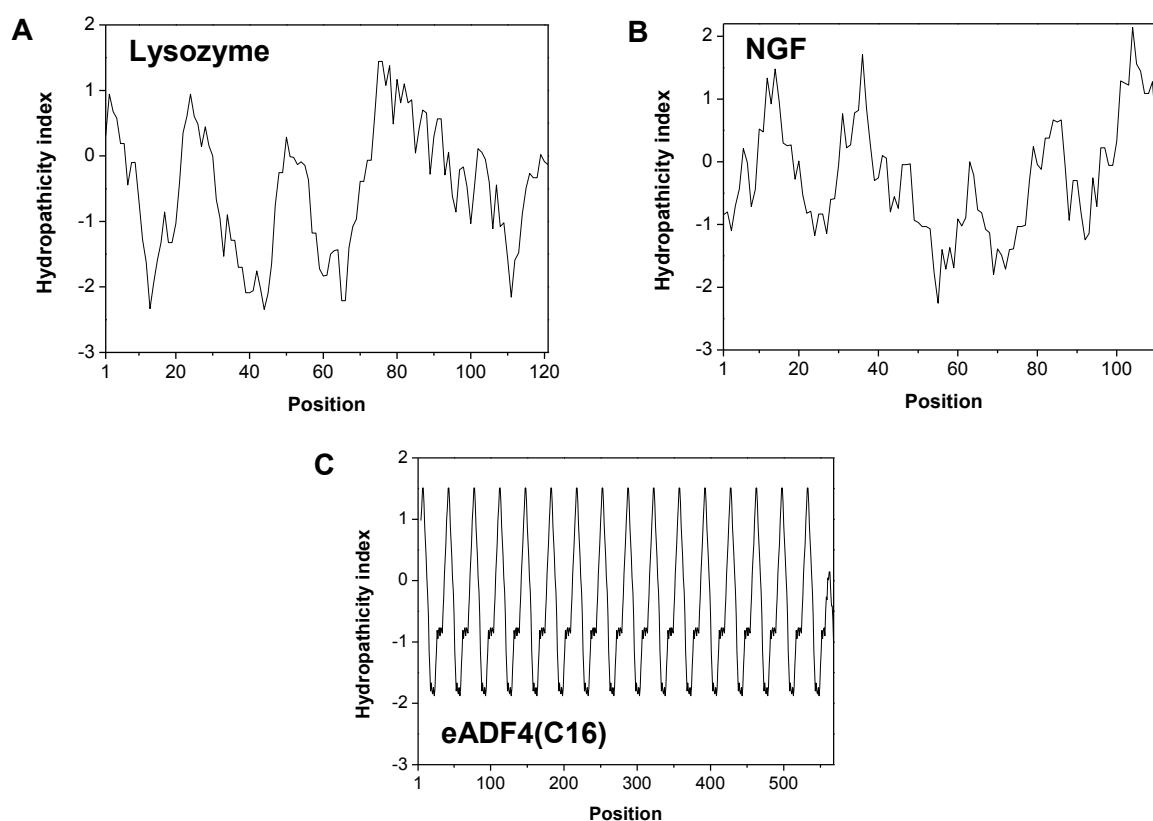


Figure 4.5. Hydropathicity plot of lysozyme (A), nerve growth factor (B) and eADF4(C16) (C) according to Kyte and Doolittle [25]. More positive values indicate stronger hydrophobicity. The position at the x axis reflects the corresponding amino acid of the protein starting at the amino terminus and ending at the carboxy terminus.

In comparison to the loading and loading efficiencies of small molecules determined by Lammel et al. [23], loading with lysozyme is more efficient at a certain w/w-ratio using the same remote loading procedure. Loading of around 13% [w/w] and a corresponding loading efficiency of 80% [w/w] was achieved with methyl violet (MV) as a model drug at a molar ratio of 21:1 (MV:eADF4). A molar ratio of 21:1 corresponds to a w/w-ratio of 17.9%. Lysozyme

was loaded onto eADF4(C16) particles at a w/w-ratio of 20% with a loading efficiency of 97.5% [w/w] and even at a w/w-ratio of 30% with an efficiency of 94.9% [w/w]. It has to be further mentioned that methyl violet was dissolved in purified water without the addition of buffer components or salts so that the obtained values present the maximum achievable loading. Therefore, the total mass of loaded drug at comparable loading conditions is distinctly higher for lysozyme compared to methyl violet or other small molecules which exhibited an even lower loading efficiency [23].

4.2.2 NERVE GROWTH FACTOR

Remote loading was further carried out using nerve growth factor which is regarded as a potential protein drug candidate for future applications of silk proteins [27, 28]. The biochemical properties of recombinant human nerve growth factor have already been described in chapter 2, section 2.1.1.3, but according to the knowledge from previous studies the charge of the protein plays a very important role. For this reason, the determination of net charge vs. pH was performed by dynamic light scattering and the resulting titration profile and IEP are displayed in Figure 4.6. Nerve growth factor exhibits a positive zeta-potential of +15 mV at pH 7, which is almost equal to the corresponding zeta-potential of lysozyme. In combination with an almost similar molecular weight of the monomer molecule (13.5 kDa vs. 14.3 kDa), the loading potential of nerve growth factors was assessed to be as good as for lysozyme. However, it has to be considered that the native conformation of NGF in an aqueous solution consists of non-covalent dimers. It can be clearly depicted from the comparison of the volume mean diameter that dimer formation leads to a larger hydrodynamic diameter for native NGF molecules compared to lysozyme.

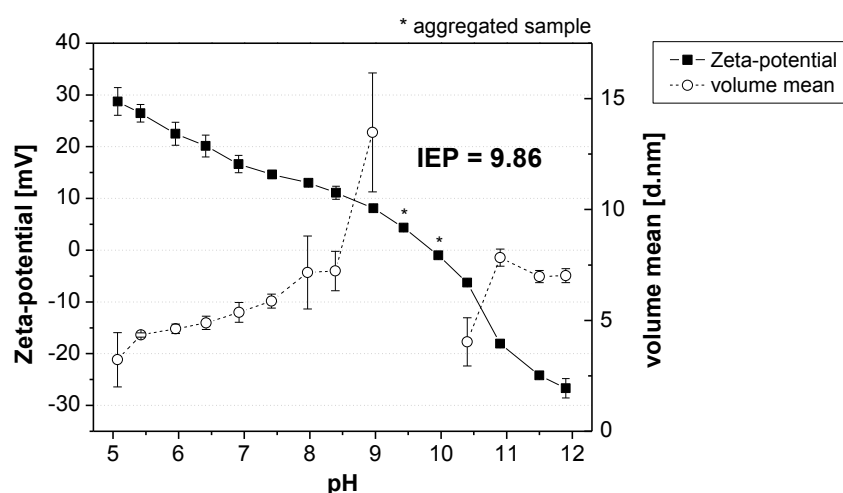


Figure 4.6. Zeta-potential, hydrodynamic diameter and calculated isoelectric point of nerve growth factor as determined by dynamic light scattering (conc. = 4.4 mg/mL, background: 10 mM sodium chloride). An aggregated sample (*) means that the volume mean diameter was too high to be displayed in the diagram.

Loading with NGF was carried out at standard loading conditions according to the previous study with lysozyme (30 mM ionic strength, pH 7.0). The residual protein concentration in the supernatant was determined by Micro BCA Protein Assay as well as by size-exclusion chromatography. The resulting payloads and loading efficiencies are shown in Figure 4.7, A. High loading of eADF4(C16) particles with NGF was possible with almost 100% loading efficiency at an incubation at 20% w/w-ratio. However, a further increase of the NGF content in the loading solution resulted in a distinct decrease of the loading efficiency to approx. 82%. At this point, the loading efficiency for lysozyme was still above 90% so that it can be concluded that lysozyme is superior to NGF regarding the payload and loading efficiency at higher w/w-ratios during remote lading.

Another important difference between loading with lysozyme and nerve growth factor was detected when the zeta-potential and particle size of NGF-loaded eADF4(C16) particles was determined (see Figure 4.7, B and C). The zeta-potential of NGF-loaded spider silk particles did not change up to a payload of 10% [w/w], but an increase in particle size, meaning agglomeration of NGF-loaded particles as shown by the SEM (see Figure 4.7, D), was already observed at this protein payload. In contrast, loading with lysozyme did not significantly alter the particles' properties till a payload of more than 20% [w/w].

In order to further clarify the influence of electrostatic interactions, the ionic strength of the loading buffer was increased to 60 mM and 100 mM by adding sodium chloride. Figure 4.8 illustrates that the impact of ionic strength was significant upon a w/w-ratio of 5% because remote loading was less efficient the higher the ionic strength had been. Again, the comparison to lysozyme (see Figure 4.4, A and B) shows that remote loading with nerve growth factor is less efficient. Besides surface charge and molecular weight, the hydrophilic or hydrophobic properties of the protein have to be taken into account to explain and compare the interactions between lysozyme, nerve growth factor and eADF4(C16) particles. The GRAVY value of NGF is -0.292 compared to -0.472 for lysozyme according to Kyte and Doolittle [25]. Additionally, the hydropathicity plot displayed in Figure 4.5 B shows more hydrophobic amino acid residues (positive index values) for the NGF molecule compared to lysozyme. Therefore, NGF is considered as more hydrophobic protein, but regarding the efficiency of remote loading this parameter had no significant influence as the more hydrophilic lysozyme was superior to nerve growth factor. This fact can be explained by stronger electrostatic interactions as lysozyme exhibits a charge distribution ('dipole') in the protein sequence of 9/17 (neg./pos.) charged amino acid residues vs. 12/17 for NGF, resulting in a higher isoelectric point of 10.9 vs. 9.86 for NGF. The larger hydrodynamic diameter of the NGF dimer is certainly further attenuating the protein-particle interactions leading to reduced loading efficiencies.

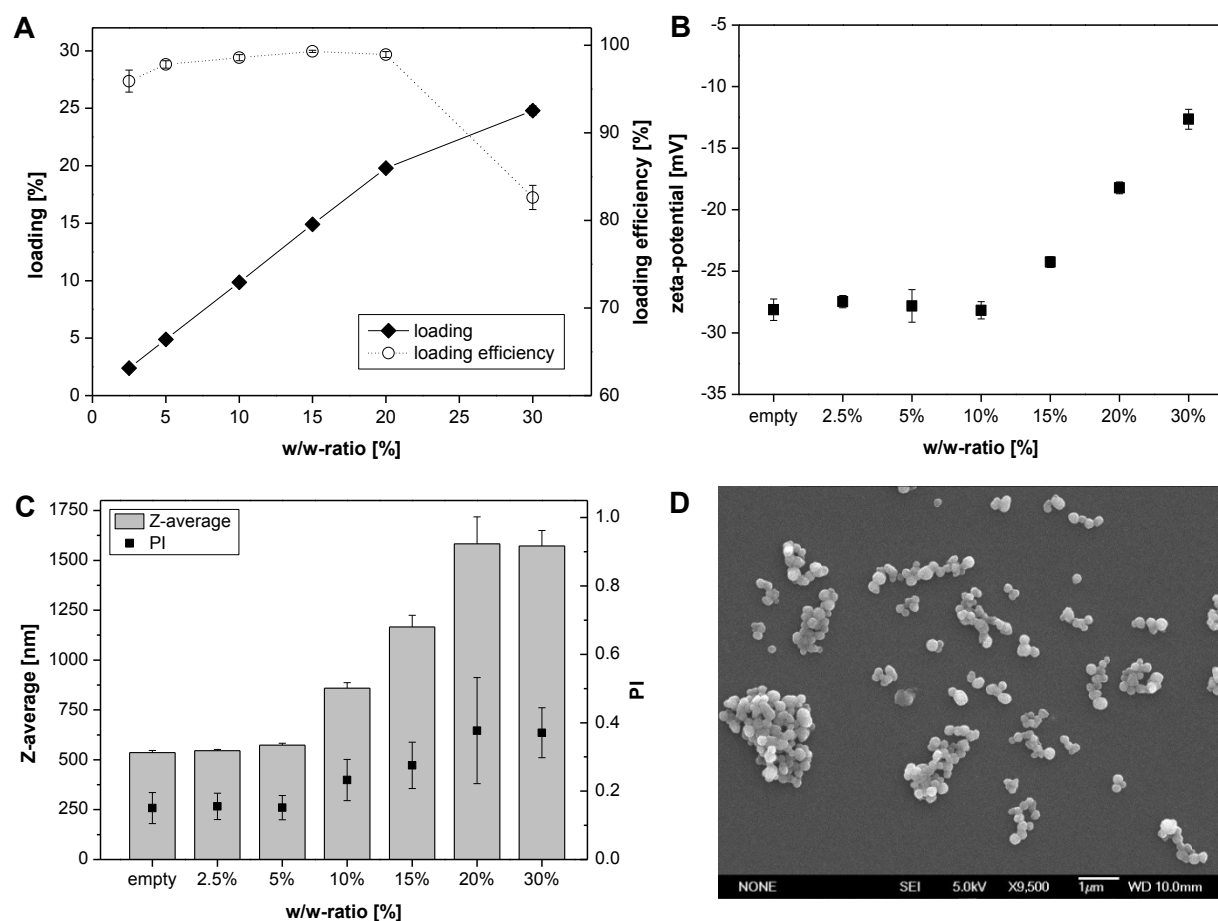


Figure 4.7. Loading of eADF4(C16) particles with nerve growth factor. (A) Loading and loading efficiencies as a function of the w/w-ratio of NGF-to-eADF4(C16) particles in the incubation dispersion at pH 7.0/30 mM ionic strength. Zeta-potential (B) and particle size (C) of different NGF-loaded eADF4(C16) particles at pH 7.0/30 mM ionic strength. (D) SEM micrograph (magnification: 9,500x) of eADF4(C16) particles loaded at 30% [w/w] NGF in the loading buffer.

Summing up the results obtained for lysozyme and NGF, it has to be stated that electrostatic interactions are the dominating forces when protein molecules are loaded onto eADF4(C16) particles. The molecular weight or rather the hydrodynamic radius of the protein molecule also influences the interaction as the charge density of the protein molecule is higher for smaller molecules. In contrast to low molecular weight substances, at which the hydrophobicity significantly influenced the loading behavior, the hydrophobicity of protein molecules does not play a decisive role as shown by comparing between lysozyme and nerve growth factor.

Remote loading with NGF performed in this work has to be compared with already published studies about the delivery of nerve growth factor using different biomaterials.

10% [w/w] NGF combined with a loading efficiency of 100% was only achieved by Lam et al. [29]. This study included the preparation of PLGA microspheres using spray freeze drying and stabilization of nerve growth factor by forming an insoluble NGF-zinc complex prior to encapsulation. All other drug delivery systems aimed for NGF delivery in peripheral nerve repair, which requires in principle only a fraction of the payload described in this thesis [27,

30-32]. Therefore, the reported colloidal instability of eADF4(C16) particles with 10% [w/w] NGF payload will not be a concern for such applications so that in summary, the developed NGF-loaded spider silk particles present a promising platform for pharmaceutical applications of NGF.

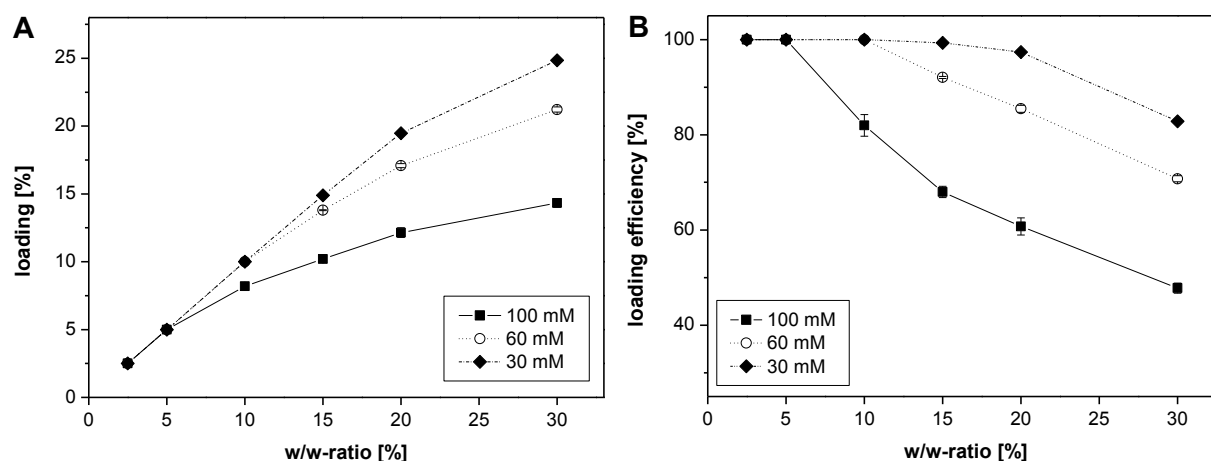


Figure 4.8. (A) Loading of eADF4(C16) particles with nerve growth factor at different ionic strengths at pH 7.0. (B) Loading efficiencies of nerve growth factor at different ionic strengths at pH 7.0

4.2.3 INVESTIGATION OF LOADING MECHANISM

The aim of this study was to prove and to visualize the hypothesis that macromolecules can permeate into the matrix of eADF4(C16) particles. Thus, loading was conducted with three fluorescently-labeled macromolecules having different charges and sizes at the investigated loading conditions of pH 2 and pH 7 (see Table 4.1).

Table 4.1. List of employed macromolecules with regard to remote loading of eADF4(C16) particles

	M_w [kDa]	IEP (theoretical)	Net charge at pH 2	Net charge at pH 7
eADF4(C16)	47.7	3.48	positive	negative
FITC - lysozyme	14.3	11.35	positive	positive
FITC - BSA	66	4.7 – 4.9	positive	negative
FITC - dextran	21.2	N.A.	uncharged	uncharged

Dextran is an uncharged polysaccharide and was used as control as no electrostatic interactions with charged spider silk particles are possible. Bovine serum albumin (BSA) has a molecular weight of 66 kDa and an isoelectric point of ~ 4.7 . Therefore, it exhibits a negative overall net charge at pH 7 and is positively charged at pH 2. The biochemical properties of lysozyme have already been discussed in section 4.2.1.

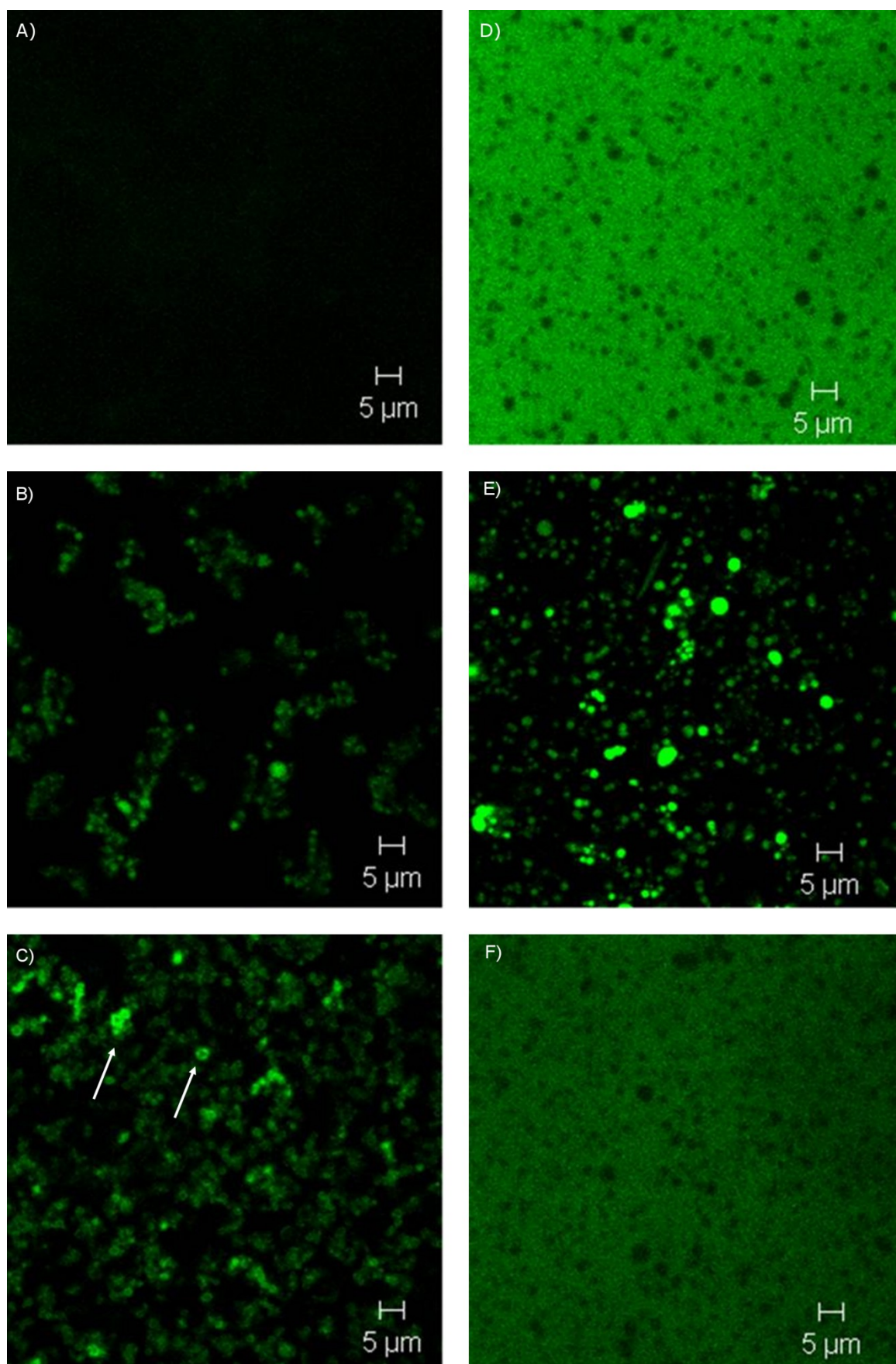


Figure 4.9. Confocal micrographs of dispersed and positively charged eADF4(C16) particles at pH 2 after loading with FITC-dextran (A), FITC-lysozyme (B) and FITC-BSA (C). Images (D), (E) and (F) show the confocal micrographs of dispersed and negatively charged eADF4(C16) particles at pH 7 after loading with FITC-dextran (D), FITC-lysozyme (E) and FITC-BSA (F)

In order to investigate eADF4(C16) particles by confocal laser scanning microscopy (CLSM), micrometer sized particles had to be prepared by dialysis. Herein, eADF4(C16) particles with a particle size of $2.1 \pm 0.06 \mu\text{m}$ determined by laser diffraction (mean size) were obtained. eADF4(C16) particles prepared by the micromixing system exhibited particle sizes in the submicron range and would have been too small to be precisely investigated by CLSM.

Confocal micrographs of the obtained spider silk suspensions are shown in Figure 4.9. It has to be noted that suspensions were investigated after mixing of eADF4(C16) particles with FITC-labeled macromolecules and incubation at room temperature for a minimum of 30 minutes. Due to the uncharged nature of FITC-dextran molecules, empty eADF4(C16) particles were detected both at pH 2 (see Figure 4.9, A) and pH 7 (see Figure 4.9, D). As a result, unloaded spider silk particles appear at pH 7 as dark spots upon strong green fluorescence caused by the unbound FITC-dextran in solution, whereas at pH 2 the fluorescence signal of FITC-dextran only present in the solution and not bound to the particles was too low to be detected. This can be explained, because the fluorescence intensity is pH-dependent and has its maximum at pH 8 and above (as per manufacturer's instructions). In contrast, FITC-labeled lysozyme was loaded onto eADF4(C16) particles as a result of its opposite charge at pH 7 (see Figure 4.9, E). The FITC-lysozyme loaded protein spheres appeared as filled bright green spots upon a dark background. Considering that no washing steps were applied after loading, almost the entire FITC-lysozyme was loaded onto eADF4(C16) particles. This finding confirms the previous results of the loading experiments (see section 4.2.1), where 15% [w/w] loading with lysozyme was achieved combined with almost 100% loading efficiency. Due to its negative charge at pH 7 (identical to eADF4(C16) particles), it was not possible to load FITC-BSA onto eADF4(C16) particles. Again, this conclusion could be derived from dark particle spots on the green fluorescent background (see Figure 4.9, F).

At pH 2, loading behavior of FITC-labeled lysozyme and FITC-BSA changed significantly. Exhibiting the identical charge as eADF4(C16) particles, both FITC-lysozyme and FITC-BSA have to overcome repulsive electrostatic forces in order to be loaded on positively charged particles. Surprisingly, eADF4(C16) particles appeared as hollow spots with green fluorescence at the surface when FITC-BSA was present in the loading suspension (see Figure 4.9, C). In contrast, FITC-lysozyme loaded eADF4(C16) particles appeared as filled green spots (see Figure 4.9, B).

To further confirm these findings, images of the suspension containing FITC-lysozyme at pH 7 were taken every 100 nm of the z-axis and are shown in Figure 4.10. It has to be highlighted that the FITC-lysozyme-loaded spider silk particles are visible as filled green spots in each section plane. Following a single particle throughout the image set, it is possible to observe that the fluorescence is covering the entire particle matrix even at the

edges of the particle (referring to the z-axis). This aspect is of major importance because the investigation of loaded eADF4(C16) particles by CLSM is on this account able to distinguish between only surface-loaded (see Figure 4.9, C) and matrix-loaded eADF4(C16) particles (see Figure 4.10).

Consequently, it was visualized that FITC-BSA molecules were only adsorbed on the eADF4(C16) particles' surface at pH 2 and that FITC-BSA was not able to permeate into the particles' matrix. On the other hand, FITC-labeled lysozyme molecules diffused and permeated into the spider silk matrix and were not only adsorbed to the particles' surface.

It was shown previously for spider silk microcapsules that their shell made of eADF4(C16) protein had an average molecular weight cutoff of 27 kDa, meaning that molecules exhibiting a smaller radius of gyration than 27 kDa dextran are expected to pass through the membrane [33, 34]. Results obtained using FITC-labeled lysozyme and BSA provide an indication that a molecular weight cutoff in the same range may exist for diffusion into eADF4(C16) particles. Proteins with a molecular weight comparable or higher than that of bovine serum albumin (66 kDa) are not likely to permeate into the eADF4(C16) particles' matrix and bind only to the surface.

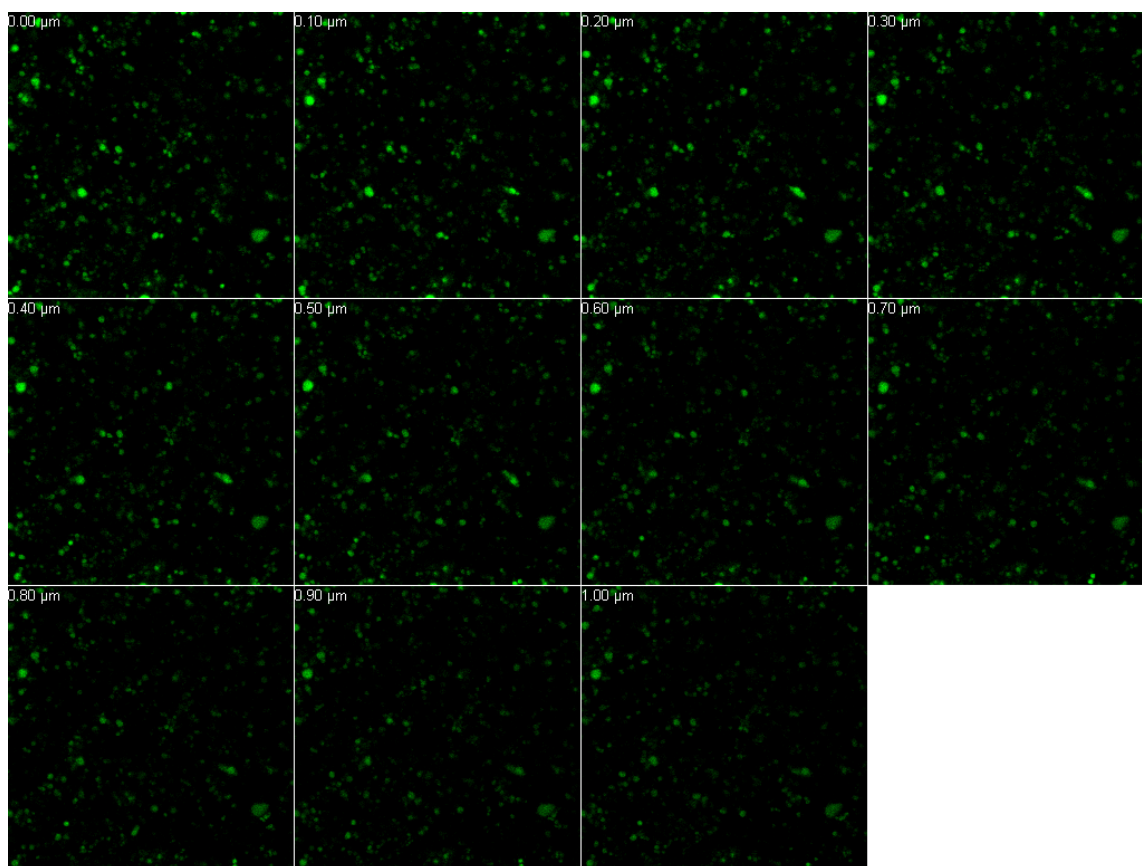


Figure 4.10. Confocal micrographs of FITC-lysozyme loaded eADF4(C16) particles at pH 7. The distance in the upper left corner represents the distance of the slice level on the z-axis (vertical) from the starting point of the z-scan.

Regarding the loading behavior of nerve growth factor, which is somehow special due to its non-covalent dimer formation, it is supposed that also matrix loading of the spider silk spheres takes place. The obtained loading efficiencies and payloads are almost comparable to lysozyme and a saturation of the surface only would not allow such high payloads.

4.2.4 *IN VITRO* RELEASE FROM PROTEIN LOADED SPIDER SILK PARTICLES

First studies on the *in vitro* release from eADF4(C16) particles were performed by Lammel et al. using low molecular weight drugs [23]. It was found that the release of methyl violet and ethacridine lactate is constant at physiological conditions over a period of 30 days with only low burst release (11%) during the first 24 hours. After this initial period, approx. 5% of the entrapped molecules were released per day. The release rate was further dependent on the pH of the release medium with higher release rates obtained at acidic release conditions. This was assigned to the importance of electrostatic interactions between small molecules and eADF4(C16) particles.

Based on these findings, different release conditions were employed to investigate the *in vitro* release from protein-loaded eADF4(C16) particles more deeply and to elucidate the underlying mechanisms.

4.2.4.1 INFLUENCE OF pH, IONIC STRENGTH AND PAYLOAD

The *in vitro* release of lysozyme from eADF4(C16) particles was studied in several different release media (see chapter 2, Table 2.4) starting with the approach to completely replace the release medium every 24 hours during the first 5 days.

The pH of the release medium was varied to evaluate its impact on the release profile of lysozyme. The total ionic strength of the release media in this study was set to 50 mM. The obtained results are illustrated in Figure 4.11. At pH 2 and pH 4, almost 90% of loaded lysozyme were released from eADF4(C16) particles within the first 48 hours. In contrast, no significant amounts of lysozyme were detected at pH 7.4, even after 28 days of release. Interestingly, the reduction from pH 7.4 to pH 6 showed no effect at all, indicating still very strong interactions between the spider silk protein particles and lysozyme at pH 6 and 50 mM ionic strength.

Figure 4.12 displays the cumulative release of lysozyme from eADF4(C16) particles incubated in release media with different ionic strength. The pH was set to 7.4 during the study and the ionic strength of the release medium was increased from purified water to 50, 100 and 160 mM. The release profiles show that the change of ionic strength had a very strong influence on the resulting release rate. The reduction of the ionic strength from 160 mM to 50 mM or purified water (HPW) resulted in a dramatic decrease of the released

lysozyme fraction from around 78% to no detectable amounts after 7 days of release. The initial burst release was small up to 100 mM ionic strength as not more than 11% lysozyme were released during the first 24 hours. No detectable amounts of lysozyme were released over the whole period of 21 days neither at 50 mM nor in highly purified water.

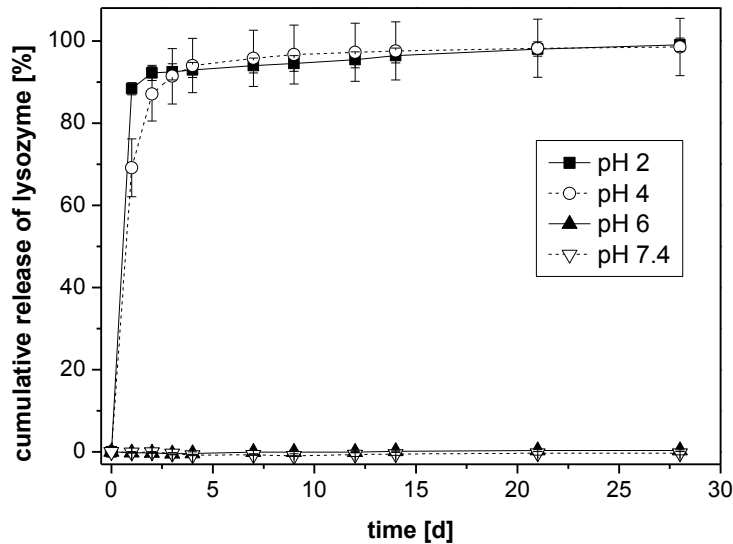


Figure 4.11. *In vitro* release of lysozyme from eADF4(C16) particles at 50 mM ionic strength and different pH determined over 28 days.

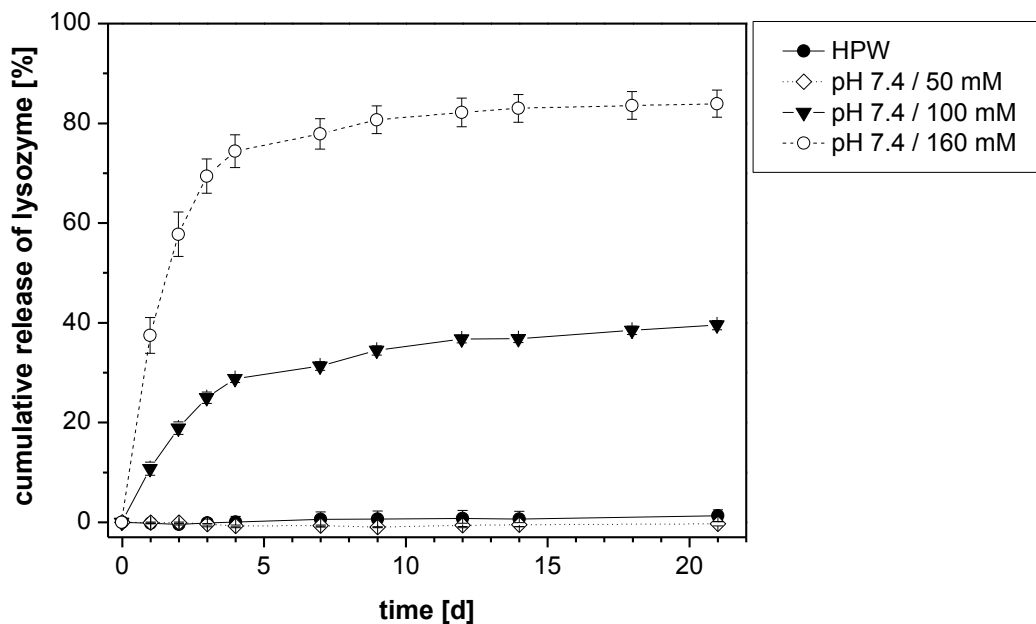


Figure 4.12. Influence of ionic strength on the *in vitro* release of lysozyme from eADF4(C16) particles at pH 7.4 determined over 21 days

Therefore, it can be concluded that the release of lysozyme from eADF4(C16) particles is mainly controlled by the degree of electrostatic interactions and not by hydrophobic forces. A decrease in pH and an increase in ionic strength weakens the electrostatic interactions between positively charged lysozyme molecules and negatively charged eADF4(C16)

particles so that lysozyme is released more easily. On the contrary, lysozyme is strongly attached to the particles at neutral pH and low ionic strength (pH 7.4 / pH 6 and 50 mM ionic strength or lower).

The lysozyme payload was varied and the *in vitro* release was investigated at physiological conditions in another experiment. As it can be seen in Figure 4.13, no significant differences between the release from spider silk particles loaded with 5, 10 and 15% [w/w] lysozyme were observed. However, these results demonstrate that the release at physiological conditions (pH 7.4 and isotonic ionic strength of 160 mM) is quite fast as over 70% lysozyme is released during the first 4 days (daily sampling). In comparison to the controlled *in vitro* release described previously for methyl violet or ethacridine lactate [23], it has to be stated that the release of lysozyme is much faster. Therefore, the interactions between eADF4(C16) particles and the protein molecule have to be weaker than between spider silk particles and small, positively charged molecules.

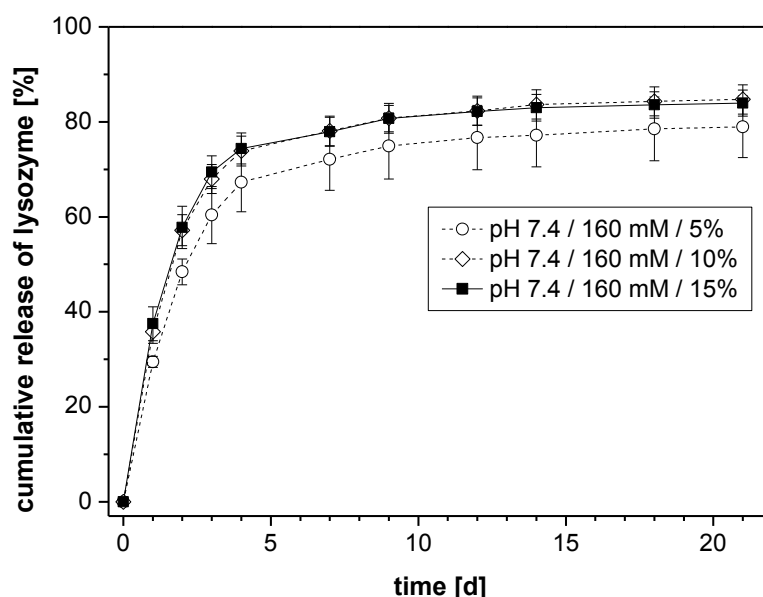


Figure 4.13. *In vitro* release of lysozyme from differently loaded spider silk particles at pH 7.4 and 160 mM ionic strength (10 mM phosphate buffer)

4.2.4.2 ANALYSIS OF DRUG RELEASE FROM REMOTE LOADED eADF4(C16) PARTICLES

During the first release studies, time points for replacing the supernatant with fresh release medium were varied in order to concentrate the released drug prior to analysis. However, an extension of the sampling interval to seven days resulted in the same release profile as obtained with a daily exchange of the release medium. This was so far not expected. The release was thought to be also driven by diffusion processes of the loaded drug inside the particle matrix (see Figure 4.1). On this account, the sampling interval was decreased to one hour to clarify whether the same release profile can be obtained again. The results of all

three different release setups are shown in Figure 4.14, in which the x-axis is displayed in logarithmic scale.

It can be observed that the release rate of lysozyme is independent of the time interval between the individual sampling points. The amount of released lysozyme is almost equal in all three experiments at the first, second, third and fourth time point of analysis, which is accompanied with the replacement of the entire volume of the release medium.

As this release behavior was quite contrary to those described in literature [23], release studies employing methyl violet were performed in order to evaluate if the discovered phenomena also occurs in case of low molecular weight substances.

Daily sampling revealed only slightly different results compared to literature as 14% and 39% of the loaded compound were released over the first 24 hours and 4 days, respectively (see Figure 4.15, A).

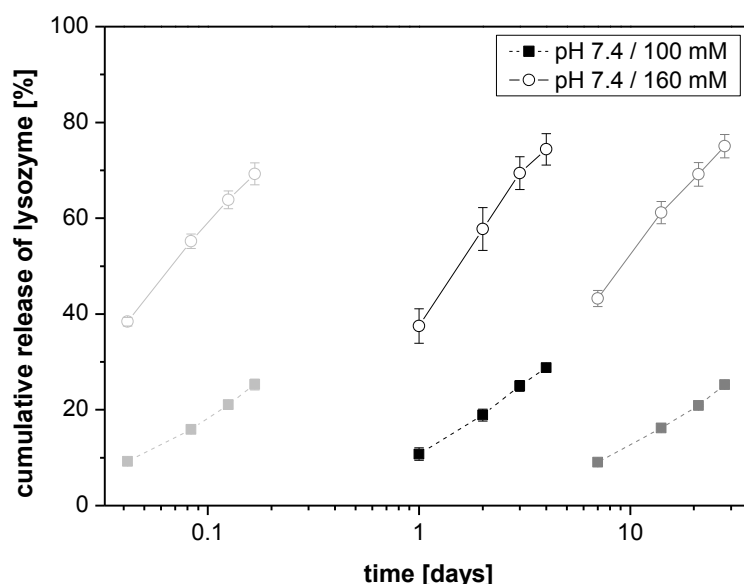


Figure 4.14. *In vitro* release of lysozyme from identically loaded eADF4(C16) particles using different time intervals for replacement of the release medium: 1 hour (light gray), 1 day (black) and 7days (gray)

This data confirms the release profile of low molecular weight substances as described in literature providing that the release medium is replaced every 24 hours. Systematic errors leading to differences in the release profiles can be therefore excluded.

Next, the release of methyl violet was determined by exchanging the release medium every hour and using release media with different ionic strength (Figure 4.15, A). The strong dependency of the release on the ionic strength was expected as it was already shown for lysozyme, but more interestingly, the same release behavior as observed for daily sampling was also obtained for hourly sampling.

Taking both results together, it was proven that the release of small molecules is also dependent on the experimental setup, but not on the time interval between the individual

sampling points. As a consequence, the hypothesis proposed by Lammel et al. (see Figure 4.1) seems to be inaccurate regarding the suggested release process. The constant and comparatively slow release rates were explained by a transport of the drug molecule from the inside of the spider silk matrix to the particle's surface. The driving force was the concentration gradient between the surface and the particle's matrix. The additional results presented in this thesis do not support this explanation any longer. In fact, the release process of a remote-loaded drug substance seems to be a result of an equilibrium state rather than a transport or diffusion based release process. The main criterion supporting this hypothesis is the fact that release rates were independent of the time interval between the sampling points both in the case of methyl violet and lysozyme. An interval of 60 minutes or seven days resulted in exactly the same concentration of lysozyme present in the supernatant of the release medium (see Figure 4.14).

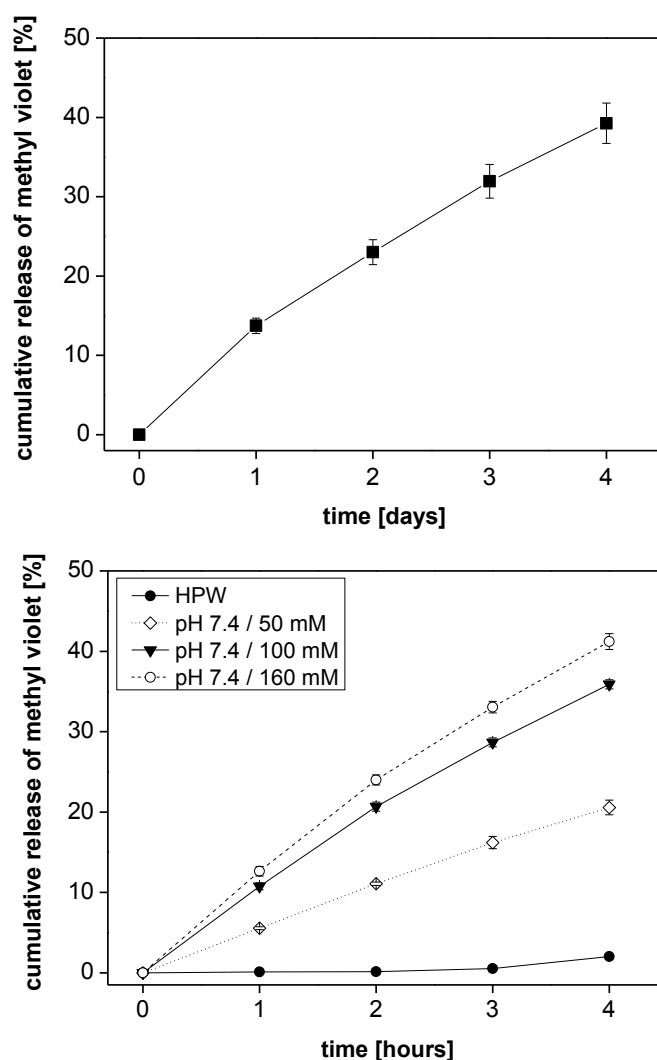


Figure 4.15. (A) *In vitro* release of methyl violet from eADF4(C16) particles at pH 7.4 / 160 mM ionic strength. eADF4(C16) particles were loaded with 10% [w/w] methyl violet according to the remote loading procedure. (B) Release of methyl violet from eADF4(C16) particles at different ionic strength. The samples were drawn every hour.

Otherwise, parameters which are able to alter the equilibrium state are strongly influencing the resulting release profile. Reducing the ionic strength in the release medium led to a significant reduction of the release rate, meaning that fewer positively charged ions are able to displace less drug molecules from the spider silk particle. Furthermore, it has to be considered that matrix loading was assumed for small molecules [23] and proteins up to a certain molecular weight (see section 4.2.3). Remote loading of eADF4(C16) particles assumes that unhindered diffusion of drug molecules into the particles' matrix is possible.

In addition to lysozyme, the *in vitro* release of nerve growth factor was determined. Figure 4.16 shows the release profiles which were obtained by exchanging the release medium every hour. Once again, a fast release of the loaded protein was observed at physiological conditions with more than 80% of NGF being already released during the first two hours. The release rate was slowed down at decreased ionic strength of the release medium. The dispersion of NGF-loaded eADF4(C16) particles in purified water showed no drug release at all, which was similar to lysozyme-loaded spider silk particles.

However, the release of NGF was significantly faster at 50 mM and 100 mM ionic strength (pH 7.4) compared to lysozyme. This confirms the statement made in section 4.2.2: interactions between spider silk particles and nerve growth factor are weaker than between the eADF4(C16) particles and lysozyme. The overall time scale of the release proved again that loaded NGF molecules were neither retarded by the interaction with the particle matrix nor that time dependent transport/diffusion processes occurred during the incubation in the release medium.

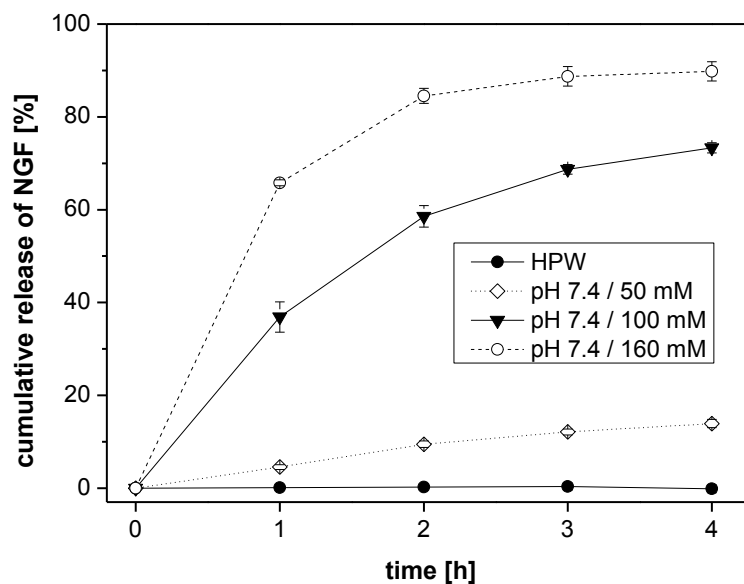


Figure 4.16. *In vitro* release of NGF from 10% [w/w] loaded eADF4(C16) particles in release media with different ionic strength (pH 7.4). The samples were drawn every hour and eADF4(C16) particles were loaded according to the remote loading procedure.

4.2.4.3 *IN VITRO* RELEASE IN THE PRESENCE OF ALBUMIN

In order to further simulate physiological conditions, albumin was added to the *in vitro* release medium. Human serum albumin (HSA) constitutes about 60% of the human plasma protein. The common range of human serum albumin in adults is 3.5 – 5 g/dL. For this reason, an albumin concentration of 40 mg/mL was chosen for the release experiments. Human serum albumin was only used in two release media due to the high albumin concentration and higher costs, and was compared to bovine serum albumin as shown in Figure 4.17, A. No difference between human and bovine serum albumin was detectable both at 100 mM and 160 mM ionic strength. Therefore, solely bovine serum albumin (BSA) was employed in the following release studies.

The release profiles of lysozyme displayed in Figure 4.17 A have to be compared to Figure 4.12. In doing so, an acceleration of the release rate in the presence of albumin could be depicted. The difference became apparent especially at 50 mM ionic strength, at which in the absence of albumin no release of lysozyme was detectable (see Figure 4.12). It was further shown that a lower albumin concentration of 4 mg/mL resulted in an identical release profile as at 40 mg/mL (data not shown). Thus, an impact of the different osmotic gradient can be excluded. Taken together, it is suggested that binding of lysozyme to albumin takes place which alters the equilibrium distribution and results in a higher release of lysozyme. Nevertheless, albumin molecules alone were not able to sufficiently alter the equilibrium as no lysozyme release was detected in purified water (see Figure 4.17, A).

This release behavior of methyl violet was considerably altered by the addition of albumin (see Figure 4.17, B compared to Figure 4.15). Very strong interactions between methyl violet and albumin shifted the equilibrium from originally electrostatic interactions between the spider silk particles and methyl violet towards the complex formed between methyl violet and albumin. Thus, very fast release of methyl violet was detected independent of the ionic strength of the release media (see Figure 4.17, B). Nevertheless, this result should not be too surprising as it is general knowledge that a wide range of low molecular weight drugs exhibit an excessively high affinity for albumin (> 95% bound), which is often driven by the lipophilicity of the drug and drug-specific molecular recognition [35]. The binding of crystal violet to albumin was investigated in detail and hydrophobic interaction forces played the major role in stabilizing the complex [36]. Crystal violet differs from methyl violet in only one methyl group attached to the amine functional group. Thus, this fact can be certainly transferred to methyl violet so that the strong affinity of methyl violet to albumin can be attributed to its high lipophilicity. As a result, the release is dramatically accelerated in the presence of albumin due to its strong influence on the equilibrium state.

On this account, these results confirm that fast equilibrium distribution and not slow, diffusive transport processes are responsible for the drug release from spider silk particles.

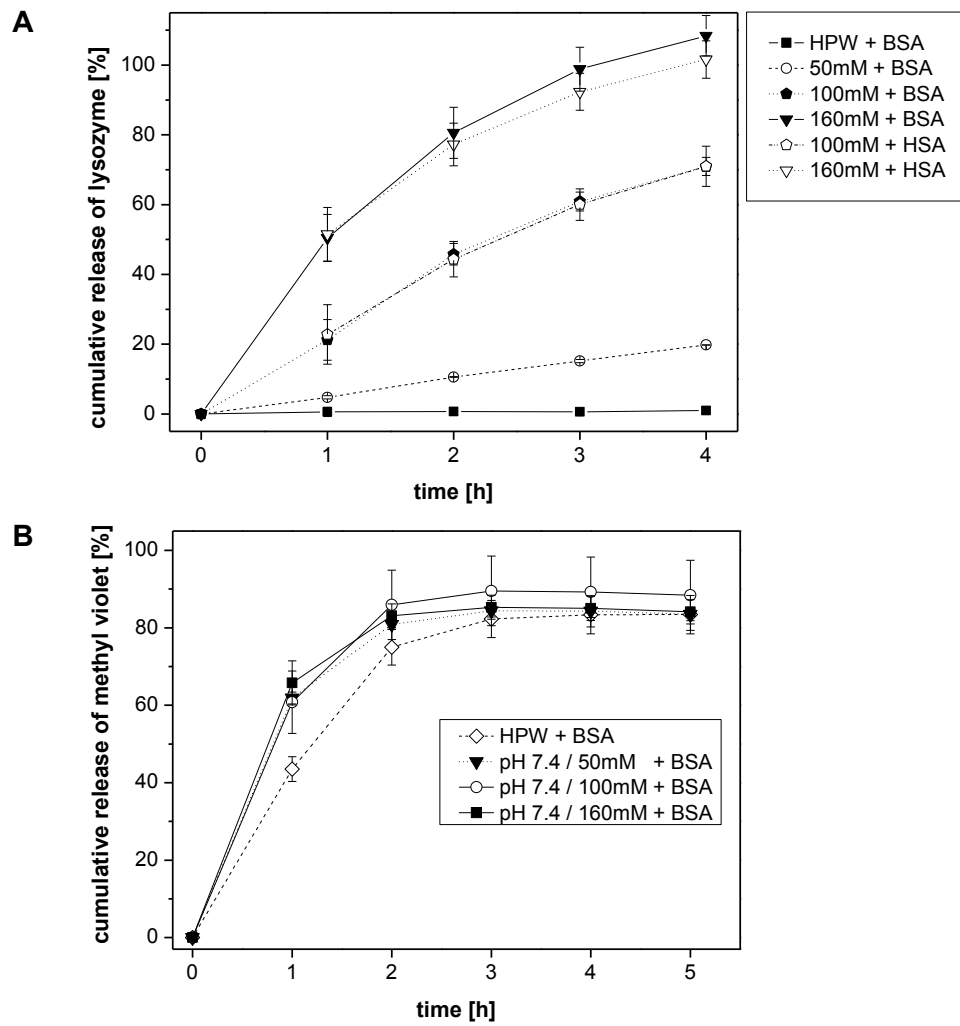


Figure 4.17. *In vitro* release from eADF4(C16) particles loaded with 15% [w/w] lysozyme (A) and 10% [w/w] methyl violet (B). BSA or HSA were added to the release media at a concentration of 40 mg/mL. The concentration of lysozyme was determined by measuring the activity of lysozyme in the release medium.

4.3 ENCAPSULATION OF DRUGS INTO eADF4(C16) PARTICLES

Besides the described procedure of loading drugs after particle preparation, drugs can be encapsulated into polymeric particles during the particle preparation process. This approach is commonly used for the development of particulate delivery systems aiming a sustained release of the incorporated drug. Several drug products comprising microparticles made of PLGA are on the market as depot formulations for Gonadotropin-releasing hormone agonists such as Leuprorelin or Triptorelin. However, encapsulation of susceptible drugs into polymer matrices constitutes different concerns which are specified in Table 4.2. It has to be considered as well that the preparation process for spider silk particles is pretty different to those processes applied for other polymers such as PLGA. Therefore, comparisons or predictions on the feasibility of drug encapsulation during eADF4(C16) particle preparation are hardly possible.

Table 4.2. Comparison of encapsulation and remote loading of drugs onto spider silk particles

Encapsulation / Co-precipitation	Remote loading
<ul style="list-style-type: none"> + Drug is completely incorporated in the spider silk protein matrix + theoretically: <ul style="list-style-type: none"> → longer diffusion pathways → slower release rates 	<ul style="list-style-type: none"> + Particles can be prepared without being influenced by the presence of the drug <ul style="list-style-type: none"> → control of particle size + Drug is not exposed to the conditions required for particle preparation <ul style="list-style-type: none"> → beneficial for susceptible drugs + Loading conditions can be set to optimal conditions
<ul style="list-style-type: none"> - Drug stability during the encapsulation process - Influence of the drug on the particle preparation process <ul style="list-style-type: none"> → particle size - Presence of high salt concentration during encapsulation <ul style="list-style-type: none"> → Encapsulation efficiency 	<ul style="list-style-type: none"> - Weak drug-matrix interactions result in fast release rates

Two different studies on the encapsulation of small molecules into eADF4(C16) particles can be found in literature [37, 38]. On the one hand, encapsulation was evaluated as an opportunity to formulate and deliver poorly soluble drugs [37]. β -carotene as a very hydrophobic compound was dissolved in tetrahydrofuran, mixed with an aqueous eADF4(C16) solution (10 mg/mL) and spider silk particle formation was induced by dialysis against 1 M potassium phosphate. It was shown that nanoparticles of β -carotene, which were formed due to dilution into the aqueous protein solution, could be embedded into the matrix

of eADF4(C16) microbeads. The obtained β -carotene loaded microbeads exhibited a rather rough surface compared to empty microbeads. In order to study the release, proteinase K was added and a complete degradation of microbeads and release of β -carotene was achieved. However, this study focused more on proving that eADF4(C16) interacts with hydrophobic molecules and is able to stabilize those substances in aqueous solution rather than on investigating eADF4(C16) microbeads as a drug delivery system for therapeutic drugs.

This approach was evaluated in a different study carried out by Blüm et al. [38]. Five different preparation routes including remote loading and encapsulation were investigated regarding loading capacity and release of the loaded substance. Rhodamine B was chosen as model drug for this study. It has to be considered that rhodamine B adopts a zwitterionic form at neutral pH in contrast to positively charged lysozyme, NGF or methyl violet. For this reason, electrostatic interactions between Rhodamine B and eADF4(C16) molecules or particles are not likely to occur. Co-precipitation was slightly superior to loading by diffusion processes (remote loading), but loading efficiencies were very low (< 1%) and the release was very fast, independent of the loading strategy (release medium: 10 mM Tris buffer). Furthermore, crosslinking of eADF4(C16) using ammonium persulfate and Rubpy (Tris(2,2'-bipyridyl)dichlororuthenium(II)) was performed in order to modify the release behavior. However, the release rates were not significantly slowed down and the amount of not released drug at the end of the release study increased due to the spider silk crosslinking.

In order to evaluate the different issues listed in Table 4.2, encapsulation was performed at first using rhodamine B in accordance to the presented study from Blüm et al. [38]. Afterwards, lysozyme was employed to compare the encapsulation data with results obtained by remote loading from section 4.2.

4.3.1 RHODAMINE B

As the influence of rhodamine B on eADF4(C16) particle characteristics during particle formation was not investigated by Blüm et al. [38], we performed identical experiments and focused on this part of the story. Figure 4.18 illustrates the results for loading and loading efficiency (A) as well as particle size and zeta-potential (B) of rhodamine B loaded particles prepared via co-precipitation. Interestingly, not more than 1% loading [w/w] could be achieved so that apparently uncharged molecules like rhodamine B can hardly be encapsulated into negatively charged eADF4(C16) particles. This data is consistent with the results reported by Blüm et al. [38] and is especially important, because it demonstrates clearly that electrostatic interactions are the basic prerequisite for sufficient loading of eADF4(C16) particles. Hydrophobic interactions, as they are the primary interactions in the

case of rhodamine B, are not at all potent enough to achieve reasonable loading capacities even for low molecular weight substances.

The addition of rhodamine B to the protein solution before particle preparation led to changes in the resulting particle size, whereas the charge of the particles was not affected. The more rhodamine B was present during phase separation, the larger the resulting eADF4(C16) particles became. At the highest Rhodamine B to eADF4(C16) particles ratio of 30% [w/w], no spider silk particles were formed at all. This shows that drug molecules can have a significant influence on the phase separation process, but the impact of the respective drug has to be considered case-to-case as the drug-protein interaction will be different regarding electrostatic and hydrophobic interactions.

Due to the unsatisfying low encapsulation capability for rhodamine B, follow-up release studies were not carried out. The data from the aforementioned study showed that even at low salt concentrations (10 mM Tris-buffer) a fast release occurred independent of the employed loading strategy [38].

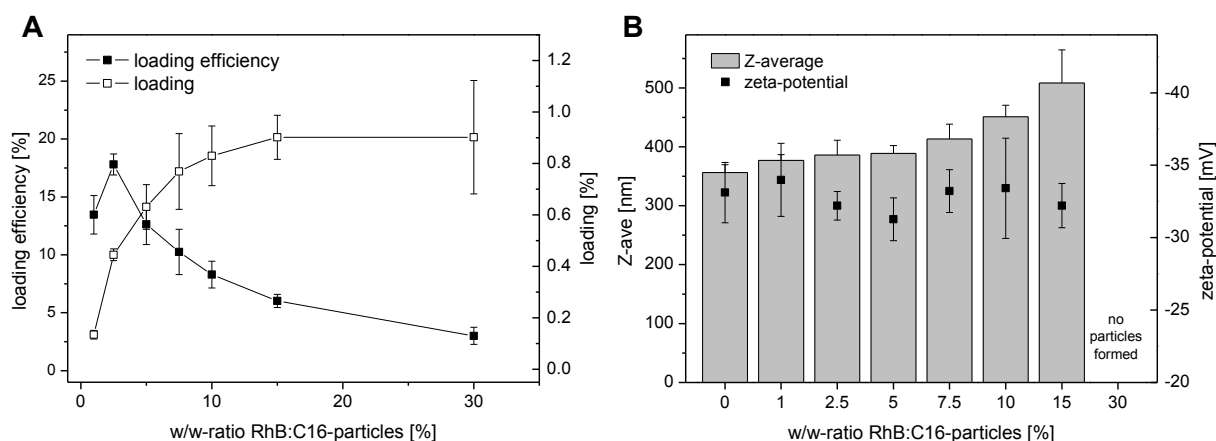


Figure 4.18. (A) Loading and loading efficiencies of the encapsulation of rhodamine B into eADF4(C16) particles at pH 7 / 30mM ionic strength. (B) Particle size and zeta-potential of eADF4(C16) particles loaded with rhodamine B. and prepared by co-precipitation

4.3.2 LYSOZYME

Co-precipitation of lysozyme was investigated to obtain data about the encapsulation behavior of negatively charged macromolecules. Encapsulation can be carried out by two different strategies, meaning that the drug can be mixed with either the spider silk protein solution or the salt solution prior to the phase separation process. However, lysozyme could not be dissolved in 2 M potassium phosphate as those conditions are used to crystallize lysozyme. On this account, only the addition of lysozyme to the eADF4(C16) solution was carried out.

First, the protein-protein interaction between lysozyme and eADF4(C16) in aqueous solution (10 mM Tris, pH 8.0) was investigated. This interaction is the major issue prior to the phase separation process and was considered as critical due to the strong electrostatic attraction between both protein molecules. AF4 was chosen as analytical technique, because it allows the simultaneous determination of soluble and insoluble protein species. Different lysozyme to eADF4(C16) ratios were analyzed at a fixed eADF4(C16) concentration of 1.0 mg/mL. An overlay of the 1:1 mixture (red) and lysozyme (green) or eADF4(C16) (blue) injection is depicted in Figure 4.19. It can be derived that at this ratio both a loss of lysozyme and spider silk protein recovery occurred most likely due to insoluble protein aggregates. Soluble, heterogeneous protein aggregates were not detected. However, at lower ratios of lysozyme to eADF4(C16) such as 1:5, both protein recoveries were determined to be adequate for encapsulation (> 90%, data not shown). Therefore, the addition of lysozyme to eADF4(C16) solutions ($c=1.0$ mg/mL) at w/w-ratios below 1:1 and followed by immediate phase separation was considered as uncritical regarding protein loss due to protein-protein interactions.

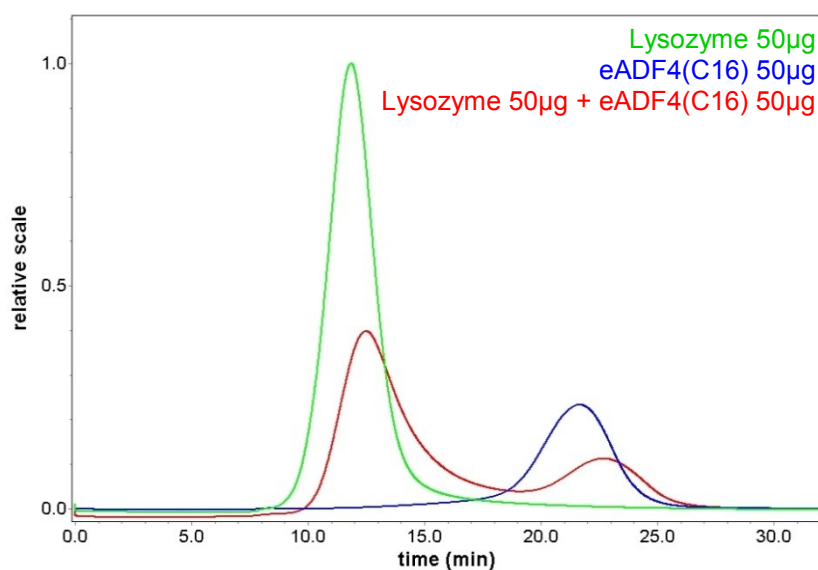


Figure 4.19. UV-chromatogram (280 nm) of lysozyme (green), eADF4(C16) (blue) and a mixture (red) of equivalent masses of lysozyme and eADF4(C16) analyzed by AF4

4.3.2.1. LYSOZYME-LOADED NANOPARTICLES

The eADF4(C16) concentration was set to 1.0 mg/mL in order to obtain spider silk nanoparticles. Different amounts of lysozyme dissolved in 10 mM Tris buffer (pH 8.0) were added and phase separation was immediately induced by flushing the buffer solution into equal volumes of 2 M potassium phosphate (pH 8) by a pipette. Nanoparticles around 350 nm were obtained for lysozyme-free solutions (see Figure 4.20, B). Loading and loading efficiencies [w/w] were determined according to the procedure for remote-loaded particles and the corresponding values are shown in Figure 4.20, A. A maximum of approx. 4%

loading was achieved at a lysozyme to eADF4(C16) ratio of 50% and 100% [w/w]. Therefore, the corresponding loading efficiencies were quite low (< 10%), representing an inefficient loading process. This situation was marginally improved at lower lysozyme to eADF4(C16) ratios, but efficiencies were still below 40% [w/w].

Particle size slightly increased with increasing lysozyme amount during precipitation (see Figure 4.20, B), but investigation by SEM did not reveal altered particle characteristics as depicted in Figure 4.21.

The low loading efficiencies can be explained by the presence of high salt concentration during particle formation. As it was shown for remote loading of lysozyme (see section 4.2), high ionic strength weakens the electrostatic interactions and releases the protein from eADF4(C16) particles. This happens now already during the loading procedure so that less lysozyme is finally incorporated into or bound to eADF4(C16) particles than using the remote loading approach at low ionic strength.

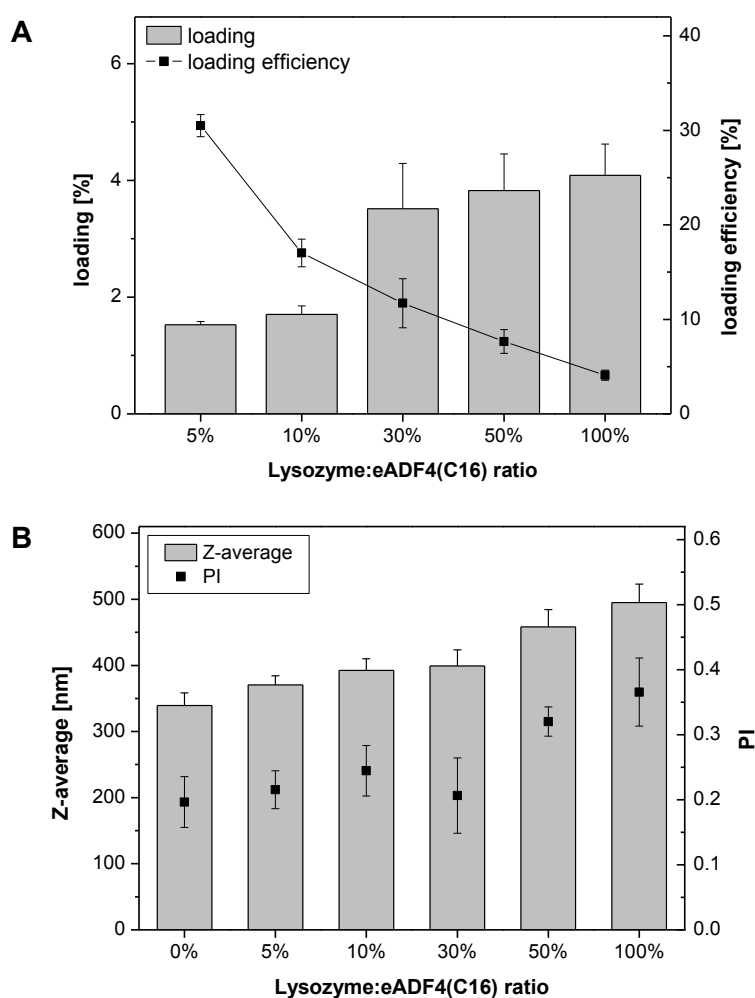


Figure 4.20. (A) Loading and loading efficiencies of lysozyme-co-precipitated eADF4(C16) particles at an eADF4(C16) concentration of 1.0 mg/mL. (B) Particle sizes and polydispersity indices of the resulting spider silk particles as determined by dynamic light scattering.

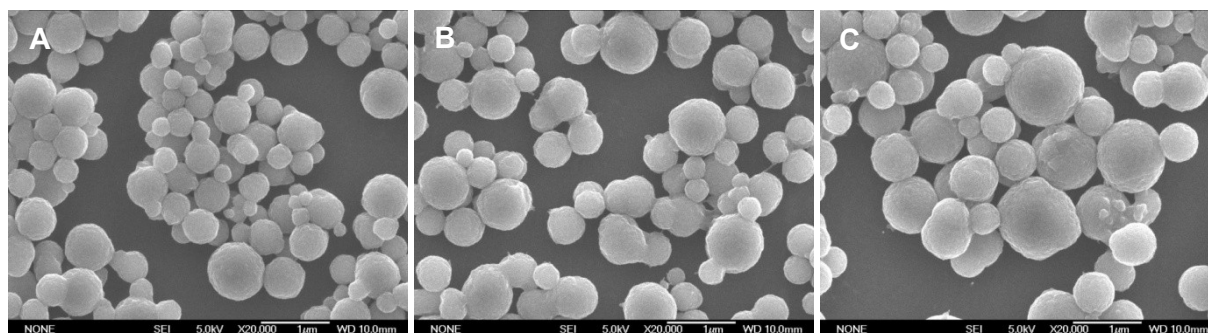


Figure 4.21. SEM micrographs (magnification: 20,000x) of particles prepared at different lysozyme to eADF4(C16) ratios and an eADF4(C16) concentration of 1.0 mg/mL: 0% (A), 30% (B) and 100% (C).

The major advantage of encapsulated lysozyme in comparison to the remote loaded delivery system is theoretically a sustained or at least slowed down release rate from the eADF4(C16) particles due to longer diffusion pathways (see Table 4.2). For this reason, release from co-precipitated particles was directly compared to release from particles loaded with a comparable amount of lysozyme via the remote loading procedure. The corresponding results are displayed in Figure 4.22.

However, co-precipitated lysozyme was released as fast as remote loaded lysozyme. Hence, encapsulation by co-precipitation was not successful in the retardation of the release from eADF4(C16) nanoparticles at physiological conditions. This result will be further discussed in section 4.4.

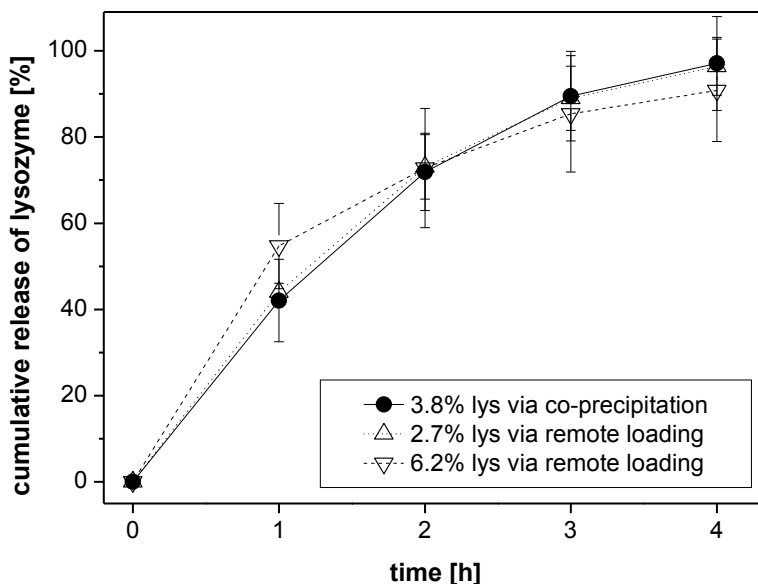


Figure 4.22. *In vitro* release of lysozyme from remote loaded and co-precipitated eADF4(C16) particles. The release study was conducted at 37°C and physiological ionic strength. The release medium was refreshed every hour. The amount of released lysozyme was determined by measuring the activity of released lysozyme.

4.3.2.2. LYSOZYME-LOADED MICROPARTICLES

In order to improve the unsatisfying results obtained for the loading and release of co-precipitated lysozyme from eADF4(C16) nanoparticles, lysozyme was added to solutions with an eADF4(C16) concentration of 10 mg/mL (10 mM Tris-buffer, pH 8.0) with the intention to prepare spider silk microparticles. However, protein-protein interactions between eADF4(C16) and lysozyme were dramatically increased at this high protein concentration.

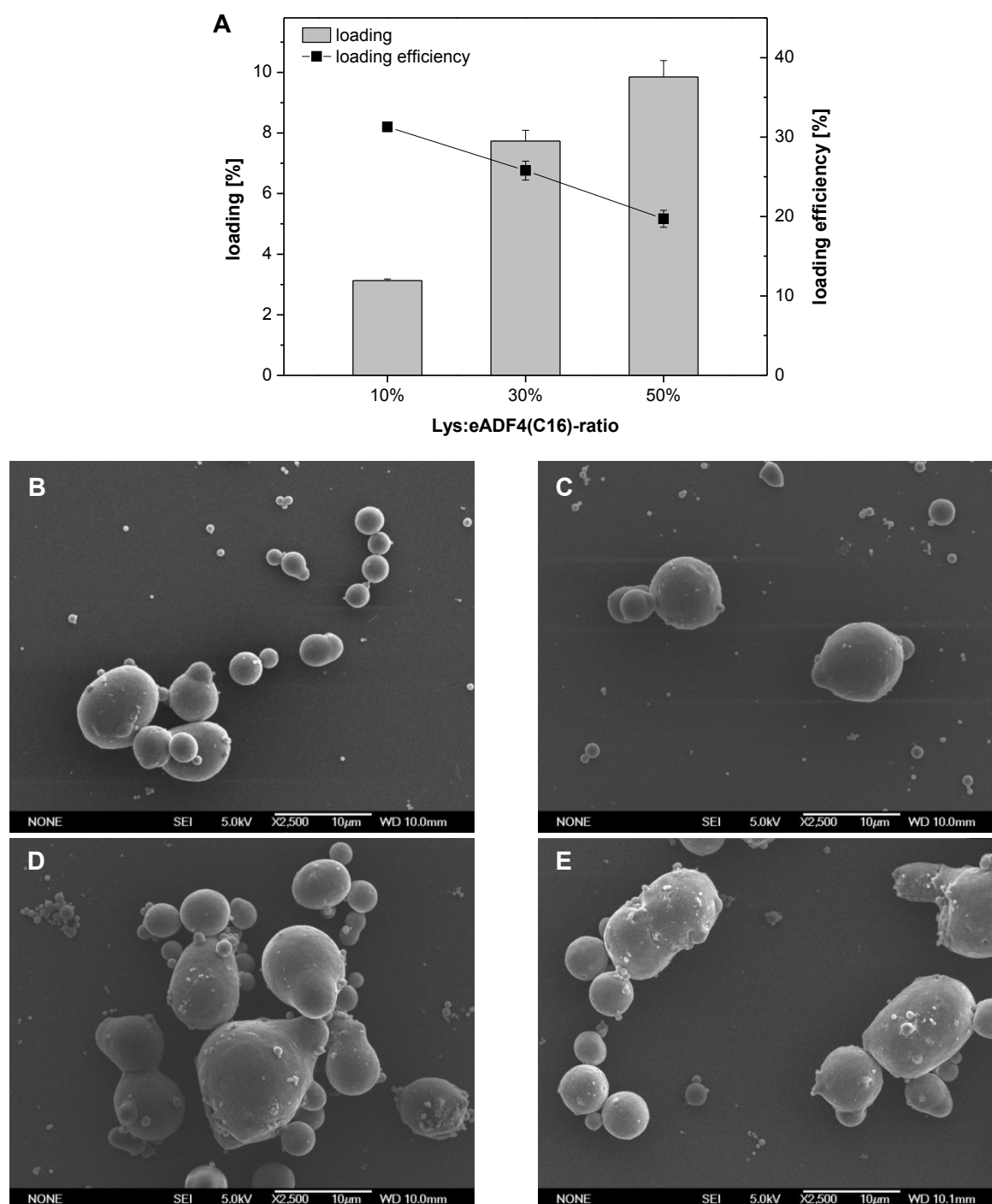


Figure 4.23. (A) Loading and loading efficiencies of lysozyme-co-precipitated eADF4(C16) particles at an eADF4(C16) concentration of 10 mg/mL. (B-E) SEM micrographs of particles prepared at different Lysozyme:eADF4(C16)-ratios and an eADF4(C16) concentration of 10 mg/ml: 0% (B), 10% (C), 30% (D) and 50% (E).

Precipitation was observed right after the addition of lysozyme to the spider silk solution as if spider silk particles would have been formed immediately. Nevertheless, atomization of the 2 M potassium phosphate solution via the ultrasonic nozzle was subsequently started and co-precipitation took place.

The resulting loading and loading efficiencies (see Figure 4.23, A) were higher compared to the co-precipitation at an eADF4(C16) concentration of 1.0 mg/mL, but still considerably below the corresponding values achieved by the remote loading procedure. The aforementioned explanation of weakened electrostatic interactions due to the presence of 2 M potassium phosphate holds also certainly true at this eADF4(C16) concentration.

The particle formation process seemed to be affected by the presence of lysozyme in a way that larger and more noncircular particles were obtained (see Figure 4.23, B-E). Nevertheless, particle yield was still satisfying with more than 99% precipitated spider silk protein also in the presence of lysozyme. The absence of eADF4(C16) in the supernatant was proven by SDS-PAGE (data not shown).

After co-precipitation and determination of the loaded amount of lysozyme, the *in vitro* release was studied from the obtained eADF4(C16) microparticles. The determined release profiles are displayed in Figure 4.24 and show a cumulative release of lysozyme of approx. 50% after 4 hours. Such low release rates were not obtained so far, but it has to be mentioned that the loading values were determined indirectly, meaning that they were calculated by measuring the concentration of lysozyme in the supernatant after the particle preparation process. Therefore, a loss of lysozyme due to protein-protein interactions prior to particle preparation could not be assessed and would result in an overestimated loading percentage of lysozyme. The course of the release indicates that release is almost finished after the investigated time period. This fact is in agreement with other release profiles obtained for remote loaded and co-precipitated nanoparticles where the release was almost completed after 4 hours. The run of the release curve is further identical to previous release experiments except the absolute value of the endpoint.

Altogether, these comments considerably argue for an inaccurate determination of the loaded amount of lysozyme so that the residual amount of the protein in eADF4(C16) particles after 4 hours of release is significantly overrated.

Albeit, a sustained release of lysozyme from eADF4(C16) microparticles was not detected, because at least 50% released lysozyme after 4 hours still represent a too fast release and can on no account be explained by a diffusion-based release mechanism.

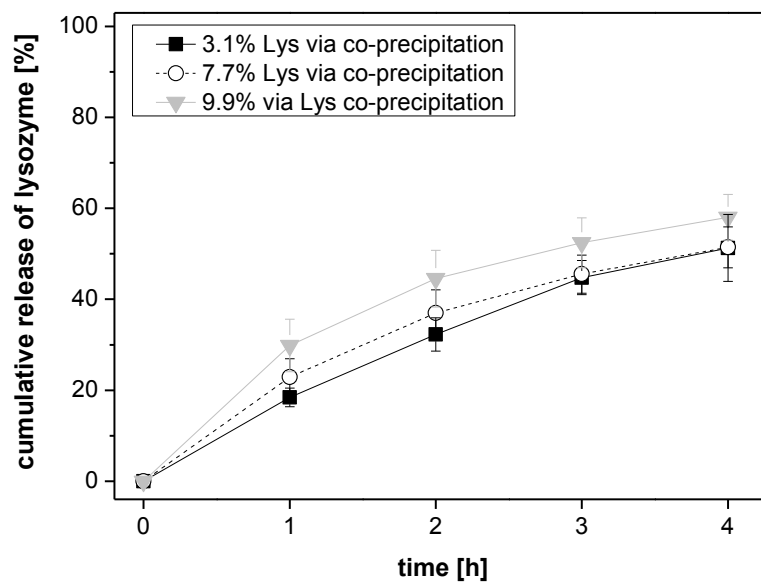


Figure 4.24. *In vitro* release of lysozyme from co-precipitated eADF4(C16) microparticles. The release study was conducted at 37°C and the release medium was refreshed every hour. The amount of released lysozyme was determined by measuring the activity of released lysozyme.

4.4 SUMMARY AND CONCLUSIONS

Two different strategies for loading eADF4(C16) particles are described in this chapter.

On the one hand, spider silk particles were loaded after particle preparation via incubation in a drug containing buffer solution. This procedure was called 'remote loading'. On the other hand, drugs were mixed with the spider silk protein solution prior to particle preparation. Subsequently, co-precipitation was induced and the drug was incorporated into the spider silk matrix. This approach is typically known as drug encapsulation.

Remote loading is most efficient when the ionic strength of the loading buffer is as low as possible. In this case, lysozyme as well as nerve growth factor were loaded into eADF4(C16) particles up to payloads of more than 20% [w/w], whereas the corresponding loading efficiencies were still sufficiently high (> 80%). The same holds true for small and essentially positively charged molecules like methyl violet which could also be loaded on eADF4(C16) particles in large amounts without losing too much drug substance during loading. The predominant driving force during loading was shown to be electrostatic attraction, whereas hydrophobic forces may only play a subsidiary role. The higher the electrostatic attraction, the higher the resulting loading efficiencies and payloads will be. It was furthermore proven by CLSM experiments that in fact matrix loaded spider silk particles were obtained by remote loading even with macromolecules like proteins.

In comparison to these results from remote loading, encapsulation did only lead to a low payload for any of the investigated drug substances. Remote loading offers the possibility to optimize the loading conditions, whereas co-precipitation has to deal with the conditions required for particle preparation. This is of special importance in the case of spider silk particles as a very high ionic strength is necessary for the induction of the phase separation process and finally particle formation. The presence of 2 M potassium phosphate inhibits the electrostatic interactions between eADF4(C16) particles and the drug molecules. Therefore, only low amounts can be co-precipitated into the spider silk protein matrix. It has also to be mentioned that uncharged molecules like rhodamine B could not be loaded on spider silk particles even during co-precipitation. Therefore, electrostatic attraction is also a prerequisite for successful encapsulation.

The *in vitro* release was investigated using several different setups and drug molecules. In summary, release from spider silk particles was very fast at physiological conditions independent of the performed loading procedure. So far data does not prove that an incorporation of drug molecules into the spider silk protein matrix lead to a sustained release rate due to diffusion through a dense polymer matrix. On the contrary, the spider silk matrix seems to be visually dense, but not in a way that diffusion out of the particle is hindered neither for small nor large drug molecules like proteins. The determined release can be better understood as the creation of an equilibrium distribution between the particle with its

loaded drug molecules and the buffer environment including ions or other molecules like albumin. Any change of this equilibrium modifies the release of the drug molecules from the spider silk particles. Therefore, pH, ionic strength and the addition of albumin strongly influence the determined amount of free drug substance.

Altogether, the usage of spider silk particles for a sustained delivery of drug substances has to be assessed as very challenging on the basis of the data presented in this chapter. However, eADF4(C16) particles may act as appropriate drug carriers for applications where the local environment may allow a slowed down release of the loaded drug substance or where a sustained release is not absolutely necessary. Physiological conditions are furthermore more complex than the employed *in vitro* conditions so that a simple transfer of the release data to the *in vivo* situation is in general difficult. Therefore, *in vivo* studies have to prove if spider silk particles fulfill the requirements for the desired application.

4.5 REFERENCES

- [1] **Edlund U. and Albertsson A. C.**, Degradable polymer microspheres for controlled drug delivery, in *Degradable aliphatic polyesters*, Albertsson, A.C., Editor. 2002, Springer: Berlin. p. 67-112
- [2] **Allen T. M. and Cullis P. R.**, Drug Delivery Systems: Entering the Mainstream. *Science* 2004, 303(5665), 1818-1822
- [3] **Gombotz W. R. and Pettit D. K.**, Biodegradable polymers for protein and peptide drug delivery. *Bioconjug. Chem.* 1995, 6(4), 332-351
- [4] **Wenk E., Merkle H. P. and Meinel L.**, Silk fibroin as a vehicle for drug delivery applications. *J. Control. Release* 2011, 150(2), 128-141
- [5] **Sinha V. R. and Trehan A.**, Biodegradable microspheres for protein delivery. *J. Control. Release* 2003, 90(3), 261-280
- [6] **Panyam J. and Labhasetwar V.**, Biodegradable nanoparticles for drug and gene delivery to cells and tissue. *Adv Drug Deliv Rev* 2003, 55(3), 329-347
- [7] **Estey T., Kang J., Schwendeman S. P. and Carpenter J. F.**, BSA degradation under acidic conditions: a model for protein instability during release from PLGA delivery systems. *J. Pharm. Sci.* 2006, 95(7), 1626-1639
- [8] **van de Weert M., Hennink W. E. and Jiskoot W.**, Protein instability in poly(lactic-co-glycolic acid) microparticles. *Pharm. Res.* 2000, 17(10), 1159-1167
- [9] **Brunner A., Mäder K. and Göpferich A.**, pH and osmotic pressure inside biodegradable microspheres during erosion. *Pharm. Res.* 1999, 16(6), 847-853
- [10] **Xu Y., Du Y., Huang R. and Gao L.**, Preparation and modification of N-(2-hydroxyl) propyl-3-trimethyl ammonium chitosan chloride nanoparticle as a protein carrier. *Biomaterials* 2003, 24(27), 5015-5022
- [11] **Xu Y. and Du Y.**, Effect of molecular structure of chitosan on protein delivery properties of chitosan nanoparticles. *Int. J. Pharm.* 2003, 250(1), 215-226
- [12] **Gan Q. and Wang T.**, Chitosan nanoparticle as protein delivery carrier - systematic examination of fabrication conditions for efficient loading and release. *Colloids Surf. B Biointerfaces* 2007, 59(1), 24-34
- [13] **Amidi M., Romeijn S. G., Borchard G., Junginger H. E., Hennink W. E. and Jiskoot W.**, Preparation and characterization of protein-loaded N-trimethyl chitosan nanoparticles as nasal delivery system. *J. Control. Release* 2006, 111(1-2), 107-116
- [14] **Prokop A., Kozlov E., Newman G. W. and Newman M. J.**, Water-based nanoparticulate polymeric system for protein delivery: permeability control and vaccine application. *Biotechnol. Bioeng.* 2002, 78(4), 459-466
- [15] **Coester C. J., Langer K., Von Briesen H. and Kreuter J.**, Gelatin nanoparticles by two step desolvation - a new preparation method, surface modifications and cell uptake. *J. Microencapsul.* 2000, 17(2), 187-193
- [16] **Altman G. H., Diaz F., Jakuba C., Calabro T., Horan R. L., Chen J., Lu H., Richmond J. and Kaplan D. L.**, Silk-based biomaterials. *Biomaterials* 2003, 24(3), 401-416
- [17] **Panilaitis B., Altman G. H., Chen J., Jin H.-J., Karageorgiou V. and Kaplan D. L.**, Macrophage responses to silk. *Biomaterials* 2003, 24(18), 3079-3085

- [18] **Vollrath F., Barth P., Basedow A., Engstrom W. and List H.**, Local tolerance to spider silks and protein polymers in vivo. *In Vivo* 2002, 16(4), 229-234
- [19] **Spieß K., Lammel A. and Scheibel T.**, Recombinant spider silk proteins for applications in biomaterials. *Macromol. Biosci.* 2010, 10(9), 998-1007
- [20] **Humenik M., Smith A. M. and Scheibel T.**, Recombinant spider silks - biopolymers with potential for future applications. *Polymers* 2011, 3(1), 640-661
- [21] **Wenk E., Wandrey A. J., Merkle H. P. and Meinel L.**, Silk fibroin spheres as a platform for controlled drug delivery. *J. Control. Release* 2008, 132(1), 26-34
- [22] **Scheibel T.**, Spider silks: recombinant synthesis, assembly, spinning, and engineering of synthetic proteins. *microbial cell factories* 2004, 3(1), 14
- [23] **Lammel A., Schwab M., Hofer M., Winter G. and Scheibel T.**, Recombinant spider silk particles as drug delivery vehicles. *Biomaterials* 2011, 32(8), 2233-2240
- [24] **Lehermayr C., Mahler H.-C., Mäder K. and Fischer S.**, Assessment of net charge and protein-protein interactions of different monoclonal antibodies. *J. Pharm. Sci.* 2011, 100(7), 2551-2562
- [25] **Kyte J. and Doolittle R. F.**, A simple method for displaying the hydrophobic character of a protein. *J. Mol. Biol.* 1982, 157(1), 105-132
- [26] *ExPASy ProtParam tool.* Available from: <http://web.expasy.org/protparam/>.
- [27] **Uebbersax L., Mattotti M., Papaliozou M., Merkle H. P., Gander B. and Meinel L.**, Silk fibroin matrices for the controlled release of nerve growth factor (NGF). *Biomaterials* 2007, 28(30), 4449-4460
- [28] **Yang Y., Chen X., Ding F., Zhang P., Liu J. and Gu X.**, Biocompatibility evaluation of silk fibroin with peripheral nerve tissues and cells in vitro. *Biomaterials* 2007, 28(9), 1643-1652
- [29] **Lam X. M., Duenas E. T. and Cleland J. L.**, Encapsulation and stabilization of nerve growth factor into poly(lactic-co-glycolic) acid microspheres. *J. Pharm. Sci.* 2001, 90(9), 1356-1365
- [30] **Xu X., Yu H., Gao S., Mao H.-Q., Leong K. W. and Wang S.**, Polyphosphoester microspheres for sustained release of biologically active nerve growth factor. *Biomaterials* 2002, 23(17), 3765-3772
- [31] **Cao X. and Shoichet M. S.**, Delivering neuroactive molecules from biodegradable microspheres for application in central nervous system disorders. *Biomaterials* 1999, 20(4), 329-339
- [32] **Saltzman W. M., Mak M. W., Mahoney M. J., Duenas E. T. and Cleland J. L.**, Intracranial Delivery of Recombinant Nerve Growth Factor: Release Kinetics and Protein Distribution for Three Delivery Systems. *Pharm. Res.* 1999, 16(2), 232-240
- [33] **Hermanson K. D., Harasim M. B., Scheibel T. and Bausch A. R.**, Permeability of silk microcapsules made by the interfacial adsorption of protein. *Phys. Chem. Chem. Phys.* 2007, 9(48), 6442-6446
- [34] **Hermanson K. D., Huemmerich D., Scheibel T. and Bausch A. R.**, Engineered Microcapsules Fabricated from Reconstituted Spider Silk. *Adv. Mater.* 2007, 19(14), 1810-1815
- [35] **Kratochwil N. A., Huber W., Müller F., Kansy M. and Gerber P. R.**, Predicting plasma protein binding of drugs: a new approach. *Biochem. Pharmacol.* 2002, 64(9), 1355-1374

- [36] **Xu H., Gao S.-L., Lv J.-B., Liu Q.-W., Zuo Y. and Wang X.**, Spectroscopic investigations on the mechanism of interaction of crystal violet with bovine serum albumin. *Journal of Molecular Structure* 2009, 919(1–3), 334-338

- [37] **Liebmann B., Hümmerich D., Scheibel T. and Fehr M.**, Formulation of poorly water-soluble substances using self-assembling spider silk protein. *Colloids and Surfaces A: Physicochemical and Engineering Aspects* 2008, 331(1-2), 126-132

- [38] **Blüm C. and Scheibel T.**, Control of Drug Loading and Release Properties of Spider Silk Sub-Microparticles. *BioNanoScience* 2012, 2(2), 67-74

CHAPTER 5

SPIDER SILK PARTICLES AS NOVEL EXCIPIENT FOR THE STABILIZATION OF NERVE GROWTH FACTOR

5.1 INTRODUCTION

The stabilization of therapeutic proteins during manufacturing processes and ensuring the shelf-life of the drug product are the major tasks in formulation development of biopharmaceuticals [1]. Due to the need of freezing, buffer-exchange, filtration or stirring during manufacturing, protein formulations are exposed to multiple and very different types of stress factors (see Table 5.1.) which may lead to physical and chemical instability of proteins [2]. Protein aggregation is arguably the most important and relevant pathway of protein instability in biopharmaceuticals and should be considered as a critical quality attribute of the drug product [3]. The reason is that protein aggregates are associated with product quality, toxicity and potentially enhanced immunogenicity [3-5]. In order to prevent aggregation therapeutic proteins are usually stabilized by the addition of excipients which act by different mechanisms [6, 7]. The most important types of excipients are certainly buffer components, tonicity agents, stabilizers like sugars or polyols, antioxidants and surfactants like polysorbates for the stabilization against surface-induced protein aggregation and the prevention of protein adsorption [8].

Table 5.1. Stress factors a protein is encountered during real-life conditions, adapted from Hawe et al. [9]

Stress factor	Encountered
Elevated temperature	Production processes, improper shipment, storage or handling
Freezing, freeze-thawing	Accidental freezing during storage or shipment, storage of (frozen) bulk material, lyophilization
Mechanical stress	Production (pumping, filtration, stirring, etc.), shipment, handling
Light	Exposure to daylight or artificial light during production, shipment, storage or handling; UV-detection during downstream processing
Oxidative stress	Contact with oxygen; excipients; metal ion traces from production equipment; light; cavitation
pH changes	Processing (downstream); freezing; formulation
Interfaces	Air-water interface; filters; primary packaging material; silicone oil; extraneous particles

Nevertheless, commonly used excipients like polysorbate or primary packaging materials exhibit important limitations and can themselves induce protein aggregation under certain conditions [10]. Thus, developing strategies to overcome these challenges and to stabilize therapeutic proteins is still in the focus of academic research [11-13]. Unfortunately, research and investment in excipient development for pharmaceutical drug products has been very complicated and expensive from an industrial perspective as excessive safety studies almost similar to those for a new drug substance were required for successful approvals [14].

For this reason, one objective of this thesis was the investigation whether protein drugs could be stabilized by adsorption to spider silk particles. The interaction of several proteins with foreign micro- or nanoparticles has already been described in literature. Bee et al. investigated the interaction of an IgG1 with glass, cellulose, stainless steel and F₂O₃ microparticles [15]. Interestingly, each particle type revealed a different result regarding the adsorption behavior of the antibody so that a transfer or comparison of the results to spider silk particles is pretty difficult. In theory, loading of a therapeutic protein onto or into the particulate spider silk matrix may be beneficial as the protein itself is less exposed to stress factors compared to the particle-free formulation. Furthermore, binding to the particles, which is mainly driven by electrostatic interactions, may stabilize the native, folded state of the protein.

The drug delivery system used in this study was a suspension of NGF-loaded spider silk particles in a phosphate buffer at pH 7.0 and 30 mM ionic strength adjusted with sodium chloride (see chapter 2, section 2.3.1.1). In literature, silk fibroin matrices have been employed for the stabilization of proteins as well but so far only silk films were investigated [16, 17]. Furthermore, these studies primarily focused on the stabilization of an API in a silk matrix which was dried after incorporation of the drug, i.e. by lyophilization. These approaches were shown to be successful for the stabilization of a vaccine (measles, mumps, rubella) and an antibiotic (tetracycline). However, this stabilization is not very surprising since the mechanism is based on the reduction of the water content which is well-known from the stabilization of liquid protein formulations by spray- or freeze-drying [16]. Another interesting study from Uebersax et al. incorporated nerve growth factor into a silk fibroin matrix [17]. The silk fibroin films and tubes were air-dried or freeze-dried, respectively, and a successful release of the biologically active protein over a period of three weeks was shown by HP-SEC, PC 12 cell bioactivity and ELISA-reactivity. However, the very low NGF payload of this study is especially noteworthy (payload: 0.02% [w/w]). In contrast, the payloads described in this thesis using eADF4(C16) particles are 2.5%, 5% and 10% [w/w].

In order to evaluate the potential of eADF4(C16) particles to stabilize bound protein molecules forced degradation studies comparing the suspension and the original protein formulation were performed. Freeze-thawing, stirring, light exposure and incubation at elevated temperatures of both types of formulations were conducted to obtain an insight into the different processes and mechanisms occurring with or without spider silk particles. Besides, this study should be considered as a first proof-of-concept study given that NGF is a protein where little information is available on the performance during degradation studies. On the other hand, nerve growth factor is an ideal candidate to be loaded onto eADF4(C16) particles due to its biochemical properties (see chapter 4, section 4.2.2).

5.2 DEVELOPMENT OF A STANDARD DESORPTION PROCEDURE

The loading and in vitro release of NGF from eADF4(C16) particles was studied and reported earlier and aimed at sustained release of the drug (see chapter 4, section 4.2.2 and 4.2.4). The goal of this study was on protein stabilization of the loaded compound during forced degradation studies. Therefore, in contrast to the setup of the release experiments, a standard desorption procedure had to be developed resulting in a sufficiently efficient release of the protein without affecting the protein's stability and conformation. A sufficiently efficient release was achieved when more than 80% of the loaded NGF amount was found in the supernatant by employing a maximal dilution factor of two. A higher dilution during desorption should be avoided due to the comparatively low protein concentration of 0.5 mg/mL of the original formulation.

The conclusions from the release studies present two different strategies to obtain a fast and complete release. The first approach is the increase of ionic strength of the medium, and the second approach is the decrease of the pH from 7.4 towards an acidic pH approximating the isoelectric point of eADF4(C16) particles (see chapter 3, section 3.4). Nevertheless, as a main criterion the desorption procedure has to maintain the protein's chemical and physical state present in the formulation before and after the degradation study. For this reason, different desorption procedures were compared to a freshly thawed, non-stressed sample of NGF in bulk solution.

In preliminary experiments the influence of acidic pH values was investigated. However, the detected NGF concentrations in the supernatant were not sufficient regarding the aforementioned definition (data not shown). Therefore, the addition of sodium hydroxide was tested and it was found that an increase of the pH towards or above the isoelectric point of NGF is more effective than acidic solutions. This result was somewhat unexpected, but lowering the charge of nerve growth factor molecules clearly improved the desorption procedure. Otherwise, it has also been reported in literature that deamidation of recombinant human nerve growth factor occurs after 16 to 18 hours incubation at pH 8.1 so that alkaline solutions above pH 10 were generally excluded from further experiments [18]. The protein content has so far been determined by UV-spectroscopy and size-exclusion chromatography, but this had to be changed to reversed phase chromatography for the study described here. This change was necessary to detect deamidation or other chemically modified protein species [18].

In order to optimize the desorption procedure samples were placed in a Thermomixer to heat and shake the suspensions under controlled and reproducible conditions. Solutions were adjusted to three different pH-values (pH 6, 8 and 10) and different amounts of sodium chloride were added to the buffer component (200 mM sodium phosphate) to modify the ionic strength (400 mM, 800 mM and 1200 mM sodium chloride).

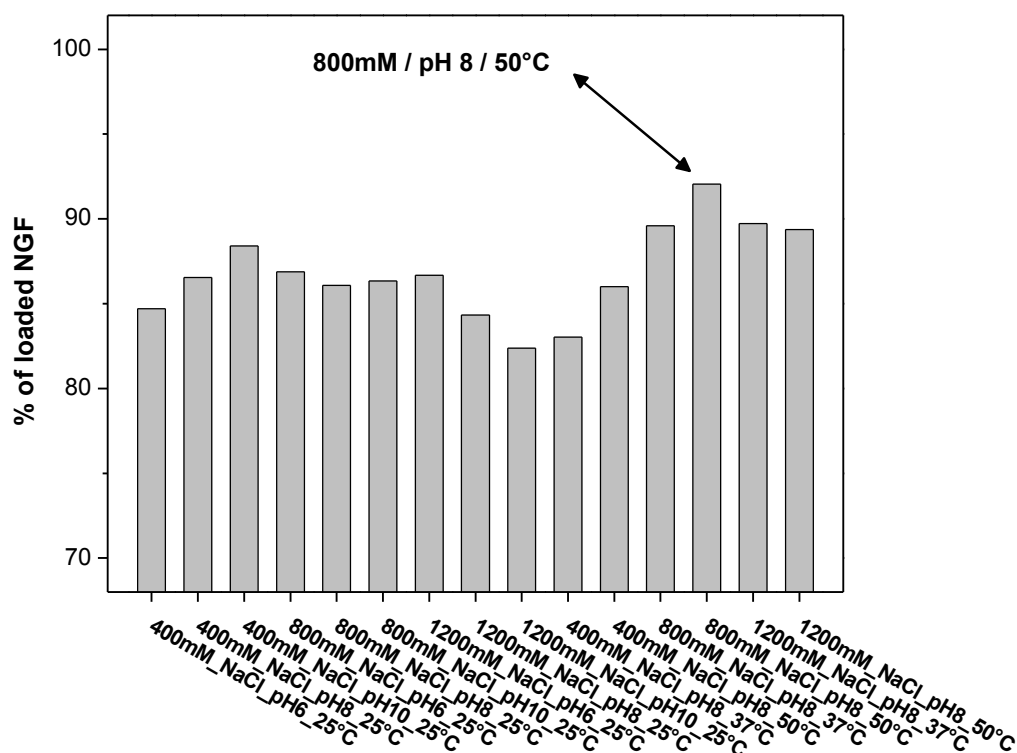


Figure 5.1. Efficacy of different solutions regarding the amount of displaced NGF from eADF4(C16) particles determined by RP-HPLC. All solutions consisted of 200 mM sodium phosphate and the declared amount of sodium chloride.

After mixing the same volume of the solution with the suspension containing 5 mg/mL NGF-loaded spider silk particles in 10 mM phosphate buffer pH 7.0 (30 mM ionic strength), the sample was agitated at 600 rpm for 30 minutes at the corresponding temperature. The pH of the resulting suspensions was 6.38 ± 0.05 , 7.90 ± 0.04 and 10.19 ± 0.09 , respectively. Desorption at 25°C revealed an impact of the pH on solutions with different amounts of sodium chloride. At 400 mM sodium chloride, the amount of released NGF is significantly increased at higher pH-values. Formulations with higher sodium chloride concentration showed an opposite behavior as the amount of released NGF was not further enhanced at 800 mM and even decreased at 1200 mM sodium chloride. Taking these results together, it seems that at comparatively low ionic strength an increase of the pH towards or above the IEP of NGF further decreased the electrostatic interactions between the spider silk particles and NGF. At higher ionic strength the change in pH was not able to affect the charge-charge interactions further. This can be explained by the fact that due to the very high ionic strength the electric charge density has already been reduced to a minimum. Therefore, using even a pH above the IEP of NGF is not able to further decrease the electrostatic interactions.

As the interaction between the eADF4(C16) particles and the loaded compound is dominated by electrostatic and hydrophobic interactions and an equilibrium is created after the addition of the required solution, elevated temperature should also enhance the dissociation of bound

NGF from eADF4(C16) particles. This assumption was confirmed when the temperature during the agitation step was increased from 25°C to 37°C and 50°C, respectively. The highest amount of released NGF of all investigated solutions and procedures was achieved using a formulation consisting of 200 mM sodium phosphate and 800 mM sodium chloride at pH 8, and a process temperature of 50°C. The released amount of NGF was 92% of the protein originally loaded onto the particles, and the protein showed no change in its chemical or physical state as determined by RP-HPLC and HP-SEC. Thus, this desorption procedure was applied for all further forced degradation studies. Samples which were treated according to this standard desorption/washing procedure are further referred as 'Liquid NGF WP'. Samples which were treated with the formulation buffer instead are further referred as 'Liquid NGF FB'.

5.3 FORCED DEGRADATION STUDIES

5.3.1 FREEZE-THAW STUDY

Freezing and thawing processes can occur at many different stages in a lifecycle of a drug product. Bulk substance is routinely stored in the frozen state due to superior storage stability to the storage of liquid formulations. In addition, accidental freezing and thawing may happen during storage at different development processes. As a consequence, the prevention of protein aggregation generated by freeze-thaw cycles plays a major role in formulation development and the development of robust manufacturing processes even for drug products where lyophilization is not necessary [19].

Protein aggregation is the result of different factors appearing during freezing and thawing: low temperature, high local solute concentration, formation of ice-water interfaces, potential pH changes and phase separation [19, 20]. As a result, soluble as well as insoluble protein aggregates can be generated, and surfactants like the non-ionic polysorbate 20 or 80 are usually added to successfully minimize protein-ice interactions. Furthermore, formulations having a low protein concentration are more prone to freeze-thaw induced aggregation because the protein to surface-ratio is larger than for higher concentrated solutions [20].

In the following study it was investigated if there is a potential stabilizing or even destabilizing effect of eADF4(C16) particles on nerve growth factor. So far it is the first study which evaluates the effect of binding a protein to nanoparticles and subsequent freezing and thawing of the nanoparticle suspension without further additives. In literature, plenty of studies have been performed on the freeze-thawing or freeze-drying of nanoparticle suspensions, but their focus was the conservation of the colloidal stability of the nanoparticles and the characterization of the freeze-drying process [21-23]. In this study the stabilization of bound protein towards freeze-thaw induced stress was investigated in order to find a possible application of spider silk particles as a novel excipient for protein stabilization during drug development and manufacturing.

Unfortunately, no information about the stability of nerve growth factor during freezing and thawing in a liquid formulation is available in the literature. The already described loading buffer (10 mM phosphate, adjusted to 30 mM ionic strength with sodium chloride, pH 7.0) was therefore chosen as formulation buffer for the complete forced degradation study as it had already been shown that NGF at the employed protein to nanoparticle ratios will completely adhere to the particles over a sufficiently long period of time (see chapter 4, section 4.2.2). The amount of spider silk particles was set to 0.5%, 1% and 2% [w/V], which corresponds to a nanoparticle concentration of 5, 10 and 20 mg/mL, respectively. As described in chapter 2, section 2.3.1.1, the NGF concentration of 0.5 mg/mL was kept constant in all formulations.

The amount of total NGF recovered after 5, 10 and 15 freeze-thaw cycles is depicted in Figure 5.2 and was determined by RP-HPLC with UV-detection at 215 nm. This diagram shows one important fact of the entire forced degradation study. If one considers the formulation 'Liquid NGF FB' as reference formulation (= 100% at t₀), it can be observed that desorption was less efficient for formulations containing more than 0.5% [w/V] eADF4(C16) particles. This can be well explained by the equilibrium between loaded and displaced NGF molecules which is created during the desorption process similar to the release process (see chapter 4, section 4.2.4). The higher the particle concentration is the less NGF molecules are displaced at the same ionic strength and pH in the solution.

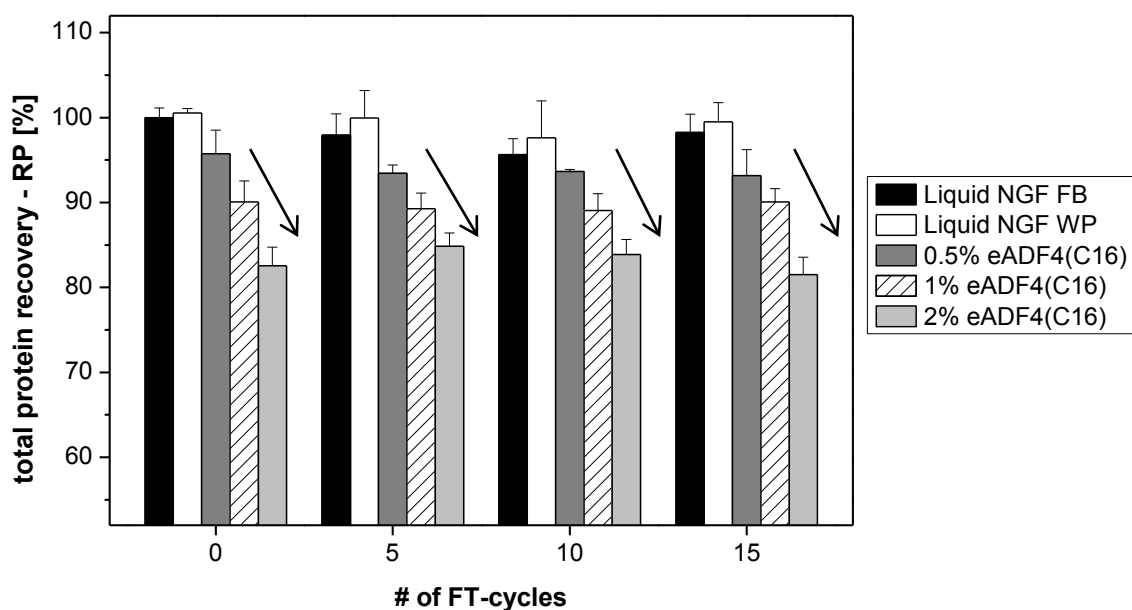


Figure 5.2. Total protein content after freeze-thawing of NGF formulations as analyzed by RP-HPLC (UV-detection at 215 nm). The displayed protein recovery is calculated regarding the total protein content of the reference formulation 'Liquid NGF FB' at t₀. The bars represent the mean of three samples \pm SD.

To improve the visualization of the stabilizing effect, the NGF content of each formulation at t₀ was set to 100%. The same calculation was carried out for the remaining dimer content which was determined by HP-SEC and referred to the total AUC of each formulation at t₀. Both diagrams are depicted in Figure 5.3.

Taking together, the result from the freeze-thaw study is clear: Neither the particle-free formulation nor the suspensions comprising bound NGF showed any significant degradation or aggregation of NGF throughout 15 freeze-thaw cycles. The total protein recoveries as well as the dimer contents of all investigated formulations remained at almost 100%. SDS-PAGE under non-reducing conditions showed no additional protein species or decreased protein content as all formulations exhibited a single band which represents the monomeric form of NGF with a molecular weight of 13 kDa (see Figure 5.4).

Subvisible particle analysis is more sensitive towards early and quite low fractions of protein aggregation compared to chromatographic methods [5, 24, 25]. Therefore, spider silk particle-free formulations were analyzed by light obscuration as depicted in Figure 5.5. The increasing number of subvisible particles indicates that protein aggregation took place throughout freeze-thawing. The difference in the particle counts between both formulations illustrated that already formed particles were partly dissolved again due to the high ionic strength of the solution used for desorption.

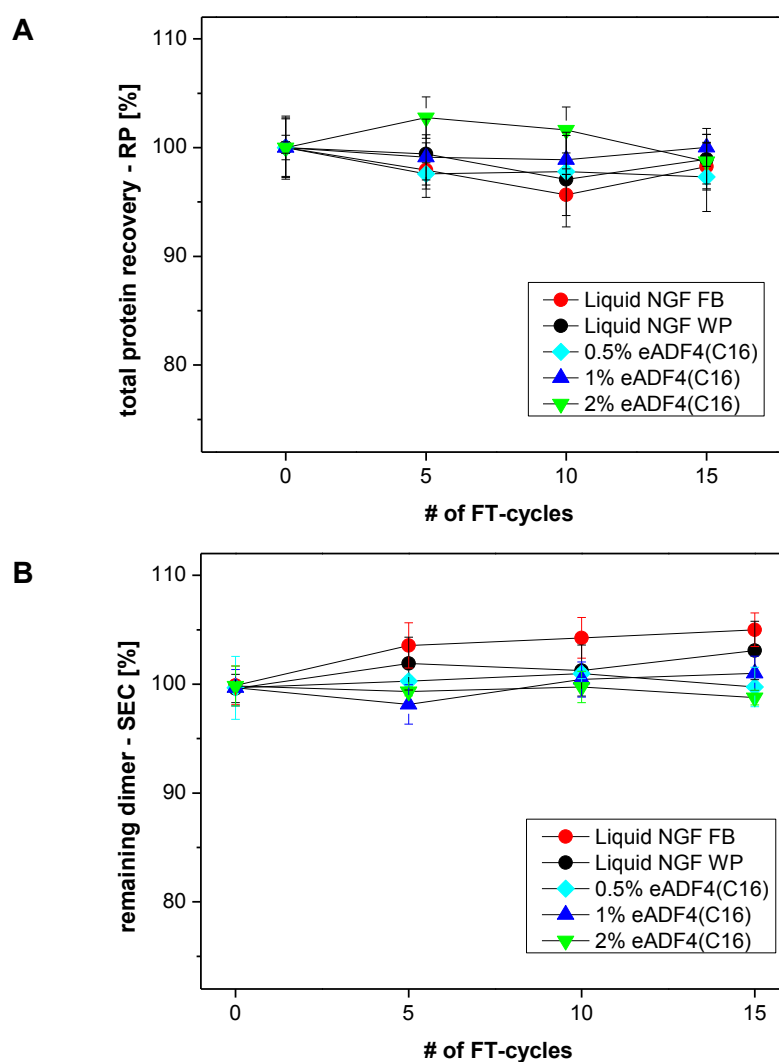


Figure 5.3. (A) Freeze-thawing of NGF formulations analyzed by RP-HPLC and UV-detection at 215 nm. (B) Freeze-thawing of NGF formulations analyzed by HP-SEC and UV-detection at 215 nm. The remaining protein/dimer content is calculated regarding the total protein/dimer content of each formulation at t₀. The symbols represent the mean of three samples \pm SD.

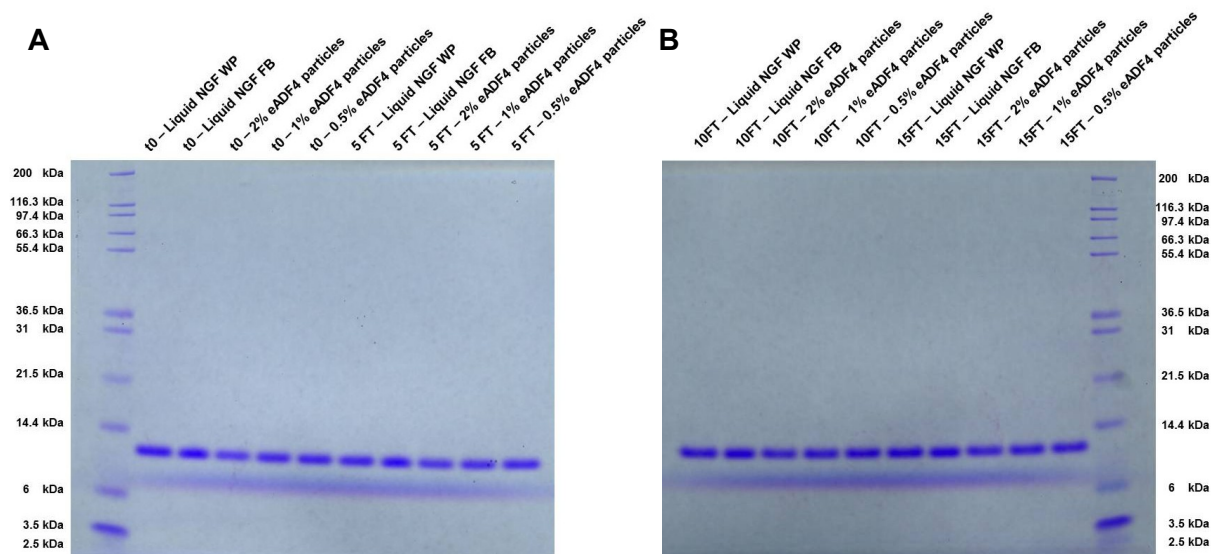


Figure 5.4. SDS-PAGE of unstressed (t0) and freeze-thawed NGF formulations after 5 (A), 10 and 15 FT-cycles (B)

This difference was also slightly visible regarding the determined turbidity as the values of the formulation 'Liquid NGF FB', which was diluted 1:1 with formulation buffer, were always a little higher than those for the formulation 'Liquid NGF WP', which was diluted 1:1 with the buffer required for desorption. This trend was observed throughout all different applied stress methods, but an interpretation of the light obscuration results is certainly still possible. Regrettably, formulations containing spider silk nanoparticles had to be centrifuged in order to obtain a spider silk particle-free, NGF containing supernatant. Thus, these formulations were not analyzed by light obscuration.

So far it can be concluded from the freeze-thaw study that only marginal protein aggregation took place under the investigated conditions, which was not enough to study any stabilizing effect of protein binding to spider silk particles. Apparently, NGF is not prone to significant aggregation during freezing and thawing even at this low concentration. At least, the presence of spider silk particles and the binding of NGF did not lead to a diminished stability of these formulations.

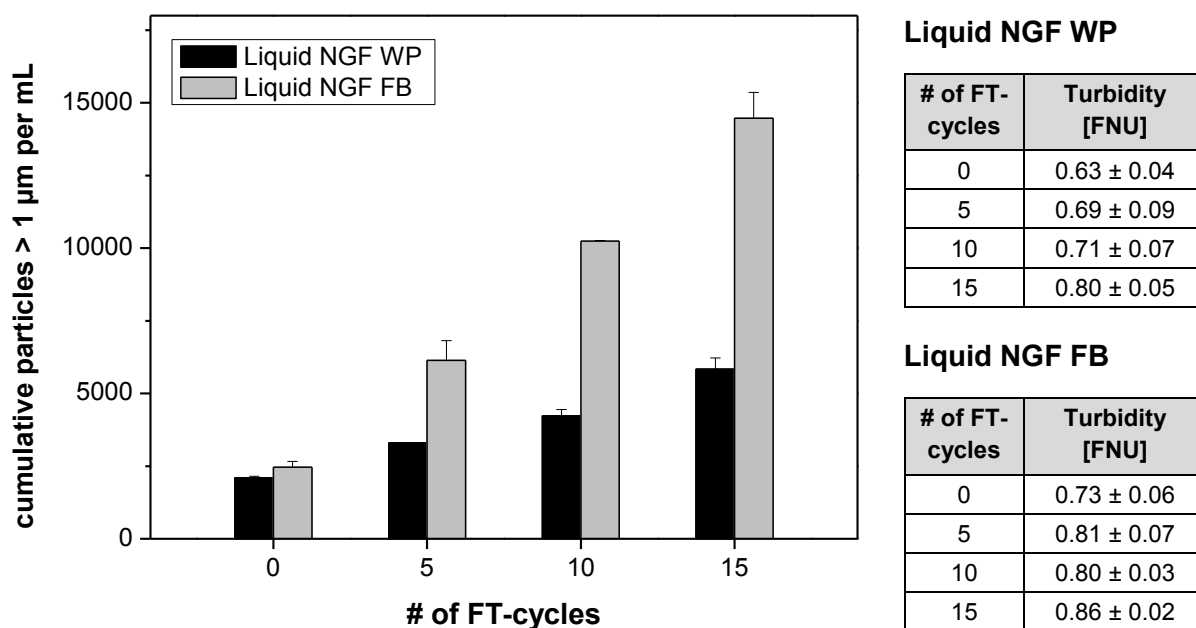


Figure 5.5. The diagram shows the subvisible particle count occurred during freeze-thawing of NGF formulations determined by light obscuration. The bars represent the mean of three samples \pm SD. The corresponding turbidity values are tabulated alongside the diagram.

5.3.2 STIRRING

In order to evaluate whether spider silk nanoparticles are capable to stabilize nerve growth factor against further stress conditions that occur during pharmaceutical processing, a stirring study was carried out. It is known from literature that stirring is more harmful to the stability of an IgG1 antibody than agitation or shaking [26, 27]. For example, it has been described in literature that non-ionic surfactants such as polysorbate 20 or 80 are able to prevent agitation and therefore air-water-interface induced protein aggregation, but fail to sufficiently stabilize antibodies during stirring studies [11, 26, 27]. Additional stress factors like cavitation, accelerated mass transport, local heating and particularly shear are held responsible for this more detrimental effect compared to agitation, where protein molecules are solely exposed to the air-water interface. Furthermore, the types of aggregates created by stirring and shaking of antibodies are quite different and depend strongly on the employed conditions of the stirring or shaking study.

As a conclusion of these findings, stirring was chosen as method of choice for studying mechanical stress on NGF formulations. For that purpose all formulations were filled into small glass vials typically used for HPLC samples and stirred over a period of 92 hours using Teflon-coated stirring bars and a stirring speed of 400 rpm. For each sampling point separate vials were used and non-stirred samples were analyzed as a control.

The amount of remaining total protein (A) and remaining dimer (B) over the investigated stirring time is depicted in Figure 5.6. The stirring stress led to a steady loss in dimer and

total protein recovery in formulations containing spider silk particles whereas NGF formulations without spider silk particles showed no significant protein loss. Interestingly, the protein loss in formulations comprising eADF4(C16) particles increased with increasing particle concentration so that the formulation comprising 20 mg/mL eADF4(C16) particles exhibited the lowest amount of residual dimer content with a recovery lower than 60%. Therefore, it can be stated that the more particles are present in the formulation, the higher the degree of protein loss during stirring will be. This result is so far contrary to the expectation which was defined in the forefront of the study. The binding of NGF onto or into eADF4(C16) particles was intended to prevent the protein from shear, surface or cavitation induced stress, but it seems that the opposite occurred.

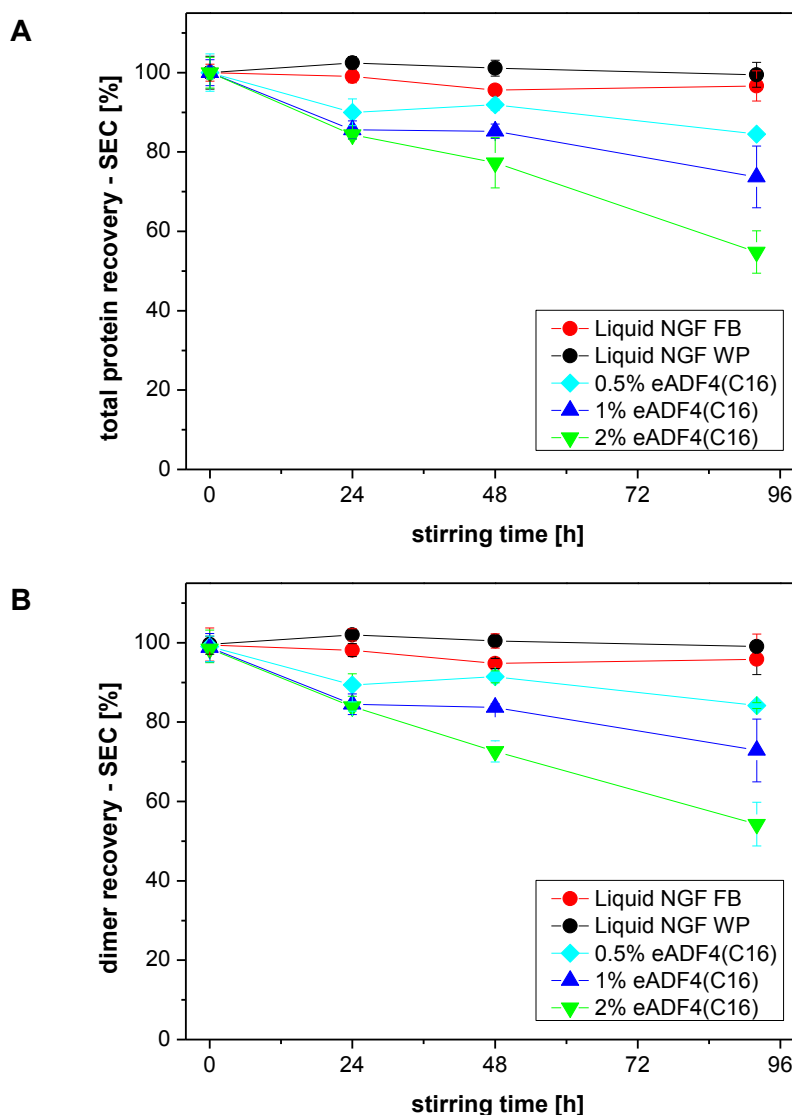


Figure 5.6. Total protein recovery (A) and remaining dimer content (B) during stirring of NGF formulations over 92 hours determined by HP-SEC (UV-detection at 215 nm). The displayed protein recoveries are calculated referring to the total AUC of each formulation at t₀. The symbols represent the mean of three samples \pm SD. Separate samples of each formulation were prepared for different sampling points.

Further analysis of the formulations was obtained by SDS-PAGE under non-reducing conditions and is illustrated in Figure 5.7. This method confirmed the loss of NGF content especially for the formulation with 2% [w/V] spider silk particles. An important additional information is that traces of soluble aggregates were neither detected by SDS-PAGE nor by HP-SEC so that the loss of protein has to be referred to the formation of insoluble protein aggregates or the enhanced adsorption of stressed, partially unfolded NGF to spider silk particles.

Light obscuration results for particle-free formulations are displayed in Figure 5.8 and reveal slightly increased particle counts for stirred formulations compared to control samples. As already described in the freeze-thaw study (see section 5.3.1), this indicates the early start of protein aggregation, but the degree was much too low to be detected by HP-SEC or RP-HPLC. Nevertheless, the issue of protein loss in the particle containing formulations remains open as the detection of protein aggregates in presence of spider silk protein nanoparticles poses a huge challenge for the analytics currently available. The differentiation just by size using light obscuration or static light scattering will be nearly impossible because of the presence of agglomerates of nanoparticles which will interfere with protein aggregates in the micrometer range. The high concentration of nanoparticles will also require the need of excessive sample dilution that will affect the particulate protein aggregates as well. A different and meaningful approach compared to light obscuration would be the use of newly developed imaging techniques such as Micro-flow Imaging™ [28, 29]. This analytical technique allows an image-based particle analysis which is e.g. able to distinguish between silicon oil droplets and protein particles. The differentiation is based on the different intensity or shape of the material after analysis of the obtained image set. For that reason, there may be an opportunity to achieve a separation between eADF4(C16) particles and NGF aggregates, but due to presumably similar refractive indices this analysis will be very difficult and was therefore not considered due to time restraints.

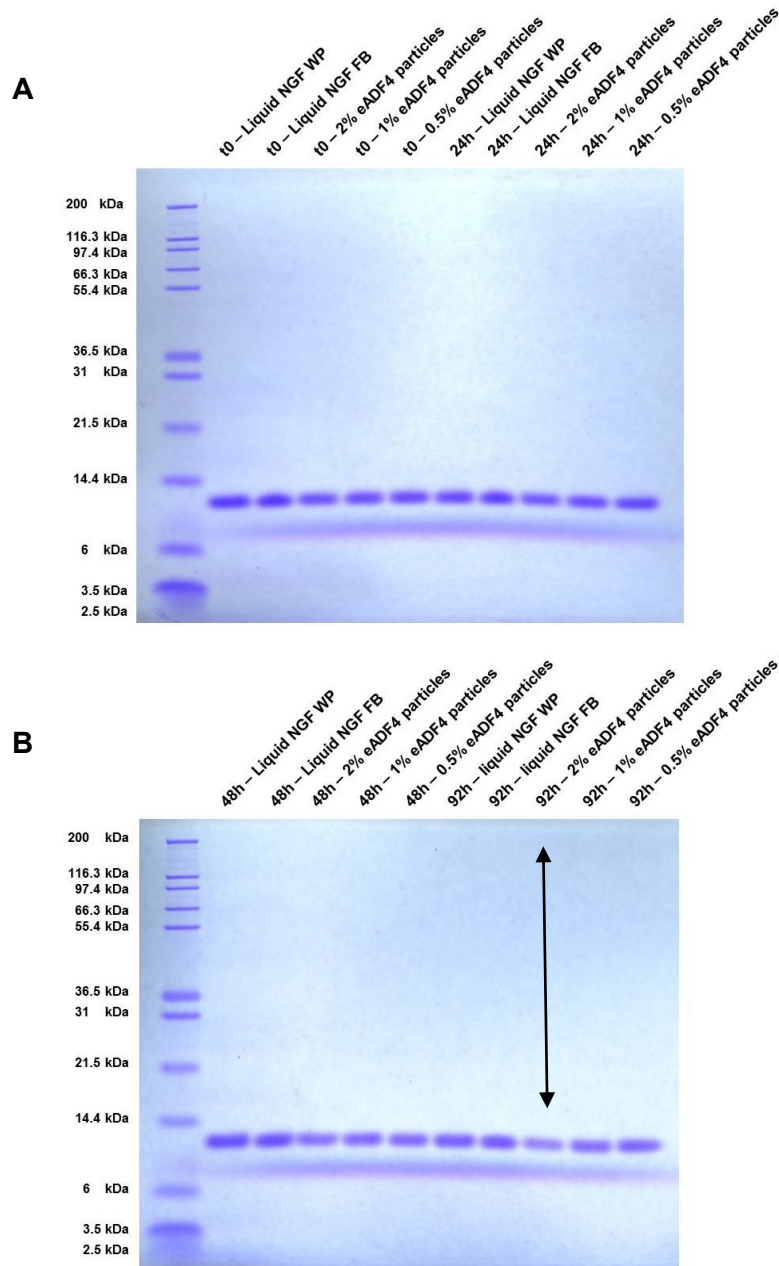


Figure 5.7. SDS-PAGE (non-reducing conditions) of unstressed (t0) and stirred NGF formulations after 24 (A), 48 and 92 hours (B) of stirring time

In summary, all formulations comprising NGF bound to spider silk particles exhibited a detrimental effect on the protein stability during stirring. The formulation without spider silk particles did not show a significant protein degradation under the investigated conditions and was therefore unambiguously superior to eADF4(C16) particle containing formulations. The mechanisms responsible for the protein loss could not be clarified due to analytical limitations. It can be only speculated whether insoluble aggregates are formed or an unfolding of protein molecules takes place that leads to very strong interactions with spider silk particles. As a result, these protein molecules would not be washed from the particles matrix and reduced protein content would be determined in the supernatant.

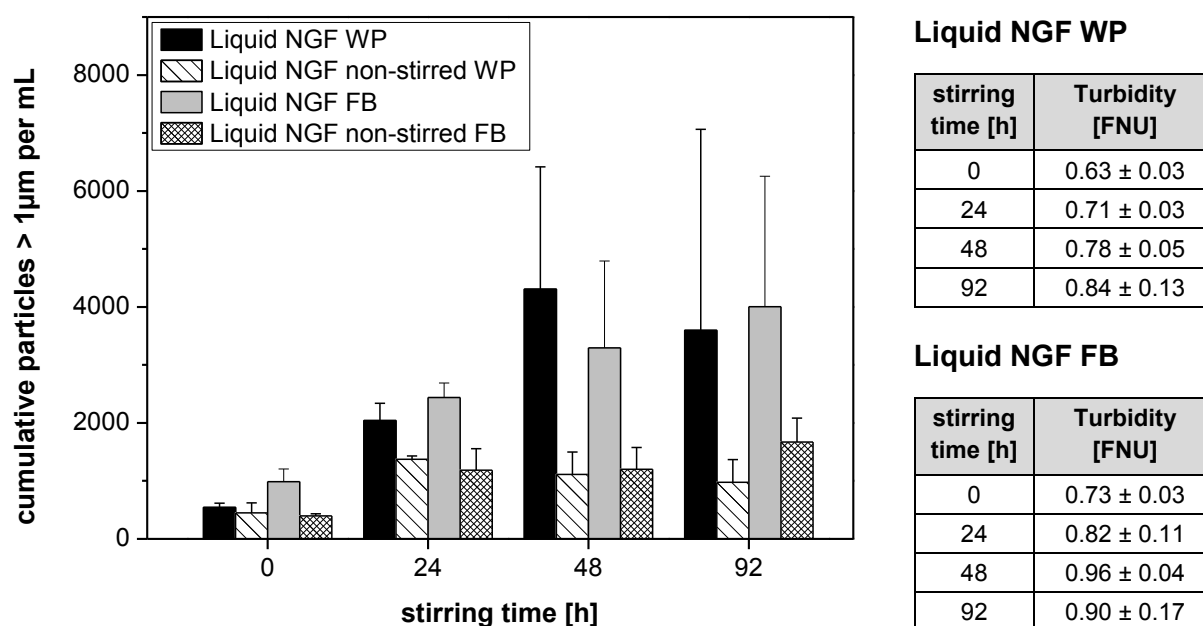


Figure 5.8. Cumulative counts for particles greater than 1 μm obtained during stirring of NGF formulations as determined by light obscuration. The bars represent the mean of three samples \pm SD. The corresponding turbidity values are tabulated alongside the diagram.

5.3.3 LIGHT EXPOSURE

Protein formulations are exposed to light several times in real-life conditions. This includes the potential exposure to UV-light during different production steps using UV-detection systems and to artificial or daylight during production, shipment, storage and administration of the drug to the patient [30, 31]. The primary target of photodegradation in proteins is their peptide backbone consisting of tryptophan, tyrosine, phenylalanine and cysteine, but absorption of light can also induce protein oxidation by the formation of reactive oxygen species. Mostly, photodegradation leads to chemical changes of the primary sequence and generates cross-linking reactions via disulfide or dityrosine formation [31]. As a consequence, protein formulations after light exposure exhibit a complex mixture of multiple protein species from soluble to insoluble and covalent to non-covalent protein aggregates. Performing studies on the photodegradation of protein formulations ICH guideline Q1B defines the type of light source needed and the procedure for confirmatory studies that should provide an overall illumination of not less than 1.2 million lux hours and an integrated near ultraviolet energy of not less than 200 watt hours/square meter [32]. Usually, confirmatory testing of protein formulations results in strong and severe protein degradation so that for forced degradation studies different settings can be used [9].

The following study was performed using a Suntest[®] CPS device equipped with a xenon arc lamp and an ultraviolet energy of 60 watt hours/square meter. Throughout preliminary experiments the appropriate time of light exposure was evaluated and samples were drawn after 8, 16 and 24 hours, respectively. It was expected from this study that NGF molecules

are protected from light by a shielding effect of the surrounding spider silk protein matrix and scattering or absorption of the incoming light by protein particles. Thus, the degree of photodegradation of NGF may be significantly reduced.

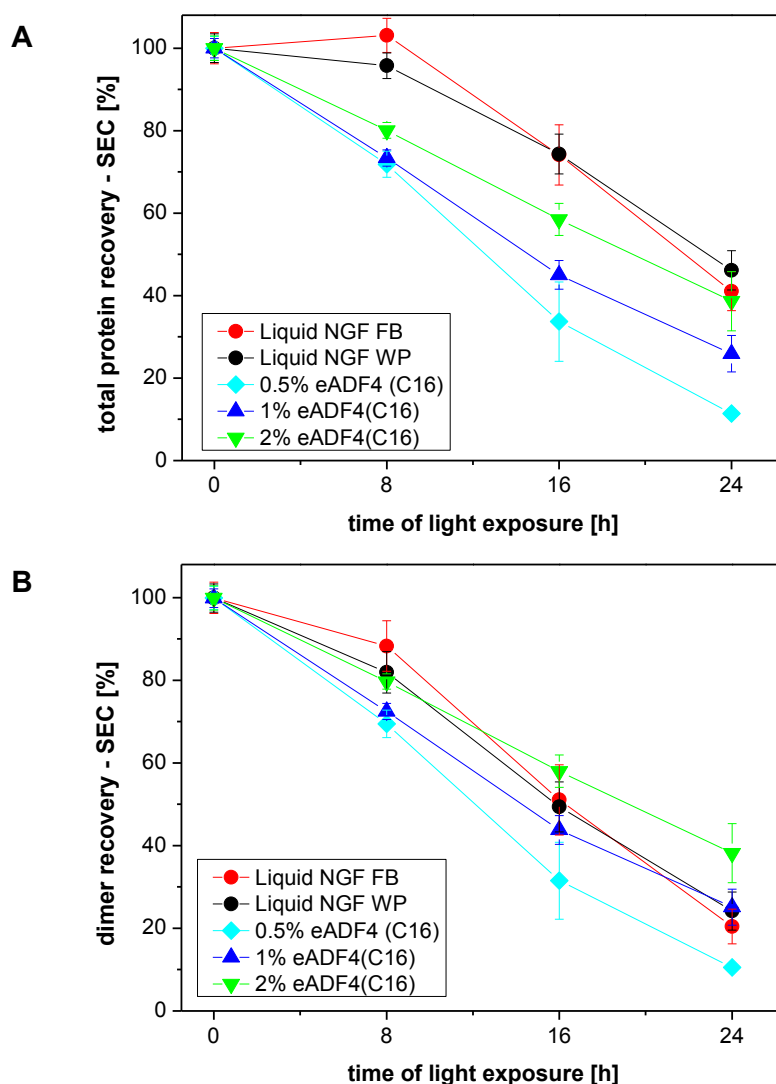


Figure 5.9. Total protein recovery (A) and remaining dimer content (B) of NGF formulations after light exposure as analyzed by HP-SEC (UV-detection at 215 nm). The displayed protein recoveries were calculated referring to the total AUC at t0 of each formulation. The symbols represent the mean of three samples \pm SD. Separate samples of each formulation were prepared for different sampling points.

Light exposure of NGF containing formulations resulted in fast and excessive protein degradation as depicted in Figure 5.9. Less than 25% dimer content was remaining after 24 hours in the case of particle-free NGF formulations (red and black dots, see Figure 5.9, B). This severe protein degradation came along with the formation of large amounts of soluble protein aggregates as the total protein recovery for these formulations decreased to only 45% of the starting value.

Figure 5.10 A shows the amount and type of soluble protein species determined by HP-SEC. An increasing fraction of tetramers and oligomers (HMW-aggregates) was detected and after 24 hours, 48% of the remaining soluble NGF was assigned to protein aggregates. This

finding was confirmed by results obtained from SDS-PAGE using the more sensitive silver staining in order to visualize also very low quantities of aggregates. As shown in Figure 5.11, significant amounts of protein aggregates with molecular weights above 26 kDa were formed. This correlated well to the results from HP-SEC. In addition, SDS-PAGE under non-reducing conditions revealed interesting information about the nature of the protein dimers present in the formulations. In HP-SEC analysis NGF elutes in its native form which is a non-covalent homodimer with a molecular weight of 26 kDa (see chapter 2, section 2.1.1.3). Therefore, this technique is not able to distinguish between non-covalent dimers consisting of two monomers stabilized via cysteine-knot motif (=native) or covalently linked dimers (=non-native aggregates). This lack of information can be filled with the result from SDS-PAGE under non-reducing conditions. Here, it is clearly visible that the amount of covalently linked NGF dimer was drastically increased following the absorption of light. This dimer formation can be easily explained by the aforementioned cross-linking reactions of cysteine groups which are a characteristic component of growth factor proteins [33].

Similar to particle-free formulations spider silk particle suspensions failed to stabilize nerve growth factor against light induced degradation as derived from the decrease in dimer and total protein recovery (see Figure 5.9). None of the employed eADF4(C16) particle concentrations showed a significant improvement. Spider silk particles seemed to be even detrimental for NGF stability at low concentrations such as 0.5% [w/V] (cyan diamonds). However, the formulation having the highest particle concentration of 2% [w/V] (green triangles) showed the best result with 38% dimer recovery vs. 25% for the particle-free formulation. This value is of course too low to declare a stabilizing effect, but at least the correlation between higher dimer recovery and higher eADF4(C16) particle concentration can be concluded at this point.

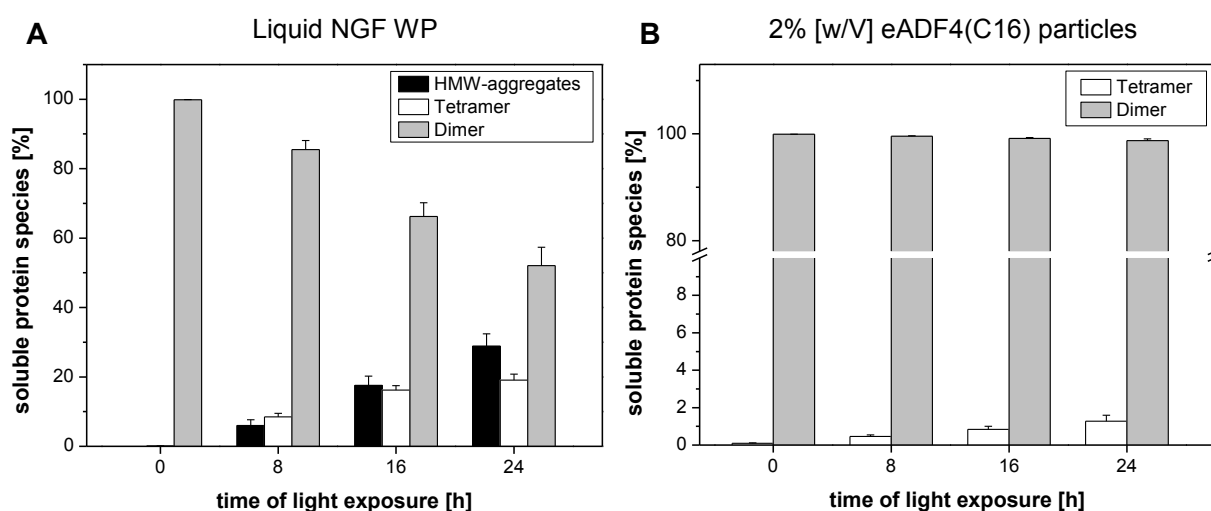


Figure 5.10. Soluble protein species of 'Liquid NGF WP' (A) and the formulation containing 2% [w/V] eADF4(C16) particles (B) determined by HP-SEC (UV-detection at 215 nm). The bars represent the mean of three samples \pm SD. Separate samples of each formulation were prepared for the different sampling points.

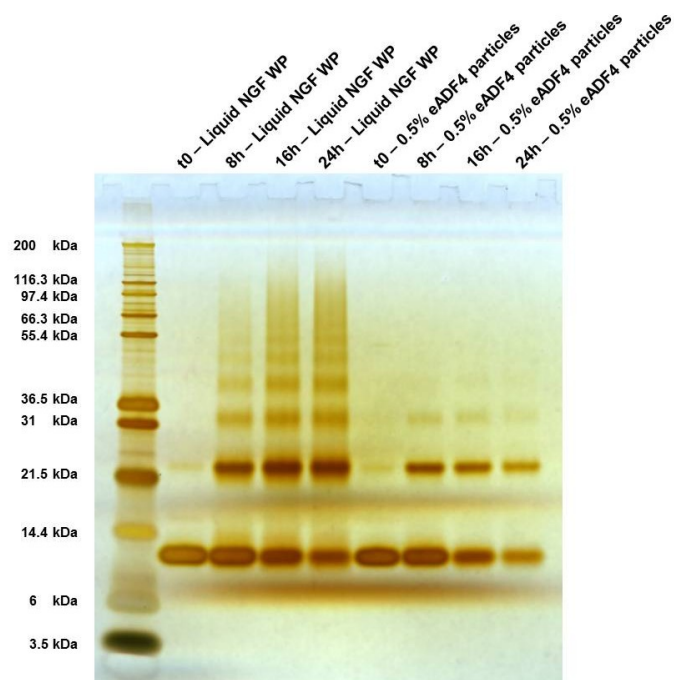


Figure 5.11. Comparison of particle-free vs. 0.5% [w/V] spider silk particle comprising NGF formulations by SDS-PAGE under non-reducing conditions (silver staining)

The Coomassie blue staining of the entire sample set is illustrated in Figure 5.12. It confirmed the already described results regarding the distinct decrease of total protein content over time. Nevertheless, the amount of NGF aggregates was quite different in spider silk particle comprising samples in contrast to particle-free samples, which was also observed in the silver staining of the formulation including 0.5% [w/V] spider silk particles (see Figure 5.11). All stressed samples showed an additional dimer bond, but especially after 24 hours of light exposure the dimer bond of particle-free samples was much more pronounced than for particle containing formulations. Consequently, the NGF monomer bond at 13 kDa showed the opposite behavior. This difference in aggregation behavior was also detected by HP-SEC as only small amounts of aggregated protein were determined (see Figure 5.10, B).

The dramatic loss in protein content suggests that also significant amounts of insoluble protein particles had been formed during degradation. As depicted in Figure 5.13 and keeping the dilution factor of 1:20 in mind, the assessed particle counts for particle-free formulations with values around 30,000 particles $\geq 1 \mu\text{m}$ per mL supported this assumption. Interestingly, the nephelometric analysis of these samples showed only a marginal increase which was not higher than for stirring or freeze-thaw stress. This finding may be considered as a hint for the formation of larger protein aggregates and will be discussed in comparison to heat-induced aggregates in the next section 5.3.4.

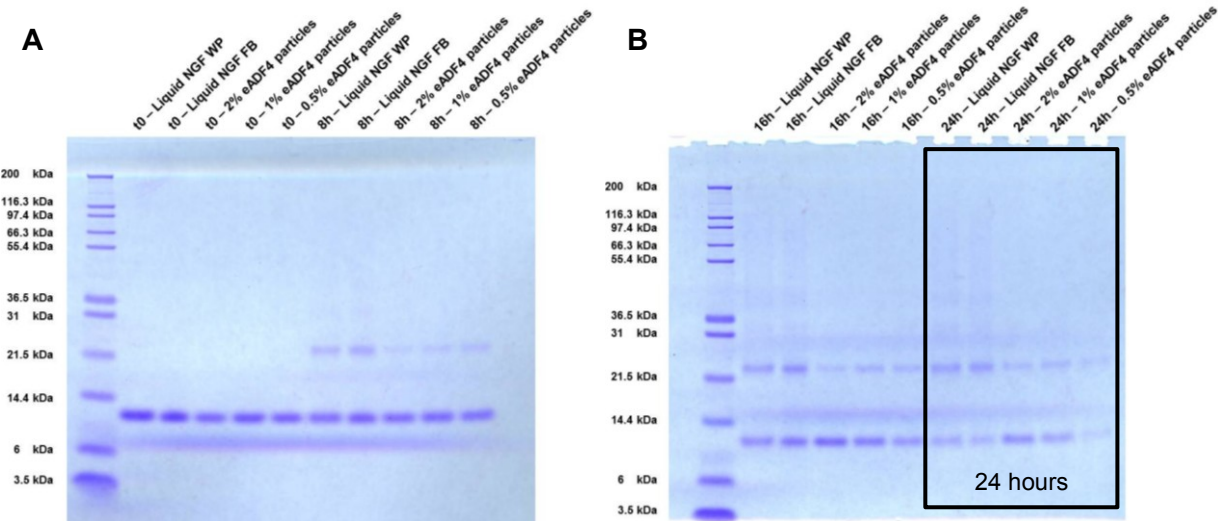


Figure 5.12. SDS-PAGE (non-reducing conditions) of unstressed NGF formulation (t0) and after 8 (A), 16 and 24 hours (B) of light exposure

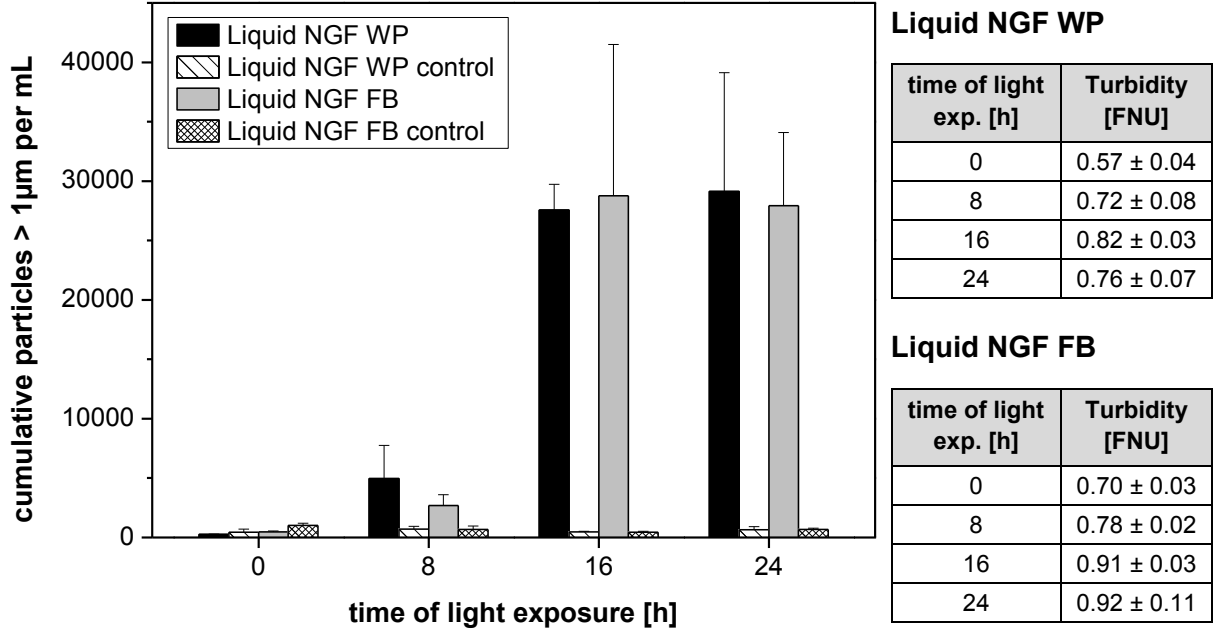


Figure 5.13. The diagram shows the subvisible particle count occurring after light exposure of NGF formulations determined by light obscuration. The bars represent the mean of three samples ± SD. The corresponding turbidity values are tabulated alongside the diagram.

To sum up the results from light exposure experiments, it has to be stated that a sufficient stabilization of NGF has not been achieved by adding spider silk particles to the formulation. Severe protein degradation took place in all samples investigated in this study and led to the formation of soluble and insoluble protein aggregates. Interestingly, the formulation containing 2% [w/V] spider silk particles showed the same amount of residual protein compared to the reference formulation, but the residual protein consisted of 99% dimer vs. 52% dimer content in the particle-free formulation. The dimer content determined by HP-SEC has to be furthermore analyzed by SDS-PAGE under non-reducing conditions to clarify the nature of the protein dimer. Particle-free formulations contained large amounts of covalently-linked molecules whereas the suspensions showed only a weak dimer and a strong monomer bond. Therefore, at least a week stabilizing effect can be attributed to the 2% [w/V] eADF4(C16) particle containing formulation, which provides an opportunity to achieve a substantial stabilizing effect by further increasing the spider silk particles' concentration. Moreover, a successful analytical differentiation between spider silk particles and particulate NGF aggregates as already discussed in section 5.3.2 may help to clarify the mechanism of protein degradation in the suspensions and thereby offer a starting point for further optimization of the formulation.

5.3.4 INCUBATION AT ELEVATED TEMPERATURE

The pathway of protein aggregation has been described as a very complex process which can broadly differ between stress factors applied during development and production and also strongly depends on the protein itself [34, 35]. Herein, thermal stress is the most common method to investigate protein degradation of biopharmaceuticals [9]. Regarding heat stress, the starting point of protein aggregation appears to be a conformational modification or partial unfolding into a non-native protein conformation which exhibits a high propensity to form irreversible protein aggregates [35]. Therefore, excipients stabilizing the native conformation provide the potential to inhibit heat-induced protein aggregation.

In order to shorten the time period required for a long-term stability study according to ICH guideline Q1A, accelerated stability testing at higher temperatures is commonly used and the experimental design has to be defined case-by-case [9]. These studies are performed to investigate and characterize protein aggregates in detail, to clarify the effect of different formulation excipients and to define lead candidates during formulation development. Therefore, incubation temperatures are required at which severe protein aggregation takes place over a limited period of time. As a rule of thumb, the incubation temperature should be 10-20°C below T_m of the protein in the corresponding formulation. The T_m is defined as the temperature where 50% of the protein molecules are unfolded during a thermal scan and can

be determined by microcalorimetry or other analytical techniques like Fourier transformed infrared spectroscopy [36].

The melting temperature of the employed particle-free NGF formulation was determined by microcalorimetry and the corresponding thermogram is shown in Figure 5.14. The calculated T_m value of 74.7°C reflects a comparatively stable protein formulation regarding heat-induced aggregation. eADF4(C16) particle containing NGF formulations were also examined by microcalorimetry, but the corresponding thermograms did not show any exo- or endothermic events. It is likely that the presence of highly concentrated eADF4(C16) particles inhibited the detection of any signals arising from folding processes of NGF. As a conclusion, an incubation temperature of 60°C and sampling points after 1, 3 and 7 days of incubation were chosen for the first study.

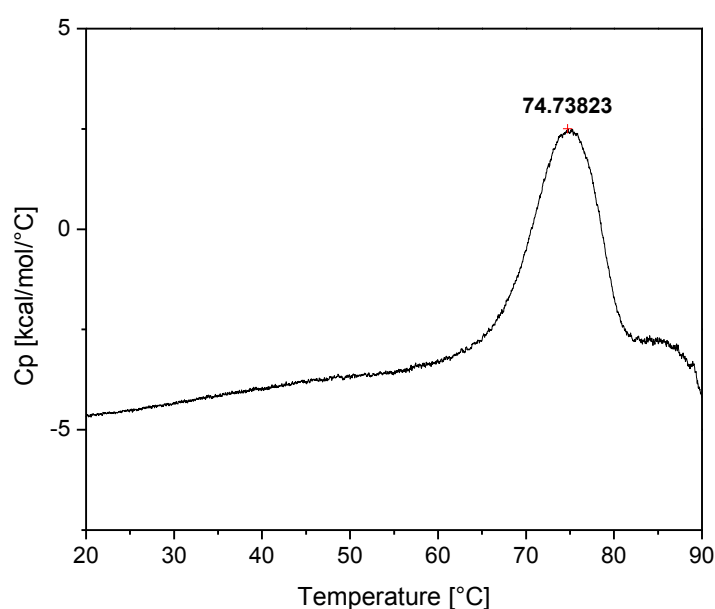


Figure 5.14. Thermogram of nerve growth factor formulated in the loading buffer (= formulation buffer) at a concentration of 0.5 mg/mL measured by μ DSC

The results from HP-SEC after 1 and 3 days of incubation are summarized in Figure 5.15. All formulations showed a fast and severe degradation of NGF already after 1 day of incubation at 60°C. For this reason, data from the last sampling point at 7 days is not displayed. Comparing the total protein recovery of all formulations with the remaining dimer fraction, it is visible that less than 1% of soluble aggregates were present. This finding is contrary to the NGF degradation detected during light stress where up to 50% soluble aggregate species were formed. This implicates that heat-induced aggregation of NGF is rather different in its mechanism compared to light-induced aggregation.

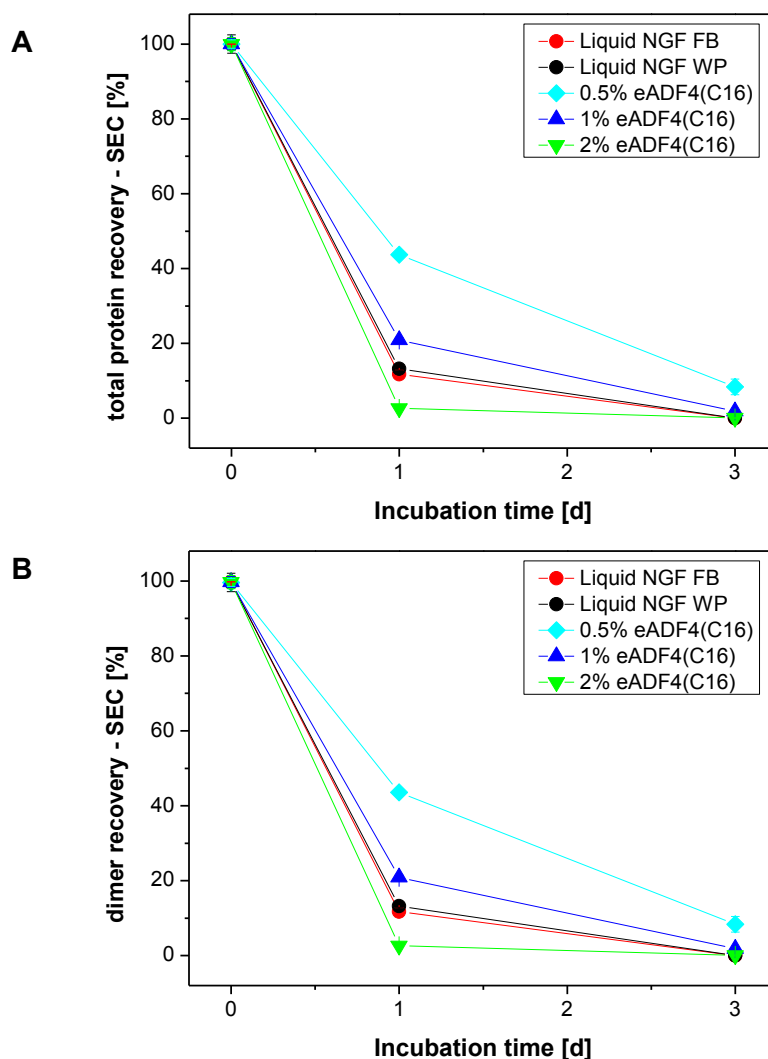


Figure 5.15. Total protein recovery (A) and dimer recovery (B) of NGF formulations after incubation at 60°C analyzed by HP-SEC (UV-detection at 215 nm). The displayed protein recoveries are calculated referring to the total AUC of each formulation at t_0 . The symbols represent the mean of three samples \pm SD. Separate samples of each formulation were prepared for different sampling points.

This difference was also observed by SDS-PAGE under non-reducing conditions (see Figure 5.16). All samples showed an intense band representing the dissociated NGF monomer with a molar mass of 13 kDa, but no significant amounts of NGF dimer or oligomers. Only a slight smearing was observed in particle-free formulations which can be explained by the fact that during denaturation of the samples parts of insoluble aggregates are dissolved again. Hence, cross-linking of cytosine or tyrosine residues did not occur during incubation at 60°C.

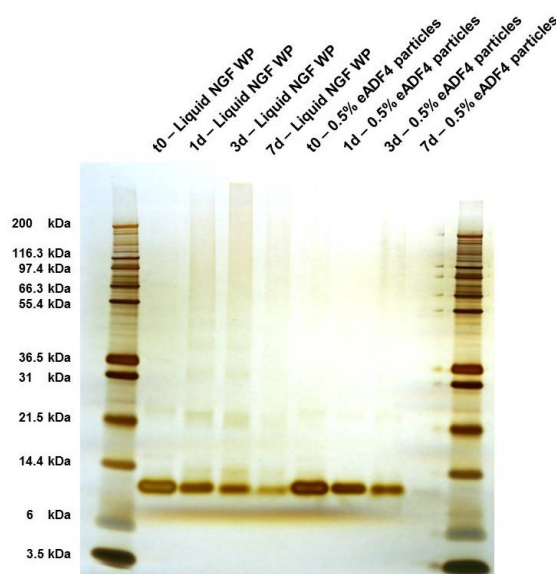


Figure 5.16. Comparison of particle-free vs. 0.5% [w/V] spider silk particle comprising NGF formulations after incubation at 60°C by SDS-PAGE (non-reducing conditions, silver staining).

The eADF4(C16) particle containing formulations showed unfortunately no significant stabilizing effect during incubation at 60°C. Interestingly, the ranking of the formulations, which was set according to results from light-exposure (2% > 1% > 0.5%), is turned upside down regarding the dimer recovery after 1 day. The formulation comprising 2% [w/V] particles was even worse, but at least the addition of 0.5% [w/V] spider silk particles resulted in significantly higher remaining dimer content than the particle-free formulation. Certainly, the stabilizing effect was not satisfying, but the formulation with the lowest employed amount of spider silk particles showed that stabilization may be possible by a further reduction of the particle concentration and the identification of the right balance between particle concentration and protein payload.

To complete the overall picture on heat-induced aggregation of NGF, samples were analyzed by light obscuration, and turbidity measurements were carried out (see Figure 5.17). The severe decrease in protein recovery detected by HP-SEC had to result in return in large amounts of insoluble aggregates as already explained. This was confirmed by more than 50,000 particles $\geq 1 \mu\text{m}$ per mL (1:20 dilution) after 3 days of incubation. For the first time also the determined FNUs showed a clear increase to values around 3 compared to values below 1 after light exposure. Taking both numbers into account, more subvisible particles as well as smaller particles were formed at 60°C than during light exposure. This outcome further confirmed the different kind of aggregation mechanism of nerve growth factor induced by different stress methods.

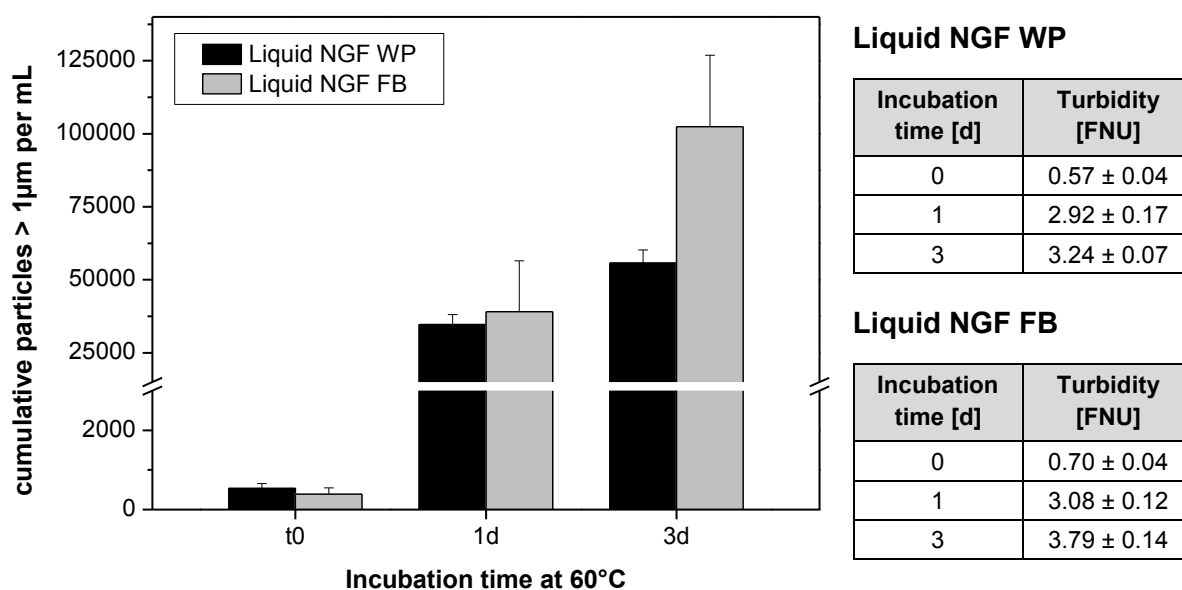


Figure 5.17. The diagram shows the subvisible particle count after incubation at 60°C determined by light obscuration. The bars represent the mean of three samples \pm SD. The corresponding turbidity values are tabulated alongside the diagram.

A second study was performed at 40°C to slow down the heat-induced aggregation. As depicted in Figure 5.18, the particle-free formulation showed no loss in NGF dimer content, whereas the spider silk particle containing formulations already indicated a detrimental effect on protein stability with 85% (2% [w/V] nanoparticles), 93% (1% [w/V] nanoparticles) and 95% (0.5% [w/V] nanoparticles) dimer recovery after only 3 days of incubation. Again, more eADF4(C16) particles led to a larger loss in dimer content and at 40°C the formulation comprising 0.5% [w/V] spider silk particles also exhibited a decreased protein recovery compared to the particle-free formulation.

Taking all results from incubation at 60°C and 40°C together, it can be concluded that in the presence of spider silk particles NGF is presumably more prone to heat-induced aggregation than in nanoparticle-free formulations. In contrast to light exposure, heat-induced aggregation did not lead to an increase in soluble protein aggregates. Otherwise, an immense appearance of comparatively small subvisible particles was found and visually turbid formulations were obtained. The particle formation may be a result of conformational changes of native NGF molecules at elevated temperatures without the occurrence of covalently-linked protein species as they were detected after light exposure.

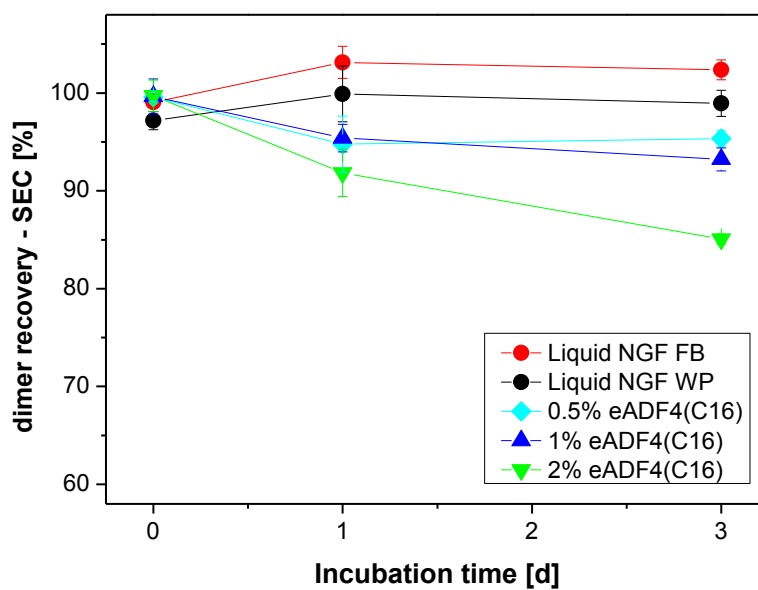


Figure 5.18. Remaining dimer content of NGF formulations after incubation at 40°C as analyzed by HP-SEC (UV-detection at 215 nm). The displayed protein recovery was calculated referring to the total AUC of each formulation at t₀. The symbols represent the mean of three samples ± SD. Separate samples of each formulation were prepared for the different sampling points.

5.4 SUMMARY AND CONCLUSIONS

The stability of nerve growth factor in a particle-free formulation vs. spider silk nanoparticle formulations was investigated. The impact of binding NGF onto foreign particles during accelerated stability studies has been performed for the first time to our knowledge. Freeze-thawing, stirring, light exposure and incubation at elevated temperature were carried out after an appropriate procedure for the desorption of NGF from eADF4(C16) particles had been developed. This procedure included the mixing of the corresponding formulation at a ratio of 1:1 with a solution containing 200 mM sodium phosphate and 800 mM sodium chloride at pH 8.0. The mixture was incubated for 30 min at 50°C and an agitation speed of 600 rpm.

As it is known from multiple studies reported in literature, different stress methods lead to different results regarding the type and degree of protein aggregation [26, 34, 35]. The underlying mechanisms strongly depend on the type of protein as well. Additionally, little knowledge is available about the behavior of proteins being bound to foreign particles and subjected to forced degradation studies so that the outcome of this study could hardly be estimated.

The results from the freeze-thaw study showed that freezing and thawing of NGF bound to eADF4(C16) particles was not detrimental regarding protein stability. All formulations including the one without spider silk particles exhibited no loss in protein or dimer content after 15 freeze-thaw cycles in liquid nitrogen. According to this data, the formation of ice-water interfaces and local freeze-concentration did not lead to significant conformational changes of the native protein. Only slightly increased subvisible particle counts were obtained giving a first hint of protein aggregation.

Stirring studies were performed in order to obtain information on the impact of shear and other stress factors associated with mechanical stress on NGF stability. The applied stirring stress of 92 hours at 400 rpm did not affect the NGF in solution, but the presence of spider silk particles deteriorated the stability of NGF significantly. The higher the particle concentration in the formulation, the larger the loss in protein and dimer recovery had been. An explanation for this effect is difficult to find, but maybe more particles enhance the probability that partially unfolded NGF molecules come close to other protein molecules and cause a higher degree of protein aggregation. More particles also create a larger surface area where NGF molecules are able to adsorb and desorb due to electrostatic and hydrophobic forces. Thereby, unfolding processes are maybe enhanced.

Exposing NGF formulations to xenon light interestingly led to a completely different behavior of the formulations. In this case, none of the formulations was able to sufficiently stabilize NGF against degradation, but more spider silk particles in the formulation were favorable compared to lower concentrations. Nevertheless, an interesting result was that in formulations with spider silk particles the dimer content of the residual protein remained

above 95% whereas NGF in the solution alone showed an almost 50% proportion of soluble NGF aggregates consisting of covalently-linked dimers and oligomers. Again, a well-defined explanation is difficult, but it can be speculated that the residual NGF content is protected through the binding to the spider silk matrix. A lower particle concentration implies a lower mass and volume of available eADF4(C16) matrix and results in a higher degree of surface adsorption where NGF molecules are not protected against light-induced degradation processes.

The formulations were additionally subjected to an accelerated stability testing at elevated temperatures of 60°C and 40°C, respectively. A fast and severe loss in NGF content was detected at 60°C. Already after 1 day of incubation all formulations showed significant protein degradation independent of the presence of nanoparticles. Therefore, incubation at 40°C was carried out. All eADF4(C16) particle comprising formulations revealed a reduced NGF content after 3 days, whereas the particle-free formulation did not show that severe protein aggregation. For this reason, enhanced desorption processes from the spider silk particles accompanied by protein unfolding are also considered as potential sources of increased protein aggregation.

In summary, nerve growth factor could not be stabilized by the addition of spider silk nanoparticles. Although different stress methods showed different results regarding the underlying mechanisms of aggregation, a significant stabilizing effect was not observed throughout the entire degradation study. In order to clarify the protein degradation in presence of spider silk particles, further studies have to be performed and an analytical technique enabling the differentiation between spider silk particles and particulate protein aggregates should be developed.

5.5 REFERENCES

- [1] **Wang W.**, Instability, stabilization, and formulation of liquid protein pharmaceuticals. *Int. J. Pharm.* 1999, 185(2), 129-188
- [2] **Wang W.**, Lyophilization and development of solid protein pharmaceuticals. *Int. J. Pharm.* 2000, 203(1-2), 1-60
- [3] **Wang W., Singh S. K., Li N., Toler M. R., King K. R. and Nema S.**, Immunogenicity of protein aggregates—Concerns and realities. *Int. J. Pharm.* 2012, 431(1–2), 1-11
- [4] **Hermeling S., Crommelin D., Schellekens H. and Jiskoot W.**, Structure-Immunogenicity Relationships of Therapeutic Proteins. *Pharm. Res.* 2004, 21(6), 897-903
- [5] **Carpenter J. F., Randolph T. W., Jiskoot W., Crommelin D. J. A., Middaugh C. R., Winter G., Fan Y.-X., Kirshner S., Verthelyi D., Kozlowski S., Clouse K. A., Swann P. G., Rosenberg A. and Cherney B.**, Overlooking subvisible particles in therapeutic protein products: Gaps that may compromise product quality. *J. Pharm. Sci.* 2009, 98(4), 1201-1205
- [6] **Gekko K. and Timasheff S. N.**, Mechanism of protein stabilization by glycerol: preferential hydration in glycerol-water mixtures. *Biochemistry* 1981, 20(16), 4667-4676
- [7] **Prestrelski S. J., Tedeschi N., Arakawa T. and Carpenter J. F.**, Dehydration-induced conformational transitions in proteins and their inhibition by stabilizers. *Biophys. J.* 1993, 65(2), 661-671
- [8] **Gokarn Y. R., Kosky A., Kras E., McAuley A. and Remmele R. L.**, Excipients for Protein Drugs, in *Excipient Development for Pharmaceutical, Biotechnology, and Drug Delivery Systems*. p. 291-331
- [9] **Hawe A., Wiggenghorn M., van de Weert M., Garbe J. H. O., Mahler H.-C. and Jiskoot W.**, Forced degradation of therapeutic proteins. *J. Pharm. Sci.* 2012, 101(3), 895-913
- [10] **Kerwin B. A.**, Polysorbates 20 and 80 used in the formulation of protein biotherapeutics: Structure and degradation pathways. *J. Pharm. Sci.* 2008, 97(8), 2924-2935
- [11] **Serno T., Geidobler R. and Winter G.**, Protein stabilization by cyclodextrins in the liquid and dried state. *Adv Drug Deliv Rev* 2011, 63(13), 1086-1106
- [12] **Veronese F. M.**, Peptide and protein PEGylation: a review of problems and solutions. *Biomaterials* 2001, 22(5), 405-417
- [13] **Besheer A., Hertel T. C., Kressler J., Mäder K. and Pietzsch M.**, Enzymatically catalyzed HES conjugation using microbial transglutaminase: Proof of feasibility. *J. Pharm. Sci.* 2009, 98(11), 4420-4428
- [14] **Pinco R. G. and Sullivan T. M.**, Regulation of Pharmaceutical Excipients, in *Excipient Development for Pharmaceutical, Biotechnology, and Drug Delivery Systems*. p. 37-50
- [15] **Bee J. S., Chiu D., Sawicki S., Stevenson J. L., Chatterjee K., Freund E., Carpenter J. F. and Randolph T. W.**, Monoclonal antibody interactions with micro- and nanoparticles: Adsorption, aggregation, and accelerated stress studies. *J. Pharm. Sci.* 2009, 98(9), 3218-3238
- [16] **Zhang J., Pritchard E., Hu X., Valentin T., Panilaitis B., Omenetto F. G. and Kaplan D. L.**, Stabilization of vaccines and antibiotics in silk and eliminating the cold chain. *P Natl Acad Sci USA* 2012, 109(30), 11981-11986

- [17] **Uebersax L., Mattotti M., Papaloizos M., Merkle H. P., Gander B. and Meinel L.**, Silk fibroin matrices for the controlled release of nerve growth factor (NGF). *Biomaterials* 2007, 28(30), 4449-4460
- [18] **Eng M., Ling V., Briggs J. A., Souza K., Canova-Davis E., Powell M. F. and De Young L. R.**, Formulation Development and Primary Degradation Pathways for Recombinant Human Nerve Growth Factor. *Anal. Chem.* 1997, 69(20), 4184-4190
- [19] **Bhatnagar B. S., Bogner R. H. and Pikal M. J.**, Protein Stability During Freezing: Separation of Stresses and Mechanisms of Protein Stabilization. *Pharm. Dev. Technol.* 2007, 12(5), 505-523
- [20] **Wang W., Nema S. and Teagarden D.**, Protein aggregation—Pathways and influencing factors. *Int. J. Pharm.* 2010, 390(2), 89-99
- [21] **Abdelwahed W., Degobert G., Stainmesse S. and Fessi H.**, Freeze-drying of nanoparticles: formulation, process and storage considerations. *Adv Drug Deliv Rev* 2006, 58(15), 1688-1713
- [22] **Zillies J. C., Zwioerek K., Hoffmann F., Vollmar A., Anchordoquy T. J., Winter G. and Coester C.**, Formulation development of freeze-dried oligonucleotide-loaded gelatin nanoparticles. *Eur. J. Pharm. Biopharm.* 2008, 70(2), 514-521
- [23] **Beirowski J., Inghelbrecht S., Arien A. and Gieseler H.**, Freeze-drying of nanosuspensions, 1: Freezing rate versus formulation design as critical factors to preserve the original particle size distribution. *J. Pharm. Sci.* 2011, 100(5), 1958-1968
- [24] **Carpenter J. F., Randolph T. W., Jiskoot W., Crommelin D. J. A., Middaugh C. R. and Winter G.**, Potential inaccurate quantitation and sizing of protein aggregates by size exclusion chromatography: Essential need to use orthogonal methods to assure the quality of therapeutic protein products. *J. Pharm. Sci.* 2010, 99(5), 2200-2208
- [25] **Barnard J. G., Singh S., Randolph T. W. and Carpenter J. F.**, Subvisible particle counting provides a sensitive method of detecting and quantifying aggregation of monoclonal antibody caused by freeze-thawing: Insights into the roles of particles in the protein aggregation pathway. *J. Pharm. Sci.* 2011, 100(2), 492-503
- [26] **Kiese S., Pappengerger A., Friess W. and Mahler H.-C.**, Shaken, not stirred: Mechanical stress testing of an IgG1 antibody. *J. Pharm. Sci.* 2008, 97(10), 4347-4366
- [27] **Mahler H.-C., Müller R., Frieß W., Delille A. and Matheus S.**, Induction and analysis of aggregates in a liquid IgG1-antibody formulation. *Eur. J. Pharm. Biopharm.* 2005, 59(3), 407-417
- [28] **Huang C.-T., Sharma D., Oma P. and Krishnamurthy R.**, Quantitation of protein particles in parenteral solutions using micro-flow imaging. *J. Pharm. Sci.* 2009, 98(9), 3058-3071
- [29] **Sharma D., King D., Oma P. and Merchant C.**, Micro-Flow Imaging: Flow Microscopy Applied to Sub-visible Particulate Analysis in Protein Formulations. *The AAPS Journal* 2010, 12(3), 455-464
- [30] **Rathore N. and Rajan R. S.**, Current Perspectives on Stability of Protein Drug Products during Formulation, Fill and Finish Operations. *Biotechnol. Prog.* 2008, 24(3), 504-514
- [31] **Kerwin B. A. and Remmele R. L.**, Protect from light: Photodegradation and protein biologics. *J. Pharm. Sci.* 2007, 96(6), 1468-1479
- [32] *ICH Guidelines - Quality Guidelines - Stability Testing: Photostability Testing of New Drug Substances and Products Q1B.* 1996; Available from: <http://www.ich.org/products/guidelines/quality/article/quality-guidelines.html>.

- [33] **Wiesmann C. and de Vos A. M.**, Nerve growth factor: structure and function. *Cell. Mol. Life Sci.* 2001, 58(5), 748-759
- [34] **Mahler H.-C., Friess W., Grauschopf U. and Kiese S.**, Protein aggregation: Pathways, induction factors and analysis. *J. Pharm. Sci.* 2009, 98(9), 2909-2934
- [35] **Philo J. S. and Arakawa T.**, Mechanisms of Protein Aggregation. *Curr. Pharm. Biotechnol.* 2009, 10(4), 348-351
- [36] **Schön A. and Velazquez-Campoy A.**, Calorimetry, in *Methods for Structural Analysis of Protein Pharmaceuticals*. 2005, AAPS Press. p. 573-589

CHAPTER 6

FINAL SUMMARY AND CONCLUSION

The **general aim** of this thesis was to investigate the recombinant spider silk protein eADF4(C16) in depths with regard to applications as new biomaterial for colloidal drug delivery of proteins. The objective originated in the work of Andreas Lammel and Martin Schwab who showed that spider silk particles can be easily prepared by a salting out process, and that particles size and size distribution can be adjusted by appropriate process parameters [1]. Small hydrophobic guest molecules were employed in their work to investigate the applicability of eADF4(C16) particles for drug delivery. However, this simple and gentle preparation technique makes such a delivery system a promising platform even for controlled drug delivery of sensitive drugs like therapeutic proteins.

In Chapter 1 a general introduction into the area of drug delivery of proteins and the biomaterial silk is given. There is still a clear need for biodegradable materials which exhibit the potential and prerequisites to be approved as delivery systems / excipients for human use by the health authorities. For this reason, it is essential to understand the biochemical and material properties of spider silk proteins and the technical processing into different morphologies including spider silk protein particles. Reviewing literature, the potential of *Bombyx mori* (silkworm) silk and the spider silk protein eADF4(C16) becomes apparent.

The materials and methods applied throughout this thesis are described **in Chapter 2**.

Particle preparation techniques, deep-dive physical characterization and freeze-drying of spider silk particles are presented **in Chapter 3**. The phase separation process was exploited by two different techniques. eADF4(C16) particles were prepared in the nanometer as well as in the micrometer range. In terms of nano-sized spider silk particles, a micromixing system consisting of two syringe pumps and a T-shaped mixing element was established as standard preparation technique due to its upscalability and excellent reproducibility. eADF4(C16) particles slightly below 300 nm with a narrow particle size distribution were obtained applying elevated process temperatures. Spider silk microparticles were produced using an ultrasonic spray nozzle to atomize potassium phosphate into aqueous eADF4(C16) solutions. Further process optimization enabled the preparation of microparticles between 5 and 7 μm and offers the potential to further increase the resulting particle size for future work. However, the intention of simultaneous atomization of potassium phosphate and the protein solution resulted only in non-spherical protein aggregates like threads and fibrils due

to an inadequate phosphate to eADF4(C16)-ratio present at the atomizing surface and in the atomized droplet mixture.

As the aqueous eADF4(C16) solution is one important factor influencing the phase separation process, detailed analysis of this protein formulation was performed. eADF4(C16) stability during incubation at 80°C was investigated since pre-heating of the protein solution is applied for the preparation of eADF4(C16) nanoparticles. It was shown that the spider silk formulation (1.0 mg/mL, 10 mM Tris-buffer, pH 8.0) exhibits only limited protein stability over a period of four hours at 80°C as thin spider silk fibers were formed. However, a short preheating step before particle preparation will not significantly affect the phase separation process according to the determined protein aggregation behavior.

Spider silk particle suspensions comprising sucrose, trehalose or mannitol were successfully freeze-dried above a threshold of an excipient-to-particles ratio of 10:1 [w/w] using a conventional freeze-drying cycle. It was possible to maintain all particle characteristics throughout the drying process. Lysozyme-loaded eADF4(C16) particles produced via remote loading were successfully freeze-dried as well. Freeze-dried nanosuspensions provide better storage stability compared to an aqueous eADF4(C16) suspension which was shown to be sensitive towards changes in pH and ionic strength. Nevertheless, the particle stock solution prepared in purified water and in the absence of additional ions could be stored over a period of six months.

In Chapter 4 two different strategies for drug loading of eADF4(C16) particles are described. First, the so-called remote loading was performed which means that drug loading was achieved in a second step after particle preparation by addition of the drug substance to the particle suspension. Lysozyme and nerve growth factor (NGF) were loaded onto eADF4(C16) particles up to payloads of more than 20% [w/w] with corresponding loading efficiencies above 80% [w/w]. It was concluded from the loading studies that the predominant driving force is electrostatic attraction and that hydrophobic forces may only play a subsidiary role. Interestingly, confocal laser scanning microscopy revealed matrix loaded spider silk particles as a result of the remote loading procedure. Matrix loading was considered to be beneficial for a sustained protein release compared to simple surface adsorption.

Secondly, a typical encapsulation process was conducted by addition of the drug substance to the aqueous eADF4(C16) solution prior to particle preparation. However, encapsulation did not lead to comparable payloads due to the required conditions for particle formation during the encapsulation process. The high ionic strength (1 M potassium phosphate) strongly diminished electrostatic interactions so that less protein molecules were co-precipitated into the eADF(C16) matrix. Additionally, neutral substances such as Rhodamine B could not be efficiently encapsulated. Hence, electrostatic attraction was also regarded as prerequisite for a successful encapsulation of drug molecules into eADF4(C16) particles.

Several *in vitro* release studies were carried out to examine the underlying release rates and mechanisms. Release from spider silk particles was very fast at physiological conditions independent of the performed loading procedure. All results indicated that an incorporation of the drug molecule into the protein matrix does not lead to a sustained release rate caused by potential slow diffusion through a dense polymer matrix. In contrast, the determined release has to be understood as the creation of equilibrium between the particle with its loaded drug molecules and the aqueous environment including ions, other substances like albumin and the potentially already released drug molecules. Any change of this equilibrium modifies the release, for which reason changes of pH, ionic strength or the addition of albumin significantly alter the release profile. Therefore, the eADF4(C16) matrix was not able to prevent fast dissolution neither of small molecules nor macromolecules like protein drugs except during storage of loaded particles in purified water. Herein, the loaded compound is not released at all which allows for a long-term storage of loaded spider silk particles in purified water. Nevertheless, a sustained delivery of drug substances from eADF4(C16) particles has to be assessed as very challenging on the basis of the current data. This kind of triggered release behavior may be especially of interest for applications in diagnostics where the loaded particles are stored in aqueous solution and the release of the loaded compound starts immediately upon dilution with e.g. salts, buffer or albumin.

A different approach for using eADF4(C16) particles was examined in **Chapter 5**. Recently, silk fibroin films were successfully employed for the stabilization of a vaccine in order to eliminate the necessary cold chain [2]. On this account, spider silk particles were employed in forced degradation studies in order to evaluate their potential to stabilize the loaded protein molecules. Different stress conditions were applied to a suspension comprising eADF4(C16) particles loaded with nerve growth factor via remote loading and the particle-free NGF formulation. A standard procedure was developed that allowed for reproducible and gentle desorption of nerve growth factor from eADF4(C16) particles at pH 8.0 and high ionic strength.

Freeze-thawing, stirring and accelerated stability testing of the formulations revealed that a potential stabilizing impact of binding NGF onto spider silk nanoparticles cannot be verified. Protein aggregation was actually provoked by the presence of eADF4(C16) particles as the occurring desorption and adsorption processes are considered to force unfolding and subsequent protein aggregation. Only light exposure of NGF formulations showed that eADF4(C16) particles were able to mitigate the degree of protein aggregation. Higher particle concentrations were superior, but the best performing formulation was still not able to prevent protein degradation even though a significantly reduced formation of soluble protein aggregates (covalently-linked dimers and oligomers) was detected. It was assumed that the amount of NGF being incorporated into the spider silk matrix is protected from light exposure.

Taking together **conclusions from all chapters**, different proof of concept studies were performed in order to show the potential benefit of using eADF4(C16) particles as an alternative to other polymeric drug delivery systems as well as the present limitations.

Although the release from eADF4(C16) particles is not retarded by the spider silk matrix, the characteristics of this drug delivery system offer certain possible applications. It may be used e.g. for diagnostics where the long-term storage in purified water and the immediate and fast release only upon a distinct trigger is of great advantage.

Furthermore, the material properties are very interesting in the area of wound healing. Negatively charged polystyrene microspheres (PolyHeal™) with a size of 5-microns were introduced as a safe and clinically effective treatment option for hard-to-heal wounds [3] and functionalized silk biomaterials (films) were recently evaluated by Kaplan et al. [4]. In this context, the development of endotoxin-free and sterile spider silk material (e.g. particles or films) has to obtain priority.

Another possible application is the area of vaccination where particulate vaccine-delivery systems with comparable dimensions to the pathogens are desired [5]. Spider silk particles may act as adjuvants per se for which reason a broad screening of different particulate formulations should be performed to proof this hypothesis. Furthermore, chemical or genetical modification as exemplarily shown by Scheibel et al. [6] using eADF4(C16) in conjunction with a specific antigen will be an innovative approach to combine the properties of both single molecules. As a result, spider silk particles with antigen sequences on the surface may be formed and act as a smart vaccine-delivery system. Future work should therefore focus on *in vitro* and *in vivo* vaccination studies to verify the potential benefits of this new biomaterial.

REFERENCES

- [1] **Lammel A., Schwab M., Slotta U., Winter G. and Scheibel T.,** Processing conditions for the formation of spider silk microspheres. *ChemSusChem* 2008, 1(5), 413-416
- [2] **Zhang J., Pritchard E., Hu X., Valentin T., Panilaitis B., Omenetto F. G. and Kaplan D. L.,** Stabilization of vaccines and antibiotics in silk and eliminating the cold chain. *P Natl Acad Sci USA* 2012, 109(30), 11981-11986
- [3] **Govrin J., Leonid K., Luger E., Tamir J., Zeilig G. and Shafir R.,** New method for treating hard-to-heal wounds: clinical experience with charged polystyrene microspheres. *Wounds UK* 2010, 6(4), 52-61
- [4] **Gil E. S., Panilaitis B., Bellas E. and Kaplan D. L.,** Functionalized Silk Biomaterials for Wound Healing. *Advanced Healthcare Materials* 2013, 2(1), 206-217
- [5] **Singh M., Chakrapani A. and O'Hagan D.,** Nanoparticles and microparticles as vaccine-delivery systems. *Expert Rev. Vaccines* 2007, 6(5), 797-808
- [6] **Wohlrab S., Müller S., Schmidt A., Neubauer S., Kessler H., Leal-Egaña A. and Scheibel T.,** Cell adhesion and proliferation on RGD-modified recombinant spider silk proteins. *Biomaterials* 2012, 33(28), 6650-6659

PUBLICATIONS AND PRESENTATIONS ASSOCIATED WITH THIS THESIS

ARTICLES

M. Hofer, G. Winter, J. Myschik

Recombinant spider silk particles for controlled delivery of protein drugs
Biomaterials, 2012, 33(5), 1554-1562

A. Lammel, M. Schwab, M. Hofer, G. Winter, T. Scheibel

Recombinant spider silk particles as drug delivery vehicles
Biomaterials, 2011, 32(8), 2233-2240

PATENTS

A. Lammel, T. Scheibel, M. Schwab, G. Winter, M. Hofer, J. Myschik

Silk particles for controlled and sustained delivery of compounds
WO2011063990

POSTER PRESENTATIONS

M. Hofer, G. Winter, J. Myschik

Protein loading of recombinant spider silk particles
AAPS Annual Meeting and Exposition, 2011, October 23rd-27th, Washington D.C., USA

M. Hofer, E. Agostini, G. Winter, J. Myschik

Recombinant spider silk proteins as new biomaterial for innovative drug delivery systems
Forum Life Science, 2011, March 23rd-24th, Munich, Germany

M. Hofer, A. Lammel, M. Schwab, J. Myschik, T. Scheibel, G. Winter

Preparation of spider silk particles and their evaluation as a new particulate drug delivery system

7th World Meeting on Pharmaceutics, Biopharmaceutics and Pharmaceutical Technology, 2010, March 8th-11th, Valetta, Malta

M. Hofer, A. Lammel, M. Schwab, J. Myschik, T. Scheibel, G. Winter

Spider Silk Proteins – A new biopolymer for drug delivery applications
Science to Market Conference – EAPB, 2009, October 6th-7th, Hannover, Germany

ORAL PRESENTATIONS

M. Hofer, G. Winter, J. Myschik

Investigation of spider silk particles as a potential drug carrier for biotec drugs

8th World Meeting on Pharmaceutics, Biopharmaceutics and Pharmaceutical Technology,
2012, March 19th-22nd, Istanbul, Turkey